COORDINATION OF PLANT ENDOMEMBRANE SYSTEM WITH DEVELOPMENTAL SIGNALS AND ENVIRONMENTAL STIMULI.

EDITED BY: Ruixi Li, Georgia Drakakaki, Yansong Miao, Ying Fu and Xiaojuan Li

PUBLISHED IN: Frontiers in Plant Science

frontiers Research Topics

frontiers

ISSN 1664-8714
ISBN 978-2-88976-937-7
DOI 10.3389/978-2-88976-937-7

About Frontiers

Frontiers is more than just an open-access publisher of scholarly articles: it is a pioneering approach to the world of academia, radically improving the way scholarly research is managed. The grand vision of Frontiers is a world where all people have an equal opportunity to seek, share and generate knowledge. Frontiers provides immediate and permanent online open access to all its publications, but this alone is not enough to realize our grand goals.

Frontiers Journal Series

The Frontiers Journal Series is a multi-tier and interdisciplinary set of open-access, online journals, promising a paradigm shift from the current review, selection and dissemination processes in academic publishing. All Frontiers journals are driven by researchers for researchers; therefore, they constitute a service to the scholarly community. At the same time, the Frontiers Journal Series operates on a revolutionary invention, the tiered publishing system, initially addressing specific communities of scholars, and gradually climbing up to broader public understanding, thus serving the interests of the lay society, too.

Dedication to Quality

Each Frontiers article is a landmark of the highest quality, thanks to genuinely collaborative interactions between authors and review editors, who include some of the world's best academicians. Research must be certified by peers before entering a stream of knowledge that may eventually reach the public - and shape society; therefore, Frontiers only applies the most rigorous and unbiased reviews.
Frontiers revolutionizes research publishing by freely delivering the most outstanding research, evaluated with no bias from both the academic and social point of view. By applying the most advanced information technologies, Frontiers is catapulting scholarly publishing into a new generation.

What are Frontiers Research Topics?

Frontiers Research Topics are very popular trademarks of the Frontiers Journals Series: they are collections of at least ten articles, all centered on a particular subject. With their unique mix of varied contributions from Original Research to Review Articles, Frontiers Research Topics unify the most influential researchers, the latest key findings and historical advances in a hot research area! Find out more on how to host your own Frontiers Research Topic or contribute to one as an author by contacting the Frontiers Editorial Office: frontiersin.org/about/contact

COORDINATION OF PLANT ENDOMEMBRANE SYSTEM WITH DEVELOPMENTAL SIGNALS AND ENVIRONMENTAL STIMULI.

Topic Editors:
Ruixi Li, Southern University of Science and Technology, China
Georgia Drakakaki, University of California, Davis, United States
Yansong Miao, Nanyang Technological University, Singapore
Ying Fu, China Agricultural University, China
Xiaojuan Li, Beijing Forestry University, China

Citation: Li, R., Drakakaki, G., Miao, Y., Fu, Y., Li, X., eds. (2022). Coordination of Plant Endomembrane System With Developmental Signals and Environmental Stimuli. Lausanne: Frontiers Media SA. doi: 10.3389/978-2-88976-937-7

Table of Contents

04 ***Editorial: Coordination of plant endomembrane system with developmental signals and environmental stimuli***
Ruixi Li, Georgia Drakakaki, Yansong Miao, Ying Fu and Xiaojuan Li

06 ***Overexpression of a Banana Aquaporin Gene* MaPIP1;1 *Enhances Tolerance to Multiple Abiotic Stresses in Transgenic Banana and Analysis of Its Interacting Transcription Factors***
Yi Xu, Juhua Liu, Caihong Jia, Wei Hu, Shun Song, Biyu Xu and Zhiqiang Jin

22 ***Erratum: Overexpression of a Banana Aquaporin Gene* MaPIP1;1 *Enhances Tolerance to Multiple Abiotic Stresses in Transgenic Banana and Analysis of Its Interacting Transcription Factors***
Frontiers Production Office

23 ***Extracellular Vesicles: Emerging Players in Plant Defense Against Pathogens***
Guosheng Liu, Guangren Kang, Shumei Wang, Yifan Huang and Qiang Cai

32 ***Functions and Mechanisms of SAC Phosphoinositide Phosphatases in Plants***
Yanbo Mao and Shutang Tan

38 ***Controlling the Gate: The Functions of the Cytoskeleton in Stomatal Movement***
Yihao Li, Xin Zhang, Yi Zhang and Haiyun Ren

47 ***An Update on Coat Protein Complexes for Vesicle Formation in Plant Post-Golgi Trafficking***
Kai Ching Law, Ka Kit Chung and Xiaohong Zhuang

56 ***ROOT HAIR DEFECTIVE3 Is a Receptor for Selective Autophagy of the Endoplasmic Reticulum in* Arabidopsis**
Jiaqi Sun, Weina Wang and Huanquan Zheng

64 ***Monitoring Autophagy in Rice With GFP-ATG8 Marker Lines***
Rui Liu, Rongxue Zhang, Yi Yang, Xuejun Liu and Qingqiu Gong

76 ***Vacuoles in Bryophytes: Properties, Biogenesis, and Evolution***
Hao-ran Liu, Chao Shen, Danial Hassani, Wan-qi Fang, Zhi-yi Wang, Yi Lu, Rui-liang Zhu and Qiong Zhao

86 ***Constitutive Active CPK30 Interferes With Root Growth and Endomembrane Trafficking in* Arabidopsis thaliana**
Ren Wang, Ellie Himschoot, Jian Chen, Marie Boudsocq, Danny Geelen, Jiří Friml, Tom Beeckman and Steffen Vanneste

frontiers | Frontiers in Plant Science

TYPE Editorial
PUBLISHED 02 August 2022
DOI 10.3389/fpls.2022.977333

OPEN ACCESS

EDITED AND REVIEWED BY
Katalin Solymosi,
Eötvös Loránd University, Hungary

*CORRESPONDENCE
Ruixi Li
lirx@sustech.edu.cn

SPECIALTY SECTION
This article was submitted to Plant Physiology, a section of the journal Frontiers in Plant Science

RECEIVED 24 June 2022
ACCEPTED 20 July 2022
PUBLISHED 02 August 2022

CITATION
Li R, Drakakaki G, Miao Y, Fu Y and Li X (2022) Editorial: Coordination of plant endomembrane system with developmental signals and environmental stimuli.
Front. Plant Sci. 13:977333.
doi: 10.3389/fpls.2022.977333

Editorial: Coordination of plant endomembrane system with developmental signals and environmental stimuli

Ruixi Li[1]*, Georgia Drakakaki[2], Yansong Miao[3], Ying Fu[4] and Xiaojuan Li[5]

[1]Key Laboratory of Molecular Design for Plant Cell Factory of Guangdong Higher Education Institutes, Institute of Plant and Food Science, Department of Biology, School of Life Sciences, Southern University of Science and Technology, Shenzhen, China, [2]Department of Plant Sciences, University of California, Davis, Davis, CA, United States, [3]School of Biological Sciences, Nanyang Technological University, Singapore, Singapore, [4]State Key Laboratory of Plant Physiology and Biochemistry, Department of Plant Sciences, College of Biological Sciences, China Agricultural University, Beijing, China, [5]Key Laboratory of Genetics and Breeding in Forest Trees and Ornamental Plants Ministry of Education, College of Biological Sciences and Biotechnology, Beijing Forestry University, Beijing, China

KEYWORDS

plant endomembrane system, biotic stress, abiotic stress, cytoskeleton dynamics, intracellular transport

Editorial on the Research Topic
Coordination of plant endomembrane system with developmental signals and environmental stimuli

Being sessile, plants have developed many plant-specific mechanisms to adapt to their unique lifestyle and respond to the changing environment. For a long time, researchers in plant biology have focused on the hormone regulation pathways and signal transduction cascades, thus the roles of endomembrane proteins in developmental program and stress response remained largely unexplored. During the past decade, however, researchers have started to unravel the mysteries of the endomembrane system under physiological conditions by integrating image analysis with forward and reverse genetics approach. Recent progresses have shed light on the extensive interactions between endomembrane proteins and signaling pathways.

In this Research Topic collection, we published nine papers, which could be grouped into three categories. In the first category, researchers reviewed recent advances about special organelles or trafficking modulators in developmental regulation and stress response. Liu, Kang et al. summarized the current understanding of plant extracellular vesicles (EVs), including their isolation technologies, biogenesis and essential roles in plant immunity. EVs are potential carriers for metabolites and nucleotides with key roles in cross-species regulation, therefore this paper has drawn broad attention after publication. Mao and Tan reviewed recent progress in the biological functions of SUPPRESSOR OF ACTIN (SAC) domain-containing phosphoinositide phosphatases in plants. Considering the vital role of phosphatidylinositol in a wide range of biological

processes, this mini review provides novel insights into its regulatory mechanism. Li et al. discussed recent advances in the organization and dynamics of actin filaments and microtubule networks in guard cells, emphasizing cytoskeletal rearrangements during stomatal movement. Stomata are the main sites for gas exchange in leaves, so their regulatory mechanisms are important to ensure efficient photosynthesis. Law et al. highlighted recent findings and potential applications of adaptor protein (AP) complexes, retromer, and retriever complexes in post-Golgi trafficking.

In the second category, the authors focused on studying a particular endomembrane protein under different physiological conditions. Xu et al. described the essential function of the aquaporin gene MaPIP1;1 in regulating multiple abiotic stresses in banana. Wang et al. showed that the constitutive active calcium-dependent protein kinase 30 (CPK30) plays an important role in root growth regulation and endomembrane trafficking. Sun et al. demonstrated that Root Hair Defective3 (RHD3) acts as an ER-phagy receptor under ER stress to promote ER-phagy in *Arabidopsis*. RHD3 is the close homolog of the Atlastin-type GTPase in mammalian cells, which has been widely reported as the key regulator of ER fusion and ER-phagy. This is the first paper in plant field revealing the conserved role of RHD3 as an important ER-phagy receptor in *Arabidopsis*.

In the third category, the researchers discussed cell biological aspects in plant species other than model plant *Arabidopsis*. Liu, Shen et al. reviewed the current knowledge about vacuoles in Bryophytes, including their special properties, biogenesis mechanism and evolutionary roles. Liu, Zhang et al. tested different GFP-ATG8 markers to monitor autophagy in rice. Since both vacuolar transport and autophagy are fundamental cell biology processes, establishing the system in different plant species other than *Arabidopsis* will benefit science and society in the long term.

Functional studies of endomembrane system during the developmental program and environmental response have been just started. We hope this research collection can open a door to researchers who are willing to bridge the gap between macroscopic/physiological analysis and subcellular details.

Author contributions

RL wrote the manuscript. All authors revised and approved the final version.

Funding

RL was supported by Guangdong Innovation Research Team Fund (2016ZT06S172) and Shenzhen Sci-Tech Fund (KYTDPT20181011104005 and JCYJ20210324105004011). YM was supported by Singapore Ministry of Education (MOE) Tier 1 grant (RT11/20; RG32/20). YF was supported by the National Natural Science Foundation of China (32061143018).

Conflict of interest

The authors declare that the research was conducted in the absence of any commercial or financial relationships that could be construed as a potential conflict of interest.

Publisher's note

frontiers in Plant Science

ORIGINAL RESEARCH
published: 25 August 2021
doi: 10.3389/fpls.2021.699230

Overexpression of a Banana Aquaporin Gene *MaPIP1;1* Enhances Tolerance to Multiple Abiotic Stresses in Transgenic Banana and Analysis of Its Interacting Transcription Factors

Yi Xu[1,3,4], Juhua Liu[2], Caihong Jia[2], Wei Hu[2], Shun Song[1,3,4], Biyu Xu[2]* and Zhiqiang Jin[2]**

[1] Key Laboratory of Genetic Improvement of Bananas, Haikou Experimental Station, Chinese Academy of Tropical Agricultural Sciences, Haikou, China, [2] Key Laboratory of Biology and Genetic Resources of Tropical Crops, Institute of Tropical Bioscience and Biotechnology, Chinese Academy of Tropical Agricultural Sciences, Haikou, China, [3] Sanya Research Institute of Chinese Academy of Tropical Agricultural Sciences, Sanya, China, [4] Hainan Key Laboratory for Biosafety Monitoring and Molecular Breeding in Off-Season Reproduction Regions, Sanya, China

Aquaporins can improve the ability of plants to resist abiotic stresses, but the mechanism is still not completely clear. In this research, overexpression of *MaPIP1;1* in banana improved tolerance to multiple stresses. The transgenic plants resulted in lower ion leakage and malondialdehyde content, while the proline, chlorophyll, soluble sugar, and abscisic acid (ABA) contents were higher. In addition, under high salt and recovery conditions, the content of Na^+ and K^+ is higher, also under recovery conditions, the ratio of K^+/Na^+ is higher. Finally, under stress conditions, the expression levels of ABA biosynthesis and response genes in the transgenic lines are higher than those of the wild type. In previous studies, we proved that the MaMADS3 could bind to the promoter region of *MaPIP1;1*, thereby regulating the expression of *MaPIP1;1* and affecting the drought tolerance of banana plants. However, the mechanism of *MaPIP1;1* gene response to stress under different adversity conditions might be regulated differently. In this study, we proved that some transcription factor genes, including MaERF14, MaDREB1G, MaMYB1R1, MaERF1/39, MabZIP53, and MaMYB22, showed similar expression patterns with *MaPIP1;1* under salt or cold stresses, and their encoded proteins could bind to the promoter region of *MaPIP1;1*. Here we proposed a novel *MaPIP1;1*-mediated mechanism that enhanced salt and cold tolerance in bananas. The results of this study have enriched the stress-resistant regulatory network of aquaporins genes and are of great significance for the development of molecular breeding strategies for stress-resistant fruit crops.

Keywords: *MaPIP1*, tolerance, banana, interaction, transcription factor

OPEN ACCESS

Edited by:
Xiaojuan Li,
Beijing Forestry University, China

Reviewed by:
Mei Zhang,
South China Botanical Garden, Chinese Academy of Sciences, China
Rajesh Kumar Jha,
West Virginia State University, United States

***Correspondence:**
Zhiqiang Jin
zhiqiangjin@itbb.org.cn
Biyu Xu
biyuxu@itbb.org.cn
Shun Song
sss1984006@163.com

Specialty section:
This article was submitted to Plant Physiology, a section of the journal Frontiers in Plant Science

Received: *23 April 2021*
Accepted: *21 July 2021*
Published: *25 August 2021*

Citation:
Xu Y, Liu J, Jia C, Hu W, Song S, Xu B and Jin Z (2021) Overexpression of a Banana Aquaporin Gene MaPIP1;1 Enhances Tolerance to Multiple Abiotic Stresses in Transgenic Banana and Analysis of Its Interacting Transcription Factors. Front. Plant Sci. 12:699230. doi: 10.3389/fpls.2021.699230

INTRODUCTION

Drought, salinity, and cold stresses can cause plants to lose water and severely affect their growth and development. Water transport is an important way to maintain tolerance to drought and high salt stresses (Cheeseman, 1988; Bray, 1993; Blumwald, 2000). As the main fruit and crop on a global scale, bananas have made important economic contributions to tropical and subtropical developing countries (Liu et al., 2017). Due to their shallow root system, banana plants are susceptible to drought, salt, and cold stress-induced water shortage conditions, which will greatly reduce the yield and quality of bananas (van Asten et al., 2011; Sreedharan et al., 2013).

Aquaporin can increase the penetration of cell membranes to water, glycerol, carbon dioxide, boron, and other small molecules (Kapilan et al., 2018). The aquaporin (AQP) family was first identified from humans and then was isolated from animals and plants. There are currently 47 AQP members in bananas (Hu et al., 2015) and tomatoes (Reuscher et al., 2013), and 33, 35, 53, and 36 AQP members in rice, *Arabidopsis*, Chinese cabbage, and corn, respectively (Chaumont et al., 2001; Johanson et al., 2001; Sakurai et al., 2005; Tao et al., 2014). Plant AQPs can be divided into eight categories, including tonoplast intrinsic proteins (TIPs), plasma membrane intrinsic proteins (PIPs), small basic intrinsic proteins (SIPs), nodulin 26-like intrinsic proteins (NIPs), hybrid intrinsic proteins (HIPs), GlpF-like intrinsic proteins (GIPs), large intrinsic proteins (LIPs), and uncategorized members designated X intrinsic proteins (XIPs), which were based on protein sequence homology and predicted subcellular location (Hussain et al., 2019).

Many biological studies have shown that AQPs not only participate in plant growth and development also can improve the tolerance of plants to drought, high salt, low temperature, and other abiotic stresses (Hu et al., 2012; Feng et al., 2018, 2019; Madrid-Espinoza et al., 2018; Hussain et al., 2019; Li W. et al., 2019). One of the AQP genes, *TaAQP8* in wheat, can improve the salt tolerance of transgenic tobacco (Hu et al., 2012). Under the high salt stress, tobacco *NtAQP1* can improve plant water absorption capacity (Sade et al., 2010). Overexpressing of *SpAQP1*, *TdPIP1;1*, *OsPIP1;1*, *SlTIP2;2*, and *TaNIP* can improve the salt tolerance of transgenic plants (Gao et al., 2010; Chang et al., 2016). Two AQP genes in rice, *OsPIP1*, and *OsPIP2*, improve the drought resistance of transgenic plants. Some members of the plant AQP family can respond to multiple stresses, such as *BnPIP1* and *VfPIP1* can enhance the drought and osmotic ability of transgenic plants (Lian et al., 2004; Guo et al., 2006). *PgTIP1* confers tolerance to drought and salt stresses. *TaAQP7* transgenic plants can respond to drought and osmotic stresses (Peng et al., 2007; Huang et al., 2014). *MaPIP2-7* improves the adaptability of transgenic bananas to drought, salt, and low temperature (Xu et al., 2020c), and bananas transformed with the *MaSIP2-1* gene had a stronger drought and cold tolerance than the control (Xu et al., 2020b). AQP can improve the tolerance of plants to abiotic stress, so further study of its mechanism is very important to improve plant growth and development.

The mechanism by which AQPs improve stress tolerance is still poorly understood. Related studies have shown that AP2/ERF transcription factors have a certain regulatory effect on the expression of AQPs (Xu et al., 2020b). AtTG, which encodes AP2/ERF transcription factors, improves the adaptability to drought tolerance of plants by directly activating the expression of *AtTIP2;3*, *AtTIP1;1*, and *AtPIP2;2* (Zhu et al., 2014). *RdreB1BI* improves the drought tolerance by combining with the *FvPIP2;1* promoter in the strawberry (Gu et al., 2017). Our previous research also showed that MaMADS3 could interact with the promoter of *MaPIP1;1* and improved the drought resistance of plants (Xu et al., 2020a).

In previous studies, we have cloned *MaPIP1;1* in bananas and proved that it could improve the adaptability of transgenic *Arabidopsis* to drought and salt (Xu et al., 2014). Next, the transcription factors that bind to *MaPIP1;1* under drought conditions were screened by the yeast one-hybrid to further analyze the mechanism of *MaPIP1;1* in improving plant drought resistance (Xu et al., 2020a). Our research also shows that *MaPIP1;1* can improve the drought, salt, and low-temperature tolerance of transgenic bananas. In addition, we identified that MaERF14, MaDREB1G, and MaMYB1R1 could regulate *MaPIP1;1* expression under high salt conditions. Furthermore, MaERF1/39, MabZIP53, and MaMYB22 can combine with the *MaPIP1;1* promoter, thereby regulating the expression of *MaPIP1;1* and affect the cold tolerance of banana plants. The results of this study will enhance our understanding of AQP, improving the tolerance of transgenic bananas to abiotic stress and the mechanism by which *MaPIP1;1* improves plant stress resistance and lays the foundation for the cultivation of stress-resistant bananas.

MATERIALS AND METHODS

Plant Materials and Treatments

Banana seedlings (*Musa acuminata* L. AAA group, cv. Brazilian) were grown in coconut medium in a greenhouse (16 h light/8 h dark cycle; 70% relative humidity; 28°C; 200 μmol m^{-2} s^{-1} light intensity). When the seedlings had five leaves (100 days old), those subjected to the stress treatment were grown in the same way.

Under the NaCl treatment, banana seedlings were treated with a Hoagland solution containing 250 mM NaCl for 2, 4, or 6 h, respectively.

In the low-temperature treatment, the banana seedlings were put in an incubator at 28, 15, 10, 7, or 5°C for 12 h (Xu et al., 2014).

Genetic Transformation and Characterization of Transgenic Plants

The open reading frame (ORF) of *MaPIP1;1* with an *Nco*I/*Spe*I restriction site was cloned into the pCAMBIA1302 vector under the control of a CaMV35S promoter, the primer pair for construction of recombinant vector was listed in **Supplementary Table 1**. The pCAMBIA1302-*MaPIP1;1*-GFP construct was introduced into Agrobacterium strain EHA105 and transformed

Agrobacterium. We transformed *MaPIP1;1* into Gongjiao (*Musa acuminata* L. AA group, cv. Mas) using our previously established *Agrobacterium*-mediated transformation method (Liu et al., 2017). The transformed hygromycin-resistant transgenic lines were detected by PCR amplification of the *GFP* gene. The primer pair for PCR verification was listed in **Supplementary Table 2**. The transgenic plants with positive results through PCR verification have been obtained and planted in the soil. Among them, two independent individuals with the strongest growth have been chosen through Southern blot analysis that further confirmed the integration of *MaPIP1;1* into line 1 (L1) and line 2 (L2) banana genomes. These two lines were randomly selected and planted in the field to obtain their sucking buds, and through their asexual reproduction of sucking buds, the third-generation tissue culture of more than 100 strains each of L1 and L2 was obtained by vegetative propagation for the next experiments.

Southern Blot Analyses

Digestion of genomic DNA in transgenic banana leaves was performed with *Hin*dIII restriction enzyme. The digested DNA was separated on a 0.8% agarose gel and transferred to a nylon membrane. Design of 35S promoter primers as probes for Southern blot amplification. The primer pair was listed in **Supplementary Table 2**. The probe was labeled using a random primer labeling system. Hybridization was carried out according to the instructions for use (Roche11745832910, DIG-High Prime DNA Labeling and Detection Starter Kit, Roche, Indianapolis, IN, United States).

Drought, Salt, and Cold Tolerance Assays of Transgenic and WT Plants

To test the drought, high salt, and low-temperature tolerance of transgenic plants compared with wild-type (WT) plants, banana seedlings were treated with drought, high salt, and cold stresses. In the drought treatment, banana seedlings (100 days old) were subjected to water control for 10 and 15 days; after 15 days of drought stress, they recovered for 10 days. Banana seedlings (100 days old) used for salt treatment were irrigated with 250 mM NaCl for 13 days and then recovered for 10 days. In the cold treatment, banana seedlings (100 days old) were placed in an 8°C incubator for 5 days and then recovered for 11 days.

Quantification of IL, MDA, and H_2O_2 Contents

The measurement method of ion leakage (IL) is as follows: strips cut from banana leaves were placed in distilled water (15 mL) at 25°C for 12 h, and conductivity (C1) was measured using a conductivity meter (DDBJ-350; INESA Scientific Instrument Co., Shanghai, China). Samples were transferred to boiling water for 30 min. When the sample cooled, it was used to test the conductivity (C2). IL was calculated as follows: IL (%) = C1/C2 × 100. The content of malondialdehyde (MDA) was determined by thiobarbituric acid colorimetry (Heath and Packer, 1968). According to the instructions, a test kit (Nanjing Jiancheng Institute of Biological Engineering, Nanjing, A064) was used to measure the content of H_2O_2.

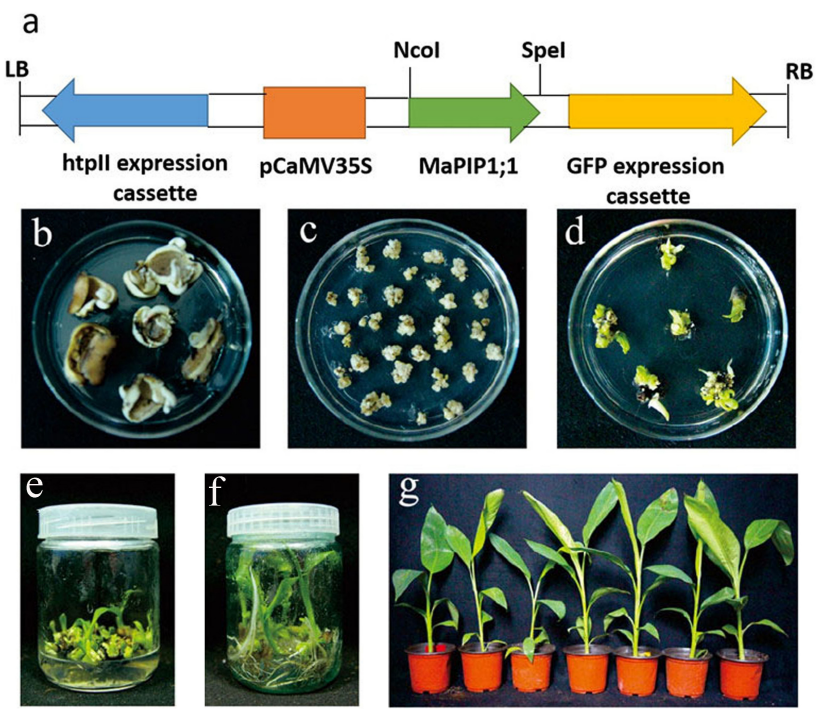

FIGURE 1 | Generation of *MaPIP1;1* overexpressing banana plants. **(a)** Schematic representation of T-DNA region used to generate transgenic plants. **(b)** Slices of the floral apex on differentiation medium. **(c)** Callus regenerated from slices. **(d)** Conversion of callus into shoots on shooting medium. **(e)** Generation of multiple shoots of putative transgenic lines. **(f)** Rooting of different transgenic lines on rooting medium. **(g)** Hardening of rooted transgenic lines.

Measurement of Soluble Sugar, Chlorophyll, Proline, GA, and ABA

The phenol reaction method was used to measure the soluble sugar content in the leaves. Banana leaves were placed in boiling water. After cooling, 9% phenol and concentrated sulfuric acid were added to the extract. The mixed solution was incubated at 25°C for 30 min, and the water extract was measured at a wavelength of 485 nm.

A chlorophyll analyzer (SPAD-502Plus, Konica Minolta, Tokyo, Japan) was used to measure the chlorophyll content. Using an ABA analysis kit (CSBE09159Pl, Cusabio, Wuhan Huamei Biotechnology Co., Ltd., Wuhan, China), we determined the ABA content according to the instructions. The proline content was determined using a PRO measurement kit (BC0290, Solarbio, Beijing, China). The gibberellin content was determined using a GA measurement kit (CK-E91022, Jinkelong, Beijing, China).

Measurement of Na^+ and K^+ Contents

Banana leaves were incubated at 105°C for 8 min and then heated to 80°C for 48 h, after which 50 mg of dried leaves was dissolved in nitric acid (6 mL) and 30% H_2O_2 (2 mL), followed by heating at 180°C for 15 min. After digestion, dilution was performed with 50 mL ultrapure water, and atomic absorption spectrometry (Analyst400, PerkinElmer, Waltham, MA, United States) was used to determine the content.

Quantitative PCR

SYBR®Premix Ex real-time qRT-PCR was used to test the expression level of *MaPIP1;1* in banana leaves after various treatments, as well as the ABA biosynthesis and biosynthesis in wild and transgenic lines under drought, high salt, and low-temperature conditions. The primer pair for qRT-PCR, was listed in **Supplementary Table 3** and the sequences were in **Supplementary Figure 4**. To respond to gene expression and determine the expression of genes screened by yeast one-hybrid under high salt and low-temperature conditions, use the Stratagene Mx3000P (Stratagene, La Jolla, CA, United States) instrument with Taq™ (TaKaRa Bio, Shiga, Japan) Reagents. To better amplify the target gene and reference gene, a series of diluted primers and templates are designed to obtain the best concentration of primers and templates. The primer pair was shown in **Supplementary Table 5**. The amplification efficiency of primers is between 0.89 and 1.12. MaActin1 was used as an internal control to normalize the expression level of target genes. Use $2^{-\Delta\Delta Ct}$ to evaluate the expression level of the tested gene.

cDNA Library Construction and Y1H Library Screening

The plant RNA kit (TIANGEN Biotech, Beijing, China) was used to extract total RNA from the high-salt and low-temperature treated (Xu et al., 2014) leaves of BX banana, and then the Matchmaker Gold Yeast OneHybrid Library Screening System Kit (Clontech, Mountain View, CA, United States) was used.

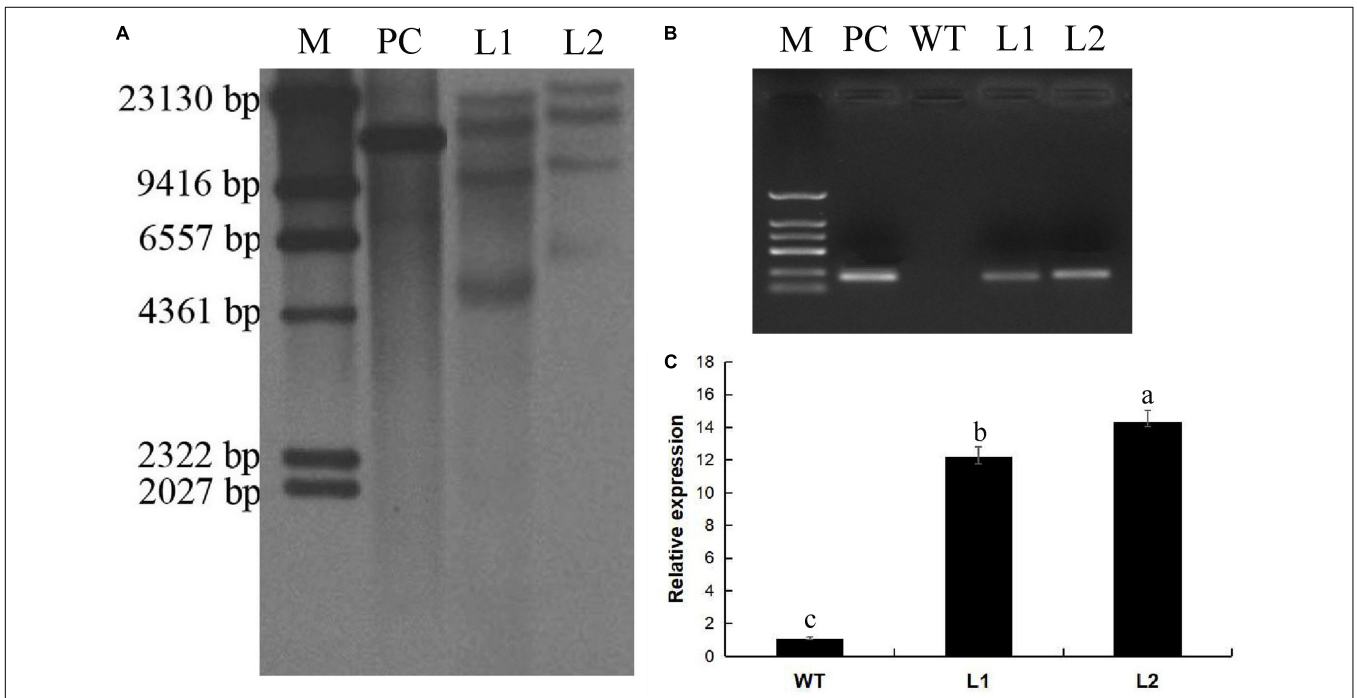

FIGURE 2 | Characterization of the transgenic lines. **(A)** Integration of *MaPIP1;1* transgene in Line 1 (L1) and Line 2 (L2) by Southern blot (35S promoter in the pcambia 1302 vector). **(B)** PCR amplification of the *GFP* gene in transgenic lines. **(C)** qRT-PCR analysis of the expression of *MaPIP1;1* in transgenic lines. Data are means ± SD of $n = 3$ biological replicates. Means denoted by the same letter do not significantly differ at $P < 0.05$ as determined by Duncan's multiple-range test. M, marker; PC, positive control.

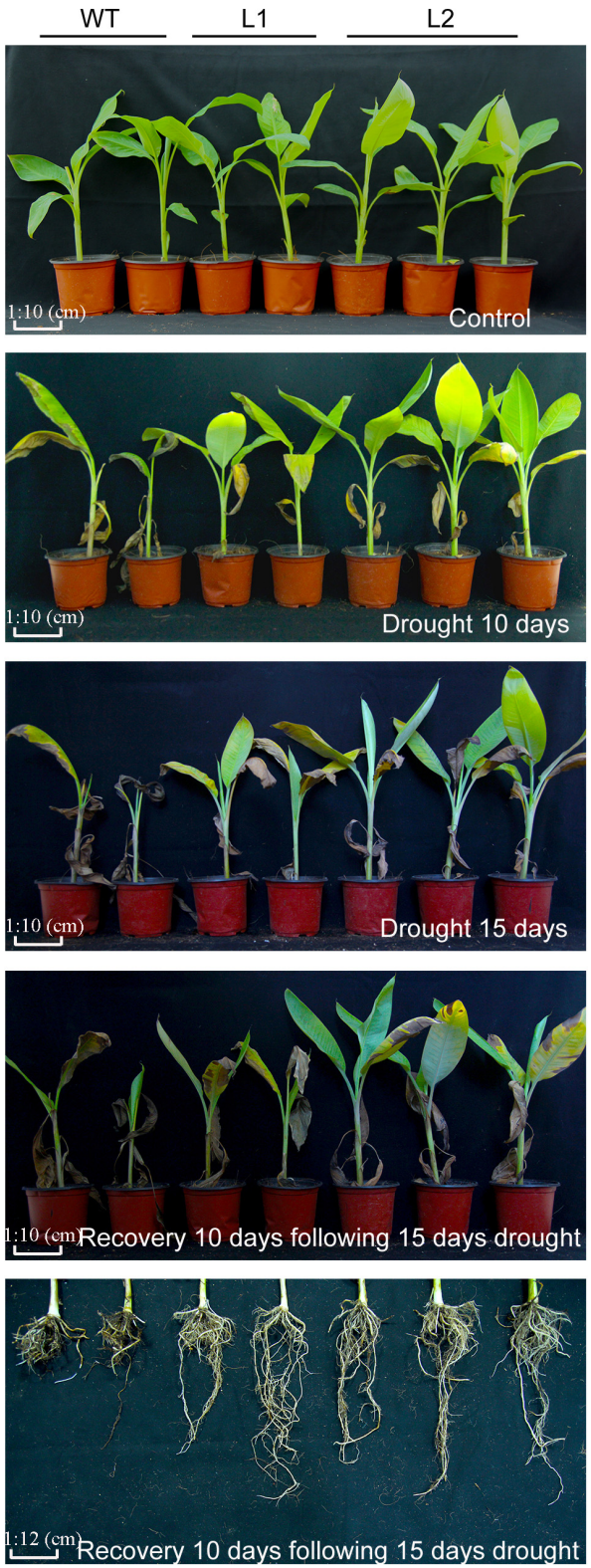

FIGURE 3 | Phenotype differences between WT and transgenic plants under normal, drought, and recovery conditions. Banana seedlings (100-day-old) were subjected to water withholding for 10 and 15 days, and recovery for 10 days following 15 days drought treatment, then the photos were taken.

Co-transform the bait and pGADT7-Rec prey vector with the cDNA library into Y1HGold (Clontech) cells, and then isolate and place them on SD/-Leu + AbA^{200} medium at 30°C for 3 days. PCR and sequence analysis further verified the selected positive colonies. The identified TF genes are annotated in the banana A genome database.

Gene Isolation and Sequence Analysis

After BLAST analysis, primers (**Supplementary Table 6**) and a SMART RACE cDNA Amplification Kit (Clontech) were used to amplify part of the coding sequence (CDS) to obtain a complete CDS. The full-length TF candidate sequence (**Supplementary Figure 7**) was confirmed and amplified with primers spanning the start and stop codons. These newly isolated TFs were named based on their homologs in Genbank and previously reported TFs in rice.

Analysis of Dual Luciferase (LUC) Activity

As described by Hellens et al. (2005), the *MaPIP1;1* promoter was cloned into the pGreenII 0800-REN-LUC vector. The primer pair was listed in **Supplementary Table 8**. The ORFs of the selected interaction genes were transformed into the pGreenII 62Sk vector and then into *Agrobacterium tumefaciens* GV3101 strain. The pGreen-*MaPIP1;1* promoter vector and the *A. tumefaciens* culture containing the expression vector constructed in pGreenII62Sk of each interaction gene were mixed in a 1:8 (v/v) proportion. After injection into the back of tobacco leaves and co-cultivation for 3 days, the luciferase and REN-LUC activities were analyzed using the double LUC reporter gene detection system (Promega, Madison, WI, United States). Three replicates were measured.

Statistical Analysis Methods

SPSS 10.0 software (SPSS Inc., Chicago, IL, United States) was used to conduct statistical analysis. The least significant test was used for the analysis of variance (ANOVA). The *t*-test was used to test the difference between the methods of analysis of variance. Each sample was composed of three replicates; $p < 0.05$ and $p < 0.01$ were considered to be statistically significant differences.

RESULTS

Generation of Banana Plants Overexpressing *MaPIP1;1*

To study the function of *MaPIP1;1* in bananas, *MaPIP1;1* was transformed into the pCAMBIA1302 expression vector (**Figure 1a**). The flowers of Gongjiao (*Musa acuminata* L. AA group, cv. Mas) were placed on the differentiation medium to induce the formation of banana callus (**Figure 1b**).

The callus was cut into 2-mm sections and infected with *A. tumefaciens* EHA105 transformed with the *MaPIP1;1*-pCAMBIA1302 expression vector. Murashige and Skoog (MS) medium induced bud growth (**Figure 1c**). It contained 8.9 μm/L benzylaminopurine (BA), 9.3 μm/L kinetin, 9.1 μm/L zeatin, 9.1 μm/L thiadazolam (TDZ), and 18 mg/L hygromycin

(HYG). About 300 pieces of co-culture were used. The explants were placed in a medium (containing 2 mg/L TDZ, 2 mg/L BA, and 18 mg/L HYG) to induce bud differentiation (**Figure 1d**). When the length of the shoot reached 3 cm (**Figure 1e**), the explants were transferred to the rooting medium (MS + 4 mg/L BA) to induce root growth. After 30 days of cultivation (**Figure 1f**), the plants with 8 cm roots were transplanted into coconut peat medium and grown for 100 days (**Figure 1g**). Finally, 251 hygromycin-resistant transgenic lines were obtained, of which 27 lines were further verified by PCR amplification of the *GFP* gene in the vector. Southern blot analysis and PCR detection verified the L1 and L2 lines. The result of the Southern blot showed that *MaPIP1;1* was successfully transferred to the bananas (**Figure 2A**). PCR results showed that the GFP gene was only present in the transgenic plants (**Figure 2B**). These two lines have been carried out vegetative reproduction to expand to the third generation. The expression of *MaPIP1;1* in L1 and L2 transgenic plants was significantly higher than that of wild type (**Figure 2C**). These results proved that *MaPIP1;1* was successfully overexpressed in bananas.

Overexpression of *MaPIP1;1* Enhanced Plant Tolerance to Drought Stress

To detect the performance of *MaPIP1;1* transgenic banana strains under drought stress, the wild type, and *MaPIP1;1*-high-expressing strains grown for 100 days were subjected to drought stress. After 10 or 15 days of water shortage, the leaves of most WT plants were curled and chlorotic, while most of the leaves of the *MaPIP1;1* transgenic lines remained green. After 15 days of drought treatment and re-watering for 10 days, the transgenic plants showed better growth vigor, with more green leaves and less damage to the root system (**Figure 3**). The above results indicate that *MaPIP1;1* improves the drought tolerance of transgenic plants.

Next, we examined the MDA level in the plant to study the physiological mechanism that *MaPIP1;1* confers in improving the drought tolerance of transgenic bananas. The MDA content in plants is a sign of damage mediated by reactive oxygen species (ROS) (Moore and Roberts, 1998). IL is an indicator of membrane damage. In addition, we measured the content of soluble sugar and proline, which are representative substances that can protect cells under stress conditions (El-Esawi et al., 2019; Xu et al., 2020b), and the contents of ABA (**Supplementary Table 9**). ABA is a hormone that responds to plant stress. Under normal growth conditions, compared with WT, transgenic plants had lower MDA and IL content and higher soluble sugar content. After drought stress treatment and recovery, the levels of MDA and IL in the transgenic plants were still lower. The contents of proline, chlorophyll, soluble sugar, and ABA in the transgenic plants were higher (**Figure 4**). Therefore, the overexpression of *MaPIP1;1* led to a reduction in membrane damage and the osmotic balance of plant cells and ABA levels under drought stress.

Overexpression of *MaPIP1;1* Increases Plant Tolerance to Salt Stress

To further examine whether the transgenic plants can improve salt tolerance, after 7 and 13 days of salt treatment, the transgenic lines showed better vigor, while their leaves were less wilted and yellowed. After 13 days of high-salt stress treatment and 10 days of recovery, the transgenic lines had more green leaves and

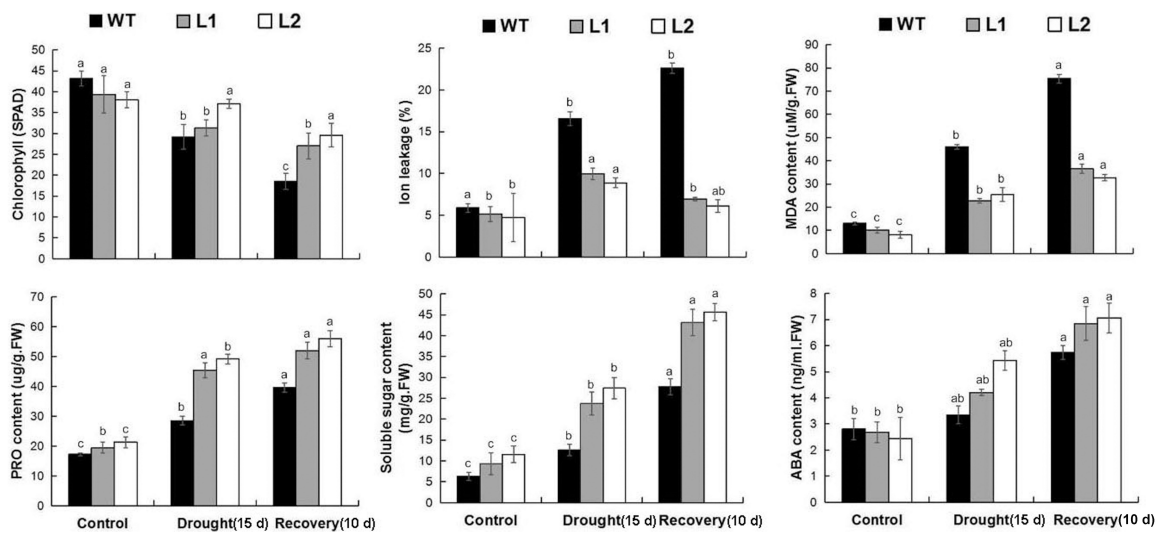

FIGURE 4 | Comparisons of physiological indices between WT and transgenic plants under normal, drought, and recovery conditions. Control means banana seedlings (100-day-old) grow normally. Drought means banana seedlings (100-day-old) were subjected to water withholding for 15 days, and recovery means banana seedlings (100-day-old) growth recovery for 10 days following 15 days drought treatment. Banana seedlings (100-day-old) were subjected to water withholding for 15 days and recovery for 10 days following 15 days drought treatment. The leaves were then sampled to perform physiological analyses. Data are means ± SD of $n = 3$ biological replicates. Means denoted by the same letter are not significantly different at $P < 0.05$ as determined by Duncan's multiple-range test.

less root damage than WT (**Figure 5**), indicating that *MaPIP1;1* overexpression can improve the salt stress tolerance of plants.

In terms of physiological response, the transgenic plants had lower IL and MDA contents, higher chlorophyll, proline, soluble sugar, and ABA contents under salt stress and recovery (**Supplementary Table 10**). In addition, under salt stress treatment and recovery conditions, *MaPIP1;1* overexpression reduced the contents of Na^+ and K^+ in the cells, while the K^+/Na^+ ratio increased during the recovery process (**Figure 6**). These results showed that *MaPIP1;1* reduces the membrane damage of transgenic bananas, improved ABA levels, and affected the contents of Na^+ and K^+ at the cellular level under salt stress.

Overexpression of *MaPIP1;1* Improves Cold Stress Tolerance

To test the cold resistance of the transgenic plants, bananas were treated with low temperatures. After 5 days of low temperature (8°C) treatment, WT leaves are more curled and withered than that of transgenic plants. After 11 days of recovery, the WT plants showed severe yellowing of leaves, while the transgenic lines showed greater vitality. In addition, under low temperature and recovery conditions (**Figure 7**), the transgenic line showed less root damage than the wild type. These results showed that *MaPIP1;1* improves the cold tolerance of transgenic bananas.

We further tested the physiological mechanism of *MaPIP1;1* improving plant cold tolerance under low-temperature conditions. Under normal growth conditions, compared with the control, the soluble sugar content of the transgenic bananas is higher, while the levels of MDA and IL are lower. After 5 days of low-temperature treatment and 11 days of the recovery period, the content of MDA and IL are lower in the transgenic plant. In the transgenic banana, the contents of chlorophyll, proline, soluble sugar, and ABA were higher than that in the wild type (**Figure 8** and **Supplementary Table 11**). Therefore, *MaPIP1;1* can reduce the ABA content and enhance osmotic balance in plant cells in transgenic plants.

Overexpression of *MaPIP1;1* Affects the Expression of ABA Biosynthetic and Responsive Genes

Abscisic acid plays a vital role in improving the drought, salt, and low-temperature resistance of plants. Under different stress treatments and recovery conditions, physiological research has found that *MaPIP1;1* can increase the level of ABA in plants. Therefore, we detected the expression of ABA biosynthetic and responsive genes in WT and transgenic plants by qRT-PCR (**Supplementary Table 12**). The ABA biosynthesis genes (*MaNCED-Ma04*, *MaNCED-Ma06*, and *MaAO*) and response genes (*MaSnRK2-11* and *MabZIP101*) in the overexpression plant showed higher expression under the drought, high salt, and low-temperature treatment (**Figure 9**). Other tested genes showed stress-specific overexpression induced by *MaPIP1;1*. Other tested genes showed that the expression of *MaSDR2* is induced under drought and NaCl treatment, high expression of *MabZIP10* under NaCl stress, and high expression of *MabZIP49* in transgenic lines under drought stress. These results further proved that

FIGURE 5 | Phenotype differences between WT and transgenic plants under normal, salt, and recovery conditions. Banana seedlings (100-day-old) were subjected to salt treatment (250 mM NaCl) for 7 and 13 days, and recovery for 10 days following 13 days salt treatment, then the photos were taken.

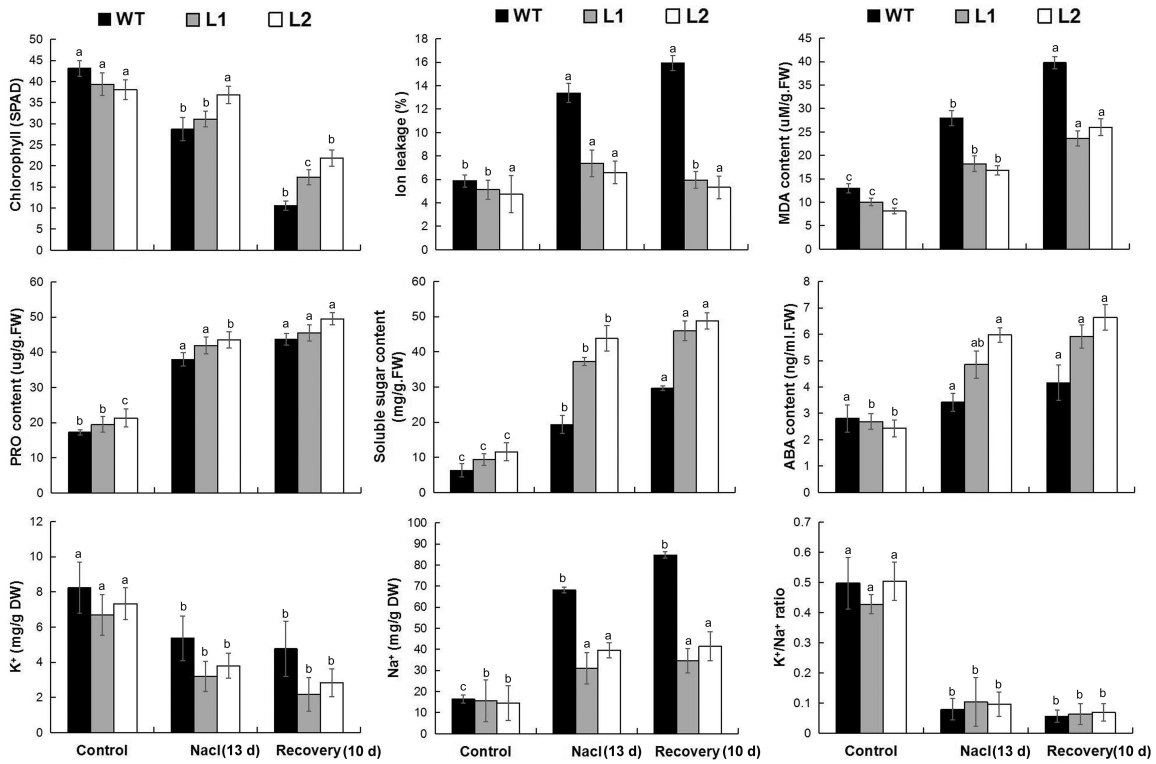

FIGURE 6 | Comparisons of physiological indices between WT and transgenic plants under normal, salt, and recovery conditions. Control means banana seedlings (100-day-old) grow normally. NaCl means banana seedlings (100-day-old) were subjected to salt treatment (250 mM NaCl) for 13 days, and recovery means banana seedlings (100-day-old) growth recovery for 10 days following 13-day salt treatment. Data are means ± SD of $n = 3$ biological replicates. Means denoted by the same letter are not significantly different at $P < 0.05$ as determined by Duncan's multiple-range test.

the overexpression of *MaPIP1;1* activated ABA biosynthesis and signal transduction.

Screening and Identifying the Transcription Factors Binding to *MaPIP1;1* Promoter in Yeast

To further analyze the mechanism of *MaPIP1;1* in improving plant resistance under high-salt and low-temperature stress, a pre-built *MaPIP1;1* promoter M-P2 bait vector (Xu et al., 2020a) in high-salt and low-temperature-treated banana cDNA one-hybrid libraries was used to screen interacting genes (**Supplementary Figure 13**).

The colonies were further flat coating on plates containing 3-amino-1,2,4-triazole (3AT). Under high salt stress, 23 colonies were screened and sequenced (**Supplementary Table 14**). Among them, there were one MaERF, one MaDREB, and one MaMYB. In subsequent verification using individual Y1H assays. In separate one-to-one Y1H analysis in subsequent verification, the yeast clones harboring pAbAi-MaPIP1;1 + pGADT7-MaERF14, pAbAi-MaPIP1;1 + pGADT7-MaDREB1G, and pAbAi-MaPIP1;1 + pGADT7-MaMYB1R1 grew normally on SD/-Leu + AbA^{200} selective medium. The result was the same with the library screening (**Figure 10A**). Under the cold treatment, a total of 25 interacting clones were screened, and the sequencing results are shown in **Supplementary Table 15**: one MaMYB, two MaERFs, and one MabZIP. In one-to-one Y1H analysis, pAbAi-MaPIP1;1 was with the pGADT7-MaMYB22/MaERF1/MaERF39/MabZIP53, normal growth on SD/-Leu + AbA^{200} selective medium, which was consistent with the results of hybrid library screening (**Figure 10A**).

Activation of the *MaPIP1;1* Promoter by MaMYB1R1, MaERF14/1/39, MaDREB1G, MabZIP53, and MaMYB22

In the early yeast one-hybrid screening, we obtained transcription factors that interacted under high-salt and low-temperature conditions: two MaMYBs, one MabZIP, one MaDREB1G, and three MaERFs bound to *MaPIP1;1 in vitro*.

The *MaPIP1;1* promoter M-P2 fragment was cloned into a reporter pGreen II 0800 vector termed pMaPIP1;1:LUC, and the full-length ORF for each transcription factor was cloned into the effector vector pGreenII 62Sk (**Figure 10B**).

Each gene and the *MaPIP1;1* promoter were co-transformed into GV3101 *Agrobacterium* and injected into tobacco leaves for expression. The results showed that all nine transcription factors screened combined with the *MaPIP1;1* promoter to increase LUC activity (**Figures 10C,D**).

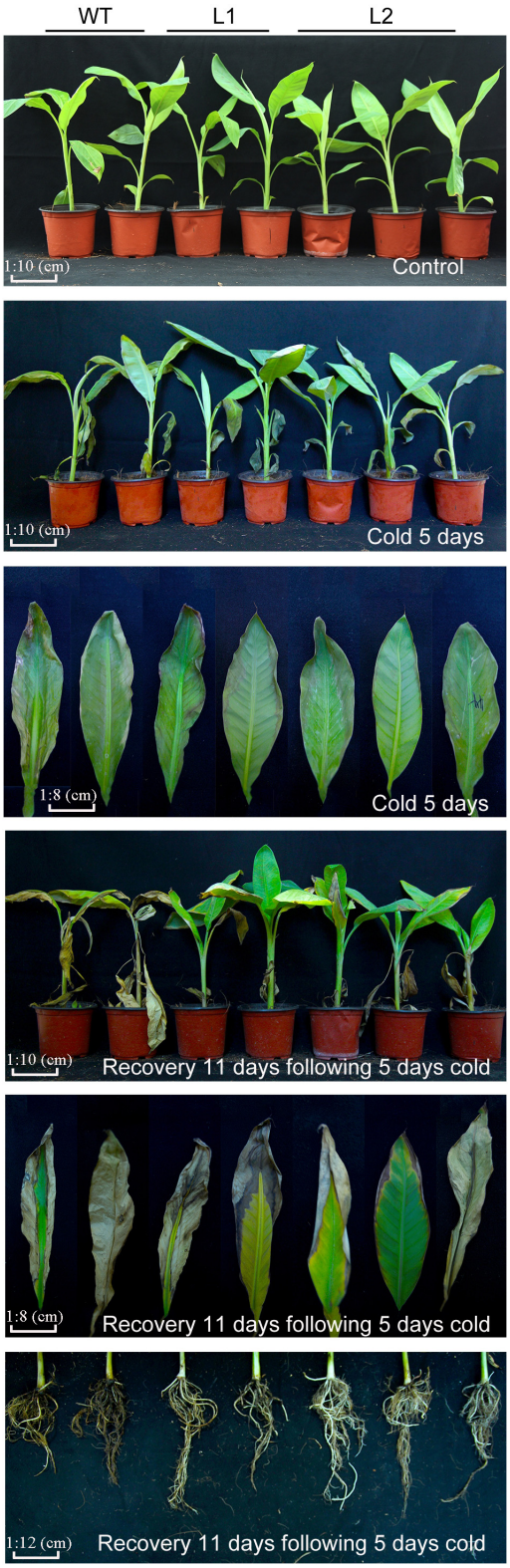

FIGURE 7 | Comparison of phenotypic differences between wild-type (WT) and transgenic lines under normal, cold, and recovery conditions. Banana seedlings (100-day-old) were subjected to cold treatment (8°C) for 5 days and recovery for 11 days after 5-day cold treatment. Then the photos were taken.

Expression of the *MaPIP1;1* Promoter-Binding Transcription Factors Under Salt and Cold Stress

The expression of the selected interaction genes *MaERFs*, *MaDREB*, *MaMYBs*, and *MabZIP* had been analyzed in the five-leaf, and one-heart banana leaves treated with high salt and low temperature. As can be seen from the results, under salt stress, the expressions of *MaERF14*, *MaDREB1G*, and *MaMYB1R1* were significantly induced. The expressions of *MaERF1/39*, *MaMYB22*, *MabZIP53* were induced under the cold stress (**Figure 11**). This is consistent with the functional description of these genes under adverse conditions.

DISCUSSION

Many abiotic stresses will affect the normal growth and development of crops, which will affect their yield and quality. Bananas are also susceptible to these abiotic stresses (van Asten et al., 2011; Sreedharan et al., 2013). Therefore, identifying genes that can improve the ability of plants to resist abiotic stresses and analyzing their gene functions and mechanisms are important ways to carry out more effective molecular breeding (Xu et al., 2020a). Molecular breeding is an important way to obtain resistant banana varieties, and genetic modification is an important means. Due to the long and cumbersome process of banana transgenics, there are few reports on banana transgenics. In addition, the research on the mechanism of transgenics to improve banana resistance is still insufficient. There are a few studies on genetically modified bananas in existing reports. *Mu-saPIP1;2* can improve the drought, salt, and cold tolerance of transgenic bananas (Sreedharan et al., 2013). Overexpression of *MusaPIP2;6* gene in banana can improve the salt tolerance of the plant (Sreedharan et al., 2015). In *MusaVND1* transgenic bananas, genes related to the biosynthetic pathway of lignin and cellulose were significantly induced to express (Negi et al., 2015). In the *AhcAPX* transgenic banana, the salt tolerance and drought resistance of the plant is improved by reducing the damage caused by ROS (Shekhar et al., 2019). In a previous study, we also obtained resistant transgenic banana plants. The *MaPIP2-7* transgenic banana has improved its drought, salt, and cold tolerance (Xu et al., 2020c). When transformed into *MaSIP2-1*, it can improve the drought and cold tolerance of genetically modified bananas (Xu et al., 2020b).

Water regulation and transport play a very important role in improving the exposure of crops to abiotic stresses such as salt, drought, and cold (Zhang et al., 2019). The AQPs of the plant can promote the transport of water in cell membranes and improve the ability of plants to resist abiotic stress. Early studies have shown that the PIPs genes in the AQP family of many plants play an active role in promoting water transport through the plasma membrane (Corey et al., 2016). At the same time, it participates in many abiotic stress responses (Maurel, 1997). Our previous research showed that AQPs could reduce the impact of external abiotic stress, the *MaPIP1;1* overexpression plants

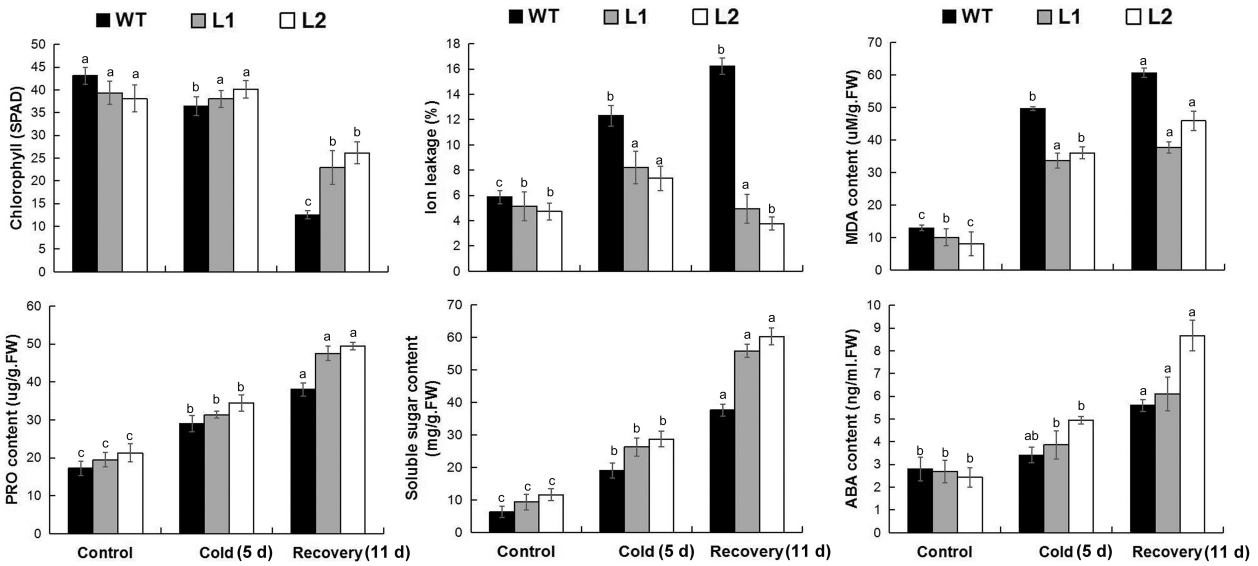

FIGURE 8 | Comparisons of physiological indices between WT and transgenic plants under normal, cold, and recovery conditions. Control means banana seedlings (100-day-old) grow normally. Cold means banana seedlings (100-day-old) were subjected to cold treatment (8°C) for 5 days, and recovery means banana seedlings (100-day-old) growth recovery for 11 days following 5-day cold treatment. The leaves were then sampled to perform physiological analyses. Data are means ± SD of $n = 3$ biological replicates. Means denoted by the same letter are not significantly different at $P < 0.05$ as determined by Duncan's multiple-range test.

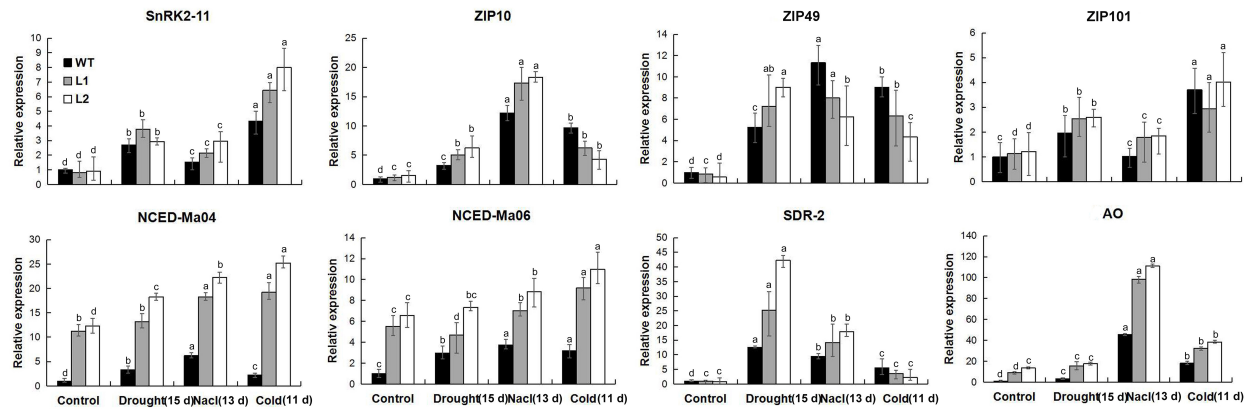

FIGURE 9 | Expression levels of ABA biosynthetic and responsive genes in WT and transgenic lines under normal, drought, cold, and salt conditions. Control means banana seedlings (100-day-old) grow normally. Drought, NaCl, and Cold means, respectively, banana seedlings (100-day-old) were subjected to water withholding for 15 days, salt (250 mM NaCl) for 13 days, and cold (8°C) for 5 days. Data are means ± SD of $n = 3$ biological replicates. Means denoted by the same letter are not significantly different at $P < 0.05$ as determined by Duncan's multiple-range test.

have stronger resistance under drought and high salt stresses (Xu et al., 2014). This study proved that *MaPIP1;1* could improve the drought resistance, salt tolerance, and low-temperature resistance of genetically modified bananas. In addition, the *MaPIP1;1* transgenic plants showed better growth vigor under the restored conditions (**Figures 3**, **5**, **7**). Therefore, *MaPIP1;1* can improve the stress resistance of plants under both stress and recovery conditions. In contrast, some AQPs exhibit negative functions in overexpressing plants. For example, under drought stress, *AtPIP1;b* leads to rapid wilting of overexpressed tobacco (Aharon et al., 2003). Plants overexpressing the *Arabidopsis* genes *AtPIP1;4* and *AtPIP2;5* can cause dehydration under drought stress (Jang et al., 2007). Therefore, different members of the AQP family show obvious functional differences.

Drought, salt, and cold stresses can disrupt the osmotic balance of plants. To cope with these stresses, there will be some accumulation of related substances in plants (Miao et al., 2020); proline and soluble sugar accumulation is extensive. The accumulation of these substances protects the cells by reducing the osmotic pressure of the cells in the plant (El-Esawi et al., 2019). In this research, compared with the wild type, *MaPIP1;1* transgenic bananas had higher proline and soluble sugar contents, indicating that it can improve the adaptability of transgenic plants under drought, salt, and cold

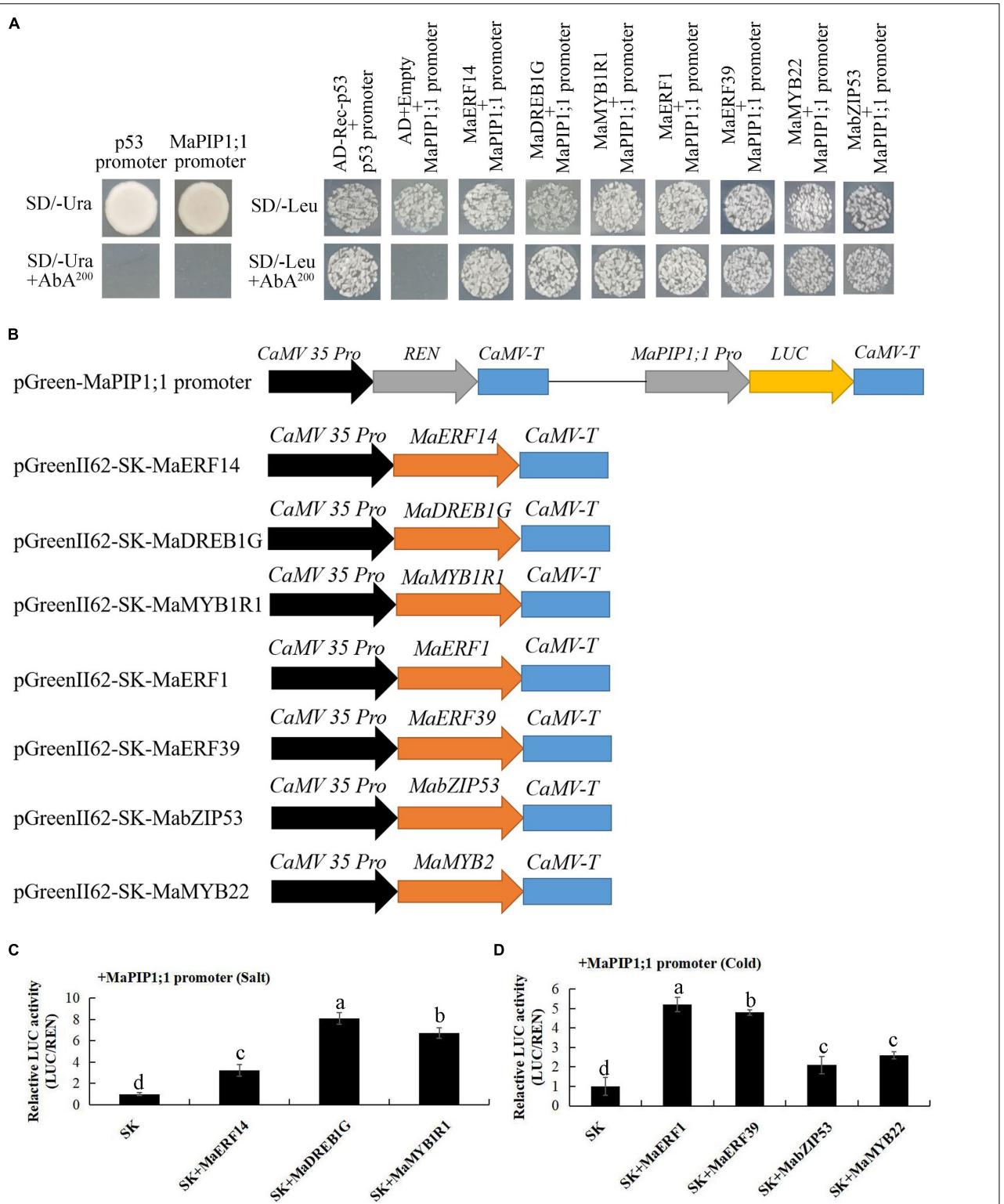

FIGURE 10 | Activation of the *MaPIP1;1* promoter by the transcription factors. **(A)** Physical interactions between MaERF14, MaDREB1G, MaMYB1R1, MaERF1/39, MabZIP53, MaMYB22, and the *MaPIP1;1* promoter according to yeast one-hybrid analysis. The autoactivation of the promoters was determined on SD/-Ura + AbA media, while the interaction between TFs and the promoter was tested on SD/-Leu + AbA media. **(B)** Schematics of transient expression vectors. **(C,D)** LUC activity resulting from the transient co-expression of the *MaPIP1;1* promoter and the transcription factors in *Agrobacterium tumefaciens* strains. There were three replicates. The data are presented as the means ± SDs. Means denoted by the same letter are not significantly different at $P < 0.05$ as determined by Duncan's multiple-range test.

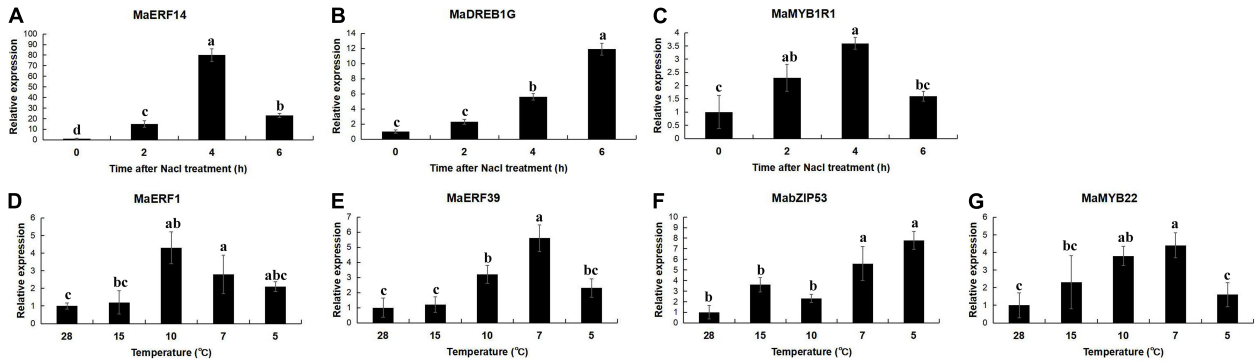

FIGURE 11 | Expression analysis of the binding transcription factors under the salt and cold stresses in the banana. Data are means ± SD of $n = 3$ biological replicates. Means denoted by the same letter are not significantly different at $P < 0.05$ as determined by Duncan's multiple-range test.

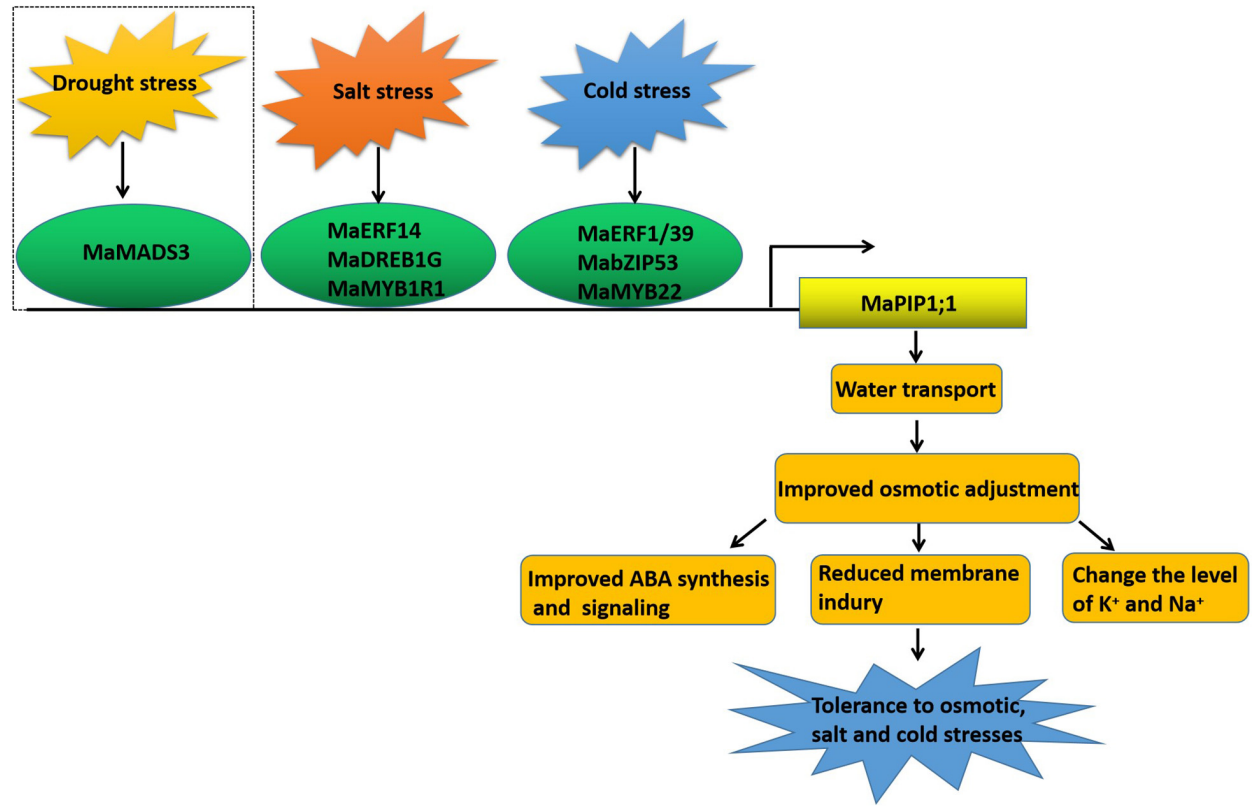

FIGURE 12 | *MaPIP1;1* combines with transcription factors under different abiotic conditions to improve the drought, salt, and low-temperature tolerance of transgenic bananas. The dotted line indicates the previous work.

stresses and recovery conditions. This is consistent with the situation where we previously expressed the AQP *MaPIP2-7* and *MaSIP2-1* in bananas (Xu et al., 2020a,b). Abiotic stress usually oxidizes DNA, lipids, and proteins, which causes the rapid accumulation of ROS (Mittler et al., 2004). MDA and IL are two important indicators for evaluating ROS-mediated cell damage under stress conditions (Sreedharan et al., 2013). The result showed that overexpression of *MaPIP1;1* reduced the accumulation of MDA and IL, indicating lipid peroxidation in the plants overexpressing *MaPIP1;1* under drought, salt, and cold stresses, and the membrane is less damaged (**Figures 4**, **6**, **8**). Consistent with our results, related reports showed that rice plants overexpressing *OsPIP2;7* had a lower IL content under low-temperature stress, and overexpression of *TaAQP7* reduced the content of MDA and IL under drought conditions (Zhou et al., 2012). Therefore, *MaPIP1;1* improves the stress resistance of overexpression plants by reducing membrane damage and oxidation under stress conditions. Na^+ harms cell metabolism

and certain proteins. A high Na^+ content will also reduce the photosynthesis of plants and cause oxidative damage (Mahajan and Tuteja, 2005). In this study, we detected the accumulation of K^+ and Na^+ in *MaPIP1;1* overexpression plants and WT plants, respectively. The figure shows that under salt stress, the K^+ and Na^+ in the cells of *MaPIP1;1* transgenic plants decreased, while the ratio of K^+/Na^+ increased. It is generally believed that a high K^+/Na^+ ratio in cells can improve the salt tolerance of plants (Ruiz-Lozano et al., 2012). *TaNIP* or *TaAQP8* will affect the distribution of Na^+ and K^+ contents in the transgenic plants under salt stress and increase their K^+/Na^+ ratio (Gao et al., 2010; Hu et al., 2012). Therefore, *MaPIP1;1* reduces the Na^+ and K^+ content of transgenic plants and increases the K^+/Na^+ ratio to improve the salt tolerance of plants.

Hormones are also involved in the process of plants responding to abiotic stress. The biosynthesis and signal transduction of ABA play a positive role in improving drought resistance of plants, high-salt, and low-temperature stress (Ben-Ari, 2012). Physiological research results showed that the expression of *MaPIP1;1* increased ABA levels in plants under stress treatment and recovery. Therefore, we tested the expression of genes related to ABA biosynthesis in control and transgenic plants under normal and stress conditions. Compared with the wild type, ABA biosynthesis genes (*MaNCED-Ma04*, *MaNCED-Ma06*, and *MaAO*) and response genes (*MabZIP49* and *MaSnRK2-11*) showed higher expression levels in the transgenic plants under drought, salt, and low-temperature conditions.

We further analyzed the molecular mechanism of *MaPIP1;1* in improving the resistance of genetically modified bananas. In a previous study, we screened out the transcription factor MaMADS3 that interacted with the yeast one-hybrid under drought stress (Xu et al., 2020a). The mechanism of the same gene response to stress under different adversity conditions might be regulated differently. In this study, we screened transcription factors that interacted with *MaPIP1;1* promoter under high-salt and low-temperature stresses. Under high-salt stress, we screened transcription factors MaERF14, MaDREB1G, and MaMYB1R1 to interact with its promoter, and under low-temperature stress conditions, we screened MaERF1/39, MabZIP53, and MaMYB22. At the same time, we found that under different stress conditions of high salt and low temperature, although the results included the ERF and MYB families, their family members were also different.

Numerous researches have indicated that transcription factors play active roles in improving plant resistance to various abiotic stresses. The ethylene-responsive factor (ERF) family encodes transcription regulators with multiple functions involved in plant development and physiological processes (Nakano et al., 2006). The apple ERF transcription factor MdERF38 can promote anthocyanin biosynthesis induced by drought stress (An et al., 2020). Li reported that the tomato ERF gene *SlERF84* could improve the adaptability of transgenic *Arabidopsis* to drought and high salt (Li et al., 2018). Another binding transcription factor is dehydration-responsive element-binding (DREB), which belongs to the AP2/ERF family. It is also widely involved in the process of improving plant abiotic stress ability. Overexpression of *ScDREB10* in the desert moss *Syntrichia caninervis* significantly improved the tolerance of transgenic *Arabidopsis* thaliana to osmotic and salt stresses in the seedling stage (Li X. S. et al., 2019). The v-myb avian myeloblastosis viral oncogene homolog transcription factor (MYB) participates in the growth and development of plants and responds to abiotic stress. *Arabidopsis AtMYB44* and *AtMYB2* can increase the resistance of transgenic plants (Jung et al., 2008). The survival rate of *GmMYB76* transgenic soybean after cold stress was much higher than that of the WT, showing that it can improve the ability of plants to resist low temperature (Liao et al., 2008). The basic region/leucine zipper (bZIP) family members can improve the drought resistance of transgenic plants (Tu et al., 2016a,b; Ma et al., 2018). The research of Tu et al. (2018) showed that the grape bZIP gene *VlbZIP30* could improve the drought resistance of transgenic *Arabidopsis* and grape seedlings.

In general, the interaction between transcription factors and the gene promoters depends on specific binding sequences, also named *cis*-acting elements. Studies have shown that ERF binds to the ethylene response element (ERE) with the core sequence of AGCCGCC (also known as the GCC-box), thereby conferring resistance to biological stress (Shinozaki and Yamaguchi-Shinozaki, 2000; Franco-Zorrilla et al., 2014). Sun's research shows that grape VaERF092 enhanced the tolerance to low-temperature stress by combining with the GCC-box in the *VaWRKY33* promoter (Sun et al., 2019). DREB can identify dehydration sensitive or the C repeat elements (DRE/CRT) A/GCCGAC core sequence, thus responding to abiotic stresses. Relevant studies have shown that MYB can improve the stress resistance of plants by combining with TAACCA elements in the promoters of downstream genes. MYB15 binds and interacts with the binding site of the *ICE1* gene promoter in *Arabidopsis* (Li J. L. et al., 2019). The studies have shown that certain bZIP proteins regulate their expression by binding to the ACGTG element in the target genes promoters (Ezer et al., 2017; Ma et al., 2018). Grape VlbZIP30 initiates gene expression by combining G-box *cis*-elements in the *VvPRXN1* and *VvNAC17* promoters (Tu et al., 2020).

In this study, we screened transcription factors that bind to *MaPIP1;1* under salt and cold stresses. In the promoter region of *MaPIP1;1*, the binding element sequences AGCCGCC, ACCGAC, TAACCA, and ACGTG are supposed to be recognized by ERF, DREB, MYB, and bZIP, respectively (**Supplementary Figure 13**). This result also provides evidence for the interaction between promoters and transcription factors. This is also the first report that AQP genes combine with these transcription factors to improve plant stress resistance. In summary, identifying these TFs lays a foundation for further elucidating the molecular regulation mechanism of *MaPIP1;1* transgenic bananas under abiotic stress.

In conclusion, here we have shown that *MaPIP1;1* improves the drought resistance, salt tolerance, and low-temperature tolerance of transgenic bananas by improving banana osmotic regulation and reducing membrane damage. In addition, the activation of *MaPIP1;1* by salt stress plays a certain role in reducing the contents of Na^+ and K^+ in plants and increasing

the ratio of K^+/Na^+, which is beneficial for improving the salt tolerance of plants. In addition, the transcription factors MaERFs, MaDREB, MaMYBs, and MabZIP interact with the *MaPIP1;1* promoter identified under high salt and low-temperature stress further reveals the mechanism of *MaPIP1;1* improving plant resistance (**Figure 12**). This research provides a theoretical basis for mining resistance-related genes and understanding their mechanism of action and has laid a good foundation for resistance breeding.

DATA AVAILABILITY STATEMENT

The original contributions presented in the study are included in the article/**Supplementary Material**, further inquiries can be directed to the corresponding authors.

AUTHOR CONTRIBUTIONS

YX, BX, and ZJ were conceived and designed the experiments. YX and SS were performed the experiments, analyzed the data, and wrote the article. CJ and WH were prepared the figures and tables. YX and JL were contributed reagents, materials, and analysis tools and reviewed drafts of the article. All authors contributed to the article and approved the submitted version.

FUNDING

This work was sponsored by the National Key R&D Program of China (2019YFD1000200), the Natural Science Foundation of Hainan Province (2019CXTD412), the Central Public-interest Scientific Institution Basal Research Fund for Chinese Academy of Tropical Agricultural Sciences (1630092020002 and 1630052020006), the China Agriculture Research System of MOF and MARA (CARS-31-03), and the National Natural Science Foundation of China (31501371).

SUPPLEMENTARY MATERIAL

The Supplementary Material for this article can be found online at: https://www.frontiersin.org/articles/10.3389/fpls.2021.699230/full#supplementary-material

REFERENCES

Aharon, R., Shahak, Y., Wininger, S., Bendov, R., Kapulnik, Y., and Galili, G. (2003). Overexpression of a plasma membrane in transgenic tobacco improves plant vigor under favorable growth conditions but not under drought or salt stress. *Plant Cell* 15, 439–447. doi: 10.1371/journal.pone.0123870

An, J. P., Zhang, X. W., Bi, S. Q., You, C. X., Wang, X. F., and Hao, Y. J. (2020). The ERF transcription factor MdERF38 promotes drought stress-induced anthocyanin biosynthesis in apple. *Plant J.* 101, 573–589. doi: 10.1111/tpj.14555

Ben-Ari, G. (2012). The ABA signal transduction mechanism in commercial crops: learning from Arabidopsis. *Plant Cell Rep.* 31, 1357–1369. doi: 10.1007/s00299-012-1292-2

Blumwald, E. (2000). Sodium transport and salt tolerance in plants. *Curr. Opin. Cell Biol.* 12, 431–434. doi: 10.1016/s0955-0674(00)00112-5

Bray, E. A. (1993). Molecular responses to water deficit. *Plant Physiol.* 103, 1035–1040. doi: 10.1104/pp.103.4.1035

Chang, W., Liu, X., Zhu, J., Fan, W., and Zhang, Z. (2016). An aquaporin gene from halophyte *Sesuvium portulacastrum*, SpAQP1, increases salt tolerance in transgenic tobacco. *Plant Cell Rep.* 35, 385–395. doi: 10.1007/s00299-015-1891-9

Chaumont, F., Barrieu, F., Wojcik, E., Chrispeels, M. J., and Jung, R. (2001). Aquaporins constitute a large and highly divergent protein family in maize. *Plant Physiol.* 125, 1206–1215. doi: 10.1104/pp.125.3.1206

Cheeseman, J. M. (1988). Mechanisms of salinity tolerance in plants. *Plant Physiol.* 87, 547–550. doi: 10.1104/pp.87.3.547

Corey, L., Lesk, C., Rowhani, P., and Ramankutty, N. (2016). Influence of extreme weather disasters on global crop production. *Nature* 529, 84–87. doi: 10.1038/nature16467

El-Esawi, M. A., Al-Ghamdi, A. A., Ali, H. M., and Ahmad, M. (2019). Overexpression of AtWRKY30 transcription factor enhances heat and drought stress tolerance in wheat (*Triticum aestivum* L.). *Genes* 10:163. doi: 10.3390/genes10020163

Ezer, D., Shepherd, S. J. K., Brestovitsky, A., Dickinson, P., Cortijo, S., Charoensawan, V., et al. (2017). The G-Box transcriptional regulatory code in Arabidopsis. *Plant Physiol.* 175, 628–640. doi: 10.1104/pp.17.01086

Feng, Z. J., Liu, N., Zhang, G. W., Niu, F. G., Xu, S. C., and Gong, Y. M. (2019). Investigation of the AQP family in soybean and the promoter activity of TIP2;6 in heat stress and hormone responses. *Int. J. Mol. Sci.* 20:262. doi: 10.3390/ijms20020262

Feng, Z. J., Xu, S. C., Liu, N., Zhang, G. W., Hu, Q. Z., Xu, Z. S., et al. (2018). Identification of the AQP members involved in abiotic stress responses from Arabidopsis. *Gene* 646, 64–73. doi: 10.1016/j.gene.2017.12.048

Franco-Zorrilla, J. M., López-Vidriero, I., Carrasco, J. L., Godoy, M., Vera, P., and Solano, R. (2014). DNA-binding specificities of plant transcription factors and their potential to define target genes. *Proc. Natl. Acad. Sci. U.S.A.* 6, 2367–2372. doi: 10.1073/pnas.1316278111

Gao, Z., He, X., Zhao, B., Zhou, C., Liang, Y., Ge, R., et al. (2010). Overexpressing a putative aquaporin gene from wheat, TaNIP, enhances salt tolerance in transgenic Arabidopsis. *Plant Cell Physiol.* 51, 767–775. doi: 10.1093/pcp/pcq036

Gu, X., Gao, Z., Yan, Y., Wang, X., Qiao, Y., and Chen, Y. (2017). RdreB1BI enhances drought tolerance by activating AQP-related genes in transgenic strawberry. *Plant Physiol. Biochem.* 119, 33–42. doi: 10.1016/j.plaphy.2017.08.013

Guo, L., Wang, Z. Y., Lin, H., Er Cui, W., Chen, J., Liu, M. H., et al. (2006). Expression and functional analysis of the rice plasma-membrane intrinsic protein gene family. *Cell Res.* 16, 277–286. doi: 10.1038/sj.cr.7310035

Heath, R. L., and Packer, L. (1968). Photoperoxidation in isolated chloroplasts. I. Kinetics and stoichiometry of fatty acid peroxidation. *Arch. Biochem. Biophys.* 125, 189–198. doi: 10.1016/0003-9861(68)90654-1

Hellens, R.P., Allan, A.C., Friel, E.N., Bolitho, K., Grafton, K., Templeton, M.D., et al. (2005). Transient expression vectors for functional genomics, quantification of promoter activity and RNA silencing in plants. *Plant Methods* 1:13.

Hu, W., Hou, X., Huang, C., Yan, Y., Tie, W., Ding, Z., et al. (2015). Genome-wide identification and expression analyses of aquaporin gene family during development and abiotic stress in banana. *Int. J. Mol. Sci.* 16, 19728–19751. doi: 10.3390/ijms160819728

Hu, W., Yuan, Q., Wang, Y., Cai, R., Deng, X., Wang, J., et al. (2012). Overexpression of a wheat aquaporin gene, TaAQP8, enhances salt stress tolerance in transgenic tobacco. *Plant Cell Physiol.* 53, 2127–2141. doi: 10.1093/pcp/pcs154

Huang, C., Zhou, S., Hu, W., Deng, X., Wei, S., Yang, G., et al. (2014). The wheat aquaporin gene TaAQP7 confers tolerance to cold stress in transgenic tobacco. *Z. Naturforsch. C. J. Biosci.* 69, 142–148. doi: 10.5560/znc.2013-0079

Hussain, A., Tanveer, R., Mustafa, G., Farooq, M., Amin, I., and Mansoor, S. (2019). Comparative phylogenetic analysis of aquaporins provides insight into the gene family expansion and evolution in plants and their role in drought tolerant and sus-ceptible chickpea cultivars. *Genomics* 112, 263–275. doi: 10.1016/j.ygeno.2019.02.005

Jang, J. Y., TLee, S. H., Rhee, J. Y., Chung, G. C., Ahn, S. J., and Kang, H. (2007). Transgenic Arabidopsis and tobacco plants overexpressing an aquaporin respond differently to various abiotic stresses. *Plant Mol. Biol.* 64, 621–632. doi: 10.1007/s11103-007-9181-8

Johanson, U., Karlsson, M., Johansson, I., Gustavsson, S., Sjövall, S., Fraysse, L., et al. (2001). The complete set of genes encoding major intrinsic proteins in Arabidopsis provides a framework for a new nomenclature for major intrinsic proteins in plants. *Plant Pyhsiol.* 126, 1358–1369. doi: 10.1104/pp.126.4.1358

Jung, C., Seo, J. S., Han, S. W., Koo Y. J., Kim, C. H., Song, S. I., et al. (2008). Overexpression of AtMYB44 enhances stomatal closure to confer abiotic stress tolerance in transgenic Arabidopsis. *J. Plant Physiol.* 146, 623–635.

Kapilan, R., Maryam Vaziri, R., and Zwiazek, J. J. (2018). Regulation of aquaporins in plants under stress. *Biol. Res.* 51:4.

Li, J. L., Han, G., Sun, C., and Sui, N. (2019). Research advances of MYB transcription factors in plant stress resistance and breeding. *Plant Signal. Behav.* 8:e1613131.

Li, W., Zhang, D., Zhu, G., Mi, X., and Guo, W. (2019). Combining genome-wide and transcriptome-wide analyses reveal the evolutionary conservation and functional diversity of aquaporins in cotton. *BMC Genomics* 20:538. doi: 10.1186/s12864-019-5928-2

Li, X. S., Liang, Y. Q., Gao, B., Mijiti, M., Bozorov, T. A., Yang, H. L., et al. (2019). ScDREB10, an A-5c type of DREB gene of the desert moss Syntrichia caninervis, confers osmotic and salt tolerances to Arabidopsis. *Genes* 10:146. doi: 10.3390/genes10020146

Li, Z. J., Tian, Y. S., Xu, J., Fu, X. Y., Gao, J. J., Wang, B., et al. (2018). A tomato ERF transcription factor, SlERF84, confers enhanced tolerance to drought and salt stress but negatively regulates immunity against *Pseudomonas syringae* pv. Tomato DC3000. *Plant Physiol. Biochem.* 132, 683–695. doi: 10.1016/j.plaphy.2018.08.022

Lian, H. L., Yu, X., Ye, Q., Ding, X. D., Kitagawa, Y., Kwak, S., et al. (2004). The role of aquaporin RWC3 in drought avoidance in rice. *Plant Cell Physiol.* 45, 481–489. doi: 10.1093/pcp/pch058

Liao, Y., Zou, H. F., Wang, H. W., Zhang, W. K., Ma, B., Zhang, J. S., et al. (2008). Soybean GmMYB76, GmMYB92, and GmMYB177 genes confer stress tolerance in transgenic Arabidopsis plants. *J. Cell Res.* 18, 1047–1060. doi: 10.1038/cr.2008.280

Liu, J., Gao, P., Sun, X., Zhang, J., Sun, P., Wang, J., et al. (2017). Efficient regeneration and genetic transformation platform applicable to five Musa varieties. *Electron. J. Biotechnol.* 25, 33–38. doi: 10.1016/j.ejbt.2016.11.002

Ma, H., Liu, C., Li, Z. X., Ran, Q., Xie, G., Wang, B., et al. (2018). ZmbZIP4 contributes to stress resistance in maize by regulating ABA synthesis and root development. *Plant Physiol.* 178, 753–770. doi: 10.1104/pp.18.00436

Madrid-Espinoza, J., Brunel-Saldias, N., Guerra, F. P., Gutiérrez, A., and Pozo, A. D. (2018). Genome-Wide identification and transcriptional regulation of aquaporin genes in bread wheat (*Triticum aestivum* L.) under water stress. *Genes* 9:497. doi: 10.3390/genes9100497

Mahajan, S., and Tuteja, N. (2005). Cold, salinity and drought stresses: an overview. *Arch. Biochem. Biophys.* 444, 139–158. doi: 10.1016/j.abb.2005.10.018

Maurel, C. (1997). Aquaporins and water permeability of plant membranes. *Annu. Rev. Plant Physiol. Plant Mol. Biol.* 48, 399–429. doi: 10.1146/annurev.arplant.48.1.399

Miao, H. X., Sun, P. G., Liu, Q., Liu, J. H., Jia, C. H., Zhao, D. F., et al. (2020). Molecular identification of the key starch branching enzyme-encoding gene SBE2.3 and its interacting transcription factors in banana fruits. *Hortic. Res.* 7:101.

Mittler, R., Vanderauwera, S., Gollery, M., and Van, B. F. (2004). Reactive oxygen gene network of plants. *Trends Plant Sci.* 9, 490–498. doi: 10.1016/j.tplants.2004.08.009

Moore, K., and Roberts, J. L. (1998). Measurement of lipid peroxidation. *Free Radic. Res.* 28, 659–671.

Nakano, T., Suzuki, K., Fujimura, T., and Shinshi, H. (2006). Genome-wide analysis of the ERF gene family in Arabidopsis and rice. *Plant Physiol.* 140, 411–432. doi: 10.1104/pp.105.073783

Negi, S., Tak, H., and Ganapathi, T. R. (2015). Cloning and functional characterization of MusaVND1 using transgenic banana plants. *Transgecni Res.* 24, 571–585. doi: 10.1007/s11248-014-9860-6

Peng, Y., Lin, W., Cai, W., and Arora, R. (2007). Overexpression of a Panax ginseng tonoplast aquaporin alters salt tolerance, drought tolerance and cold acclimation ability in transgenic Arabidopsis plants. *Planta* 226, 729–740. doi: 10.1007/s00425-007-0520-4

Reuscher, S., Akiyama, M., Mori, C., Aoki, K., Shibata, D., and Shiratake, K. (2013). Genome-wide identification and expression analysis of aquaporins in tomato. *PLoS One* 8:e79052. doi: 10.1371/journal.pone.0079052

Ruiz-Lozano, J. M., Porcel, R., Azcón, C., and Aroca, R. (2012). Regulation by arbuscular mycorrhizae of the integrated physiological response to salinity in plants: new challenges in physiological and molecular studies. *J. Exp. Bot.* 63, 4033–4044. doi: 10.1093/jxb/ers126

Sade, N., Gebretsadik, M., Seligmann, R., Schwartz, A., Wallach, R., and Moshelion, M. (2010). The role of tobacco Aquaporin1 in improving water use efficiency, hydraulic conductivity, and yield production under salt stress. *Plant Physiol.* 152, 245–254. doi: 10.1104/pp.109.145854

Sakurai, J., Ishikawa, F., Yamaguchi, T., Uemura, M., and Maeshima, M. (2005). Identification of 33 rice aquaporin genes and analysis of their expression and function. *Plant Cell Physiol.* 46, 1568–1577. doi: 10.1093/pcp/pci172

Shekhar, S., Rustagi, A., Kumar, D., Yusuf, M. A., Sarin, N. B., and Lawrence, K. (2019). Groundnut AhcAPX conferred abiotic stress tolerance in transgenic banana through modulation of the ascorbate-glutathione pathway. *Physiol. Mol. Biol. Plants* 25, 1349–1366. doi: 10.1007/s12298-019-00704-1

Shinozaki, K., and Yamaguchi-Shinozaki, K. (2000). Molecular responses to dehydration and low temperature: differences and cross-talk between two stress signaling pathways. *Curr. Opin. Plant Biol.* 3, 217–223. doi: 10.1016/s1369-5266(00)00067-4

Sreedharan, S., Shekhawat, U. K. S., and Ganapathi, T. R. (2013). Transgenic banana plants overexpressing a native plasma membrane aquaporin MusaPIP1;2 display high tolerance levels to different abiotic stresses. *Plant Biotechnol. J.* 11, 942–952. doi: 10.1111/pbi.12086

Sreedharan, S., Shekhawat, U. S., and Ganapathi, T. R. (2015). Constitutive and stress-inducible overexpression of a native aquaporin gene (MusaPIP2;6) in transgenic banana plants signals its pivotal role in salt tolerance. *Plant Mol. Biol.* 88, 41–52. doi: 10.1007/s11103-015-0305-2

Sun, X. M., Zhang, L. L., Wong, D. C. J., Wang, Y., Zhu, Z., Xu, G., et al. (2019). The ethylene response factor VaERF092 from Amur grape regulates the transcription factor VaWRKY33, improving cold tolerance. *Plant J.* 99, 988–1002.

Tao, P., Zhong, X., Li, B., Wang, W., Yue, Z., Lei, J., et al. (2014). Genome-wide identification and characterization of aquaporin genes (AQPs) in Chinese cabbage (Brassica rapa ssp. pekinensis). *Mol. Genet. Genom.* 289, 1131–1145. doi: 10.1007/s00438-014-0874-9

Tu, M. X., Wang, X. H., Feng, T. Y., Sun, X., Wang, Y., Huang, L., et al. (2016a). Expression of a grape (Vitis vinifera) bZIP transcription factor, VIbZIP36, in Arabidopsis thaliana confers tolerance of drought stress during seed germination and seedling establishment. *Plant Sci.* 252, 311–323. doi: 10.1016/j.plantsci.2016.08.011

Tu, M. X., Wang, X. H., and Huang, L. (2016b). Expression of a grape bZIP transcription factor, VqbZIP39, in transgenic Arabidopsis thaliana confers tolerance of multiple abiotic stresses. *Plant Cell Tissue Organ. Cult.* 125, 537–551. doi: 10.1007/s11240-016-0969-6

Tu, M. X., Wang, X. H., Yin, W. C., Wang, Y., Li, Y., Zhang, G. et al. (2020). Grapevine VlbZIP30 improves drought resistance by directly activating VvNAC17 and promoting lignin biosynthesis through the regulation of three peroxidase genes. *Hortic. Res.* 7:150.

Tu, M. X., Wang, X. H., Zhu, Y. X., Wang, D., Zhang, X., Cui, Y., et al. (2018). VlbZIP30 of grapevine functions in dehydration tolerance via the abscisic acid core signaling pathway. *Hortic. Res.* 5:49.

van Asten, P. J. A., Fermont, A. M., and Taulya, G. (2011). Drought is a major yield loss factor for rainfed East African highland banana. *Agric. Water Manag.* 98, 541–552. doi: 10.1016/j.agwat.2010.10.005

Xu, Y., Hu, W., Liu, J., Zhang, J., Jia, C., Miao, H., et al. (2014). A banana aquaporin gene, MaPIP1;1, is involved in tolerance to drought and salt stresses. *BMC Plant Biol.* 14:59. doi: 10.1186/1471-2229-14-59

Xu, Y., Jin, Z., Xu, B., Li, Y., Wang, X., Wang, A., et al. (2020a). Identification of transcription factors interacting with a 1274 bp promoter of MaPIP1;1 which confers high-level gene expression and drought stress Inducibility in transgenic *Arabidopsis thaliana*. *BMC Plant Biol.* 20:278. doi: 10.1186/s12870-020-02472-7

Xu, Y., Li, J., Song, S., Liu, J., Hou, X., Li, Y., et al. (2020b). A novel aquaporin gene MaSIP2-1 confers tolerance to drought and cold stresses in transgenic banana. *Mol. Breeding* 40:62.

Xu, Y., Liu, J., Song, S., Hou, X., Jia, C., Li, J., et al. (2020c). An aquaporin gene MaPIP2-7 is involved in tolerance to drought, cold and salt stresses in transgenic banana (*Musa acuminata* L.). *Plant Physiol. Biochem.* 147, 66–76. doi: 10.1016/j.plaphy.2019.12.011

Zhang, S., Feng, M., Chen, W., Zhou, X., Lu, J., Wang, Y., et al. (2019). In rose, transcription factor PTM balances growth and drought survival via PIP2;1 aquaporin. *Nat. Plants* 5, 290–299. doi: 10.1038/s41477-019-0376-1

Zhou, S., Hu, W., Deng, X., Ma, Z., Chen, L., Huang, C., et al. (2012). Overexpression of the wheat aquaporin gene, TaAQP7, enhances drought tolerance in transgenic tobacco. *PLoS One* 7:e52439. doi: 10.1371/journal.pone.0052439

Zhu, D., Wu, Z., Cao, G., Li, J., Wei, J., Tsuge, T., et al. (2014). Translucent green, an ERF family transcription factor, controls water balance in Arabidopsis by activating the expression of aquaporin genes. *Mol. Plant* 7, 601–615. doi: 10.1093/mp/sst152

Conflict of Interest: The authors declare that the research was conducted in the absence of any commercial or financial relationships that could be construed as a potential conflict of interest.

Publisher's Note: All claims expressed in this article are solely those of the authors and do not necessarily represent those of their affiliated organizations, or those of the publisher, the editors and the reviewers. Any product that may be evaluated in this article, or claim that may be made by its manufacturer, is not guaranteed or endorsed by the publisher.

frontiers in Plant Science

ERRATUM
published: 06 October 2021
doi: 10.3389/fpls.2021.780544

Erratum: Overexpression of a Banana Aquaporin Gene *MaPIP1;1* Enhances Tolerance to Multiple Abiotic Stresses in Transgenic Banana and Analysis of Its Interacting Transcription Factors

*Frontiers Production Office**

Frontiers Media SA, Lausanne, Switzerland

Keywords: *MaPIP1*, tolerance, banana, interaction, transcription factor

An Erratum on:

Overexpression of a Banana Aquaporin Gene *MaPIP1;1* Enhances Tolerance to Multiple Abiotic Stresses in Transgenic Banana and Analysis of Its Interacting Transcription Factors
by Xu, Y., Liu, J., Jia, C., Hu, W., Song, S., Xu, B., and Jin, Z. (2021). Front. Plant Sci. 12:699230. doi: 10.3389/fpls.2021.699230

Due to a production error, there were errors in the affiliations in the originally published article. Instead of

"Yi Xu[1,2,3], Juhua Liu[4], Caihong Jia[4], Wei Hu[4], Shun Song[1,2,3]*, Biyu Xu[4]* and Zhiqiang Jin[4]*

[1]Key Laboratory of Genetic Improvement of Bananas, Haikou Experimental Station, Chinese Academy of Tropical Agricultural Sciences, Haikou, China

[2]Sanya Research Institute of Chinese Academy of Tropical Agricultural Sciences, Sanya, China

[3]Hainan Key Laboratory for Biosafety Monitoring and Molecular Breeding in Off-Season Reproduction Regions, Sanya, China

[4]Key Laboratory of Biology and Genetic Resources of Tropical Crops, Institute of Tropical Bioscience and Biotechnology, Chinese Academy of Tropical Agricultural Sciences, Haikou, China",

the affiliations should have been presented as

"Yi Xu[1,3,4], Juhua Liu[2], Caihong Jia[2], Wei Hu[2], Shun Song[1,3,4]*, Biyu Xu[2]* and Zhiqiang Jin[2]*

[1]Key Laboratory of Genetic Improvement of Bananas, Haikou Experimental Station, Chinese Academy of Tropical Agricultural Sciences, Haikou, China

[2]Key Laboratory of Biology and Genetic Resources of Tropical Crops, Institute of Tropical Bioscience and Biotechnology, Chinese Academy of Tropical Agricultural Sciences, Haikou, China

[3]Sanya Research Institute of Chinese Academy of Tropical Agricultural Sciences, Sanya, China

[4]Hainan Key Laboratory for Biosafety Monitoring and Molecular Breeding in Off-Season Reproduction Regions, Sanya, China".

The publisher apologizes for this mistake. The original article has been updated.

OPEN ACCESS

Approved by:
Frontiers Editorial Office, Frontiers Media SA, Switzerland

***Correspondence:**
Frontiers Production Office
production.office@frontiersin.org

Specialty section:
This article was submitted to Plant Physiology, a section of the journal Frontiers in Plant Science

Received: *21 September 2021*
Accepted: *21 September 2021*
Published: *06 October 2021*

Citation:
Frontiers Production Office (2021) Erratum: Overexpression of a Banana Aquaporin Gene MaPIP1;1 Enhances Tolerance to Multiple Abiotic Stresses in Transgenic Banana and Analysis of Its Interacting Transcription Factors. Front. Plant Sci. 12:780544. doi: 10.3389/fpls.2021.780544

frontiers in Plant Science

MINI REVIEW
published: 30 September 2021
doi: 10.3389/fpls.2021.757925

Extracellular Vesicles: Emerging Players in Plant Defense Against Pathogens

*Guosheng Liu[1,2], Guangren Kang[1,2], Shumei Wang[3], Yifan Huang[1,2] and Qiang Cai[1,2]**

[1]State Key Laboratory of Hybrid Rice, College of Life Science, Wuhan University, Wuhan, China, [2]Hubei Hongshan Laboratory, Wuhan, China, [3]Department of Microbiology and Plant Pathology, Center for Plant Cell Biology, Institute for Integrative Genome Biology, University of California, Riverside, Riverside, CA, United States

Communication between plants and interacting microorganisms requires functional molecule trafficking, which is essential for host defense and pathogen virulence. Extracellular vesicles (EVs) are single membrane-bound spheres that carry complex cargos, including lipids, proteins, and nucleic acids. They mediate cell-to-cell communication *via* the transfer of molecules between cells. Plant EVs have been isolated from many plant species and play a prominent role in immune system modulation and plant defense response. Recent studies have shown that plant EVs are emerging players in cross-kingdom regulation and contribute to plant immunity by mediating the trafficking of regulatory small RNA into pathogens, leading to the silencing of pathogen virulence-related genes. This review summarizes the current understanding of plant EV isolation technologies, the role of plant EVs in plant immunity, and the mechanism of plant EV biogenesis, as well as approaches for how these findings can be developed into innovative strategies for crop protection.

Keywords: extracellular vesicles, cell-to-cell communication, plant immunity, cross-kingdom RNA interference, endomembrane trafficking

OPEN ACCESS

Edited by:
Ruixi Li,
Southern University of Science and Technology, China

Reviewed by:
Caiji Gao,
South China Normal University, China
Yingnan Hou,
Shanghai Jiao Tong University, China

****Correspondence:***
Qiang Cai
qiang.cai@whu.edu.cn

Specialty section:
This article was submitted to Plant Physiology, a section of the journal Frontiers in Plant Science

Received: *13 August 2021*
Accepted: *07 September 2021*
Published: *30 September 2021*

Citation:
Liu G, Kang G, Wang S, Huang Y and Cai Q (2021) Extracellular Vesicles: Emerging Players in Plant Defense Against Pathogens. Front. Plant Sci. 12:757925. doi: 10.3389/fpls.2021.757925

INTRODUCTION

Numerous plant pathogens, including bacteria, fungi, and nematodes, are responsible for many plant diseases, which reduce the yield and quality of agricultural production worldwide every year (Fisher et al., 2012; Savary et al., 2019). Exploring the interaction between plants and pathogens is conducive to plant disease control and agricultural production. Plants and pathogens secrete multitudes of molecules into the extracellular environment for cross-border communication, which is crucial to plant defense and pathogen virulence (Delaunois et al., 2014; Toruno et al., 2016). Based on our current understanding, extracellular vesicles (EVs) represent a major way to achieve this communication (Cai et al., 2021).

EVs are single membrane-bound heterogeneous spheres that are released by cells into the extracellular space (Colombo et al., 2014). They contain a diverse variety of enclosed bioactive cargos, such as proteins, nucleic acids, and metabolites (Colombo et al., 2014). EVs are currently categorized as exosomes, microvesicles, and apoptosis-derived vesicles on the basis of their origins and sizes (van Niel et al., 2018). Exosomes, which have diameters ranging from 30 nm to 150 nm, are derived from multivesicular bodies (MVBs) after fusing with the plasma membrane to release their intraluminal vesicles (ILVs; Colombo et al., 2014). Microvesicles normally refer

to 150–1,000 nm vesicles, which are shed from the plasma membrane during cell stress (Heijnen et al., 1999; Colombo et al., 2014; van Niel et al., 2018). Apoptosis-derived vesicles, which are characterized by their large size range of 30–10,000 nm, result from cell apoptosis (Atkin-Smith et al., 2015).

In the 1980s, EVs were initially thought to be a disposal mechanism for waste removal from cells (Johnstone et al., 1987). However, decades of studies have shown that numerous active molecules are transported by EVs and are featured in various biological processes, including cellular communication, immune response, antigen presentation, and cancer cell migration (Colombo et al., 2014). The latest studies have indicated that plant-released EVs play a major role in transboundary communication between plants and pathogens (Cai et al., 2018b, 2019, 2021). However, owing to the limitations of EV isolation methods, the research on plant EVs is only beginning.

PLANT EVs

EVs widely exist in eukaryotes, and numerous studies have shown that in animals, EVs are heterogeneous groups that encompass diverse subclasses and perform different functions (Kowal et al., 2016; Jeppesen et al., 2019). In plants, EVs have been isolated and purified from apoplastic washing fluid (AWF) collected from leaves and seeds or from pollen germination media (Cai et al., 2021; **Table 1**). At least three different subtypes of EVs have been characterized in *Arabidopsis* by taking advantage of their markers: tetraspanin (TET) 8, penetration 1 (PEN1), and exocyst subunit Exo70 family protein (Exo70) E2 (Wang et al., 2010; Rutter and Innes, 2017; Cai et al., 2018b; **Figure 1**).

Animal TETs, such as CD9, CD81, and CD63, are highly enriched in the membranes of exosomes and therefore serve as exosome markers (Escola et al., 1998; Simpson et al., 2012; Andreu and Yanez-Mo, 2014; Kowal et al., 2016). TET8 and TET9 are plant homologs of animal TET proteins (Cai et al., 2018b). TET8 and TET9-positive vesicles partially colocalize with the MVB marker Rab5-like guanosine triphosphatase ARA6 (also known as RABF1) inside of cells, and TET8-positive EVs have been observed outside of cells (Cai et al., 2018b; He et al., 2021). Thus, TET8-positive EVs are considered as plant exosomes. Furthermore, evidence has shown that the expression of *TET8* can be induced by *Botrytis cinerea* infection, and TET8-positive vesicles have been observed to accumulate at *B. cinerea* infection sites (Cai et al., 2018b), showing that TET8-associated EVs are involved in response to pathogen attack.

PEN1 has been previously shown to mediate trafficking between the Golgi complex and the plasma membrane (Kwon et al., 2008). PEN1 is also present in EVs induced by bacterial pathogen infection or salicylic acid treatment (Rutter and Innes, 2017). The secretion of PEN1 is dependent on ADP ribosylation factor-GTP exchange factor GNOM (Nielsen et al., 2012), and PEN1 does not colocate with ARA6, indicating that the biogenic pathway of TET8-positive EVs is different from that of PEN1-positive EVs (He et al., 2021). Moreover, EVs isolated from transgenic plants co-express two fluorescence-tagged fusion proteins, TET8-GFP and mCherry-PEN1, and display two distinct GFP-labeled and mCherry-labeled EVs (He et al., 2021). These characteristics confirm that PEN1-positive EVs and TET8-positive EVs are two subtypes of EVs (He et al., 2021).

Exocyst-positive organelle (EXPO) is a novel organelle that is identified by using live cell imaging and immunogold labeling in plants (Wang et al., 2010; Ding et al., 2014). Although EXPO and autophagosomes are bilayer structures, they do not co-locate with each other except in vacuoles upon autophagic induction (Wang et al., 2010; Lin et al., 2015). EXPO has been observed to fuse with the plasma membrane and deliver Exo70E2-positive EVs into the extracellular space. The secretory pathway of Exo70E2 is independent of MVB pathways, and EXPO is unaffected by secretory and endocytosis inhibitors in protoplasts (Wang et al., 2010; Ding et al., 2014).

TECHNIQUES FOR PLANT EV ISOLATION

The isolation of plant EVs remains a challenge (Liu et al., 2020b). In contrast to animal EVs, which are isolated from biofluids, plant EVs are isolated from AWF (Colombo et al., 2014). Currently, a simple well-established infiltration–centrifugation method is widely used for plant AWF collection (Wang et al., 2005; Sanmartin et al., 2007; Hatsugai et al., 2009; O'Leary et al., 2014). The detached leaf protocol is the ideal method for collecting AWF before EV isolation (O'Leary et al., 2014; Madsen et al., 2016; Cai et al., 2018b; He et al., 2021). This protocol has the merit of the removal of the distinct proximal (petiole) parts of leaves. This approach could remove irrelevant RNAs in the phloem stream (Zhang et al., 2009; Liu and Chen, 2018). In addition, the leaves are supported and unlikely to be squeezed with each other during centrifugation (He et al., 2021).

Differential centrifugation is commonly used for EV isolation from plants (Rutter and Innes, 2017; Cai et al., 2018b; Liu et al., 2020b; He et al., 2021). In this method, dead cells, cell debris, and large vesicles are removed through low-velocity centrifugation at 2,000× *g* and 10,000× *g*, and the separation rate is then progressively increased to 100,000× *g* to pellet small plant EVs (Prado et al., 2014; Cai et al., 2018b; Liu et al., 2020b; He et al., 2021). However, the low centrifugal force of 40,000× *g* has also been used for the final pelleting of EVs derived from *Arabidopsis* and sunflower seeds and seedlings (Regente et al., 2009, 2017; Rutter and Innes, 2017). Notably, the separation efficiency for the isolation of TET8-positive EVs obtained by centrifugation at 100,000× *g* is much higher than that obtained by centrifugation at 40,000× *g* (He et al., 2021).

Given that plant EVs are heterogeneous populations of nanosized membrane vesicles, researchers have developed additional separation methods based on EV density and specific EV markers. Currently, the most common and practical methods for separating the subtypes of plant EVs are density

TABLE 1 | List of the protein markers, confirmed cargoes, isolation methods, and biological functions of various EVs isolated from plants.

Plant	EV marker	EV Cargo	Function	Isolation method	Method advantages	Method disadvantages	Ref.
Arabidopsis	TET8	sRNAs, RBPs	Transport sRNAs to *B. cinerea* to silence virulence genes	Differential centrifugation	Enable isolation from large volumes	Unable to separate different EVs	Cai et al., 2018b, He et al., 2021
				Density gradient centrifugation	Enable separate EV sub-types	Unable to separate EVs with similar density	
				Immunoaffinity capture	High purity, high selectivity	Require specific antibodies	
Arabidopsis	PEN1	PATL1, PATL2	Enriched in plant defense components	Differential centrifugation	Enable isolation from large volumes	Unable to separate different EVs	Rutter and Innes, 2017
				Density gradient centrifugation	Enable separate EV sub-types	Unable to separate EVs with similar density	
Sunflower	nd	PMR5, GDSL, Lectins	Antifungal activity, enriched in cell wall enzymes	Differential centrifugation	Enable isolation from large volumes	Unable to separate different EVs	Regente et al., 2017, de la Canal and Pinedo, 2018
Olive	Ole e1, Ole e11, Ole e12	PCBER, GADPH	Secreted during pollen germination and pollen tube growth	Differential centrifugation	Enable isolation from large volumes	Unable to separate different EVs	Prado et al., 2014
				Density gradient centrifugation	Enable separate EV sub-types	Unable to separate EVs with similar density	
N. benthamiana	nd	HSP70, AGO2	Release virus components	Differential centrifugation	Enable isolation from large volumes	Unable to separate different EVs	Movahed et al., 2019

AGO2, Argonaute 2; GADPH, glyceraldehyde 3-phosphate dehydrogenase; HSP70, heat shock 70 kDa protein; n.d., no date (reference materials); PATL1, PATELLIN 1; PATL2, PATELLIN 2; PEN1, Penetration 1; RBPs, RNA binding protein; PCBER, phenylcoumaran benzylic ether reductase PT1; PMR5, powdery mildew resistance protein 5; sRNA, small RNA; TET8, tetraspanin 8.

gradient centrifugation and immunoaffinity capture-based techniques (Rutter and Innes, 2017; He et al., 2021). In density gradient centrifugation, sucrose and iodixanol are used as the classical media (Kowal et al., 2016; Paolini et al., 2016; Rutter and Innes, 2017; He et al., 2021). Through separation by density gradient centrifugation, TET8-positive exosomes are enriched in the gradient fraction of approximately 1.12–1.19 g ml^{-1}, whereas PEN1-positive EVs are enriched in the gradient fraction of 1.029–1.056 g ml^{-1} (Rutter and Innes, 2017; He et al., 2021).

Although density gradient centrifugation can yield high-quality EVs, different EV types may have similar physical properties. Separating EVs by immunoaffinity with EV markers may be needed. Immunoaffinity can capture specific EV subtypes with high quality at a low cost and within a short period. The activity of captured EVs is preserved to a great extent, and the captured EVs can be directly used for downstream analysis after elution (Tauro et al., 2012; Li et al., 2019). Recently, He et al. developed an immunoaffinity capture method for plant EVs (He et al., 2021). In this method, agarose beads conjugated with TET8 antibodies can efficiently isolate TET8-positive EVs (He et al., 2021). By using this method, several RNA-binding proteins (RBPs), such as argonaute 1 (AGO1), annexin1, and RNA helicases (RH11 and RH37), have been identified in TET8-positive EVs (He et al., 2021).

EVs IN CROSS-KINGDOM RNA INTERFERENCE

sRNAs are short noncoding molecules that induce RNA interference (RNAi; Baulcombe, 2004). RNAi is a regulatory mechanism for gene expression that is conserved throughout the domain Eukarya. During microbial infection, host sRNA functions endogenously by regulating gene expression to balance plant immunity and growth (Katiyar-Agarwal and Jin, 2010). Emerging studies have shown that bidirectional sRNA trafficking between hosts and interacting microorganisms/pests silence target genes *in trans* in a mechanism referred to as cross-kingdom RNAi (Cai et al., 2018a; Huang et al., 2019). For example, *Arabidopsis* delivers small interfering RNAs (siRNAs), including phased secondary siRNAs, into interacting *B. cinerea* cells, inducing the silencing of fungal genes that are involved in vesicle trafficking pathways (Cai et al., 2018b). Cross-kingdom RNA trafficking from the host into the pathogen to induce the silencing of corresponding pathogenic genes has also been observed in other plant pathosystems, such as in the cotton—*Verticillium dahliae*, and wheat—*Fusarium graminearum* systems (Zhang et al., 2016; Jiao and Peng, 2018). Pathogens also transfer sRNAs to plant hosts as effectors to promote infection and plant defense (Cai et al., 2021). The trafficking of *B. cinerea* sRNA into *Arabidopsis* cells suppresses host immune

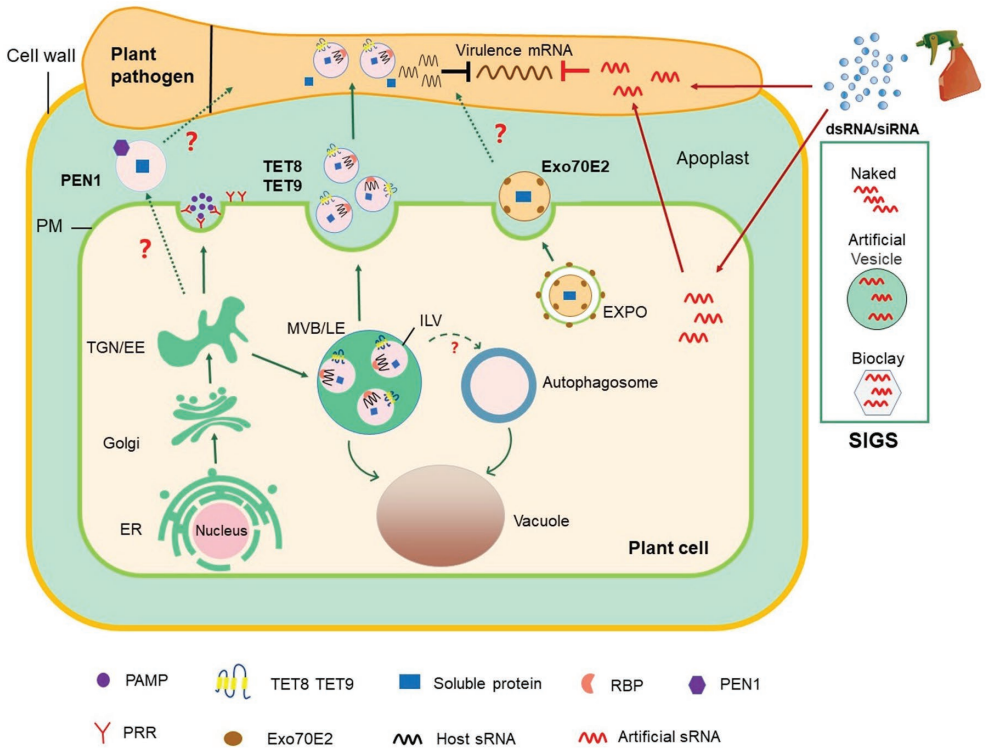

FIGURE 1 | Roles of EV-mediated RNAi in plant–microbial interactions and plant protection. The conventional secretion pathway delivers PAMPs to the extracellular space or transport surface PRRs to PM. In unconventional secretion pathway, MVBs release TET8/9-positive EVs, which contain defense proteins and host-derived sRNAs, into the extracellular space. TET8/9-positive EVs contain a variety of RBPs, including AGO1, RHs, and ANNs, which load sRNAs into EVs. PEN1-positive EVs are secreted into the extracellular space with an unknown mechanism (marked with ? in the Figure). EXPO is a novel bilayer membrane organelle that fuses with PM to produce another subtype of EVs. Whether PEN1-positive and EXPO-positive EVs contribute to cross-kingdom RNAi between plant and pathogens (marked with ? in the figure) is unknown. On the basis of the knowledge on cross-kingdom RNAi, the spray application of dsRNAs and sRNAs that target pathogen genes can potentially control plant diseases. In SIGS approaches, dsRNAs are applied exogenously or carried by nanocarriers, such as BioClay and artificial vesicles. Exogenous RNAs can either be directly internalized into fungal cells or indirectly *via* passage through plant cells before transport into fungal cells. dsRNA, double-stranded RNA; EE, early endosome; ER, endoplasmic reticulum; EVs, extracellular vesicles; EXPO, exocyst-positive organelle; MVB/LE, multivesicular body/late endosome; ILV, intraluminal vesicle; PAMP, pathogen-associated molecular pattern; PEN1, Penetration 1; PM, plasma membrane; PRR, pattern recognition receptor; RBPs, RNA binding protein; SIGS, spray-induced gene silencing; siRNA, small interfering RNA; sRNA, small RNA; TGN, *trans*-Golgi network.

genes by using the host RNAi machinery component AGO1 (Weiberg et al., 2013). Moreover, the translocated sRNAs of *Hyaloperonospora arabidopsidis* associate with the host *Arabidopsis* AGO1/RISC to regulate plant host defense genes (Dunker et al., 2020). *Puccinia striiformis* f. sp. *Tritici* (*Pst*), one of the most destructive pathogens of wheat (*Triticum aestivum* L.), produces the microRNA-like RNA 1 to silence the wheat *pathogenesis-related 2* gene, which impairs wheat defenses during wheat–Pst interactions (Wang et al., 2017).

Further studies have revealed that cross-boundary sRNA trafficking depends on EVs (Buck et al., 2014; Cai et al., 2018b, 2021; Hou et al., 2019). sRNA trafficking between cells *via* EVs has been studied in mammalian cells (Valadi et al., 2007; Colombo et al., 2014). In animal systems, the parasite nematode *Heligmosomoides polygyrus* delivers sRNAs *via* EVs into mouse gut epithelial cells to modulate host innate immunity (Buck et al., 2014). However, whether hosts use EVs to send sRNAs into interacting pathogen/parasite cells has long remained unclear. A recent study has revealed that more than 70% of the *Arabidopsis* sRNAs transported into *B. cinerea* cells are present in plant EVs, indicating that in plants, EV-mediated transport is one of the major pathways for the cross-kingdom trafficking of sRNA (Cai et al., 2018b). Furthermore, *Arabidopsis tet8/tet9* double mutants transfer less sRNAs into fungal cells and enhance susceptibility to *B. cinerea* challenge, suggesting that plant EVs contribute to plant immunity by cross-kingdom RNAi (Cai et al., 2018b). This finding was supported by the recent study where in *Arabidopsis*-derived secondary siRNAs were found in EVs and likely silenced target genes in *P. capsici* during natural infection (Hou et al., 2019). However, how sRNAs are selectively loaded into EVs during vesicle biogenesis is poorly understood. A recent study illustrated that plant TET8 positive-EVs contain a variety of RBPs, including AGO1, RHs, and ANNs (He et al., 2021). These RBPs bind to sRNAs to load sRNAs into plant EVs (He et al., 2021). Interestingly, AGO1, RH11, and RH37 selectively load sRNAs into EVs, whereas ANN1/2 bind to RNA nonspecifically, indicating that they contribute to stabilizing sRNAs in EVs (He et al., 2021).

Fungal and bacterial RNA cargoes in EVs have been shown to play a pivotal role in animal host cells by regulating gene

expression and immunity (Munhoz da Rocha et al., 2020). For example, the fatal human fungal pathogen *Cryptococcus gattii* secretes EVs for transferring RNAs to host cells as virulence factors (Bielska et al., 2018). In addition, sRNAs cargos have been detected in EVs derived from several bacterial pathogens, such as *Aggregatibacter actinomycetemcomitans*, *Porphyromonas gingivalis*, *Pseudomonas aeruginosa*, and *Treponema denticola* (Koeppen et al., 2016; Choi et al., 2017). These Gram-negative bacteria-derived EVs are released from the outer membranes and are also named as outer membrane vesicles (OMVs; Nahui Palomino et al., 2021). The bidirectional translocation of sRNAs has been observed in plant–pathogen interactions (Wang et al., 2016). However, studies on RNA in EVs derived from plant fungal and bacterial pathogens have not been reported. The fungal pathogen *B. cinerea* and the oomycete pathogen *H. arabidopsidis* have recently been shown to deliver sRNAs into plant host cells (Weiberg et al., 2013; Dunker et al., 2020). Further studies are needed to determine whether the eukaryotic plant pathogens that deliver RNA species into hosts require EVs.

BIOGENESIS AND SECRETION OF PLANT EVs

Exosomes are derived from MVB trafficking and finally fuse with the plasma membrane (Pegtel and Gould, 2019). The perimeter membrane of the late endosome buds inward to the endosome lumen, forming ILVs, which lead to the formation of multivesicular endosomes (van Niel et al., 2018; Mathieu et al., 2019). Therefore, they are also considered as MVBs. Two major mechanisms of ILV formation exist in animals: Endosomal Sorting Complex Required for Transport (ESCRT)-mediated pathway and ceramide-mediated pathway (van Niel et al., 2018; Mathieu et al., 2019). Mechanisms that drive the mobilization of secretory MVBs and fusion with the plasma membrane require the participation of Rab family proteins (Rab11, Rab35, and Rab27), and SNARE family proteins (vesicle-associated membrane protein 7 and YKT6 V-SNARE homolog; Hsu et al., 2010; Ostrowski et al., 2010; Kowal et al., 2014; Tian et al., 2020; Ferro et al., 2021). In fact, in animal cells, MVBs also fuse with autophagosomes and further form amphisomes following the release of EVs containing autophagy components (Klionsky et al., 2014; Jeppesen et al., 2019). However, the mechanism of the formation of plant EVs remains unclear. The fusion of MVBs with the plasma membrane during plant biotic stress responses or plant growth has been demonstrated (An et al., 2006a,b; Wang et al., 2011; Cai et al., 2018b). During the infection of barley (*Hordeum vulgare*) by powdery mildew fungus (*B. graminis* f. sp. *hordei*), multivesicular compartments fuse with the plasma membrane and then release paramural vesicles that are similar to exosomes and may participate in papilla deposition (An et al., 2006a,b). In lily and tobacco pollen tubes, vacuolar sorting receptors (VSRs) mediate the vacuolar transport of soluble cargoes *via* MVBs and localize to the plasma membrane, indicating that VSR proteins have an additional role in mediating protein transport to the plasma membrane (Wang et al., 2011). A recent study has demonstrated that sphingolipids in plant EVs mainly comprise pure glycol inositol phosphate ceramides (GIPCs; Liu et al., 2020a). Furthermore, the *Arabidopsis tet8* mutant has a low amount of cellular GIPCs and secretes few EVs, suggesting that GIPCs may play a part in the biogenesis of EVs (Liu et al., 2020a).

NOVEL EV- AND RNAi-BASED TOOLS FOR CROP PROTECTION

Host-induced gene silencing (HIGS) is an effective strategy for developing resistant varieties by expressing double-stranded RNAs (dsRNAs) targeting pathogen genes in plants to induce the silencing of essential pathogen genes (Nowara et al., 2010). For example, expressing a dsRNA targeting the *Fusarium verticillioides* gene *gus* enhances tobacco resistance to fungal pathogens (Tinoco et al., 2010). Silencing the *Magnaporthe oryzae* transcription factor *MoAP1* by HIGS in transgenic rice leads to improved blast disease resistance (Guo et al., 2019). HIGS has also been used to inhibit the growth of western corn rootworm (*D. virgifera* LeConte) in corn and rust fungi (*Puccinia triticina*) in wheat (Yin et al., 2011; Bolognesi et al., 2012; Panwar et al., 2013). This strategy also can effectively prevent and control root diseases that are difficult to control *via* traditional chemical control. An example of such a disease is cotton Verticillium wilt caused by *V. dahlia* (Wang et al., 2016). Recently, SmartStax Pro, a genetically modified organism (GMO) crop developed by Bayer on the basis of RNAi technologies against insect pests, has been approved by the US government (Rosa et al., 2018). This GMO can express dsRNA corresponding to rootworm *Snf7* messenger RNA (mRNA; Rosa et al., 2018).

However, HIGS has some disadvantages: (1) Transgenic expression is not always stable and is inhibited or silenced after generations; (2) uncertainty about government approvals and public concerns about GMOs; (3) currently, many plants cannot be genetically modified by transgenic technology. Recent studies have indicated that spraying dsRNAs or sRNAs that target crucial pathogen genes can provide efficient and sustainable protection to plants to solve the above problems (**Figure 1**). This new and innovative technology is called spray-induced gene silencing (SIGS), which has been applied to control numerous economically important plant pathogens (Wang et al., 2016; Cai et al., 2018a). For example, spraying the long noncoding dsRNA *CYP3*, which targets three fungal cytochrome P450 lanosterol C-14α-demethylases, inhibits the growth of *F. graminearum* on barley (Koch et al., 2016). Spraying dsRNA and sRNAs that target *B. cinerea Dicer-like 1* and *2* on the surfaces of fruits, vegetables, and flowers can effectively inhibit gray mold disease caused by *B. cinerea* (Wang et al., 2016). *H. arabidopsidis* is an obligate biotrophic oocyte pathogen that induces downy mildew in *Arabidopsis*. The application of exogenous sRNA or dsRNAs synthesized *in vitro* and targeting the conserved *cellulose synthase A3* gene of *H. arabidopsidis* impairs spore germination and hence prevents the infection of *Arabidopsis* (Bilir et al., 2019).

The success of SIGS for plant disease management is largely determined by RNA uptake efficiency, which varies among different

pathogens. Some eukaryotic microbes, including *B. cinerea*, *Rhizoctonia solani*, *Aspergillus niger*, and *V. dahliae*, could uptake environmental RNA efficiently, whereas RNA uptake is modest in *Trichoderma virens*, undetectable in *Colletotrichum gloeosporioides*, and limited in *P. infestans* (Qiao et al., 2021). The efficiency of SIGS application also depends on RNA stability in the environment. Many studies have shown that EVs can protect sRNAs from degradation in the environment and have high uptake efficiency by host cells (Colombo et al., 2014; Liu et al., 2020b). Liposomes, also called artificial vesicles, are spherical vesicles that are encased by a lipid bilayer with nontoxicity, low immunogenicity, and high biocompatibility (Tseng et al., 2009). Liposomes and lipid-based nanoparticles are the most advanced and potent delivery systems for RNA drugs, which can effectively deliver siRNAs to their targets, reducing total siRNA doses and thus attenuating their potential toxicity (Ickenstein and Garidel, 2019). For therapeutic applications in mammalian systems, EVs and artificial vesicles not only carry RNAs but also carry other beneficial molecules, such as celastrol and curcumin for anticancer therapy and gold nanoparticles for improved imaging (Aqil et al., 2016; Meng et al., 2020). Current studies in the field of plant–pathogen interaction have shown that plants use EVs to transport sRNAs into their fungal pathogens (Cai et al., 2018b). Given this new knowledge, incorporating RNAs into artificial vesicles/liposomes or nanoparticles will likely facilitate RNA delivery *via* SIGS approaches to protect RNAs from degradation or water rinsing (**Figure 1**). Indeed, dsRNA loaded on nanoparticles, such as nontoxic layered double hydroxide clay nanosheets (BioClay), can continuously protect plants against virus even after 30 days of spraying (Mitter et al., 2017). Thus, the use of EVs and nanoparticles as carriers of RNAi for crop protection is a promising field in the future.

CONCLUDING REMARKS AND FUTURE PERSPECTIVES

In the past few decades, EVs have been considered as effective carriers for intercellular communication in prokaryotes and eukaryotes due to their capability to transfer proteins, lipids, nucleic acids, and other biologically active substances, thus affecting a variety of the physiological and pathological functions of their receptor cells (Colombo et al., 2014). In recent years, many studies have revealed that EVs are crucial tools for communication between plants and pathogens and execute considerable functions in host immunity and pathogen virulence (Cai et al., 2021). Plant cells secrete EVs containing sRNAs into fungal cells to induce the silencing of fungal genes that are critical for pathogenicity (Cai et al., 2018b). Recent studies have shown that EVs from the cotton pathogen *Fusarium oxysporum* f. sp. *vasinfectum* induce a phytotoxic response in plants (Bleackley et al., 2019). In addition, OMVs derived from bacteria play a vital part in biofilm formation, virulence, and plant immune regulation during plant–bacterium interactions (Katsir and Bahar, 2017). However, reports on RNAs in EVs derived from plant pathogens or interacting microbes still not exist. Further studies need to be performed to determine whether plant pathogen EVs contain RNAs that are functional within host plant cells.

RNA interference is a conserved biological defense mechanism and is thus an effective method for controlling a variety of pests and pathogens (Majumdar et al., 2017; Zhang et al., 2017). sRNAs can move between interacting organisms, inducing gene silencing in each other, in a process called cross-kingdom RNAi (Cai et al., 2018a). HIGS by the transgenic expression of pathogen dsRNA is thus expected to be an important disease control method (Rosa et al., 2018). Given the disadvantages of transgenic approaches, sRNAs can be directly sprayed on host plants or postharvest products to silence target pathogenic genes in an approach known as SIGS (Cai et al., 2018a). Such an approach can provide effective and sustainable protection to plants. However, the success of SIGS for plant disease management largely depends on the efficiency of dsRNA uptake, which varies among different pathogens (Qiao et al., 2021). The stability of RNA in the environment also affects the efficiency of SIGS (Mitter et al., 2017). Strikingly, EVs can protect sRNAs from environmental degradation and can be efficiently absorbed by host cells (Colombo et al., 2014; Liu et al., 2020b). Artificial vesicles and lipid-based nanoparticles can effectively send siRNAs to their targets at low overall doses and with low potential toxicity (Ickenstein and Garidel, 2019). Therefore, the combined use of artificial vesicles/nanoparticles and SIGS is a desirable method for crop protection.

The current research on the role of EVs in plant immune response remains in its infancy. Many momentous molecular mechanisms of EVs, such as biogenesis (MVB formation and secretion), and receptor cell absorption, remain to be further investigated. In addition to siRNAs, whether long noncoding RNAs and mRNAs exist in plant EVs is unclear. Additional plant EV cargos and their functions require urgent confirmation. In addition, due to the heterogeneity of EVs and their complex functions, further isolating different EVs and determining the effect of each type of EV are very meaningful. He et al. developed an immunoaffinity capture-based technique that can accurately isolate the subtypes of specific EVs (He et al., 2021). Different types of EVs can be obtained *via* direct immunoaffinity capture by using specific antibodies to determine the components and subsequent functions of each kind of vesicle. Studying and identifying additional EV markers in plants is the most current urgent task. Undoubtedly, EVs are a treasured land to seek.

AUTHOR CONTRIBUTIONS

GL reviewed the published data and prepared the initial draft. GK, SW, and YH collaborated in manuscript preparation. QC designed the structure of the review, supervised the manuscript preparation and revised and finalized the manuscript. All authors read and approved the final manuscript.

FUNDING

Work in the Q.C. laboratory was supported by grants from the National Natural Science Foundation of China (32070288).

REFERENCES

An, Q., Ehlers, K., Kogel, K. H., Van Bel, A. J., and Huckelhoven, R. (2006a). Multivesicular compartments proliferate in susceptible and resistant MLA12-barley leaves in response to infection by the biotrophic powdery mildew fungus. *New Phytol.* 172, 563–576. doi: 10.1111/j.1469-8137.2006.01844.x

An, Q., Huckelhoven, R., Kogel, K. H., and Van Bel, A. J. (2006b). Multivesicular bodies participate in a cell wall-associated defence response in barley leaves attacked by the pathogenic powdery mildew fungus. *Cell. Microbiol.* 8, 1009–1019. doi: 10.1111/j.1462-5822.2006.00683.x

Andreu, Z., and Yanez-Mo, M. (2014). Tetraspanins in extracellular vesicle formation and function. *Front. Immunol.* 5:442. doi: 10.3389/fimmu.2014.00442

Aqil, F., Kausar, H., Agrawal, A. K., Jeyabalan, J., Kyakulaga, A. H., Munagala, R., et al. (2016). Exosomal formulation enhances therapeutic response of celastrol against lung cancer. *Exp. Mol. Pathol.* 101, 12–21. doi: 10.1016/j.yexmp.2016.05.013

Atkin-Smith, G. K., Tixeira, R., Paone, S., Mathivanan, S., Collins, C., Liem, M., et al. (2015). A novel mechanism of generating extracellular vesicles during apoptosis via a beads-on-a-string membrane structure. *Nat. Commun.* 6:7439. doi: 10.1038/ncomms8439

Baulcombe, D. (2004). RNA silencing in plants. *Nature* 431, 356–363. doi: 10.1038/nature02874

Bielska, E., Sisquella, M. A., Aldeieg, M., Birch, C., O'donoghue, E. J., and May, R. C. (2018). Pathogen-derived extracellular vesicles mediate virulence in the fatal human pathogen *Cryptococcus gattii*. *Nat. Commun.* 9:1556. doi: 10.1038/s41467-018-03991-6

Bilir, O., Telli, O., Norman, C., Budak, H., Hong, Y., and Tor, M. (2019). Small RNA inhibits infection by downy mildew pathogen *Hyaloperonospora arabidopsidis*. *Mol. Plant Pathol.* 20, 1523–1534. doi: 10.1111/mpp.12863

Bleackley, M. R., Samuel, M., Garcia-Ceron, D., Mckenna, J. A., Lowe, R. G. T., Pathan, M., et al. (2019). Extracellular vesicles from the cotton pathogen *Fusarium oxysporum* f. sp. vasinfectum induce a phytotoxic response in plants. *Front. Plant Sci.* 10:1610. doi: 10.3389/fpls.2019.01610

Bolognesi, R., Ramaseshadri, P., Anderson, J., Bachman, P., Clinton, W., Flannagan, R., et al. (2012). Characterizing the mechanism of action of double-stranded RNA activity against western corn rootworm (*Diabrotica virgifera* virgifera LeConte). *PLoS One* 7:e47534. doi: 10.1371/journal.pone.0047534

Buck, A. H., Coakley, G., Simbari, F., Mcsorley, H. J., Quintana, J. F., Le Bihan, T., et al. (2014). Exosomes secreted by nematode parasites transfer small RNAs to mammalian cells and modulate innate immunity. *Nat. Commun.* 5:5488. doi: 10.1038/ncomms6488

Cai, Q., He, B. Y., and Jin, H. L. (2019). A safe ride in extracellular vesicles - small RNA trafficking between plant hosts and pathogens. *Curr. Opin. Plant Biol.* 52, 140–148. doi: 10.1016/j.pbi.2019.09.001

Cai, Q., He, B., Kogel, K. H., and Jin, H. (2018a). Cross-kingdom RNA trafficking and environmental RNAi-nature's blueprint for modern crop protection strategies. *Curr. Opin. Microbiol.* 46, 58–64. doi: 10.1016/j.mib.2018.02.003

Cai, Q., He, B., Wang, S., Fletcher, S., Niu, D., Mitter, N., et al. (2021). Message in a bubble: shuttling small RNAs and proteins between cells and interacting organisms using extracellular vesicles. *Annu. Rev. Plant Biol.* 72, 497–524. doi: 10.1146/annurev-arplant-081720-010616

Cai, Q., Qiao, L. L., Wang, M., He, B. Y., Lin, F. M., Palmquist, J., et al. (2018b). Plants send small RNAs in extracellular vesicles to fungal pathogen to silence virulence genes. *Science* 360, 1126–1129. doi: 10.1126/science.aar4142

Choi, J. W., Kim, S. C., Hong, S. H., and Lee, H. J. (2017). Secretable small RNAs via outer membrane vesicles in periodontal pathogens. *J. Dent. Res.* 96, 458–466. doi: 10.1177/0022034516685071

Colombo, M., Raposo, G., and Thery, C. (2014). Biogenesis, secretion, and intercellular interactions of exosomes and other extracellular vesicles. *Annu. Rev. Cell Dev. Biol.* 30, 255–289. doi: 10.1146/annurev-cellbio-101512-122326

de la Canal, L., and Pinedo, M. (2018). Extracellular vesicles: a missing component in plant cell wall remodeling. *J. Exp. Bot.* 69, 4655–4658. doi: 10.1093/jxb/ery255

Delaunois, B., Jeandet, P., Clement, C., Baillieul, F., Dorey, S., and Cordelier, S. (2014). Uncovering plant-pathogen crosstalk through apoplastic proteomic studies. *Front. Plant Sci.* 5:249. doi: 10.3389/fpls.2014.00249

Ding, Y., Wang, J., Lai, J. H. C., Chan, V. H. L., Wang, X. F., Cai, Y., et al. (2014). Exo70E2 is essential for exocyst subunit recruitment and EXPO formation in both plants and animals. *Mol. Biol. Cell* 25, 412–426. doi: 10.1091/mbc.e13-10-0586

Dunker, F., Trutzenberg, A., Rothenpieler, J. S., Kuhn, S., Prols, R., Schreiber, T., et al. (2020). Oomycete small RNAs bind to the plant RNA-induced silencing complex for virulence. *eLife* 9:e56096. doi: 10.7554/eLife.56096

Escola, J. M., Kleijmeer, M. J., Stoorvogel, W., Griffith, J. M., Yoshie, O., and Geuze, H. J. (1998). Selective enrichment of tetraspan proteins on the internal vesicles of multivesicular endosomes and on exosomes secreted by human B-lymphocytes. *J. Biol. Chem.* 273, 20121–20127. doi: 10.1074/jbc.273.32.20121

Ferro, E., Bosia, C., and Campa, C. C. (2021). RAB11-mediated trafficking and human cancers: an updated review. *Biology* 10:26. doi: 10.3390/biology10010026

Fisher, M. C., Henk, D. A., Briggs, C. J., Brownstein, J. S., Madoff, L. C., Mccraw, S. L., et al. (2012). Emerging fungal threats to animal, plant and ecosystem health. *Nature* 484, 186–194. doi: 10.1038/nature10947

Guo, X. Y., Li, Y., Fan, J., Xiong, H., Xu, F. X., Shi, J., et al. (2019). Host-induced gene silencing of MoAP1 confers broad-spectrum resistance to *Magnaporthe oryzae*. *Front. Plant Sci.* 10:433. doi: 10.3389/fpls.2019.00433

Hatsugai, N., Iwasaki, S., Tamura, K., Kondo, M., Fuji, K., Ogasawara, K., et al. (2009). A novel membrane fusion-mediated plant immunity against bacterial pathogens. *Genes Dev.* 23, 2496–2506. doi: 10.1101/gad.1825209

He, B., Cai, Q., Qiao, L., Huang, C. Y., Wang, S., Miao, W., et al. (2021). RNA-binding proteins contribute to small RNA loading in plant extracellular vesicles. *Nat. Plants* 7, 342–352. doi: 10.1038/s41477-021-00863-8

Heijnen, H. F. G., Schiel, A. E., Fijnheer, R., Geuze, H. J., and Sixma, J. J. (1999). Activated platelets release two types of membrane vesicles: microvesicles by surface shedding and exosomes derived from exocytosis of multivesicular bodies and alpha-granules. *Blood* 94, 3791–3799. doi: 10.1182/blood.V94.11.3791

Hou, Y. N., Zhai, Y., Feng, L., Karimi, H. Z., Rutter, B. D., Zeng, L. P., et al. (2019). A phytophthora effector suppresses trans-kingdom RNAi to promote disease susceptibility. *Cell Host Microbe* 25, 153.e5–165.e5. doi: 10.1016/j.chom.2018.11.007

Hsu, C., Morohashi, Y., Yoshimura, S., Manrique-Hoyos, N., Jung, S. Y., Lauterbach, M. A., et al. (2010). Regulation of exosome secretion by Rab35 and its GTPase-activating proteins TBC1D10A-C. *J. Cell Biol.* 189, 223–232. doi: 10.1083/jcb.200911018

Huang, C. Y., Wang, H., Hu, P., Hamby, R., and Jin, H. (2019). Small RNAs - big players in plant-microbe interactions. *Cell Host Microbe* 26, 173–182. doi: 10.1016/j.chom.2019.07.021

Ickenstein, L. M., and Garidel, P. (2019). Lipid-based nanoparticle formulations for small molecules and RNA drugs. *Expert Opin. Drug Deliv.* 16, 1205–1226. doi: 10.1080/17425247.2019.1669558

Jeppesen, D. K., Fenix, A. M., Franklin, J. L., Higginbotham, J. N., Zhang, Q., Zimmerman, L. J., et al. (2019). Reassessment of exosome composition. *Cell* 177, 428.e18–445.e18. doi: 10.1016/j.cell.2019.02.029

Jiao, J., and Peng, D. (2018). Wheat microRNA1023 suppresses invasion of *Fusarium graminearum* via targeting and silencing FGSG_03101. *J. Plant Interact.* 13, 514–521. doi: 10.1080/17429145.2018.1528512

Johnstone, R. M., Adam, M., Hammond, J. R., Orr, L., and Turbide, C. (1987). Vesicle formation during reticulocyte maturation - Association of plasma-membrane activities with released vesicles (exosomes). *J. Biol. Chem.* 262, 9412–9420. doi: 10.1016/S0021-9258(18)48095-7

Katiyar-Agarwal, S., and Jin, H. (2010). Role of small RNAs in host-microbe interactions. *Annu. Rev. Phytopathol.* 48, 225–246. doi: 10.1146/annurev-phyto-073009-114457

Katsir, L., and Bahar, O. (2017). Bacterial outer membrane vesicles at the plant-pathogen interface. *PLoS Pathog.* 13:e1006306. doi: 10.1371/journal.ppat.1006306

Klionsky, D. J., Eskelinen, E. L., and Deretic, V. (2014). Autophagosomes, phagosomes, autolysosomes, phagolysosomes, autophagolysosomes. Wait, I'm confused. *Autophagy* 10, 549–551. doi: 10.4161/auto.28448

Koch, A., Biedenkopf, D., Furch, A., Weber, L., Rossbach, O., Abdellatef, E., et al. (2016). An RNAi-based control of *Fusarium graminearum* infections through spraying of long dsRNAs involves a plant passage and is controlled by the fungal silencing machinery. *PLoS Pathog.* 12:e1005901. doi: 10.1371/journal.ppat.1005901

Koeppen, K., Hampton, T. H., Jarek, M., Scharfe, M., Gerber, S. A., Mielcarz, D. W., et al. (2016). A novel mechanism of host-pathogen interaction through sRNA in bacterial outer membrane vesicles. *PLoS Pathog.* 12:e1005672. doi: 10.1371/journal.ppat.1005672

Kowal, J., Arras, G., Colombo, M., Jouve, M., Morath, J. P., Primdal-Bengtson, B., et al. (2016). Proteomic comparison defines novel markers to characterize heterogeneous populations of extracellular vesicle subtypes. *Proc. Natl. Acad. Sci. U. S. A.* 113, E968–E977. doi: 10.1073/pnas.1521230113

Kowal, J., Tkach, M., and Thery, C. (2014). Biogenesis and secretion of exosomes. *Curr. Opin. Cell Biol.* 29, 116–125. doi: 10.1016/j.ceb.2014.05.004

Kwon, C., Neu, C., Pajonk, S., Yun, H. S., Lipka, U., Humphry, M., et al. (2008). Co-option of a default secretory pathway for plant immune responses. *Nature* 451, 835–840. doi: 10.1038/nature06545

Li, J., He, X. Q., Deng, Y. Y., and Yang, C. X. (2019). An update on isolation methods for proteomic studies of extracellular vesicles in biofluids. *Molecules* 24:3516. doi: 10.3390/molecules24193516

Lin, Y. S., Ding, Y., Wang, J., Shen, J. B., Kung, C. H., Zhuang, X. H., et al. (2015). Exocyst-positive organelles and autophagosomes are distinct organelles in plants. *Plant Physiol.* 169, 1917–1932. doi: 10.1104/pp.15.00953

Liu, L., and Chen, X. (2018). Intercellular and systemic trafficking of RNAs in plants. *Nat. Plants* 4, 869–878. doi: 10.1038/s41477-018-0288-5

Liu, N. J., Wang, N., Bao, J. J., Zhu, H. X., Wang, L. J., and Chen, X. Y. (2020a). Lipidomic analysis reveals the importance of GIPCs in Arabidopsis leaf extracellular vesicles. *Mol. Plant* 13, 1523–1532. doi: 10.1016/j.molp.2020.07.016

Liu, Y., Wu, S., Koo, Y., Yang, A., Dai, Y., Khant, H., et al. (2020b). Characterization of and isolation methods for plant leaf nanovesicles and small extracellular vesicles. *Nanomedicine* 29:102271. doi: 10.1016/j.nano.2020.102271

Madsen, S. R., Nour-Eldin, H. H., and Halkier, B. A. (2016). Collection of apoplastic fluids from *Arabidopsis thaliana* leaves. *Methods Mol. Biol.* 1405, 35–42. doi: 10.1007/978-1-4939-3393-8_4

Majumdar, R., Rajasekaran, K., and Cary, J. W. (2017). RNA interference (RNAi) as a potential tool for control of mycotoxin contamination in crop plants: concepts and considerations. *Front. Plant Sci.* 8:200. doi: 10.3389/fpls.2017.00200

Mathieu, M., Martin-Jaular, L., Lavieu, G., and Thery, C. (2019). Specificities of secretion and uptake of exosomes and other extracellular vesicles for cell-to-cell communication. *Nat. Cell Biol.* 21, 9–17. doi: 10.1038/s41556-018-0250-9

Meng, W., He, C., Hao, Y., Wang, L., Li, L., and Zhu, G. (2020). Prospects and challenges of extracellular vesicle-based drug delivery system: considering cell source. *Drug Deliv.* 27, 585–598. doi: 10.1080/10717544.2020.1748758

Mitter, N., Worrall, E. A., Robinson, K. E., Li, P., Jain, R. G., Taochy, C., et al. (2017). Clay nanosheets for topical delivery of RNAi for sustained protection against plant viruses. *Nat. Plants* 3:16207. doi: 10.1038/nplants.2016.207

Movahed, N., Cabanillas, D. G., Wan, J., Vali, H., Laliberte, J. F., and Zheng, H. Q. (2019). Turnip mosaic virus components are released into the extracellular space by vesicles in infected leaves. *Plant Physiol.* 180, 1375–1388. doi: 10.1104/pp.19.00381

Munhoz da Rocha, I. F., Amatuzzi, R. F., Lucena, A. C. R., Faoro, H., and Alves, L. R. (2020). Cross-kingdom extracellular vesicles EV-RNA communication as a mechanism for host-pathogen interaction. *Front. Cell. Infect. Microbiol.* 10:593160. doi: 10.3389/fcimb.2020.593160

Nahui Palomino, R. A., Vanpouille, C., Costantini, P. E., and Margolis, L. (2021). Microbiota-host communications: Bacterial extracellular vesicles as a common language. *PLoS Pathog.* 17:e1009508. doi: 10.1371/journal.ppat.1009508

Nielsen, M. E., Feechan, A., Bohlenius, H., Ueda, T., and Thordal-Christensen, H. (2012). Arabidopsis ARF-GTP exchange factor, GNOM, mediates transport required for innate immunity and focal accumulation of syntaxin PEN1. *Proc. Natl. Acad. Sci. U. S. A.* 109, 11443–11448. doi: 10.1073/pnas.1117596109

Nowara, D., Gay, A., Lacomme, C., Shaw, J., Ridout, C., Douchkov, D., et al. (2010). HIGS: host-induced gene silencing in the obligate biotrophic fungal pathogen *Blumeria graminis*. *Plant Cell* 22, 3130–3141. doi: 10.1105/tpc.110.077040

O'Leary, B. M., Rico, A., Mccraw, S., Fones, H. N., and Preston, G. M. (2014). The infiltration-centrifugation technique for extraction of apoplastic fluid from plant leaves using *Phaseolus vulgaris* as an example. *J. Vis. Exp.* 94:52113. doi: 10.3791/52113

Ostrowski, M., Carmo, N. B., Krumeich, S., Fanget, I., Raposo, G., Savina, A., et al. (2010). Rab27a and Rab27b control different steps of the exosome secretion pathway. *Nat. Cell Biol.* 12, 19–30. doi: 10.1038/ncb2000

Panwar, V., Mccallum, B., and Bakkeren, G. (2013). Host-induced gene silencing of wheat leaf rust fungus *Puccinia triticina* pathogenicity genes mediated by the *Barley stripe mosaic virus*. *Plant Mol. Biol.* 81, 595–608. doi: 10.1007/s11103-013-0022-7

Paolini, L., Zendrini, A., Di Noto, G., Busatto, S., Lottini, E., Radeghieri, A., et al. (2016). Residual matrix from different separation techniques impacts exosome biological activity. *Sci. Rep.* 6:23550. doi: 10.1038/srep23550

Pegtel, D. M., and Gould, S. J. (2019). Exosomes. *Annu. Rev. Biochem.* 88, 487–514. doi: 10.1146/annurev-biochem-013118-111902

Prado, N., Alche Jde, D., Casado-Vela, J., Mas, S., Villalba, M., Rodriguez, R., et al. (2014). Nanovesicles are secreted during pollen germination and pollen tube growth: a possible role in fertilization. *Mol. Plant* 7, 573–577. doi: 10.1093/mp/sst153

Qiao, L. L., Lan, C., Capriotti, L., Ah-Fong, A., Sanchez, J. N., Hamby, R., et al. (2021). Spray-induced gene silencing for disease control is dependent on the efficiency of pathogen RNA uptake. *Plant Biotechnol. J.* doi: 10.1111/pbi.13589 [Epub ahead of print]

Regente, M., Corti-Monzon, G., Maldonado, A. M., Pinedo, M., Jorrin, J., and De La Canal, L. (2009). Vesicular fractions of sunflower apoplastic fluids are associated with potential exosome marker proteins. *FEBS Lett.* 583, 3363–3366. doi: 10.1016/j.febslet.2009.09.041

Regente, M., Pinedo, M., San Clemente, H., Balliau, T., Jamet, E., and De La Canal, L. (2017). Plant extracellular vesicles are incorporated by a fungal pathogen and inhibit its growth. *J. Exp. Bot.* 68, 5485–5495. doi: 10.1093/jxb/erx355

Rosa, C., Kuo, Y. W., Wuriyanghan, H., and Falk, B. W. (2018). RNA interference mechanisms and applications in plant pathology. *Annu. Rev. Phytopathol.* 56, 581–610. doi: 10.1146/annurev-phyto-080417-050044

Rutter, B. D., and Innes, R. W. (2017). Extracellular vesicles isolated from the leaf apoplast carry stress-response proteins. *Plant Physiol.* 173, 728–741. doi: 10.1104/pp.16.01253

Sanmartin, M., Ordonez, A., Sohn, E. J., Robert, S., Sanchez-Serrano, J. J., Surpin, M. A., et al. (2007). Divergent functions of VTI12 and VTI11 in trafficking to storage and lytic vacuoles in Arabidopsis. *Proc. Natl. Acad. Sci. U. S. A.* 104, 3645–3650. doi: 10.1073/pnas.0611147104

Savary, S., Willocquet, L., Pethybridge, S. J., Esker, P., Mcroberts, N., and Nelson, A. (2019). The global burden of pathogens and pests on major food crops. *Nat. Ecol. Evol.* 3, 430–439. doi: 10.1038/s41559-018-0793-y

Simpson, R. J., Kalra, H., and Mathivanan, S. (2012). ExoCarta as a resource for exosomal research. *J. Extracell. Vesicles* 1:18374. doi: 10.3402/jev.v1i0.18374

Tauro, B. J., Greening, D. W., Mathias, R. A., Ji, H., Mathivanan, S., Scott, A. M., et al. (2012). Comparison of ultracentrifugation, density gradient separation, and immunoaffinity capture methods for isolating human colon cancer cell line LIM1863-derived exosomes. *Methods* 56, 293–304. doi: 10.1016/j.ymeth.2012.01.002

Tian, X. Y., Teng, J. L., and Chen, J. G. (2020). New insights regarding SNARE proteins in autophagosome-lysosome fusion. *Autophagy*, 1–9. doi: 10.1080/15548627.2020.1823124 [Epub ahead of print]

Tinoco, M. L., Dias, B. B., Dall'astta, R. C., Pamphile, J. A., and Aragao, F. J. (2010). In vivo trans-specific gene silencing in fungal cells by in planta expression of a double-stranded RNA. *BMC Biol.* 8:27. doi: 10.1186/1741-7007-8-27

Toruno, T. Y., Stergiopoulos, I., and Coaker, G. (2016). Plant-pathogen effectors: cellular probes interfering with plant defenses in spatial and temporal manners. *Annu. Rev. Phytopathol.* 54, 419–441. doi: 10.1146/annurev-phyto-080615-100204

Tseng, Y. C., Mozumdar, S., and Huang, L. (2009). Lipid-based systemic delivery of siRNA. *Adv. Drug Deliv. Rev.* 61, 721–731. doi: 10.1016/j.addr.2009.03.003

Valadi, H., Ekstrom, K., Bossios, A., Sjostrand, M., Lee, J. J., and Lotvall, J. O. (2007). Exosome-mediated transfer of mRNAs and microRNAs is a novel

mechanism of genetic exchange between cells. *Nat. Cell Biol.* 9, 654–659. doi: 10.1038/ncb1596

van Niel, G., D'angelo, G., and Raposo, G. (2018). Shedding light on the cell biology of extracellular vesicles. *Nat. Rev. Mol. Cell Biol.* 19, 213–228. doi: 10.1038/nrm.2017.125

Wang, J. A., Ding, Y., Wang, J. Q., Hillmer, S., Miao, Y. S., Lo, S. W., et al. (2010). EXPO, an exocyst-positive organelle distinct from multivesicular endosomes and autophagosomes, mediates cytosol to cell wall exocytosis in Arabidopsis and tobacco cells. *Plant Cell* 22, 4009–4030. doi: 10.1105/tpc.110.080697

Wang, B., Sun, Y., Song, N., Zhao, M., Liu, R., Feng, H., et al. (2017). *Puccinia striiformis* f. sp. tritici microRNA-like RNA 1 (Pst-milR1), an important pathogenicity factor of Pst, impairs wheat resistance to Pst by suppressing the wheat pathogenesis-related 2 gene. *New Phytol.* 215, 338–350. doi: 10.1111/nph.14577

Wang, D., Weaver, N. D., Kesarwani, M., and Dong, X. N. (2005). Induction of protein secretory pathway is required for systemic acquired resistance. *Science* 308, 1036–1040. doi: 10.1126/science.1108791

Wang, M., Weiberg, A., Lin, F. M., Thomma, B. P., Huang, H. D., and Jin, H. (2016). Bidirectional cross-kingdom RNAi and fungal uptake of external RNAs confer plant protection. *Nat. Plants* 2:16151. doi: 10.1038/nplants.2016.151

Wang, H., Zhuang, X. H., Hillmer, S., Robinson, D. G., and Jiang, L. W. (2011). Vacuolar sorting receptor (VSR) proteins reach the plasma membrane in germinating pollen tubes. *Mol. Plant* 4, 845–853. doi: 10.1093/mp/ssr011

Weiberg, A., Wang, M., Lin, F. M., Zhao, H., Zhang, Z., Kaloshian, I., et al. (2013). Fungal small RNAs suppress plant immunity by hijacking host RNA interference pathways. *Science* 342, 118–123. doi: 10.1126/science.1239705

Yin, C. T., Jurgenson, J. E., and Hulbert, S. H. (2011). Development of a host-induced RNAi system in the wheat stripe rust fungus *Puccinia striiformis* f. sp tritici. *Mol. Plant-Microbe Interact.* 24, 554–561. doi: 10.1094/MPMI-10-10-0229

Zhang, J., Khan, S. A., Heckel, D. G., and Bock, R. (2017). Next-generation insect-resistant plants: RNAi-mediated crop protection. *Trends Biotechnol.* 35, 871–882. doi: 10.1016/j.tibtech.2017.04.009

Zhang, S., Sun, L., and Kragler, F. (2009). The phloem-delivered RNA pool contains small noncoding RNAs and interferes with translation. *Plant Physiol.* 150, 378–387. doi: 10.1104/pp.108.134767

Zhang, T., Zhao, Y. L., Zhao, J. H., Wang, S., Jin, Y., Chen, Z. Q., et al. (2016). Cotton plants export microRNAs to inhibit virulence gene expression in a fungal pathogen. *Nat. Plants* 2:16153. doi: 10.1038/nplants.2016.153

Conflict of Interest: The authors declare that the research was conducted in the absence of any commercial or financial relationships that could be construed as a potential conflict of interest.

Publisher's Note: All claims expressed in this article are solely those of the authors and do not necessarily represent those of their affiliated organizations, or those of the publisher, the editors and the reviewers. Any product that may be evaluated in this article, or claim that may be made by its manufacturer, is not guaranteed or endorsed by the publisher.

frontiers in Plant Science

MINI REVIEW
published: 16 December 2021
doi: 10.3389/fpls.2021.803635

Functions and Mechanisms of SAC Phosphoinositide Phosphatases in Plants

Yanbo Mao and Shutang Tan**

MOE Key Laboratory for Cellular Dynamics, School of Life Sciences, Division of Molecular and Cell Biophysics, Division of Life Sciences and Medicine, Hefei National Science Center for Physical Sciences at the Microscale, University of Science and Technology of China, Hefei, China

Phosphatidylinositol (PtdIns) is one type of phospholipid comprising an inositol head group and two fatty acid chains covalently linked to the diacylglycerol group. In addition to their roles as compositions of cell membranes, phosphorylated PtdIns derivatives, termed phosphoinositides, execute a wide range of regulatory functions. PtdIns can be phosphorylated by various lipid kinases at 3-, 4- and/or 5- hydroxyls of the inositol ring, and the phosphorylated forms, including PtdIns3P, PtdIns4P, PtdIns5P, PtdIns(3,5)P_2, PtdIns(4,5)P_2, can be reversibly dephosphorylated by distinct lipid phosphatases. Amongst many other types, the SUPPRESSOR OF ACTIN (SAC) family of phosphoinositide phosphatases recently emerged as important regulators in multiple growth and developmental processes in plants. Here, we review recent advances on the biological functions, cellular activities, and molecular mechanisms of SAC domain-containing phosphoinositide phosphatases in plants. With a focus on those studies in the model plant *Arabidopsis thaliana* together with progresses in other plants, we highlight the important roles of subcellular localizations and substrate preferences of various SAC isoforms in their functions.

Keywords: phosphoinositides, SAC phosphatases, subcellular localization, trafficking, *Arabidopsis*

OPEN ACCESS

Edited by:
Ruixi Li,
Southern University of Science and Technology, China

Reviewed by:
Martin Potocký,
Institute of Experimental Botany, Academy of Sciences of the Czech Republic, Czechia
Takashi Aoyama,
Kyoto University, Japan

****Correspondence:***
Yanbo Mao
ybmao@ustc.edu.cn
Shutang Tan
sttan@ustc.edu.cn

Specialty section:
This article was submitted to Plant Physiology, a section of the journal Frontiers in Plant Science

Received: *28 October 2021*
Accepted: *30 November 2021*
Published: *16 December 2021*

Citation:
Mao Y and Tan S (2021) Functions and Mechanisms of SAC Phosphoinositide Phosphatases in Plants. Front. Plant Sci. 12:803635. doi: 10.3389/fpls.2021.803635

INTRODUCTION

The biological membrane doesn't only separate the cell from the outer environment, but also defines specific territory for subcellular compartments. It is mainly composed of sterols, sphingolipids and structural glycerophospholipids together with regulatory phospholipids including phosphatidylinositol and its phosphorylated derivatives phosphatidylinositol phosphates (PtdInsPs, also referred to as phosphoinositides) (Ejsing et al., 2009; Andreyev et al., 2010; Colin and Jaillais, 2020). Despite representing a small fraction of total phospholipids, these negatively charged phosphoinositides play a vital role in various cellular activities, including membrane trafficking and cellular dynamics (Gerth et al., 2017; Noack and Jaillais, 2020). Different phosphoinositides are enriched in different membranes and execute specific cellular functions (Noack and Jaillais, 2020). By application of fluorescent probes, PtdIns3P was found to distribute at multivesicular bodies/late endosomes/prevacuolar compartment (MVB/LE/PVC) and the vacuolar membrane (Vermeer et al., 2006; Simon et al., 2014); PtdIns(3,5)P_2 localizes predominantly in MVB/LE (Hirano et al., 2017) and PtdIns(4,5)P_2 mainly at the plasma membrane (PM; Van Leeuwen et al., 2007). These subcellular localizations may vary according to distinct cell types. In *Arabidopsis* root

hairs, PtdIns(3,5)P_2 localizes to the PM along the shank region and is involved in the hardening of the shank, whereas PtdIns(4,5)P_2 was observed to accumulate at the apex and it is required for tip growth (Hirano et al., 2018). In root epidermal cells, PtdIns4P exhibited a gradient distribution from the highest concentration at the PM, intermediate concentration in post-Golgi/endosomal compartments to the lowest level in Golgi (Simon et al., 2014). Although both PtdIns(4,5)P_2 and PtdIns4P accumulate at the PM, they contribute differently to PM surface charges, which give rise to different electrostatic filed along the membrane (Simon et al., 2016; Dubois and Jaillais, 2021). It is exactly these special biophysiochemical properties that determine membrane specificity and thus contribute to the organellar identity (Noack and Jaillais, 2017, 2020; Platre et al., 2018). In addition, these PtdInsPs can also recruit different lipid-binding proteins, ensuring their subcelluar localizations and functions at local membranes.

In eukaryotes, phosphoinositides can be interconverted through corresponding modifying enzymes, phosphoinositide kinases and phosphatases respectively. In plants, phosphoinositide phosphatases can be categorized into three major families, the PHOSPHATASE AND TENSIN homologs (PTEN) family, 5-Phosphatases (5-PTases) and Suppressor of Actin (SAC) domain containing phosphatases (hereafter SAC phosphatases) (Gerth et al., 2017). Here, we summarize and discuss the recent advances on this SAC family, especially the subcellular localization, substrate specificity, as well as their interacting proteins and regulators.

OVERVIEW OF PLANT SAC FAMILY

The SAC phosphatase Sac1p was first identified in a genetic screen for the suppressor of actin defective mutant in yeast. The loss of Sac1p led to increased sensitivity to cold treatment, disorganized intracellular actin as well as decreased secretion rate in yeast (Novick et al., 1989), whereas absence of *SAC1* resulted in embryonic and preimplantation lethality in *Drosophila* and mice (Wei et al., 2003; Liu et al., 2008). In yeast and mammals, SAC domain proteins can be further divided into two subfamilies. Members of the first subfamily contain the SAC domain and the type II phosphatidylinositol phosphatase 5-phosphatase domain, including yeast Inp51p, Inp52p, and Inp53p, and mammalian synaptojanin1 and synaptojanin2. The other subfamily includes yeast Sac1p and Fig4p, and mammalian counterparts Sac1, Sac2/INPP5f, and Sac3 (Hughes et al., 2000a; Manford et al., 2010). Based on sequence homology, nine SAC phosphatases (SAC1∼SAC9) have been found in both *Arabidopsis thaliana* and rice (*Oryza sativa* L.) genome, respectively, forming three subgroups (**Table 1** and **Figure 1A**; Zhong and Ye, 2003; Novakova et al., 2014): (I) AtSAC1 ∼ AtSAC5 form a clade with medium protein size, exhibiting high similarity to yeast Fig4p (Zhong et al., 2005; Novakova et al., 2014). (II) The Sac1p closest homologs AtSAC6/AtSAC1b, AtSAC7/ROOT HAIR DEFFECTIVE4 (RHD4)/NON-CYTOLEDON PHENOTYPE2 (NCP2)/AtSAC1c, and AtSAC8/AtSAC1a all contain the two transmembrane domains (TMD) at their C-termini (Despres et al., 2003; Zhong and Ye, 2003; Thole et al., 2008). Notably, ectopic expression of *AtSAC6* to *AtSAC8* rescued the cold-sensitive phenotype associated with ablation of yeast Sac1p (Despres et al., 2003). The recently characterized rice GRAIN NUMBER AND PLANT HEIGHT (OsGH1) was also classified into this subclade according to its protein size and domain organization (Guo et al., 2020; **Figure 1B**). (III) The third clade only contains one member, AtSAC9, which possesses a larger protein size and a unique protein sequence, a WW protein-protein interaction domain following the N-terminal SAC catalytic domain plus around 1,100 amino acid residues at the C-terminus with unknown function (Zhong and Ye, 2003; Williams et al., 2005; **Figure 1B**).

SUBSTRATE SPECIFICITY

The SAC domain is highly conserved and profiled with PtdInsP phosphatase activity among eukaryotes (Del Bel and Brill, 2018). *In vitro* biochemical studies revealed that mouse Sac1 and yeast Sac1p are capable of dephosphorylating PtdIns3P, PtdIns4P and PtdIns(3,5)P_2. Whereas the levels of PtdIns3P only slightly increased (around 1.5-fold) in yeast *sac1* mutant, 8- to 10-fold elevated levels of PtdIns4P were detected in this mutant (Guo et al., 1999; Hughes et al., 2000b; Nemoto et al., 2000). These data indicated that PtdIns4P, rather than PtdIns3P, might be a preferential substrate for Sac1p, and that enzyme specificities do not always correlate between *in vitro* and *in vivo* assays. This could be due to the differences in the subcellular distributions of phospholipids and SAC1 enzymes, or potential additional components involved in the catalysis *in vivo*.

In *Arabidopsis*, AtSAC1 exhibited phosphatase activity toward PtdIns(3,5)P_2 as observed by an *in vitro* activity assay (Zhong et al., 2005). Overexpression of *AtSAC2*∼*AtSAC5* resulted in the reduction of PtdIns(3,5)P_2, whereas the level of PtdIns(3,5)P_2 was unchanged in the *sac3 sac4 sac5* triple mutant, perhaps due to a compensatory response. Nevertheless, together with the abundance of PtdIns3P in the tonoplast, it is implied that AtSAC2∼AtSAC5 are responsible for the conversion of PtdIns(3,5)P_2 to PtdIns3P (Zhong et al., 2005; Novakova et al., 2014). Overall, AtSAC1∼AtSAC5 share high similarity to the homologous yeast Fig4p on the phosphatase activity toward PtdIns(3,5)P_2 (Rudge et al., 2004; Duex et al., 2006).

In line with the *in vitro* data that AtSAC7 displayed a preference for PtdIns4P, around a 50% increase of PtdIns4P was detected in the root of the *sac7* mutant compared to wild type (Thole et al., 2008). By use of an ion chromatography system, both PtdIns4P and PtdIns(4,5)P_2 contents were found to dramatically increase in *sac6/7*, *sac6/8* and *sac7/8* double mutants, while a slight increase was detected in single mutants (Song et al., 2021), suggesting that PtdIns4P and PtdIns(4,5)P_2 might be the substrates for AtSAC6/7/8. In rice, the close related homolog OsGH1 specifically dephosphorylated PtdIns4P and PtdIns(4,5)P_2 from both *in vitro* phosphatase activity assay and binding studies. Moreover, the *OsGH1* knockout plant showed a significant increase in endogenous PtdIns4P and PtdIns(4,5)P_2 levels, whereas *OsGH1*-overexpressing plants

TABLE 1 | Subcellular localization and substrate specificity of currently characterized plant SAC family members.

Subgroup	Name	Localization	Putative substrate	References
Clade I	AtSAC1/FRA7	Golgi apparatus	PtdIns(3,5)P_2	Zhong et al., 2005
	AtSAC2/3/4/5	Tonoplast	PtdIns(3,5)P_2	Novakova et al., 2014
Clade II	AtSAC6/AtSAC1b	Endoplasmic reticulum	PtdIns4P, PtdIns(4,5)P_2	Despres et al., 2003; Song et al., 2021
	AtSAC7/RHD4/NCP2/AtSAC1c	Endoplasmic reticulum	PtdIns4P, PtdIns(4,5)P_2	Despres et al., 2003; Thole et al., 2008; Song et al., 2021
	AtSAC8/AtSAC1a	Endoplasmic reticulum	PtdIns4P, PtdIns(4,5)P_2	Despres et al., 2003; Song et al., 2021
	OsGH1	Endoplasmic reticulum	PtdIns4P, PtdIns(4,5)P_2	Guo et al., 2020
Clade III	AtSAC9	Subpopulation of trans-Golgi network/early endosomes	Ins(1,4,5)P_3, PtdIns(4,5)P_2	Williams et al., 2005; Doumane et al., 2021

exhibited reduced PtdIns4P and PtdIns(4,5)P_2 levels (Guo et al., 2020), differently from the yeast homolog Sac1p and mammalian SAC1, indicating the functional diversity among the eukaryotes. These findings suggested that the plant SAC family clade II displayed phosphatase activity toward PtdIns4P and PtdIns(4,5)P_2. In addition, AtSAC9 was also reported to act as a PtdIns(4,5)P_2 phosphatase based on the observation of approximately 4-fold higher PtdIns(4,5)P_2 levels in root extracts of loss-of-function *sac9* mutant (Williams et al., 2005). Nevertheless, the elevated level of Ins(1,4,5)P_3 was also detected in *sac9* (Williams et al., 2005), indicating the catalytic diversity of AtSAC9. The overall substrate preference is summarized here based on the previous research (**Table 1**), but more direct biochemical evidence is still required to validate the substrate specificity for each SAC enzyme.

THE EXPRESSION PATTERN AND SUBCELLULAR LOCALIZATION OF SACS

In *Arabidopsis*, transcripts of all the nine *AtSACs* were detected in most tissues (Despres et al., 2003; Zhong and Ye, 2003; Song et al., 2021), implying pleotropic functions in various life activities. Among the members of subgroup I, AtSAC1 was reported to colocalize with the Golgi marker AVP2-ECFP when co-expressed in carrot protoplasts. The truncation of its C terminus by the *fra7* mutation resulted in its mislocalization at the cytoplasm, but the phosphatase catalytic activity was unaffected. These results suggest that the sub-cellular localization of AtSAC1 might be essential for its biological functions (Zhong et al., 2005). Interestingly, in pollen and pollen tubes, over-expression of AtSAC1-GFP under the *LAT52* promoter was found to reside at the PVC (Zhang et al., 2018), implying the subcellular distribution pattern may vary in distinct cell types. Furthermore, AtSAC2∼AtSAC5 were all observed to localize in the tonoplast, and this thus ensures the abundance of PtdIns3P in the tonoplast for appropriate maintenance of vacuolar morphology (Novakova et al., 2014). Similarly, the yeast homolog Fig4p was also identified to localize in the limiting membrane of yeast vacuoles, controlling the level of PtdIns(3,5)P_2 upon hyperosmotic shock (Rudge et al., 2004), suggesting a conserved role of SACs from this subgroup in vacuole development among eukaryotes.

In yeast, Sac1p is an integral protein residing at endoplasmic reticulum (ER) and Golgi apparatus membrane, and regulates the PtdIns4P pool that is important for vacuolar morphology and Golgi trafficking (Whitters et al., 1993; Foti et al., 2001). The endoplasmic reticulum localization was also identified for mammalian and *Drosophila* Sac1 (Nemoto et al., 2000; Liu et al., 2008; Forrest et al., 2013). Consistently, the rice homolog OsGH1 was reported to co-localize with the ER marker in rice protoplasts. Disruption of OsGH1 destroyed homeostasis of membrane PtdIns4P and PtdIns(4,5)P_2, thus affecting organelle morphology and cell development (Guo et al., 2020). In *Arabidopsis*, AtSAC6/7/8 targeted to the ER compartment when expressed in tobacco BY2 cells together with a C-terminally fused GFP (Despres et al., 2003), and they are required for both the maintenance of PtdIns(4,5)P_2 polarity and the restriction of PtdIns4P at PM in root hairs (Thole et al., 2008; Song et al., 2021). Intriguingly, the N-terminal fusion version EYFP-AtSAC7 which is functional, as demonstrated by rescuing the phenotype of the *sac7* loss-of-function mutant, localized at the post-Golgi secretory compartments and regulated the accumulation of PtdIns4P on membrane compartments at the tips of growing root hairs (Thole et al., 2008). Future experimental validations are thus needed to address whether all these three SAC isoforms share the same subcellular localization. A recent study has shown that AtSAC9 localizes to a subpopulation of trans-Golgi network/early endosomes in close vicinity to the PM in meristematic epidermal cells of *Arabidopsis* roots, restricting the distribution of its substrate PtdIns(4,5)P_2 at the PM for proper regulation of endocytosis (Doumane et al., 2021; **Table 1** and **Figure 1C**).

FUNCTIONS AND MECHANISMS OF SACS AND PHOSPHOINOSITIDES

The anionic lipids, PtdIns4P, PtdIns(3,5)P_2, and PtdIns(4,5)P_2, regulate many cellular processes, including endocytosis, vacuolar

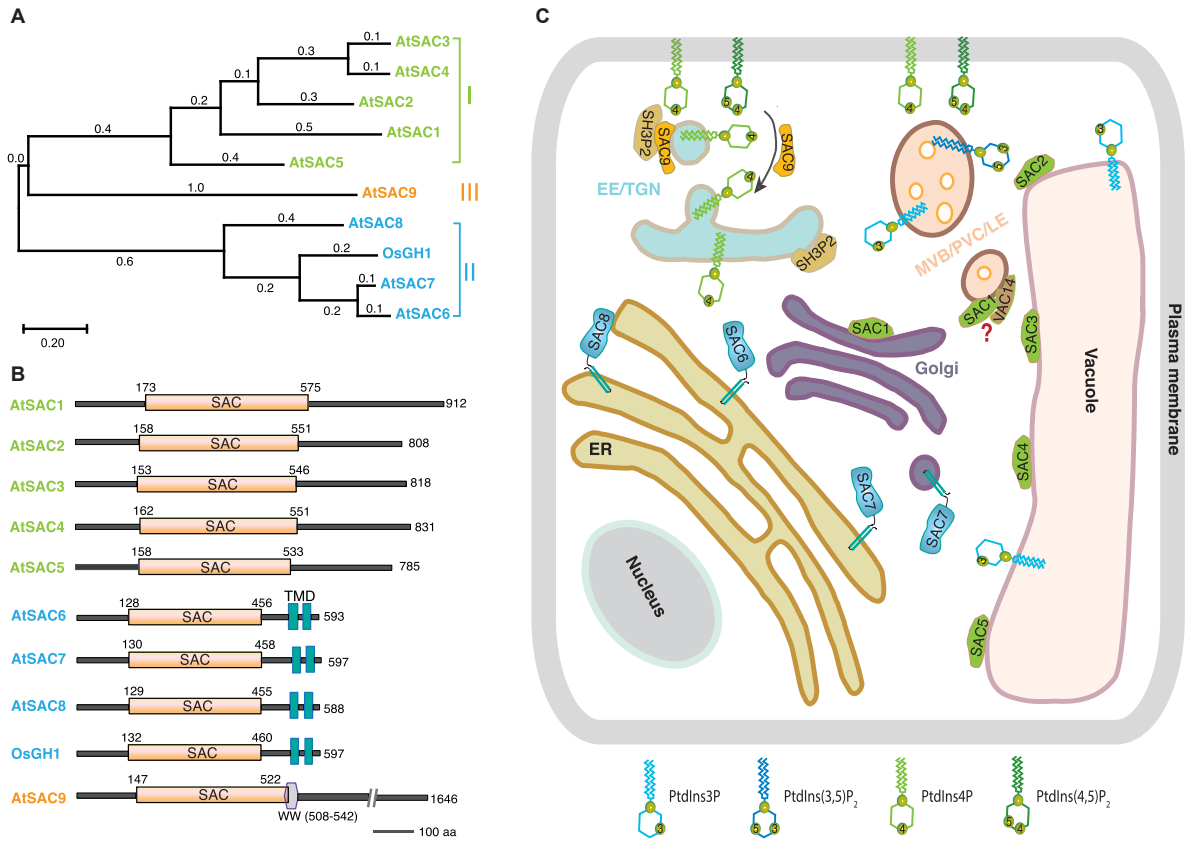

FIGURE 1 | The current overview of plant SACs.**(A)** Phylogenetic analysis and **(B)** schematic domain structures of the experimentally characterized plant SACs. The phylogenetic tree was conducted by MEGA X10.2.4 with a maximum likelihood method and a Poisson correction model. The aligned protein sequences were based on 10 plant SAC members, AtSAC1 (At1g22620.1), AtSAC2 (At3g14205.1), AtSAC3 (At3g43220.1), AtSAC4 (At5g20840.1), AtSAC5 (At1g17340.1), AtSAC6 (At5g66020.1), AtSAC7 (At3g51460.1), AtSAC8 (At3G51830.1), AtSAC9 (At3g59770.3), and OsGH1 (Os02g0554300). Domain structures were determined by using the PROSITE program (https://prosite.expasy.org/). Abbreviations, SAC, suppressor of actin domain; TMD, transmembrane domain; WW, a domain with two conserved tryptophan residues. The numbers denote the amino acid residue positions. **(C)** Schematic representation of sub-cellular distribution of SACs and their putative substrates in the plant cell. AtSAC1 (green) localizes at the Golgi, whereas all the other members (AtSAC2∼AtSAC5) from subgroup I locate in the tonoplast. AtSAC6∼AtSAC8 (blue) from subgroup II are all integrated on ER through two transmembrane motifs. Additionally, AtSAC7 also localizes in post-Golgi secretory compartments. The subclade III member AtSAC9 (orange) localizes in a subpopulation of TGN/EEs close to cell cortex and thus also regulates the distribution pattern of PtdIns(4,5)P_2. Meanwhile, AtSAC9 interacts and colocalizes with the endocytic component SH3P2. AtSAC1 colocalizes with VAC14 in MVB/LE/PVC in pollen, but it is still unclear if they can form a complex or not in plants. Abbreviations: TGN/EE, trans-Golgi network/early endosome; ER, endoplasmic reticulum; MVB/LE/PVC, multivesicular body/late endosome/pre-vacuolar compartments. The black arrow indicates the conversion of PtdIns(4,5)P_2 to PtdIns4P during endocytosis regulated by AtSAC9.

trafficking and actin dynamics, though in low abundance (Gerth et al., 2017; Hirano and Sato, 2019; Noack and Jaillais, 2020). Deficiency in these phosphoinositides or dysfunction of their related metabolic enzymes SAC phosphatases usually causes defects in endocytic trafficking and results in abnormal vacuole, Golgi and endosome morphology (Rudge et al., 2004; Liu et al., 2008; Whitley et al., 2009; He et al., 2017). In *Arabidopsis*, the *AtSAC1*-truncated mutant *fra7* (*fragile fiber7*) displayed a wide range of defects in plant growth and architecture, including a decrease of cell wall thickness and cell length in fiber cells and vessel elements, and aberrant actin organization (Zhong et al., 2005). However, how loss of *AtSAC1* and accumulation of PtdIns(3,5)P_2 are related with these various phenotypes is still elusive. Interestingly, seedlings overexpressing *AtSAC2* ∼*AtSAC5* or the *sac2 sac3 sac4 sac5* quadruple mutant and *sac3 sac4 sac5* triple mutant all exhibited arrested growth on medium without sucrose. It is proposed that fragmented vacuoles and abnormal protein trafficking toward the vacuole in the *sac* mutants might explain for the decreased viability in seedlings (Novakova et al., 2014). In yeast, the vacuole-localized Fig4p physically associates with an adaptor-like protein Vac14p in FAB1/PIKfyve protein complex and thus regulates the biosynthesis and turnover of PtdIns(3,5)P_2, controlling the vacuolar size (Rudge et al., 2004; Duex et al., 2006; Jin et al., 2008). Moreover, Vac14 can also control Fig4p localization in yeast (Rudge et al., 2004), indicating that the subcellular distribution of the phosphatase is directed by its interacting partner. AtSAC1 was also found to colocalize with the yeast Vac14p homolog VAC14 at PVC in wortmannin (an inhibitor of PI3K)-treated pollen tubes in *Arabidopsis* (Zhang et al., 2018).

Consistent with the functional redundancy among the SAC family, the single mutant of *sac6*, *sac7*, and *sac8* didn't show any obvious defects in plant development except the short-bulged root hairs in *sac7/rhd4-1* (Schiefelbein and Somerville, 1990; Thole et al., 2008). However, in the double and triple mutants, significantly delayed embryonic development or even lethal embryos were observed, correlated with a decreased auxin distribution (Song et al., 2021). Furthermore, the retrograde trafficking of auxin efflux carrier PIN-FORMED1 (PIN1) and PIN2 proteins was also affected in the loss of *AtSAC7/8*, suggesting a role of AtSAC6-AtSAC8 in auxin-mediated development (Song et al., 2021). In rice, over-accumulation of PtdIns4P and PtdIns(4,5)P_2 caused by dysfunction of *OsGH1* disrupted the activity of actin-related protein 2/3 (Arp2/3) complex for actin nucleation, thus resulting in the reduced plant height, panicle and grain size. In addition, the morphology of Golgi apparatus and chloroplast was also perturbed by elevated PtdInsP4 and PtdIns(4,5)P_2 levels (Guo et al., 2020), highlighting the conserved role of PtdInsP homeostasis in organellar organization in rice. In *Drosophila*, Vesicle-associated membrane protein (VAMP)-Associated Protein (DVAP) physically interacts with SAC1 in controlling phosphoinositide metabolism (Forrest et al., 2013), providing the evidence for the potential working mechanism of SACs in vesicle trafficking.

In *Arabidopsis*, the endocytic component Src Homology 3 Domain Protein 2 (SH3P2) was identified as a AtSAC9-interacting partner through yeast two-hybrid screening. Absence of AtSAC9 resulted in mis-localization of PtdIns(4,5)P_2, and also triggered the altered SH3P2 localization and reduced clathrin-mediated endocytosis rate (Doumane et al., 2021). Moreover, *sac9* knock-out mutant exhibited cell wall defects and overall stressed phenotype, including dwarfism, closed stomata, anthocyanin accumulation, and increased transcription of stress response genes (Williams et al., 2005; Vollmer et al., 2011). These results suggest that the AtSAC9 phosphatase is required for modulating phosphoinositide distribution during stress response and cell wall deposition.

CONCLUSION

In plants, three types of phosphoinositides, PtdIns4P, PtdIns(3,5)P_2, and PtdIns(4,5)P_2, have been identified so far as substrates of SAC phosphatases within distinct endomembrane compartments. Malfunction of SACs severely disrupts PtdInsP homeostasis reflected on both contents and distribution patterns, thus affecting endomembrane trafficking and organellar organization, and results in a wide range of developmental defects. However, it is still less understood how SACs execute their catalytic functions and associate with membrane in the case of those isoforms lacking TMDs. Future studies might be required to determine the regulatory molecules and interacting partners to better understand cellular pathways in which SACs are involved.

AUTHOR CONTRIBUTIONS

YM and ST conceptualized and wrote the manuscript. YM made the figures. Both authors contributed to the article and approved the submitted version.

FUNDING

This work was supported by Youth Innovation Fund of University of Science and Technology of China (No. WK9100000021).

ACKNOWLEDGMENTS

We acknowledge University of Science and Technology of China for support. We are sorry for those whose work is not included due to limited space.

REFERENCES

Andreyev, A. Y., Fahy, E., Guan, Z., Kelly, S., Li, X., McDonald, J. G., et al. (2010). Subcellular organelle lipidomics in TLR-4-activated macrophages1[S]. *J. Lipid Res.* 51, 2785–2797. doi: 10.1194/jlr.M008748

Colin, L. A., and Jaillais, Y. (2020). Phospholipids across scales: lipid patterns and plant development. *Curr. Opin. Plant Biol.* 53, 1–9. doi: 10.1016/j.pbi.2019.08.007

Del Bel, L. M., and Brill, J. A. (2018). Sac1, a lipid phosphatase at the interface of vesicular and nonvesicular transport. *Traffic* 19, 301–318. doi: 10.1111/tra.12554

Despres, B., Bouissonnié, F., Wu, H.-J., Gomord, V., Guilleminot, J., Grellet, F., et al. (2003). Three SAC1-like genes show overlapping patterns of expression in Arabidopsis but are remarkably silent during embryo development. *Plant J.* 34, 293–306. doi: 10.1046/j.1365-313X.2003.01720.x

Doumane, M., Lebecq, A., Fangain, A., Bayle, V., Rozier, F., Marquès-Bueno, M. D. M., et al. (2021). The Arabidopsis SAC9 Enzyme defines a cortical population of early endosomes and restricts PI(4,5)P₂ to the Plasma Membrane. *bioRxiv* [Preprint]. doi: 10.1101/2021.09.10.459735

Dubois, G. A., and Jaillais, Y. (2021). Anionic phospholipid gradients: an uncharacterized frontier of the plant endomembrane network. *Plant Physiol.* 185, 577–592. doi: 10.1093/plphys/kiaa056

Duex, J. E., Nau, J. J., Kauffman, E. J., and Weisman, L. S. (2006). Phosphoinositide 5-phosphatase Fig 4p is required for both acute rise and subsequent fall in stress-induced phosphatidylinositol 3,5-bisphosphate levels. *Eukaryot. Cell* 5, 723–731. doi: 10.1128/ec.5.4.723-731.2006

Ejsing, C. S., Sampaio, J. L., Surendranath, V., Duchoslav, E., Ekroos, K., Klemm, R. W., et al. (2009). Global analysis of the yeast lipidome by quantitative shotgun mass spectrometry. *Proc. Natl. Acad. Sci. U. S. A.* 106, 2136–2141. doi: 10.1073/pnas.0811700106

Forrest, S., Chai, A., Sanhueza, M., Marescotti, M., Parry, K., Georgiev, A., et al. (2013). Increased levels of phosphoinositides cause neurodegeneration in a Drosophila model of amyotrophic lateral sclerosis. *Hum. Mol. Genet.* 22, 2689–2704. doi: 10.1093/hmg/ddt118

Foti, M., Audhya, A., and Emr, S. D. (2001). Sac1 lipid phosphatase and Stt4 phosphatidylinositol 4-kinase regulate a pool of phosphatidylinositol 4-phosphate that functions in the control of the actin cytoskeleton and vacuole morphology. *Mol. Biol. Cell* 12, 2396–2411. doi: 10.1091/mbc.12.8.2396

Gerth, K., Lin, F., Menzel, W., Krishnamoorthy, P., Stenzel, I., Heilmann, M., et al. (2017). Guilt by Association: a Phenotype-Based View of the Plant

Phosphoinositide Network. *Annu. Rev. Plant Biol.* 68, 349–374. doi: 10.1146/annurev-arplant-042916-041022

Guo, S., Stolz, L. E., Lemrow, S. M., and York, J. D. (1999). SAC1-like domains of yeast SAC1, INP52, and INP53 and of human synaptojanin encode polyphosphoinositide phosphatases. *J. Biol. Chem.* 274, 12990–12995. doi: 10.1074/jbc.274.19.12990

Guo, T., Chen, H. C., Lu, Z. Q., Diao, M., Chen, K., Dong, N. Q., et al. (2020). A SAC Phosphoinositide Phosphatase Controls Rice Development via Hydrolyzing PI4P and PI(4,5)P2. *Plant Physiol.* 182, 1346–1358. doi: 10.1104/pp.19.01131

He, K., Marsland Iii, R., Upadhyayula, S., Song, E., Dang, S., Capraro, B. R., et al. (2017). Dynamics of phosphoinositide conversion in clathrin-mediated endocytic traffic. *Nature* 552, 410–414. doi: 10.1038/nature25146

Hirano, T., Konno, H., Takeda, S., Dolan, L., Kato, M., Aoyama, T., et al. (2018). PtdIns(3,5)P2 mediates root hair shank hardening in Arabidopsis. *Nat. Plants* 4, 888–897. doi: 10.1038/s41477-018-0277-8

Hirano, T., Munnik, T., and Sato, M. H. (2017). Inhibition of phosphatidylinositol 3,5-bisphosphate production has pleiotropic effects on various membrane trafficking routes in Arabidopsis. *Plant Cell Physiol.* 58, 120–129. doi: 10.1093/pcp/pcw164

Hirano, T., and Sato, M. H. (2019). Diverse Physiological Functions of FAB1 and Phosphatidylinositol 3,5-Bisphosphate in Plants. *Front. Plant Sci.* 10:274. doi: 10.3389/fpls.2019.00274

Hughes, W. E., Cooke, F. T., and Parker, P. J. (2000a). Sac phosphatase domain proteins. *Biochem. J.* 350, 337–352. doi: 10.1042/bj3500337

Hughes, W. E., Woscholski, R., Cooke, F. T., Patrick, R. S., Dove, S. K., McDonald, N. Q., et al. (2000b). SAC1 encodes a regulated lipid phosphoinositide phosphatase, defects in which can be suppressed by the homologous Inp52p and Inp53p phosphatases. *J. Biol. Chem.* 275, 801–808. doi: 10.1074/jbc.275.2.801

Jin, N., Chow, C. Y., Liu, L., Zolov, S. N., Bronson, R., Davisson, M., et al. (2008). VAC14 nucleates a protein complex essential for the acute interconversion of PI3P and PI(3,5)P2 in yeast and mouse. *EMBO J.* 27, 3221–3234. doi: 10.1038/emboj.2008.248

Liu, Y., Boukhelifa, M., Tribble, E., Morin-Kensicki, E., Uetrecht, A., Bear, J. E., et al. (2008). The Sac1 Phosphoinositide Phosphatase Regulates Golgi Membrane Morphology and Mitotic Spindle Organization in Mammals. *Mol. Biol. Cell* 19, 3080–3096. doi: 10.1091/mbc.e07-12-1290

Manford, A., Xia, T., Saxena, A. K., Stefan, C., Hu, F., Emr, S. D., et al. (2010). Crystal structure of the yeast Sac1: implications for its phosphoinositide phosphatase function. *EMBO J.* 29, 1489–1498. doi: 10.1038/emboj.2010.57

Nemoto, Y., Kearns, B. G., Wenk, M. R., Chen, H., Mori, K., Alb, J. G., et al. (2000). Functional Characterization of a Mammalian Sac1 and Mutants Exhibiting Substrate-specific Defects in Phosphoinositide Phosphatase Activity*. *J. Biol. Chem.* 275, 34293–34305. doi: 10.1074/jbc.M003923200

Noack, L. C., and Jaillais, Y. (2017). Precision targeting by phosphoinositides: how PIs direct endomembrane trafficking in plants. *Curr. Opin. Plant Biol.* 40, 22–33. doi: 10.1016/j.pbi.2017.06.017

Noack, L. C., and Jaillais, Y. (2020). Functions of Anionic Lipids in Plants. *Annu. Rev. Plant Biol.* 71, 71–102. doi: 10.1146/annurev-arplant-081519-035910

Novakova, P., Hirsch, S., Feraru, E., Tejos, R., van Wijk, R., Viaene, T., et al. (2014). SAC phosphoinositide phosphatases at the tonoplast mediate vacuolar function in Arabidopsis. *Proc. Natl. Acad. Sci. U. S. A.* 111, 2818–2823. doi: 10.1073/pnas.1324264111

Novick, P., Osmond, B. C., and Botstein, D. (1989). Suppressors of yeast actin mutations. *Genetics* 121, 659–674. doi: 10.1093/genetics/121.4.659

Platre, M. P., Noack, L. C., Doumane, M., Bayle, V., Simon, M. L. A., Maneta-Peyret, L., et al. (2018). A Combinatorial Lipid Code Shapes the Electrostatic Landscape of Plant Endomembranes. *Dev. Cell* 45, 465–480.e11. doi: 10.1016/j.devcel.2018.04.011

Rudge, S. A., Anderson, D. M., and Emr, S. D. (2004). Vacuole size control: regulation of PtdIns(3,5)P2 levels by the vacuole-associated Vac14-Fig4 complex, a PtdIns(3,5)P2-specific phosphatase. *Mol. Biol. Cell* 15, 24–36. doi: 10.1091/mbc.e03-05-0297

Schiefelbein, J. W., and Somerville, C. (1990). Genetic Control of Root Hair Development in Arabidopsis thaliana. *Plant Cell* 2, 235–243. doi: 10.1105/tpc.2.3.235

Simon, M. L., Platre, M. P., Marques-Bueno, M. M., Armengot, L., Stanislas, T., Bayle, V., et al. (2016). A PtdIns(4)P-driven electrostatic field controls cell membrane identity and signalling in plants. *Nat. Plants* 2:16089. doi: 10.1038/nplants.2016.89

Simon, M. L. A., Platre, M. P., Assil, S., van Wijk, R., Chen, W. Y., Chory, J., et al. (2014). A multi-colour/multi-affinity marker set to visualize phosphoinositide dynamics in Arabidopsis. *Plant J.* 77, 322–337. doi: 10.1111/tpj.12358

Song, L., Wang, Y., Guo, Z., Lam, S. M., Shui, G., and Cheng, Y. (2021). NCP2/RHD4/SAC7, SAC6 and SAC8 phosphoinositide phosphatases are required for PtdIns4P and PtdIns(4,5)P2 homeostasis and Arabidopsis development. *New Phytol.* 231, 713–725. doi: 10.1111/nph.17402

Thole, J. M., Vermeer, J. E., Zhang, Y., Gadella, T. W. Jr., and Nielsen, E. (2008). Root hair defective4 encodes a phosphatidylinositol-4-phosphate phosphatase required for proper root hair development in Arabidopsis thaliana. *Plant Cell* 20, 381–395. doi: 10.1105/tpc.107.054304

Van Leeuwen, W., Vermeer, J. E. M., Gadella, T. W. J. Jr., and Munnik, T. (2007). Visualization of phosphatidylinositol 4,5-bisphosphate in the plasma membrane of suspension-cultured tobacco BY-2 cells and whole Arabidopsis seedlings. *Plant J.* 52, 1014–1026. doi: 10.1111/j.1365-313X.2007.03292.x

Vermeer, J. E. M., van Leeuwen, W., Tobeña-Santamaria, R., Laxalt, A. M., Jones, D. R., Divecha, N., et al. (2006). Visualization of PtdIns3P dynamics in living plant cells. *Plant J.* 47, 687–700. doi: 10.1111/j.1365-313X.2006.02830.x

Vollmer, A. H., Youssef, N. N., and DeWald, D. B. (2011). Unique cell wall abnormalities in the putative phosphoinositide phosphatase mutant AtSAC9. *Planta* 234, 993–1005. doi: 10.1007/s00425-011-1454-4

Wei, H.-C., Sanny, J., Shu, H., Baillie, D. L., Brill, J. A., Price, J. V., et al. (2003). The Sac1 Lipid Phosphatase Regulates Cell Shape Change and the JNK Cascade during Dorsal Closure in Drosophila. *Curr. Biol.* 13, 1882–1887. doi: 10.1016/j.cub.2003.09.056

Whitley, P., Hinz, S., and Doughty, J. (2009). Arabidopsis FAB1/PIKfyve Proteins Are Essential for Development of Viable Pollen. *Plant Physiol.* 151, 1812–1822. doi: 10.1104/pp.109.146159

Whitters, E. A., Cleves, A. E., McGee, T. P., Skinner, H. B., and Bankaitis, V. A. (1993). SAC1p is an integral membrane protein that influences the cellular requirement for phospholipid transfer protein function and inositol in yeast. *J. Cell Biol.* 122, 79–94. doi: 10.1083/jcb.122.1.79

Williams, M. E., Torabinejad, J., Cohick, E., Parker, K., Drake, E. J., Thompson, J. E., et al. (2005). Mutations in the Arabidopsis phosphoinositide phosphatase gene SAC9 lead to overaccumulation of PtdIns(4,5)P2 and constitutive expression of the stress-response pathway. *Plant Physiol.* 138, 686–700. doi: 10.1104/pp.105.061317

Zhang, W.-T., Li, E., Guo, Y.-K., Yu, S.-X., Wan, Z.-Y., Ma, T., et al. (2018). Arabidopsis VAC14 Is Critical for Pollen Development through Mediating Vacuolar Organization. *Plant Physiol.* 177, 1529–1538. doi: 10.1104/pp.18.00495

Zhong, R., Burk, D. H., Nairn, C. J., Wood-Jones, A., Morrison, W. H. III, and Ye, Z. H. (2005). Mutation of SAC1, an Arabidopsis SAC domain phosphoinositide phosphatase, causes alterations in cell morphogenesis, cell wall synthesis, and actin organization. *Plant Cell* 17, 1449–1466. doi: 10.1105/tpc.105.031377

Zhong, R., and Ye, Z. H. (2003). The SAC domain-containing protein gene family in Arabidopsis. *Plant Physiol.* 132, 544–555. doi: 10.1104/pp.103.021444

Conflict of Interest: The authors declare that the research was conducted in the absence of any commercial or financial relationships that could be construed as a potential conflict of interest.

Publisher's Note: All claims expressed in this article are solely those of the authors and do not necessarily represent those of their affiliated organizations, or those of the publisher, the editors and the reviewers. Any product that may be evaluated in this article, or claim that may be made by its manufacturer, is not guaranteed or endorsed by the publisher.

frontiers in Plant Science

REVIEW
published: 23 February 2022
doi: 10.3389/fpls.2022.849729

Controlling the Gate: The Functions of the Cytoskeleton in Stomatal Movement

Yihao Li[1], Xin Zhang[1], Yi Zhang[2] and Haiyun Ren[1,2]**

[1]*Center for Biological Science and Technology, Guangdong Zhuhai-Macao Joint Biotech Laboratory, Advanced Institute of Natural Science, Beijing Normal University, Zhuhai, China,* [2]*Key Laboratory of Cell Proliferation and Regulation Biology of Ministry of Education, College of Life Sciences, Beijing Normal University, Beijing, China*

Stomata are specialized epidermal structures composed of two guard cells and are involved in gas and water exchange between plants and the environment and pathogen entry into the plant interior. Stomatal movement is a response to many internal and external stimuli to increase adaptability to environmental change. The cytoskeleton, including actin filaments and microtubules, is highly dynamic in guard cells during stomatal movement, and the destruction of the cytoskeleton interferes with stomatal movement. In this review, we discuss recent progress on the organization and dynamics of actin filaments and microtubule network in guard cells, and we pay special attention to cytoskeletal-associated protein-mediated cytoskeletal rearrangements during stomatal movement. We also discuss the potential mechanisms of stomatal movement in relation to the cytoskeleton and attempt to provide a foundation for further research in this field.

Keywords: stomatal movement, actin filament, microtubule, actin-binding proteins, microtubule-associated proteins

OPEN ACCESS

Edited by:
Ying Fu,
China Agricultural University, China

Reviewed by:
Takashi Hashimoto,
Nara Institute of Science and Technology (NAIST), Japan
Yun Xiang,
Lanzhou University, China

****Correspondence:***
Yi Zhang
yi.zhang@bnu.edu.cn
Haiyun Ren
hren@bnu.edu.cn

Specialty section:
This article was submitted to Plant Physiology, a section of the journal Frontiers in Plant Science

Received: *06 January 2022*
Accepted: *26 January 2022*
Published: *23 February 2022*

Citation:
Li Y, Zhang X, Zhang Y and Ren H (2022) Controlling the Gate: The Functions of the Cytoskeleton in Stomatal Movement. Front. Plant Sci. 13:849729. doi: 10.3389/fpls.2022.849729

INTRODUCTION

The plant leaf epidermis and cuticle protect water against transpiration in relatively dry terrestrial environments but also limit gas exchange with the external environment for photosynthesis. Plants have evolved stomata on the leaf and stem epidermis; these structures consist of two kidney-shaped or dumbbell-shaped guard cells and are responsible for 95% gas exchange between the external atmosphere and the interior of the leaf (Keenan et al., 2013; Lawson and Matthews, 2020). Furthermore, stomata provide major sites for pathogen entry (Gudesblat et al., 2009; Zeng et al., 2010; Melotto et al., 2017). Plants are able to adjust stomatal opening and closure in response to environmental changes (Hetherington and Woodward, 2003; Murata et al., 2015). Hence, an attractive research system for investigations of signal transduction and physiological responses has been developed on the basis of stomatal functions.

The key factor driving stomatal movement is the turgor pressure change provoked by ions and water across plasma and vacuolar membranes, giving rise to swelling or deflation of the cells and opening or closing of the pores (Kollist et al., 2014; Woolfenden et al., 2018; Lawson and Matthews, 2020). In recent decades, a series of ion channels and transporters and their upstream regulators fine-tuning osmotic pressure in guard cells have been identified (Kollist et al., 2014; Lawson and Matthews, 2020). The activities of these channels and transporters depend on voltage sensing, ligand binding, or protein posttranslational modification. For example, the H^+-ATPase

AHA1 is activated by blue light, which leads to hyperpolarization of the plasma membrane in guard cells (Kinoshita and Shimazaki, 1999; Kinoshita et al., 2001; Hayashi et al., 2011). The change in membrane potential drives K^+ influx through KAT1/2voltage-gated K^+ channels, accompanied by anion Cl^- and malate influx (Lebaudy et al., 2010; Yamauchi et al., 2016). Increased levels of osmotically active substances further increase water uptake, resulting in the inflation of guard cells and stomatal opening.

Emerging studies provide evidences indicating that the cytoskeleton, including actin filaments (AFs) and microtubules (MTs), is considered as an important factor involved in stomatal movement, possibly *via* affecting turgor pressure in guard cells (Zhang and Fan, 2009; Khanna et al., 2014). The cytoskeleton participates in cell division and cell wall synthesis, which affect guard cell shape, structure, and mechanics (Galatis and Apostolakos, 2004; Panteris et al., 2018; Woolfenden et al., 2018; Muroyama et al., 2020). MTs guide cellulose synthesis complexes and determine cellulose microfibril orientation, which might provide high tensile strength in guard cells during stomatal movement (Woolfenden et al., 2018). On the other hand, the cytoskeleton undergoes rapid dynamic changes during stomatal movement, and stomatal movement is inhibited in cytoskeleton-deficient plants. In this review, we discuss current knowledge of cytoskeletal dynamics and their regulation in guard cells and aim to provide novel insights into the mechanisms of cytoskeleton-dependent stomatal movement.

DYNAMICS AND FUNCTIONS OF ACTIN FILAMENTS IN GUARD CELLS

Pharmacological inhibitors are commonly used to study the dynamics and functions of cytoskeleton and have demonstrated a prerequisite for actin remodeling in stomatal movement. Treatment with the AF stabilizers, such as phalloidin or jasplakinolide, inhibits stomatal closure induced by ABA, H_2O_2, and darkness, and phalloidin (but not jasplakinolide) also inhibited light-induced stomatal opening (Kim et al., 1995; MacRobbie and Kurup, 2007; Li et al., 2014). In contrast, the application of the AF-depolymerizing agent latrunculin B (but not cytochalasin B or D) accelerates ABA-induced stomatal closure, whereas cytochalasin B and D facilitate light-induced stomatal opening (Kim et al., 1995; MacRobbie and Kurup, 2007). The different effects of phalloidin versus jasplakinolide treatment and latrunculin B versus cytochalasin treatment may be due to the different mechanisms on AFs of these drugs and different drug sensitivity for plant materials. For example, latrunculin B binds to actin monomers and cytochalasin D binds to the barbed end of AF to inhibit AF polymerization. Nevertheless, these pharmacological experiments support the necessity of AFs in both stomatal opening and closing. The interconversion and configurations of AFs are highly correlated with the movement of stomatal aperture. Based on orientation, bundling and density, AF configurations in guard cells have been classified into three types during stomatal movement: (1) "radial arrays" or "radial bundles": sparse AFs or bundles are distributed radially from stomatal pores in three-dimensional projection images, and actually cortical AFs are arranged in a circular pattern in cross-sections; (2) "random meshwork": AFs are randomly distributed and organized into mesh-like networks with a high density; and (3) "longitudinal arrays": most AFs form long bundles aligned in the longitudinal direction in guard cells (Gao et al., 2008; Higaki et al., 2010; Li et al., 2014; Shimono et al., 2016; Isner et al., 2017). In general, radial array and radial bundle configurations are more likely to be present in open stomata; filaments are reorganized into promiscuous mesh-like arrangements in the transition state; and longitudinal array configurations are dominant in closed stomata (Higaki et al., 2010; Shimono et al., 2016). Consistently, live-cell imaging of AF configurations in stomatal apertures revealed that AF remodeling during stomatal movement can be summarized as follows: the cortical radial AFs in open stomata first disassemble and are randomly distributed in response to environmental or endogenous signals, followed by reassembly into long bundles that are parallel to the long axis of guard cells, leading to stomatal closure. By observing AF behaviors in guard cells in the early stage of stomatal closure induced by the bacterial flagellin peptide flg22 at the single-filament level, Zou et al. observed that the AF-bundling frequency decreased while the severing frequency increased, which contributed to rapid AF disassembly (Zou et al., 2021). Cotreatment with phalloidin inhibits ABA or darkness-induced stomatal closure, supporting the notion that AF disassembly may be a critical step for initializing stomatal closure (Gao et al., 2008).

AF dynamics is important factor regulating the activity of ion channels and NADPH oxidase at the membrane that participates in stomata movement. A study in cytochalasin D-treated guard cells evaluated the activity of plasma membrane-localized osmo-sensitive voltage-dependent inward K^+ channels and Ca^{2+}-permeable channels at the single-channel level and found that the whole-cell current was increased (Hwang et al., 1997; Liu and Luan, 1998; Zhang and Fan, 2009). In contrast, AF stabilizer phalloidin treatment restrained inward whole-cell Ca^{2+} current (Zhang and Fan, 2009). Latrunculin B treatment enhances the vacuolar efflux transient induced by 10 μM ABA (Ca^{2+} influx rather than internal Ca^{2+} release at this concentration of ABA) but inhibits that induced by 0.1 μM ABA (triggering internal Ca^{2+} release rather than Ca^{2+} influx), indicating that AFs also regulate vacuolar ion efflux transient (MacRobbie and Kurup, 2007). The depolymerization of AFs by latrunculin B also enhances ABA-induced H_2O_2 production through increasing the activity of plasma membrane-localized NADPH oxidase RbohD (Li et al., 2014). Whereas it is still poorly understood how the activity of these proteins is influenced by AF turnover, several possible mechanisms could be tested. A tethering model has been proposed in mammalian cells and *Drosophila*, where the channel is gated by tethering to the cytoskeleton for mechanosensing (Jiang et al., 2021). For examples, AFs tether Piezo channels in mammalian cells and MTs tether NOMPC channels (belonging to the TRP family) in *Drosophila* for mechanogating (Zhang et al., 2015; Wang et al., 2020). Whether a similar mechanism whereby the cytoskeleton directly controls the activity of ion channels is conserved in guard cells still awaits further investigation. The distribution patterns and dynamic properties are also critical for membrane protein function. A recent study revealed that AFs and MTs participate in the dynamics of the aquaporin AtPIP2;1 at the plasma membrane during flg22-induced stomatal closure. Lat B treatment promotes the aggregation

of AtPIP2;1 at the plasma membrane and accelerates water loss in response to flg22 (Cui et al., 2021). This study provides a new point of view on the activity of plasma membrane proteins regulated by the cytoskeleton.

Vacuoles play a critical role in the regulation of turgor pressure in guard cells. Large vacuoles invaginate to form transvascular strands in opened stomata and split into small vacuoles during stomatal closure, which contributes to changes in the volume of guard cells and the excessive storage of membrane materials (Gao et al., 2005; Tanaka et al., 2007; Yang et al., 2021). AF dynamics is also involved in regulating the morphology of vacuoles in guard cells. AFs colocalize with tonoplasts and encircle small vacuoles (Li et al., 2013). Both depolymerizing or stabilizing AFs by pharmacological agents inhibit the fusion of small vacuoles in guard cells during stomatal opening, as in other cell types (Higaki et al., 2006; Li et al., 2013; Scheuring et al., 2016). SCAB1 is a plant-specific actin-binding protein that can bind, stabilize, and cross-link AFs through dimerization (Zhao et al., 2011; Zhang et al., 2012b; Wang et al., 2015). The mutation of *SCAB1* affects the morphological remodeling of the vacuole, and an increased number of transvascular strands appear in the guard cells of *scab1* mutants (Yang et al., 2021). The ARP2/3 multi-subunit complex, containing two actin-related proteins ARP2 and ARP3, and five other actin-related protein complex units (ARPC1-5), is an important nucleation-promoting and branching factor for AFs (Deeks and Hussey, 2005; Yanagisawa et al., 2013). Vacuole fusion is impaired during stomatal opening in AF nucleator *arp2* and *arp3* mutants owing to abnormal reorganization of AFs (Li et al., 2013). AFs are also involved in vesicle trafficking from Golgi and release to vacuole (Kim et al., 2005; Akkerman et al., 2011) and the disassembly of AFs affects cargo trafficking from the Golgi complex to the vacuole (Kim et al., 2005). AP3M, the medium subunit of the AP3 complex, serves as an AF-severing protein that participates AF reorganization and vacuole morphology. The mutation of *AP3M* alters AF status in guard cells and abolishes the transportation of Golgi cargoes, such as the sucrose exporter SUC4, to the tonoplast, leading to defects in stomatal closure under drought stress (Zheng et al., 2019).

RESPONSE OF ACTIN-BINDING PROTEINS TO UPSTREAM SIGNALS IN GUARD CELLS

Actin-binding proteins (ABPs), which modulate AF nucleation, severing, bundling, polymerization, and depolymerization, alter AF dynamics to markedly respond to environmental changes (Li et al., 2015). Recent studies have demonstrated that several ABPs are involved in the regulation of stomatal movement. Mutations in the ARP2/3 complex subunits *arpc4, arpc5, arpc2* (referred to as *hsr3*), *arp2* (referred to as *wrm*), or *arp3* (referred to as *dis1*) cause a similar phenotype: reduced or abolished dark-, ABA-, and H_2O_2-induced stomatal closure and retarded light-induced stomatal opening (Jiang et al., 2012; Li et al., 2013, 2014; Isner et al., 2017). *arpc4* and *arpc5* mutants show sparser but thicker actin bundles in the guard cells of both opened and closed stomata, suggesting that AFs tend to form bundles in the mutants. AF reorganization is also hysteretic during stomatal closure in the mutants (Li et al., 2014). The ABA-induced mesh-like network organization of AFs is suppressed and thus a more radial array of AFs is retained in the *arpc2* mutant compared to the wild type (Jiang et al., 2012). Cytochalasin D can restore the defect of stomatal closure in response to ABA in the *hsr3* mutant, suggesting that ABA-induced AF disassembly is disrupted in *hsr3* (Jiang et al., 2012). The ARP2/3 complex is in an intrinsically inactive conformation, which could be converted to an active conformation by the WAVE/SCAR (WASP family Verprolin homologous protein/Suppressor of cAMP Repressor) complex (Frank et al., 2004; Deeks and Hussey, 2005; Yanagisawa et al., 2013). A mutation in the *PIR1* gene encoding a subunit of the SCAR/WAVE complex results in reduced dark-induced stomatal closure, while a normal response to ABA or $CaCl_2$ is retained, and the dark-insensitive phenotype can be restored by latrunculin B or cytochalasin D treatment (Isner et al., 2017). These results indicate that the ARP2/3 complex, along with its upstream regulator, the SCAR/WAVE complex, is required for stomatal movement through their roles in modulating AF disorganization and remodeling. However, it is still unclear how the ARP2/3 complex and the SCAR/WAVE complex contribute to AF disassembly or rearrangement in guard cells.

Actin-Depolymerizing Factor (ADF) family is a conserved class of ABPs that are involved in plant development and stress responses. The *Arabidopsis* genome encodes 11 ADF genes categorized into four subclasses (Inada, 2017; Nan et al., 2017), among which most members have conserved actin filament depolymerizing functions, while subclass III members have instead evolved filament bundling functions (Nan et al., 2017). ADF4, a member of subclass I, regulates stomatal closure in response to ABA. The *adf4* mutant displays lower AF occupancy but thicker bundles in guard cells than the wild type (Zhao et al., 2016). In contrast, the subclass III member ADF5 regulates drought- and ABA-induced stomatal closure *via* its AF-bundling activity. ABA and drought directly promote ADF5 expression mediated by ABF/AREB transcription factors in *Arabidopsis* and *Populus* (Qian et al., 2019; Yang et al., 2020). The guard cells of the *adf5* mutant exhibit fewer and thinner bundles of actin filaments in open stomata and delayed actin filament reorganization during stomatal closure (Qian et al., 2019). The activity of ADF proteins is governed by many factors, including pH, phosphorylation modifications, and phosphoinositide binding (Inada, 2017). The phosphorylation of the conserved sixth serine (Ser-6) of plant ADF1 and ADF4 inhibits their binding to AFs and therefore abolishes the AF-disassembling activity (Porter et al., 2012; Dong and Hong, 2013). Recently, Shi et al. reported that ABA accumulates and inhibits PP2Cs activity through the ABA-PYLs-PP2Cs complex, resulting in the activation of CKL2 in guard cells (Shi et al., 2021). The ABA-activated CKL2 (Casein Kinase 1-Like Protein 2) phosphorylates ADF4 at Ser-6, which contributes to AF reorganization in ABA- and drought-induced stomatal closure (Zhao et al., 2016). More AF-severing events can be observed in the *ckl2* mutant, and the severing activity of ADF4 is inhibited in the presence of CKL2 *in vitro* (Zhao et al., 2016). Ser-6, Ser-105, and Ser-106 of ADF4 can be phosphorylated by calcium-dependent protein kinase 3 (CPK3), which is required for the association with AFs, and stomatal immunity and

pattern-triggered immunity (Lu et al., 2020). Moreover, the activity of ADFs is pH sensitive (Zhang et al., 2001; Nan et al., 2017; Wioland et al., 2019). As stomatal movement is associated with changes in intracellular pH due to the influx or efflux of proton, it is plausible to speculate that pH changes may control stomatal movement at least partially by modulating the activity of ADFs.

Villin belongs to a multifunctional villin/gelsolin/fragmin superfamily that exhibits multiple biochemical activities, including AF bundling, Ca^{2+}-dependent AF severing, and barbed end capping (Huang et al., 2015). A recent study detailed investigated the functions of Villin3 in stomatal immunity. Zou et al. reported that the *vln3* mutant showed reduced AF turnover in guard cells treated with flg22, resulting in failure to close stomata upon bacterial infection (Zou et al., 2021). Flg22-activated MPK3/MPK6 phosphorylates Villin3 at Ser779 to specifically enhance its severing activity. Neither reduced AF bundling nor increased severing is observed in the guard cells of *vln3* or *mpk3/6* double mutant plants in the early stage of flg22 treatment compared to wild type. A phosphorylation mimic version of Villin3 can restore AF dynamics and stomatal movement in the *vln3* and *mpk3/6* mutants to the WT level, supporting the importance of VLN3 phosphorylation by MPK3/6 in modulating actin remodeling to activate stomatal defense in Arabidopsis (Zou et al., 2021).

Phosphoinositide exhibits an important function in stomatal movement and ABP activity regulation. The light-induced accumulation of PI (4,5)P2 triggers stomatal opening (Lee et al., 2007). Phosphatidylinositol 4-phosphate (PI4P), a precursor of PI(4,5)P2, and phosphatidylinositol 3-phosphate (PI3P) are required for light-induced stomatal opening and ABA-induced stomatal closure and modulate actin dynamics in guard cells (Jung et al., 2002; Choi et al., 2008). The PI3P and PI4P synthesis inhibitors LY294002 and wortmannin inhibit the ABA-induced random orientation of AF arrays in the guard cells of dayflower (*Commelina communis*) (Choi et al., 2008). Both overexpression and mutation of the AF cross-linking protein SCAB1 have similar effects, including a reduced rate of actin reorganization and a delay of stomatal closure induced by ABA. However, SCAB1 overexpression results in a higher frequency of bundled actin forms compared to the control, while the *scab1* mutant shows similar actin filament reorganization to the wild type (Zhao et al., 2011). Recent research has revealed that SCAB1 binds to PI3P through its RXLR-dEER PI3P-binding motifs. PI3P binding inhibits SCAB1 oligomerization, which further impairs AF destabilization and reorganization during ABA-induced stomatal closure (Yang et al., 2021). Several members of other ABP families, such as Villins and ADFs, as well as the upstream regulator of ARP2/3 complex, the WAVE/SCAR complex (Xiang et al., 2007; Zhao et al., 2010; Qin et al., 2021), bind to and are regulated by phospholipids. These interactions pose the possibility that phospholipids may regulate stomatal movement *via* multiple mechanism.

MICROTUBULE ORGANIZATION CHANGES DURING STOMATAL MOVEMENT

The function of MTs in stomatal movement has long been debated due to conflicting results from different experiments (Assmann and Baskin, 1998; Fukuda et al., 1998; Marcus et al., 2001). Assmann et al. reported that neither the microtubule-destabilizing drug colchicine nor the stabilization drug paclitaxel had any effect on stomatal opening or closing in epidermal peels of *Vicia faba* (Assmann and Baskin, 1998). Contrary results were observed by Fukuda et al. and Marcus et al., where they showed that the microtubule-destabilizing drugs propyzamide, oryzalin, and trifluralin inhibited stomatal opening and that paclitaxel treatment suppressed stomatal closing in the same material (Fukuda et al., 1998; Marcus et al., 2001). It is still unclear why these experiments resulted in totally distinct conclusion. Nevertheless, accumulating evidences from recent decades favor the notion that the MT arrays participate in stomatal movement. During light-induced stomatal opening, oryzalin treatment blocks stomatal opening (Eisinger et al., 2012a; Qu et al., 2017), while stabilization of microtubules by paclitaxel accelerates stomatal opening in a dose-dependent manner (Qu et al., 2017). ABA-, darkness-, and NO-induced stomatal closure was markedly inhibited by cotreatment with paclitaxel, but no significant changes were observed when oryzalin was applied (Zhang et al., 2008; Eisinger et al., 2012a; Qu et al., 2017; Biel et al., 2020). It has also been reported that treatment with oryzalin alone affects stomatal closure (Khanna et al., 2014).

Live-cell imaging revealed that the number and arrangement pattern of MTs in guard cells are correlated with the stomatal aperture. In open stomata, MTs radiate from the ventral side to the dorsal side in a more parallel, straighter and denser fashion relative to AF organization (Eisinger et al., 2012a; Qu et al., 2017; Biel et al., 2020). Following stomatal closing, MT structures decrease in number and become diffused. Some studies have shown that MTs completely depolymerized (Qu et al., 2017; Yu et al., 2020), while other studies have indicated that MTs are still present, but with reduced density, in closed stomata (Khanna et al., 2014; Biel et al., 2020; Yu et al., 2020; Dou et al., 2021). In the latter case, observable MTs tend to have a longitudinal arrangement and become crisscrossed or randomly patterned near the ventral side (Fukuda et al., 1998; Lahav et al., 2004; Zhang et al., 2008; Eisinger et al., 2012a; Biel et al., 2020). By using end-binding protein 1 (EB1) to label the growing plus ends of microtubules, it was observed that there were no significant changes in the number of growing ends or the growth velocity rate of microtubules during stomatal closure. This observation suggested that the reduction of microtubule density during stomatal closure was most likely resulted from microtubule disassembly (Eisinger et al., 2012a,b). Recently, increasing observations indicate that cortical microtubules are sensitive to tensile stress (Hamant et al., 2008, 2019; Gorelova et al., 2021). Based on the observations from atomic force microscopy and finite element method simulations, MT organization is found to be consistent with the tensile pattern of guard cell (Sampathkumar et al., 2014; Gorelova et al., 2021). Thus, changes in microtubule organization may be a consequence of stomatal movement.

The functions of MTs in stomata movement are still poorly understood. MTs play essential roles in determining the arrangement of cellulose microfibrils and other non-cellulosic compounds in the cell walls, which provides mechanical properties for stomatal movement (Oda, 2015; Rui and Anderson, 2016; Yi et al., 2018). MT guides the trajectories of the cellulose synthesis complexes

(CSCs) for cellulose synthesis at the cell surface (Gutierrez et al., 2009). Colocalization between CSCs and MTs is reduced and CSC motility speed increase during dark-induced stomata closure (Rui and Anderson, 2016). During stomatal movement, cellulose in guard cell walls undergoes reorganization from a more diffuse distribution in opened stomata to extensive bundles in the closed state (Rui and Anderson, 2016). MTs also determine the alignment mode of callose deposition and disassembly of MTs by oryzalin disturbs the pattern of callose deposition in the guard cell (Apostolakos et al., 2009). Thus, MT organization may impact on cell wall organization during stomatal movement and the detail mechanism deserves further investigation.

MICROTUBULE-ASSOCIATED PROTEINS AND UPSTREAM SIGNALING IN REGULATING MICROTUBULE ORGANIZATION IN GUARD CELLS

Several microtubule-associated proteins (MAPs) and their upstream regulators play vital roles in regulating MT organization and stomatal movement. WDL7, a member of the WAVE-DAMPENED2 (WVD2)/WVD2-LIKE family, directly binds to and bundles MTs *in vitro*. WDL7-overexpressing plants show delayed stomatal closure in response to ABA compared to WT plants. MTs are less sensitive to oryzalin- and ABA-induced MT disruption in WDL7-overexpressing guard cells, indicating that WDL7 serves as a MT stabilizer. Consistently, the *wdl7* mutant shows impairment of MT assembly and the stomatal opening response to light (Dou et al., 2021). WDL7 protein stability is regulated by ubiquitination. MREL57 (MICROTUBULE RELATED E3 LIGASE 57) directly targets and ubiquitinates WDL7 for degradation. *mrel57* mutant exhibits ABA insensitivity of stomatal closure and microtubule disassembly in guard cells (Dou et al., 2021). Several other ubiquitin E3 ligases, including JUL1 (JAV1-ASSOCIATED UBIQUITIN LIGASE1) and COP1 (CONSTITUTIVE PHOTOMORPHOGENIC 1), also participate in MT remodeling during stomatal movement (Khanna et al., 2014). JUL1 mediates ABA-induced microtubule disorganization and stomatal closure downstream of H_2O_2 and calcium. JUL1 binds to polymerized microtubules but not tubulin heterodimers (Yu et al., 2020). Darkness- and ABA-induced stomatal closure and MT disassembly are suppressed in the *cop1* mutant, and oryzalin is able to reduce this effect, indicating that the function of COP1 is critical for MT destabilization upon darkness and ABA treatment in guard cells (Mao et al., 2005; Khanna et al., 2014; Chen et al., 2021). It has been reported that COP1 directly ubiquitinates the MT stabilizer WDL3 in hypocotyl cells grown under darkness (Lian et al., 2017). Whether an analogous mechanism exists in guard cells requires further evaluation.

Phosphatidic acid (PA) has emerged as a vital signaling molecule involved in regulating cytoskeletal organization and dynamics under abiotic and biotic stresses, including the regulation of stomatal movement (Pleskot et al., 2013). PA is produced through the hydrolysis of phosphatidylcholine (PC) by phospholipase D (PLD) or the phosphorylation of diacylglycerol (DAG) by DAG kinase (Testerink and Munnik, 2011; Pleskot et al., 2013). Heat shock triggers ROS production to stimulate the activity of plasma membrane-localized PLDδ, and PLDδ directly binds to and disassembles MTs and causes stomatal closure under heat stress (Zhang et al., 2017; Song et al., 2020). The mutation of *PLDα1* maintains stomatal opening and well-organized MTs in the presence of ABA. Exogenous application of PA but not PC, PE or PS promotes microtubule depolymerization in stomatal cells, suggesting that PA may regulate stomatal movement through its impact on MTs (Jiang et al., 2014). However, the molecular mechanism underlying how PA induces MT depolymerization remains unclear. It has been reported that PA binds to MAP65-1 and promotes MT polymerization and bundling under salt stress (Zhang et al., 2012a). It still needs to be explored whether PA activates a MAP or a signaling pathway to disassemble MTs in guard cells.

SINE1 and SINE2 (SUN-INTERACTING NUCLEAR ENVELOPE PROTEIN 1 AND2), which are two components of the plant LINC (LINKER OF NUCLEOSKELETON AND CYTOSKELETON) complex, are involved in regulating the reorganization of MTs in guard cells during stomatal movement. The loss of function of either *SINE1* or *SINE2* results in a disordered MT organization in open stomata (Biel et al., 2020). There are fewer MT filaments or bundles in *sine 1* or *sine 2* mutants compared to the wild type during stomatal closure, leading to insensitivity to ABA-induced stomatal closure (Biel et al., 2020). Translationally controlled tumor protein (TCTP) is a calcium- and tubulin-binding protein, and the binding of calcium facilitates TCTP binding to microtubules. The overexpression of TCTP increases ABA- and calcium-induced stomatal closure ratios to limit water evaporation by accelerating MT depolymerization (Kim et al., 2012). The detailed characterization of the biochemical activities of SINE1/2 and TCTP toward MTs should be further defined.

CONCLUSION AND PERSPECTIVE

Based on the knowledge available, we propose a model of current progress about AF and MT dynamics that are regulated by different functional ABPs and MAPs during stomatal movement. In opened stomata, the ARP2/3 complex is activated by WAVE/SCAR complex and promotes AF nucleation and branching, contributing to AF network formation. In the transition stage of stomatal closure, AF-severing factors, such ADF4 and Villin3, lead to AF depolymerization, and an increasing content of PI3P inhibits the cross-linking function of SCAB1, promoting the disassembly of the AF network. Subsequently, the phosphorylation of ADF4 inhibits its severing activity, and the upregulation of *ADF5* and SCAB1 dimer contributes to the formation of long AF bundles in closed stomata. WDL7 binds and stabiles MT in opened stomata. During ABA-induced stomatal closing, E3 ligase MREL57 ubiquitinates WDL7 for degradation; ABA-triggered calcium influx activated TCTP to stimulate MT disassembly. PLDδ activated in an H_2O_2- and calcium-dependent manner and disassembles MTs upon heat stress (**Figure 1**).

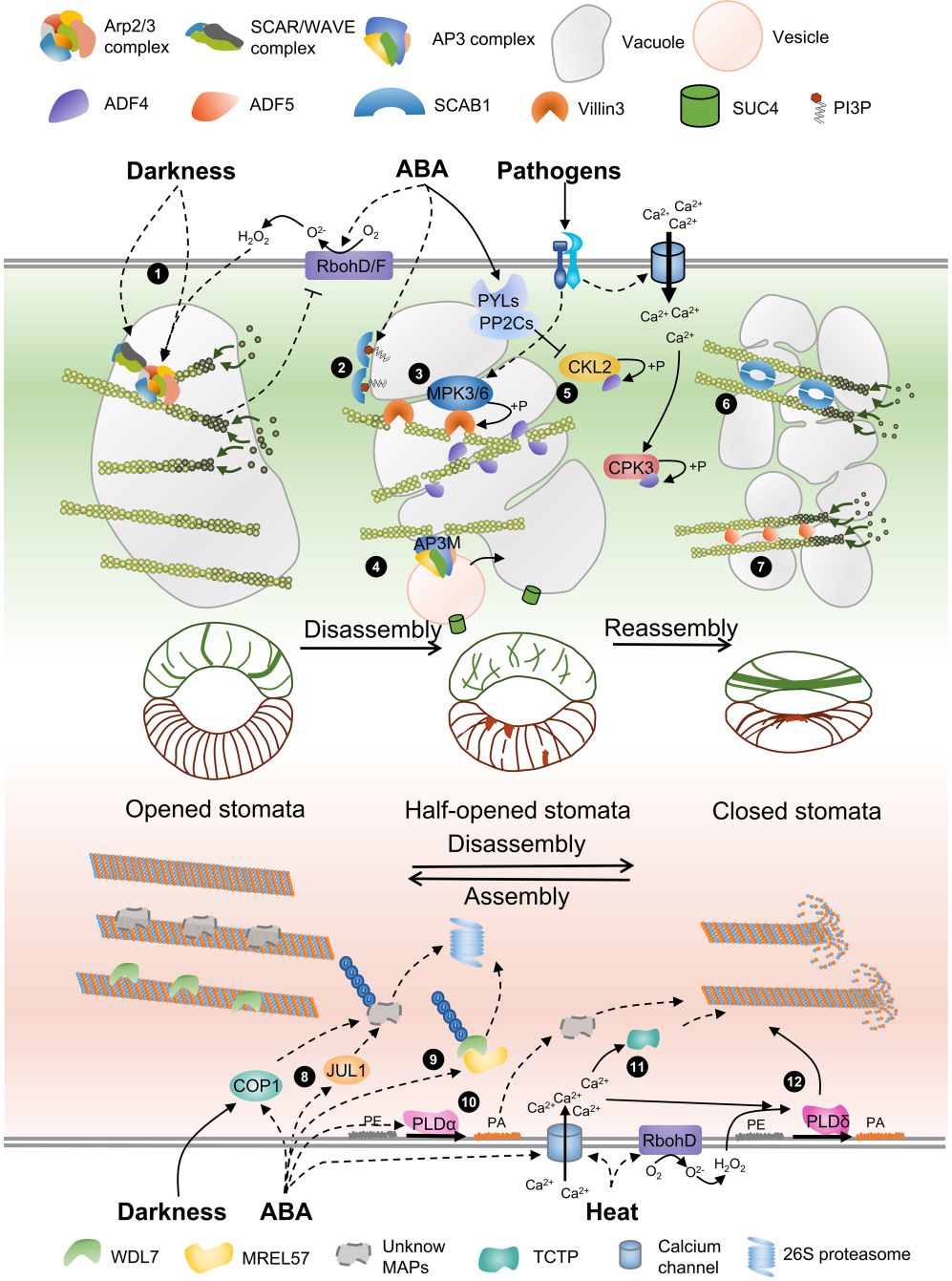

FIGURE 1 | A schematic model of AF and MT remodeling accompanied by vacuole morphology during stomatal closure. The schematic model of stomata in the middle of the panel shows the distribution of AFs and MTs in guard cells with different stomatal apertures. The gray circular charts present the different morphology of vacuole during stomata movement. Several actin-binding proteins and microtubule-associated proteins are involved in regulating cytoskeletal rearrangement. (1) The Arp2/3 complex and the activator SCAR/WAVE complex are required for AF nucleation and branching, and darkness-induced stomata closure. ABA-triggered H_2O_2 generation by RbohD/RbohF regulates AF dynamics through the Arp2/3 complex but does not regulate the SCAR/WAVE complex, and AF feedback regulates H_2O_2 production. (2) ABA-triggered PI3P biosynthesis inhibits the oligomerization of SCAB1. (3) A pathogen triggers MPK3/MPK6 activation, and Villin3 is then phosphorylated to increase AF-severing activity. (4) AP3M of the AP3 complex severs AFs and regulates vesicles from Golgi carrying SUC4 fused to the tonoplast. (5) ADF4 binds to and severs AFs, and ABA-activated CKL2 and calcium-activated CPK32 induced by pathogens phosphorylate ADF4 to inhibit its activity and promote AF reorganization. (6 and 7) SCAB1 dimers and ADF5 monomers bundle and stabilize AFs and promote AF reassembly. (8) JUL1 and COP1, two other E3 ubiquitin ligases, may control the degradation of unknown MT-stabilizing factors and promote MT disassembly. (9) WDL7 stabilizes MTs in open stomata. The E3 ubiquitin ligase MREL57 interacts with and ubiquitinates WDL7 for 26S proteasome degradation during ABA-induced stomatal closure. (10) ABA-triggered PA produced by PLDα induces MT depolymerization through an unknown mechanism. (11) An ABA-induced increase in cytosolic calcium increases TCTP binding to MTs and MT destabilization. (12) Heat shock stimulates H_2O_2 production, and calcium influx activates PLDδ, which is required for MT depolymerization.

Although the dynamic distribution of AFs and MTs during stomatal movement has been reported, the underlying molecular mechanism is still not well understood. Additional ABPs, MAPs and upstream proteins involved in stomatal movement need to be detailed analyzed, which will facilitate to dissect the roles of cytoskeleton in transducing environmental signals to stomatal movement. The arrangement mode of AFs and MTs is somewhat similar in guard cells, posing the possibility that they may coordinate to control stomata movement. Some ABPs, such as formin proteins, have been reported to interact with both AFs and MTs (Li et al., 2010; Wang et al., 2013; Sun et al., 2017). It is worthy to further investigate the interaction between AFs and MTs, as well as the underlying molecular mechanism in stomata. Although many evidences have demonstrated the potential for cytoskeleton in regulating the activity of ion channels, vesicles trafficking, and cell wall dynamics of guard cell, the detailed mechanisms need to be explored in further for advancing our understanding of the cytoskeleton function contributed to stomatal movement.

Stomata are of great importance in the response and adaptation of plants to environmental changes. Previous research in this context has mainly focused on kidney-shaped guard cells in *Arabidopsis*, *Vicia,* and tobacco. The distribution of AFs and MTs in dumbbell-shaped guard cells in most crop plants is different from that in kidney-shaped guard cells (Spiegelhalder and Raissig, 2021). Advances in research on cytoskeletal dynamics in dumbbell-shaped guard cells remain relatively stagnant. Studies on the mechanisms of stomatal movement in crops will help to improve the efficiency of carbon assimilation and water use under the trend of global warming.

AUTHOR CONTRIBUTIONS

YL and XZ collected the references and wrote the manuscript. YZ and HR revised the manuscript. All authors have read and approved the final manuscript.

FUNDING

This work was supported by the National Natural Science Foundation of China (91854206 and 32170335 to HR; 31870174 and 32070194 to YZ).

REFERENCES

Akkerman, M., Overdijk, E. J., Schel, J. H., Emons, A. M., and Ketelaar, T. (2011). Golgi body motility in the plant cell cortex correlates with actin cytoskeleton organization. *Plant Cell Physiol.* 52, 1844–1855. doi: 10.1093/pcp/pcr122

Apostolakos, P., Livanos, P., and Galatis, B. (2009). Microtubule involvement in the deposition of radial fibrillar callose arrays in stomata of the fern *Asplenium nidus* L. *Cell Motil Cytoskel.* 66, 342–349. doi: 10.1002/cm.20366

Assmann, S. M., and Baskin, T. I. (1998). The function of guard cells does not require an intact array of cortical microtubules. *J. Exp. Bot.* 49, 163–170. doi: 10.1093/jxb/49.319.163

Biel, A., Moser, M., and Meier, I. (2020). *Arabidopsis* KASH proteins SINE1 and SINE2 are involved in microtubule reorganization during ABA-induced stomatal closure. *Front. Plant Sci.* 11:575573. doi: 10.3389/fpls.2020.575573

Chen, Q., Bai, L., Wang, W., Shi, H., Ramon Botella, J., Zhan, Q., et al. (2021). COP1 promotes ABA-induced stomatal closure by modulating the abundance of ABI/HAB and AHG3 phosphatases. *New Phytol.* 229, 2035–2049. doi: 10.1111/nph.17001

Choi, Y., Lee, Y., Jeon, B. W., Staiger, C. J., and Lee, Y. (2008). Phosphatidylinositol 3- and 4-phosphate modulate actin filament reorganization in guard cells of day flower. *Plant Cell Environ.* 31, 366–377. doi: 10.1111/j.1365-3040.2007.01769.x

Cui, Y., Zhao, Y., Lu, Y., Su, X., Chen, Y., Shen, Y., et al. (2021). In vivo single-particle tracking of the aquaporin AtPIP2;1 in stomata reveals cell type-specific dynamics. *Plant Physiol.* 185, 1666–1681. doi: 10.1093/plphys/kiab007

Deeks, M. J., and Hussey, P. J. (2005). ARP2/3 and SCAR: plants move to the fore. *Nat. Rev. Mol. Cell Biol.* 6, 954–964. doi: 10.1038/nrm1765

Dong, C. H., and Hong, Y. (2013). *Arabidopsis* CDPK6 phosphorylates ADF1 at N-terminal serine 6 predominantly. *Plant Cell Rep.* 32, 1715–1728. doi: 10.1007/s00299-013-1482-6

Dou, L., He, K., Peng, J., Wang, X., and Mao, T. (2021). The E3 ligase MREL57 modulates microtubule stability and stomatal closure in response to ABA. *Nat. Commun.* 12:2181. doi: 10.1038/s41467-021-22455-y

Eisinger, W., Ehrhardt, D., and Briggs, W. (2012a). Microtubules are essential for guard cell function in *Vicia* and *Arabidopsis*. *Mol. Plant* 5, 601–610. doi: 10.1093/mp/sss002

Eisinger, W. R., Kirik, V., Lewis, C., Ehrhardt, D. W., and Briggs, W. R. (2012b). Quantitative changes in microtubule distribution correlate with guard cell function in *Arabidopsis*. *Mol. Plant* 5, 716–725. doi: 10.1093/mp/sss033

Frank, M., Egile, C., Dyachok, J., Djakovic, S., Nolasco, M., Li, R., et al. (2004). Activation of ARP2/3 complex-dependent actin polymerization by plant proteins distantly related to SCAR/WAVE. *Proc. Natl. Acad. Sci. U. S. A.* 101, 16379–16384. doi: 10.1073/pnas.0407392101

Fukuda, M., Hasezawa, S., Asai, N., Nakajima, N., and Kondo, N. (1998). Dynamic organization of microtubules in guard cells of *Vicia faba* L. with diurnal cycle. *Plant Cell Physiol.* 39:80. doi: 10.1093/oxfordjournals.pcp.a029293

Galatis, B., and Apostolakos, P. (2004). The role of the cytoskeleton in the morphogenesis and function of stomatal complexes. *New Phytol.* 161, 613–639. doi: 10.1046/j.1469-8137.2003.00986.x

Gao, X. Q., Chen, J., Wei, P. C., Ren, F., Chen, J., and Wang, X. C. (2008). Array and distribution of actin filaments in guard cells contribute to the determination of stomatal aperture. *Plant Cell Rep.* 27, 1655–1665. doi: 10.1007/s00299-008-0581-2

Gao, X. Q., Li, C. G., Wei, P. C., Zhang, X. Y., and Wang, X. C. (2005). The dynamic changes of tonoplasts in guard cells are important for stomatal movement in *Vicia faba*. *Plant Physiol.* 139, 1207–1216. doi: 10.1104/pp.105.067520

Gorelova, V., Sprakel, J., and Weijers, D. (2021). Plant cell polarity as the nexus of tissue mechanics and morphogenesis. *Nat. Plants.* 7, 1548–1559. doi: 10.1038/s41477-021-01021-w

Gudesblat, G. E., Torres, P. S., and Vojnov, A. A. (2009). Stomata and pathogens: warfare at the gates. *Plant Signal. Behav.* 4, 1114–1116. doi: 10.4161/psb.4.12.10062

Gutierrez, R., Lindeboom, J. J., Paredez, A. R., Emons, A. M., and Ehrhardt, D. W. (2009). *Arabidopsis* cortical microtubules position cellulose synthase delivery to the plasma membrane and interact with cellulose synthase trafficking compartments. *Nat. Cell Biol.* 11, 797–806. doi: 10.1038/ncb1886

Hamant, O., Heisler, M. G., Jonsson, H., Krupinski, P., Uyttewaal, M., Bokov, P., et al. (2008). Developmental patterning by mechanical signals in *Arabidopsis*. *Science* 322, 1650–1655. doi: 10.1126/science.1165594

Hamant, O., Inoue, D., Bouchez, D., Dumais, J., and Mjolsness, E. (2019). Are microtubules tension sensors? *Nat. Commun.* 10:2360. doi: 10.1038/s41467-019-10207-y

Hayashi, M., Inoue, S., Takahashi, K., and Kinoshita, T. (2011). Immunohistochemical detection of blue light-induced phosphorylation of the plasma membrane H^+-ATPase in stomatal guard cells. *Plant Cell Physiol.* 52, 1238–1248. doi: 10.1093/pcp/pcr072

Hetherington, A. M., and Woodward, F. I. (2003). The role of stomata in sensing and driving environmental change. *Nature* 424, 901–908. doi: 10.1038/nature01843

Higaki, T., Kutsuna, N., Okubo, E., Sano, T., and Hasezawa, S. (2006). Actin microfilaments regulate vacuolar structures and dynamics: dual observation of actin microfilaments and vacuolar membrane in living tobacco BY-2 cells. *Plant Cell Physiol.* 47, 839–852. doi: 10.1093/pcp/pcj056

Higaki, T., Kutsuna, N., Sano, T., Kondo, N., and Hasezawa, S. (2010). Quantification and cluster analysis of actin cytoskeletal structures in plant cells: role of actin bundling in stomatal movement during diurnal cycles in *Arabidopsis* guard cells. *Plant J.* 61, 156–165. doi: 10.1111/j.1365-313x.2009.04032.x

Huang, S., Qu, X., and Zhang, R. (2015). Plant villins: versatile actin regulatory proteins. *J. Integr. Plant Biol.* 57, 40–49. doi: 10.1111/jipb.12293

Hwang, J. U., Suh, S., Yi, H. J., Kim, J., and Lee, Y. (1997). Actin filaments modulate both stomatal opening and inward K^+-channel activities in guard cells of *Vicia faba* L. *Plant Physiol.* 115, 335–342. doi: 10.1104/Pp.115.2.335

Inada, N. (2017). Plant actin depolymerizing factor: actin microfilament disassembly and more. *J. Plant Res.* 130, 227–238. doi: 10.1007/s10265-016-0899-8

Isner, J. C., Xu, Z., Costa, J. M., Monnet, F., Batstone, T., Ou, X., et al. (2017). Actin filament reorganisation controlled by the SCAR/WAVE complex mediates stomatal response to darkness. *New Phytol.* 215, 1059–1067. doi: 10.1111/nph.14655

Jiang, K., Sorefan, K., Deeks, M. J., Bevan, M. W., Hussey, P. J., and Hetherington, A. M. (2012). The ARP2/3 complex mediates guard cell actin reorganization and stomatal movement in *Arabidopsis*. *Plant Cell* 24, 2031–2040. doi: 10.1105/tpc.112.096263

Jiang, Y., Wu, K., Lin, F., Qu, Y., Liu, X., and Zhang, Q. (2014). Phosphatidic acid integrates calcium signaling and microtubule dynamics into regulating ABA-induced stomatal closure in *Arabidopsis*. *Planta* 239, 565–575. doi: 10.1007/s00425-013-1999-5

Jiang, Y., Yang, X., Jiang, J., and Xiao, B. (2021). Structural designs and mechanogating mechanisms of the mechanosensitive PIEZO channels. *Trends Biochem. Sci.* 46, 472–488. doi: 10.1016/j.tibs.2021.01.008

Jung, J.-Y., Kim, Y.-W., Kwak, J. M., Hwang, J.-U., Young, J., Schroeder, J. I., et al. (2002). Phosphatidylinositol 3- and 4-phosphate are required for normal stomatal movements. *Plant Cell* 14, 2399–2412. doi: 10.1105/tpc.004143

Keenan, T. F., Hollinger, D. Y., Bohrer, G., Dragoni, D., Munger, J. W., Schmid, H. P., et al. (2013). Increase in forest water-use efficiency as atmospheric carbon dioxide concentrations rise. *Nature* 499, 324–327. doi: 10.1038/nature12291

Khanna, R., Li, J., Tseng, T. S., Schroeder, J. I., Ehrhardt, D. W., and Briggs, W. R. (2014). COP1 jointly modulates cytoskeletal processes and electrophysiological responses required for stomatal closure. *Mol. Plant* 7, 1441–1454. doi: 10.1093/mp/ssu065

Kim, Y. M., Han, Y. J., Hwang, O. J., Lee, S. S., Shin, A. Y., Kim, S. Y., et al. (2012). Overexpression of *Arabidopsis* translationally controlled tumor protein gene AtTCTP enhances drought tolerance with rapid ABA-induced stomatal closure. *Mol. Cells* 33, 617–626. doi: 10.1007/s10059-012-0080-8

Kim, M., Hepler, P. K., Eun, S. O., Ha, K. S., and Lee, Y. (1995). Actin filaments in mature guard cells are radially distributed and involved in stomatal movement. *Plant Physiol.* 109, 1077–1084. doi: 10.1104/pp.109.3.1077

Kim, H., Park, M., Kim, S. J., and Hwang, I. (2005). Actin filaments play a critical role in vacuolar trafficking at the Golgi complex in plant cells. *Plant Cell* 17, 888–902. doi: 10.1105/tpc.104.028829

Kinoshita, T., Doi, M., Suetsugu, N., Kagawa, T., Wada, M., and Shimazaki, K. (2001). PHOT1 and PHOT2 mediate blue light regulation of stomatal opening. *Nature* 414:656. doi: 10.1038/414656a

Kinoshita, T., and Shimazaki, K. (1999). Blue light activates the plasma membrane H^+-ATPase by phosphorylation of the C-terminus in stomatal guard cells. *EMBO J.* 18, 5548–5558. doi: 10.1093/emboj/18.20.5548

Kollist, H., Nuhkat, M., and Roelfsema, M. R. (2014). Closing gaps: linking elements that control stomatal movement. *New Phytol.* 203, 44–62. doi: 10.1111/nph.12832

Lahav, M., Abu-Abied, M., Belausov, E., Schwartz, A., and Sadot, E. (2004). Microtubules of guard cells are light sensitive. *Plant Cell Physiol.* 45, 573–582. doi: 10.1093/pcp/pch067

Lawson, T., and Matthews, J. (2020). Guard cell metabolism and stomatal function. *Annu. Rev. Plant Biol.* 71, 273–302. doi: 10.1146/annurev-arplant-050718-100251

Lebaudy, A., Pascaud, F., Very, A. A., Alcon, C., Dreyer, I., Thibaud, J. B., et al. (2010). Preferential KAT1-KAT2 heteromerization determines inward K^+ current properties in *Arabidopsis* guard cells. *J. Biol. Chem.* 285, 6265–6274. doi: 10.1074/jbc.M109.068445

Lee, Y., Kim, Y. W., Jeon, B. W., Park, K. Y., Suh, S. J., Seo, J., et al. (2007). Phosphatidylinositol 4,5-bisphosphate is important for stomatal opening. *Plant J.* 52, 803–816. doi: 10.1111/j.1365-313X.2007.03277.x

Li, J., Blanchoin, L., and Staiger, C. J. (2015). Signaling to actin stochastic dynamics. *Annu. Rev. Plant Biol.* 66, 415–440. doi: 10.1146/annurev-arplant-050213-040327

Li, X., Li, J. H., Wang, W., Chen, N. Z., Ma, T. S., Xi, Y. N., et al. (2014). ARP2/3 complex-mediated actin dynamics is required for hydrogen peroxide-induced stomatal closure in *Arabidopsis*. *Plant Cell Environ.* 37, 1548–1560. doi: 10.1111/pce.12259

Li, L. J., Ren, F., Gao, X. Q., Wei, P. C., and Wang, X. C. (2013). The reorganization of actin filaments is required for vacuolar fusion of guard cells during stomatal opening in *Arabidopsis*. *Plant Cell Environ.* 36, 484–497. doi: 10.1111/j.1365-3040.2012.02592.x

Li, Y., Shen, Y., Cai, C., Zhong, C., Zhu, L., Yuan, M., et al. (2010). The type II *Arabidopsis* formin14 interacts with microtubules and microfilaments to regulate cell division. *Plant Cell* 22, 2710–2726. doi: 10.1105/tpc.110.075507

Lian, N., Liu, X., Wang, X., Zhou, Y., Li, H., Li, J., et al. (2017). COP1 mediates dark-specific degradation of microtubule-associated protein WDL3 in regulating *Arabidopsis* hypocotyl elongation. *Proc. Natl. Acad. Sci. U. S. A.* 114, 12321–12326. doi: 10.1073/pnas.1708087114

Liu, K., and Luan, S. (1998). Voltage-dependent K^+ channels as targets of osmosensing in guard cells. *Plant Cell* 10, 1957–1970. doi: 10.1105/tpc.10.11.1957

Lu, Y. J., Li, P., Shimono, M., Corrion, A., Higaki, T., He, S. Y., et al. (2020). *Arabidopsis* CALCIUM-DEPENDENT PROTEIN KINASE 3 regulates actin cytoskeleton organization and immunity. *Nat. Commun.* 11:6234. doi: 10.1038/s41467-020-20007-4

MacRobbie, E. A. C., and Kurup, S. (2007). Signalling mechanisms in the regulation of vacuolar ion release in guard cells. *New Phytol.* 175, 630–640. doi: 10.1111/j.1469-8137.2007.02131.x

Mao, J., Zhang, Y. C., Sang, Y., Li, Q. H., and Yang, H. Q. (2005). From the cover: a role for *Arabidopsis* cryptochromes and COP1 in the regulation of stomatal opening. *Proc. Natl. Acad. Sci. U. S. A.* 102, 12270–12275. doi: 10.1073/pnas.0501011102

Marcus, A. I., Moore, R. C., and Cyr, R. J. (2001). The role of microtubules in guard cell function. *Plant Physiol.* 125, 387–395. doi: 10.1104/Pp.125.1.387

Melotto, M., Zhang, L., Oblessuc, P. R., and He, S. Y. (2017). Stomatal defense a decade later. *Plant Physiol.* 174, 561–571. doi: 10.1104/pp.16.01853

Murata, Y., Mori, I. C., and Munemasa, S. (2015). Diverse stomatal signaling and the signal integration mechanism. *Annu. Rev. Plant Biol.* 66, 369–392. doi: 10.1146/annurev-arplant-043014-114707

Muroyama, A., Gong, Y., and Bergmann, D. C. (2020). Opposing, polarity-driven nuclear migrations underpin asymmetric divisions to pattern *Arabidopsis* stomata. *Curr. Biol.* 30, 4467.e4–4475.e4. doi: 10.1016/j.cub.2020.08.100

Nan, Q., Qian, D., Niu, Y., He, Y., Tong, S., Niu, Z., et al. (2017). Plant actin-depolymerizing factors possess opposing biochemical properties arising from key amino acid changes throughout evolution. *Plant Cell* 29, 395–408. doi: 10.1105/tpc.16.00690

Oda, Y. (2015). Cortical microtubule rearrangements and cell wall patterning. *Front. Plant Sci.* 6:236. doi: 10.3389/fpls.2015.00236

Panteris, E., Achlati, T., Daras, G., and Rigas, S. (2018). Stomatal complex development and F-actin organization in maize leaf epidermis depend on cellulose synthesis. *Molecules* 23:1365. doi: 10.3390/molecules23061365

Pleskot, R., Li, J., Zarsky, V., Potocky, M., and Staiger, C. J. (2013). Regulation of cytoskeletal dynamics by phospholipase D and phosphatidic acid. *Trends Plant Sci.* 18, 496–504. doi: 10.1016/j.tplants.2013.04.005

Porter, K., Shimono, M., Tian, M., and Day, B. (2012). *Arabidopsis* ACTIN-DEPOLYMERIZING FACTOR-4 links pathogen perception, defense activation and transcription to cytoskeletal dynamics. *PLoS Pathog.* 8:e1003006. doi: 10.1371/journal.ppat.1003006

Qian, D., Zhang, Z., He, J., Zhang, P., Ou, X., Li, T., et al. (2019). *Arabidopsis* ADF5 promotes stomatal closure by regulating actin cytoskeleton remodeling in response to ABA and drought stress. *J. Exp. Bot.* 70, 435–446. doi: 10.1093/jxb/ery385

Qin, L., Liu, L., Tu, J., Yang, G., Wang, S., Quilichini, T. D., et al. (2021). The ARP2/3 complex, acting cooperatively with class I formins, modulates penetration resistance in *Arabidopsis* against powdery mildew invasion. *Plant Cell* 33, 3151–3175. doi: 10.1093/plcell/koab170

Qu, Y., Song, P., Hu, Y., Jin, X., Jia, Q., Zhang, X., et al. (2017). Regulation of stomatal movement by cortical microtubule organization in response to darkness and ABA signaling in *Arabidopsis*. *Plant Growth Regul.* 84, 467–479. doi: 10.1007/s10725-017-0353-5

Rui, Y., and Anderson, C. T. (2016). Functional analysis of cellulose and xyloglucan in the walls of stomatal guard cells of *Arabidopsis*. *Plant Physiol.* 170, 1398–1419. doi: 10.1104/pp.15.01066

Sampathkumar, A., Krupinski, P., Wightman, R., Milani, P., Berquand, A., Boudaoud, A., et al. (2014). Subcellular and supracellular mechanical stress prescribes cytoskeleton behavior in *Arabidopsis* cotyledon pavement cells. *Elife* 3:e01967. doi: 10.7554/eLife.01967

Scheuring, D., Lofke, C., Kruger, F., Kittelmann, M., Eisa, A., Hughes, L., et al. (2016). Actin-dependent vacuolar occupancy of the cell determines auxin-induced growth repression. *Proc. Natl. Acad. Sci. U. S. A.* 113, 452–457. doi: 10.1073/pnas.1517445113

Shi, Y., Liu, X., Zhao, S., and Guo, Y. (2021). The PYR-PP2C-CKL2 module regulates ABA-mediated actin reorganization during stomatal closure. *New Phytol.* 233, 2168–2184. doi: 10.1111/nph.17933

Shimono, M., Higaki, T., Kaku, H., Shibuya, N., Hasezawa, S., and Day, B. (2016). Quantitative evaluation of stomatal cytoskeletal patterns during the activation of immune signaling in *Arabidopsis thaliana*. *PLoS One* 11:e0159291. doi: 10.1371/journal.pone.0159291

Song, P., Jia, Q., Chen, L., Jin, X., Xiao, X., Li, L., et al. (2020). Involvement of *Arabidopsis* phospholipase D δ in regulation of ROS-mediated microtubule organization and stomatal movement upon heat shock. *J. Exp. Bot.* 71, 6555–6570. doi: 10.1093/jxb/eraa359

Spiegelhalder, R. P., and Raissig, M. T. (2021). Morphology made for movement: formation of diverse stomatal guard cells. *Curr. Opin. Plant Biol.* 63:102090. doi: 10.1016/j.pbi.2021.102090

Sun, T., Li, S., and Ren, H. (2017). OsFH15, a class I formin, interacts with microfilaments and microtubules to regulate grain size via affecting cell expansion in rice. *Sci. Rep.* 7:6538. doi: 10.1038/s41598-017-06431-5

Tanaka, Y., Kutsuna, N., Kanazawa, Y., Kondo, N., Hasezawa, S., and Sano, T. (2007). Intra-vacuolar reserves of membranes during stomatal closure: the possible role of guard cell vacuoles estimated by 3-D reconstruction. *Plant Cell Physiol.* 48, 1159–1169. doi: 10.1093/pcp/pcm085

Testerink, C., and Munnik, T. (2011). Molecular, cellular, and physiological responses to phosphatidic acid formation in plants. *J. Exp. Bot.* 62, 2349–2361. doi: 10.1093/jxb/err079

Wang, J., Jiang, J., Yang, X., Wang, L., and Xiao, B. (2020). Tethering Piezo channels to the actin cytoskeleton for mechanogating via the E-cadherin-β-catenin mechanotransduction complex. bioRxiv [Preprint].

Wang, J., Zhang, Y., Wu, J., Meng, L., and Ren, H. (2013). AtFH16, an *Arabidopsis* type II formin, binds and bundles both microfilaments and microtubules, and preferentially binds to microtubules. *J. Integr. Plant Biol.* 55, 1002–1015. doi: 10.1111/jipb.12089

Wang, C., Zheng, Y., Zhao, Y., Zhao, Y., Li, J., and Guo, Y. (2015). SCAB3 is required for reorganization of actin filaments during light quality changes. *J. Genet. Genomics* 42, 161–168. doi: 10.1016/j.jgg.2015.02.005

Wioland, H., Jegou, A., and Romet-Lemonne, G. (2019). Quantitative variations with ph of actin depolymerizing factor/cofilin's multiple actions on actin filaments. *Biochemistry* 58, 40–47. doi: 10.1021/acs.biochem.8b01001

Woolfenden, H. C., Baillie, A. L., Gray, J. E., Hobbs, J. K., Morris, R. J., and Fleming, A. J. (2018). Models and mechanisms of stomatal mechanics. *Trends Plant Sci.* 23, 822–832. doi: 10.1016/j.tplants.2018.06.003

Xiang, Y., Huang, X., Wang, T., Zhang, Y., Liu, Q., Hussey, P. J., et al. (2007). ACTIN BINDING PROTEIN 29 from Lilium pollen plays an important role in dynamic actin remodeling. *Plant Cell* 19, 1930–1946. doi: 10.1105/tpc.106.048413

Yamauchi, S., Takemiya, A., Sakamoto, T., Kurata, T., Tsutsumi, T., Kinoshita, T., et al. (2016). The plasma membrane H^+-ATPase AHA1 plays a major role in stomatal opening in response to blue light. *Plant Physiol.* 171, 2731–2743. doi: 10.1104/pp.16.01581

Yanagisawa, M., Zhang, C., and Szymanski, D. B. (2013). ARP2/3-dependent growth in the plant kingdom: SCARs for life. *Front. Plant Sci.* 4:166. doi: 10.3389/fpls.2013.00166

Yang, Y., Li, H. G., Wang, J., Wang, H. L., He, F., Su, Y., et al. (2020). ABF3 enhances drought tolerance via promoting ABA-induced stomatal closure by directly regulating ADF5 in Populus euphratica. *J. Exp. Bot.* 71, 7270–7285. doi: 10.1093/jxb/eraa383

Yang, Y., Yang, Y., Zhao, Y., Zheng, W., Zhao, Y., Zhao, S., et al. (2021). Phosphatidylinositol 3-phosphate regulates SCAB1-mediated F-actin reorganization during stomatal closure in *Arabidopsis*. *Plant Cell* 34, 477–494. doi: 10.1093/plcell/koab264

Yi, H., Rui, Y., Kandemir, B., Wang, J. Z., Anderson, C. T., and Puri, V. M. (2018). Mechanical effects of cellulose, xyloglucan, and pectins on stomatal guard cells of *Arabidopsis* thaliana. *Front. Plant Sci.* 9:1566. doi: 10.3389/fpls.2018.01566

Yu, S. G., Kim, J. H., Cho, N. H., Oh, T. R., and Kim, W. T. (2020). *Arabidopsis* RING E3 ubiquitin ligase JUL1 participates in ABA-mediated microtubule depolymerization, stomatal closure, and tolerance response to drought stress. *Plant J.* 103, 824–842. doi: 10.1111/tpj.14775

Zeng, W., Melotto, M., and He, S. Y. (2010). Plant stomata: a checkpoint of host immunity and pathogen virulence. *Curr. Opin. Biotechnol.* 21, 599–603. doi: 10.1016/j.copbio.2010.05.006

Zhang, X., Dong, F. C., Gao, J. F., and Song, C. P. (2001). Hydrogen peroxide-induced changes in intracellular pH of guard cells precede stomatal closure. *Cell Res.* 11, 37–43. doi: 10.1038/sj.cr.7290064

Zhang, W., and Fan, L. M. (2009). Actin dynamics regulates voltage-dependent calcium-permeable channels of the Vicia faba guard cell plasma membrane. *J. Integr. Plant Biol.* 51, 912–921. doi: 10.1111/j.1744-7909.2009.00859.x

Zhang, Q., Lin, F., Mao, T., Nie, J., Yan, M., Yuan, M., et al. (2012a). Phosphatidic acid regulates microtubule organization by interacting with MAP65-1 in response to salt stress in *Arabidopsis*. *Plant Cell* 24, 4555–4576. doi: 10.1105/tpc.112.104182

Zhang, Q., Song, P., Qu, Y., Wang, P., Jia, Q., Guo, L., et al. (2017). Phospholipase Dδ negatively regulates plant thermotolerance by destabilizing cortical microtubules in *Arabidopsis*. *Plant Cell Environ.* 40, 2220–2235. doi: 10.1111/pce.13023

Zhang, W., Cheng, L. E., Kittelmann, M., Li, J., Petkovic, M., Cheng, T., et al. (2015). Ankyrin repeats convey force to gate the NOMPC mechanotransduction channel. *Cell* 162, 1391–1403.

Zhang, Y., Wu, Z., Wang, X., and Yu, R. (2008). Rearrangements of microtubule cytoskeleton in stomatal closure of *Arabidopsis* induced by nitric oxide. *Sci. Bull.* 53, 848–852. doi: 10.1007/s11434-008-0142-7

Zhang, W., Zhao, Y., Guo, Y., and Ye, K. (2012b). Plant actin-binding protein SCAB1 is dimeric actin cross-linker with a typical pleckstrin homology domain. *J. Biol. Chem.* 287, 11981–11990. doi: 10.1074/jbc.M111.338525

Zhao, H., Hakala, M., and Lappalainen, P. (2010). ADF/cofilin binds phosphoinositides in a multivalent manner to act as a PIP_2-density sensor. *Biophys. J.* 98, 2327–2336. doi: 10.1016/j.bpj.2010.01.046

Zhao, S., Jiang, Y., Zhao, Y., Huang, S., Yuan, M., Zhao, Y., et al. (2016). CASEIN KINASE1-LIKE PROTEIN2 regulates actin filament stability and stomatal closure via phosphorylation of actin depolymerizing factor. *Plant Cell* 28, 1422–1439. doi: 10.1105/tpc.16.00078

Zhao, Y., Zhao, S., Mao, T., Qu, X., Cao, W., Zhang, L., et al. (2011). The plant-specific actin binding protein SCAB1 stabilizes actin filaments and regulates stomatal movement in *Arabidopsis*. *Plant Cell* 23, 2314–2330. doi: 10.1105/tpc.111.086546

Zheng, W., Jiang, Y., Wang, X., Huang, S., Yuan, M., and Guo, Y. (2019). AP3M harbors actin filament binding activity that is crucial for vacuole morphology and stomatal closure in *Arabidopsis*. *Proc. Natl. Acad. Sci. U. S. A.* 116, 18132–18141. doi: 10.1073/pnas.1901431116

Zou, M., Guo, M., Zhou, Z., Wang, B., Pan, Q., Li, J., et al. (2021). MPK3- and MPK6-mediated VLN3 phosphorylation regulates actin dynamics during stomatal immunity in *Arabidopsis*. *Nat. Commun.* 12:6474. doi: 10.1038/s41467-021-26827-2

Conflict of Interest: The authors declare that the research was conducted in the absence of any commercial or financial relationships that could be construed as a potential conflict of interest.

Publisher's Note: All claims expressed in this article are solely those of the authors and do not necessarily represent those of their affiliated organizations, or those of the publisher, the editors and the reviewers. Any product that may be evaluated in this article, or claim that may be made by its manufacturer, is not guaranteed or endorsed by the publisher.

frontiers in Plant Science

MINI REVIEW
published: 23 February 2022
doi: 10.3389/fpls.2022.826007

An Update on Coat Protein Complexes for Vesicle Formation in Plant Post-Golgi Trafficking

*Kai Ching Law†, Ka Kit Chung† and Xiaohong Zhuang**

Centre for Cell and Developmental Biology, State Key Laboratory of Agrobiotechnology, School of Life Sciences, The Chinese University of Hong Kong, Hong Kong, Hong Kong SAR, China

Endomembrane trafficking is an evolutionarily conserved process for all eukaryotic organisms. It is a fundamental and essential process for the transportation of proteins, lipids, or cellular metabolites. The aforementioned cellular components are sorted across multiple membrane-bounded organelles. In plant cells, the endomembrane mainly consists of the nuclear envelope, endoplasmic reticulum (ER), Golgi apparatus, trans-Golgi network or early endosome (TGN/EE), prevacuolar compartments or multivesicular bodies (PVCs/MVBs), and vacuole. Among them, Golgi apparatus and TGN represent two central sorting intermediates for cargo secretion and recycling from other compartments by anterograde or retrograde trafficking. Several protein sorting machineries have been identified to function in these pathways for cargo recognition and vesicle assembly. Exciting progress has been made in recent years to provide novel insights into the sorting complexes and also the underlying sorting mechanisms in plants. Here, we will highlight the recent findings for the adaptor protein (AP) complexes, retromer, and retriever complexes, and also their functions in the related coated vesicle formation in post-Golgi trafficking.

Keywords: protein sorting, coated vesicle formation, adaptor protein complex, retromer, retriever

OPEN ACCESS

Edited by:
Ruixi Li,
Southern University of Science and Technology, China

Reviewed by:
Tomohiro Uemura,
Ochanomizu University, Japan
Yan Zhang,
Shandong Agricultural University, China

****Correspondence:***
Xiaohong Zhuang
xhzhuang@cuhk.edu.hk

† These authors have contributed equally to this work

Specialty section:
This article was submitted to Plant Physiology, a section of the journal Frontiers in Plant Science

Received: *30 November 2021*
Accepted: *11 January 2022*
Published: *23 February 2022*

Citation:
Law KC, Chung KK and Zhuang X (2022) An Update on Coat Protein Complexes for Vesicle Formation in Plant Post-Golgi Trafficking. Front. Plant Sci. 13:826007. doi: 10.3389/fpls.2022.826007

INTRODUCTION

Protein trafficking is a complex of tightly regulated physiological processes in plant. The fundamental principle of protein secretion is after a protein is synthesized in the endoplasmic reticulum (ER), it will be transported within the endomembrane system and finally reach its destiny to perform the corresponding cellular functions there. Proteins that synthesized at the ER are either retained or transported to post-Golgi compartments. It is determined by the properties of the protein, including conformation, amino acid-based retention signal, and the presence of transmembrane domain (Banfield, 2011). After modification, secretory proteins are transported following a cis-to-trans direction and eventually packaged into vesicles, which subsequently bud off from trans-Golgi cisternae. The formation of the budding vesicles is achieved by distorting the membrane conformation of the Golgi apparatus. The cytosolic face of the transport vesicles is coated with proteins, which are responsible for structural maintenance and cargo recognition of the vesicle.

The anterograde transport (also known as forward transport) under the secretory pathway starts at the ER. Conventionally, after translation, proteins with transmembrane domains or signal peptides are targeted into the ER. Afterward, these proteins are transported to Golgi

through the coat protein complex II (COPII) machinery for further modifications (Brandizzi and Barlowe, 2013). The Golgi apparatus is separated into three functionally distinct cisternae: the cis-Golgi, medial-Golgi, and trans-Golgi. These compartments are categorized by their corresponding resident proteins. The cis face of the Golgi is closest to the ER (**Figure 1**). From the trans face of the Golgi apparatus, various types of budding vesicles are formed and transported *via* the trans-Golgi network or early endosome (TGN/EE) to the plasma membrane (PM), apoplast, vacuole, or for cell plate formation (**Figure 1**), which requires a set of adaptor protein (AP) complexes localized on different subdomains.

On the other hand, some proteins can be transported back to the Golgi apparatus or TGN from PM or endosomes, instead of being sent into the lytic vacuole for degradation, which is also known as retrograde transport. The retromer complex was first identified in the yeast *Saccharomyces cerevisiae* and was shown to mediate endosome-to-Golgi retrieval of the carboxypeptidase Y (CPY) receptor Vps10p (Seaman et al., 1998). Later, conserved retromer complex was also found in other species, including mammals and plants. Recently, another complex named retriever has been discovered to function in retrograde trafficking in a retromer-independent manner (Mcnally et al., 2017). Retromer- or retriever-mediated protein transport is considered to be independent of coat assembly. However, recent structural studies in animal system have revealed the retromer and retriever assemble into arch-like coat to aid tubular vesicle formation from the endosomes (Leneva et al., 2021). In this article, we will update the recent discoveries for the functions of these complexes in protein sorting and vesicle formation for plant post-Golgi trafficking.

Multiple Adaptor Protein Complexes, Same Coat?

Adaptor proteins are evolutionarily conserved among yeast, mammals, and plants (Arora and Van Damme, 2021). APs are divided into five complexes (AP1–5), which function in different localizations. Except the poorly understood AP5, other APs in plants have been found to form heterotetrametric complexes, which consisting of two large adaptin subunits (γ1/2 and β1/2 for AP1, α and β1/2 for AP2, δ and β3 for AP3, and ε and β4 for AP4), a medium subunit (μ1–4), and a small subunit (σ1–4) (**Figure 1** and **Table 1**). Regarding AP5, it has been shown that it consists two large subunits (β5 and ζ) and a medium subunit (μ5); yet, the presence of σ subunit is still not clear in *Arabidopsis* (Hirst et al., 2011).

Among all the APs, AP2 is one of the most well-categorized complexes in mediating clathrin-mediated endocytosis (CME) from the PM to endosomes (**Figure 1**; Jackson et al., 2010). The clathrin coat in *Arabidopsis*, which has been extensively reviewed, forms a triskelion shape that consists of three heavy chains and three light (Paul and Frigerio, 2007). Generally, the assembly of CCV is divided into several steps: recruitment of AP complexes, cargo selection, coat nucleation, and vesicle budding.

In animal model, it is suggested that only AP1 and AP2, but neither AP3 nor AP4, are clathrin-dependent (Hirst et al., 1999). However, recent findings showed that AP3 may also interact with clathrin (Kural et al., 2012; Zelazny et al., 2013). APs recognize and interact with multiple motifs that can be identified on their cargos. The tyrosine (YXXØ; Y, tyrosine residue; X, any amino acid; and Ø, an amino acid with a bulky hydrophobic side chain) and dileucine ([D/E]XXXL[L/I]; D, aspartic acid; E, glutamic acid residue; and L, leucine residue) motifs are the most well-documented (Bonifacino and Traub, 2003; Mattera et al., 2011). Tyrosine motif has a binding affinity toward μ subunit of APs, whereas dileucine motifs are recognized by σ subunit of APs. Different from other APs, AP5, which was identified in 2011 in Hela cell line, is localized to a late endosomal compartment for retrograde transport to Golgi (Hirst et al., 2011). Notably, a novel complex, named TPLATE complex (TPC), was recently identified to mediate AP2-independent CME, which however seems lost in animals and fungi (Gadeyne et al., 2014; Hirst et al., 2014). In the followings, we will further discuss the different functions of each AP subcomplex in plant developments.

AP1

AP1 is localized at TGN, which plays an important role in lysosomal or vacuolar trafficking in yeast, mammals, and plants (Arora and Van Damme, 2021). There are two isoforms of AP1 μ subunit (AP1 μ1 and AP1 μ2), which are localized at TGN, and double-knockout of two AP1 μ subunits is nearly pollen-lethal (Park et al., 2013). Loss-of-function of AP1 μ1 adaptin leads to pleiotropic growth defects in *Arabidopsis*, and auxin signaling is compromised due to asymmetric localization of PIN-FORMED2 (PIN2) auxin transporter (Wang et al., 2013). In addition, it is also reported that the formation of cell plate requires AP1-dependent vesicle transport during cytokinesis (Teh et al., 2013). Particularly, AP1 is also involved in cargo recycling from endosomes in yeast, mammals, and plants (Robinson, 2004; Zysnarski et al., 2019). For example, it has been shown that AP1 μ subunit deficiency suppresses the recycling of brassinosteroid insensitive1 (BRI1), a key receptor for the plant hormone brassinosteroid, from Brefeldin A (BFA) compartments to the PM (Wang et al., 2013). The dileucine sorting motif serves as one main sorting signal recognized by AP1, which is demonstrated by studying vacuolar targeting of *Arabidopsis* vacuolar ion transporter1 (VIT1), showing that knockdown of AP-1 γ subunit results in relocalization of VIT1 to the PM (Wang et al., 2014). Other types of sorting signals have also been reported for AP1. For example, plant vacuolar sorting receptor 4 (VSR4), which is required for the transportation of vacuole-localized protein from ER to vacuole, interacts with AP1 μ2 subunit through the tyrosine-sorting motif (Nishimura et al., 2016). Recently, it has been demonstrated that AP1 can physically interact with EPSIN1 for AP1 vesicle formation from a specific subdomain of TGN/EE (Heinze et al., 2020). This finding thus provides a novel insight into the role of accessory protein in AP1-dependent vesicle transport.

AP2

AP2 localizes exclusively at the PM (**Figure 1**). During CME, AP2 is involved in nucleation, cargo selection, and clathrin coat assembly (Mcmahon and Boucrot, 2011). Similar to AP1,

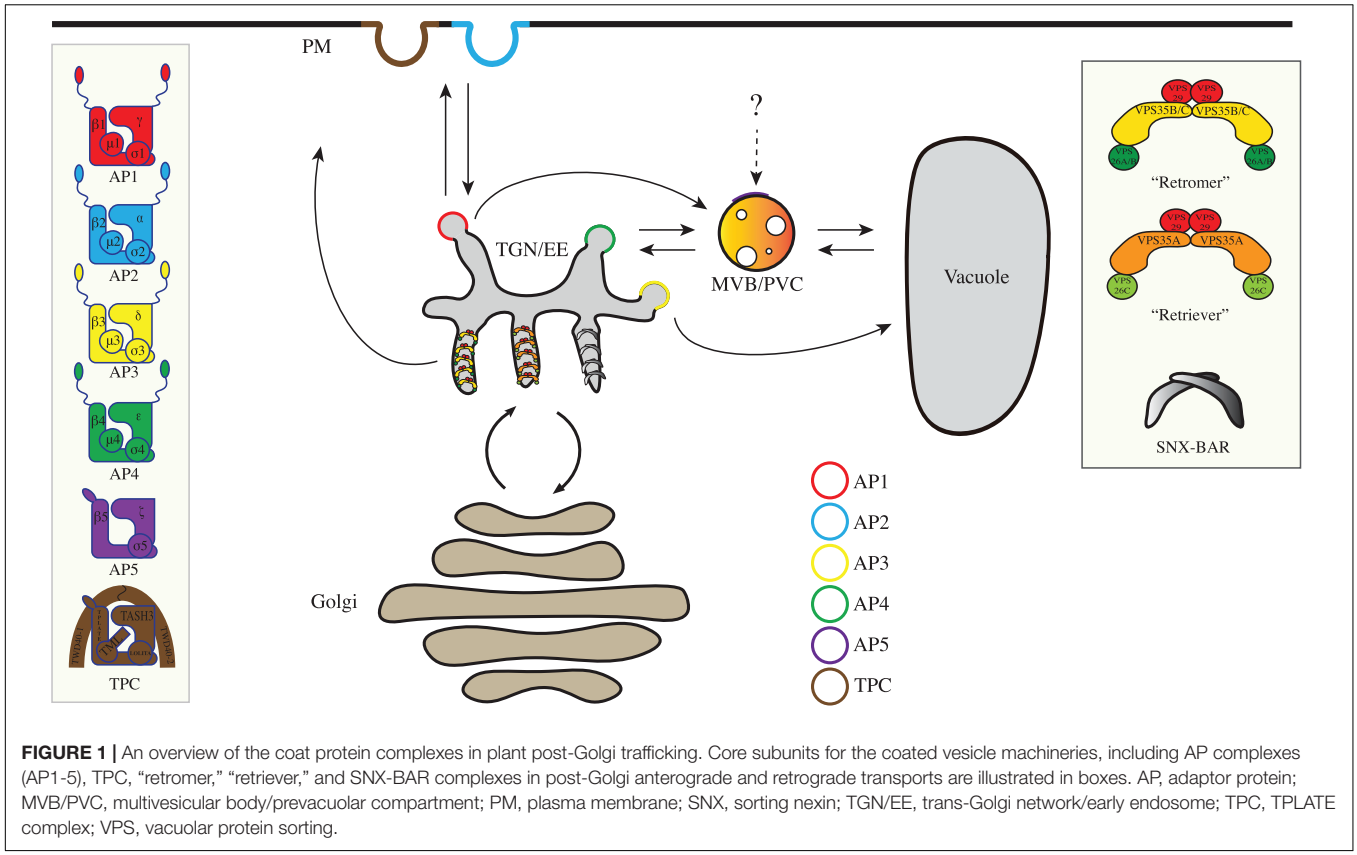

FIGURE 1 | An overview of the coat protein complexes in plant post-Golgi trafficking. Core subunits for the coated vesicle machineries, including AP complexes (AP1-5), TPC, "retromer," "retriever," and SNX-BAR complexes in post-Golgi anterograde and retrograde transports are illustrated in boxes. AP, adaptor protein; MVB/PVC, multivesicular body/prevacuolar compartment; PM, plasma membrane; SNX, sorting nexin; TGN/EE, trans-Golgi network/early endosome; TPC, TPLATE complex; VPS, vacuolar protein sorting.

tyrosine and dileucine motifs are also recognized by AP2 during cargo selection (Fan et al., 2013). By far, AP2 has been implicated to function in various plant physiological processes. For example, AP2 mediates endocytosis of several hormone regulators, including PIN1/2 (auxin signaling) and BRI1 (brassinosteroid signaling) (Di Rubbo et al., 2013; Fan et al., 2013; Kim et al., 2013). Moreover, AP2 μ subunit is required for effector-triggered immunity (ETI) response (Hatsugai et al., 2016). Phenotypic analysis of homozygous *ap2* σ mutant shows dwarfism, altered vascular pattern, and multiple abnormalities in cotyledon development and organogenesis (Fan et al., 2013; Kim et al., 2013). Additionally, AP2-deficient mutant displays defects in floral organ development and reproduction (Kim et al., 2013; Yamaoka et al., 2013). Interestingly, depletion or inhibition of the AP1 adaptor subunit and clathrin recruitment to TGN also disturbs AP2-mediated CME, and vice versa, suggesting a crosstalk between AP2-dependent CME and AP1-dependent post-Golgi trafficking (Yan et al., 2021).

AP3

AP3 was discovered by searching sequence analogy after the identification of AP1 and AP2. Each subunit of AP3 is encoded by a single copy of gene (Diane et al., 2008), but the function of AP3 in plants is still not well understood. AP3 has the ability to bind with clathrin, which however seems dispensable for AP3-coated vesicle formation. AP3 colocalizes with TGN markers in different eukaryotic systems (Feraru et al., 2010); yet, AP3-mediated trafficking bypasses the traditional prevacuolar compartment or multivesicular body (PVC/MVB)-vacuole route (Zwiewka et al., 2011). Genetic mutant screening showed that *protein affected trafficking2* (*pat2*) mutant, which was later been categorized as the β subunit of AP3, displays defects in vacuolar morphology and protein degradation (Feraru et al., 2010). Interestingly, *ap3* mutants (either β or μ subunit) show almost normal morphology under normal growth conditions (Feraru et al., 2010; Kansup et al., 2013). In addition, a recent study showed that AP-3 mediates the transport of PROTEIN S-ACYL TRANSFERASE10 (PAT10) and VAMP711 to tonoplast in a Rab5-independent manner (Feng et al., 2017). Of note, abnormal vacuole organization was also observed in *ap3* pollen cells, further supporting the role of AP3 in vacuolar trafficking for pollen tube growth (Feng et al., 2018).

AP4

In *Arabidopsis*, each subunit of AP4 is encoded by a single copy of gene (Fuji et al., 2016). AP4 colocalizes with TGN marker SYNTAXIN OF PLANTS 43 (SYP43), but not with the μ subunit of AP1, implying that different subdomains of TGN are required for the localization of AP1 and AP4 (Fuji et al., 2016). The root lengths of *ap4ß* and *ap4*μ are significantly shorter than that in wild type; yet, double-knockout of these two subunits does not induce an additive effect (Müdsam et al., 2018). AP4 mutants are also hypersensitive to avirulent bacterial infection, probably due to defects in membrane fusion

TABLE 1 | A list of the core coat protein complexes in plant post-Golgi trafficking.

Coat protein complex	*H. sapiens*	*S. cerevisiae*	*A. thaliana*	Accessory Proteins	Known Cargo Motif	Pathway
AP1	γ1, 2	γ1	γ1, 2	EPSIN,	?	TGN/EE to PM
	β1, 2	β1, 2	β1, 2	GGAs	?	
	μ1A, B	μ1	μ1, 2		YXXØ*	
	σ1A, B, C	σ1	σ1, 2		[D/E]XXXL[L/I]	
AP2	αA, C	α	α1, 2	CALM,	?	PM to TGN/EE
	β1, 2	β1, 2	β1, 2	epsin,	?	
	μ2	μ2	μ2	ARH,	YXXØ*	
	σ2	σ2	σ2	β-arrestin	[D/E]XXXL[L/I]	
AP3	δ	δ	δ	?	?	EE to vacuole/lysosome,
	β3A, B	β3	β3		?	TGN/EE to vacuole/lysosome
	μ3A, B	μ3	μ3		YXXØ*	
	σ3A, B	σ3	σ3		[D/E]XXXL[L/I]	
AP4	ε	ε	ε	Tepsin,	?	TGN to vacuole, TGN to
	β4	β4	β4	MTV	?	specialized compartments
	μ4	μ4	μ4		YXXØ*	
	σ4	σ4	σ4		[D/E]XXXL[L/I]	
AP5	ζ	ζ	ζ	SPG11/15	?	late endosome to TGN, ?
	β5	β5	β5			
	μ5	μ5	μ5			
	σ5	σ5	/			
TPC	/	/	TSPOON (LOLITA)	CALM,	?	PM to TGN/EE
	/	/	TSAUCER (TASH3)	Epsin,		
	/	/	TCUP (TML)	ARH,		
	/	/	TPLATE	β-arrestin		
	/	/	TTRAY1,TTRAY2 (TWD40-1, TWD40-2)			
	/	/	AtEH1(Pan1), AtEH12(Pan1)			
Retromer	VPS26	Vps26p	VPS26A, VPS26B	SNX3,	ØX[L/M/V]; [ILMV]x[FY]xx2-13ØxØ or [FYW]x[FY]x3-15ØxØ; [-][-]x[-][ST]xØ	Vacuole/lysosome to Endosome,Endosome to Golgi/PM
	VPS29	Vps29p	VPS29	SNX27,		
	VPS35	Vps26p	VPS35B, VPS35C	WASH		
Retriever	VPS26c	/	VPS26C	SNX17,	NPxY/NxxY	
	VPS29	/	VPS29	CCC complex,		
	VPS35L	/	VPS35A	WASH		
SNX-BAR	SNX1	Vps5p	SNX1	SNX5/6,	[ILMV]x[FY]xx2-13ØxØ or [FYW]x[FY]x3-15ØxØ; [-][-]x[-][ST]xØ	
	SNX2		SNX2A,SNX2B	WASH		

**Ø represent hydrophobic amino acid, and X represent any amino acid.*

of vacuoles, suggesting that AP4-meidated protein trafficking plays additional role in plant immunity (Hatsugai et al., 2018). Moreover, mutagenesis experiment demonstrates that sorting of NATURAL RESISTANCE-ASSOCIATED MACROPHAGE PROTEIN 3 (NRAMP3) and NRAMP4 to vacuole requires interaction between AP4 and the dileucine motifs in NRAMP3/4 (Müdsam et al., 2018). Recently, MODIFIED TRANSPORT TO THE VACUOLE1 (MTV1), an EPSIN-like protein, which locates at TGN in mediating vacuolar transport, shows a strong binding affinity with AP4 than other AP complexes (Heinze et al., 2020). MTV1 has been previously discovered to function in clathrin-dependent vacuolar transport (Sauer et al., 2013). The MTV1/AP4 interaction defines a unique subdomain on TGN/EE, which is separated from the aforementioned EPSIN1/AP1

region. Recently, using super-resolution confocal live imaging microscopy, it has been nicely showed that AP1-mediated secretory and AP4-mediated vacuolar trafficking pathways are indeed initiated from distinct zones on TGN in *Arabidopsis*, further supporting that different cargo sorting subdomains exist on plant TGN (Shimizu et al., 2021).

TPLATE Complex

Very recently, another novel AP complex termed TSET/TPC was reported, which consists of TSPOON (LOLITA), TSAUCER (TASH3), TCUP (TML), TPLATE, TTRAY1 (TWD40-1), and TTRAY2 (TWD40-2), and the counterpart in *Arabidopsis* plants involves additional two plant-specific subunits, named AtEH1/Pan1 and AtEH2/Pan1 (Gadeyne et al., 2014; Hirst et al., 2014; **Figure 1**). One of the TPC subunits, TPLATE, was first identified in *Arabidopsis* to participate in clathrin-mediated vesicle trafficking and cell plate formation (Van Damme et al., 2006). Later on, data from different organisms suggest that TPC in *Arabidopsis* plants is an octameric complex, whereas TSET is a hexametric complex in *Dictyostelium* (Gadeyne et al., 2014; Hirst et al., 2014). In plants, it was demonstrated that both TPC and AP2 participate in CME (Zhang et al., 2015). In a recent study, it has been shown that TPC is necessary for PM association of clathrin independent of AP2 (Wang et al., 2016). These results indicate that plant cells may initiate corresponding AP complexes for CME in response to different developmental signals. The molecular architectures of TPC are recently solved, revealing high similarities between TPC and the AP2-clathrin complex at the structural level (Yperman et al., 2021). In another study, a remarkable membrane-bending activity of TPC subunits during CCV formation was observed, which indicates a distinct mechanism of TPC in mediating plant endocytosis (Johnson et al., 2021). It would be interesting for future studies to further investigate how different signals are perceived by TPC- and the AP20-clathrin-mediated pathways.

Retromer and Retriever: Non-classical Coats for Tubular Vesicle Formation

Once the proteins have accomplished their functions, some will be recycled back to the Golgi apparatus or TGN, from PM or endosomes through the retrograde trafficking to reduce energy expense. In addition to the classical coated vesicle formation, tubular vesicles containing retrograde cargoes are often observed on the edges of endosomes in animal cells (Chen et al., 2019). Different from the AP complex-mediated anterograde transport which requires extra structural proteins (e.g., clathrin) for creating membrane curvature, tubular vesicle formation is largely dependent on a different set of machineries which possess the ability to induce membrane remodeling and tubulation (Oliviusson et al., 2006). In tubular vesicle formation during retrograde transport, cargoes are recognized by their corresponding sorting nexin (SNX) partners. SNX proteins associate with the phosphatidylinositol 3-phosphate on the membrane and provide a platform for the rest of the machineries to attach to. The core retromer or retriever subunits are then recruited to the membrane surfaces to form a super complex. Subsequently, the super complexes form a chain extending along the endosome, which further induces membrane curvature and constructs a tubule-shape extension (Chen et al., 2019). Next, we will mainly discuss the functions of three core complexes, which include retromer, retriever, and SNX-BAR in retrograde transport from endosomes (**Figure 1** and **Table 1**).

Retromer

Originally, retromer system was discovered in yeast 24 years ago by screening mutants with the mislocalization of Vps10p and the abnormal excretion of CPY in yeast (Seaman et al., 1998). It is proposed that Vps26p, Vps29p, and Vps35p in yeast form a multimeric complex to maintain the correct localization of Vps10p and CPY with a vacuolar sorting function (Seaman et al., 1998). Later, this system was found to be conserved in most eukaryotes and extended further, rather than a simple vacuolar cargo sorting system to the vacuole (Oliviusson et al., 2006; Koumandou et al., 2011). Moreover, the retromer complex is responsible for recycling materials from endosome to PM, TGN, and Golgi (Chen et al., 2019).

In yeast, Vps26p, Vps29p, and Vps35p together form a trimeric core retromer, and lack of these subunits would result in abnormal endosomal morphology (Banta et al., 1988), abnormal protein transport (Steinfeld et al., 2021), and excretion of vacuolar enzyme (Seaman et al., 1998). In mammals, deficiency of VPS35 and VPS26 would lead to the dysfunction of hippocampal and neurodegeneration (Muhammad et al., 2008). It is suggested that suppression of retromer would cause an accumulation of soluble α5β1-integrin, a neurotoxic peptide, and subsequently result in the abnormality in neurons (Muhammad et al., 2008). Further studies have found that the absence of retromer would lead to a similar accumulation of other peptides related to neurodegeneration (Sullivan et al., 2011).

Key subunits in retromer complexes are also conserved in *Arabidopsis* plants. There are two VPS26 paralogues, three isoforms of VPS35, and one VPS29 in *Arabidopsis*, which have been long considered to function redundantly in the retromer complex. However, recently, it has been shown that VPS26A/B-VPS29-VPS35B/C might function as the core retromer complex, whereas the other subunits, VPS26C-VPS29-VPS35A, probably constitute the core retriever complex, which will be introduced later (Oliviusson et al., 2006; Mcnally et al., 2017). Up till now, our understanding of the core retromer complex is largely derived from genetic studies of the retromer subunits, which have unveiled the essential roles of different subunits in plant survival and development. VPS26A and VPS26B might function redundantly in the retromer complex, which is supported by the observation that the double-knockout mutant showed a severely compromised growth, whereas single-knockout of VPS26A or VPS26B would not cause any phenotype (Zelazny et al., 2013). VPS35B and VPS35C have also been suggested to play a redundant role in the core retromer. Two mutant lines have been identified for VPS35B, a total knockout line *vps35b-1* and a knockdown line *vps35b-2* (Yamazaki et al., 2008). Evident developmental defects, such as early leaf senescence and dwarfism, are only observed in the *vps35b-1 vps35c-1* double-mutant, whereas no significant growth defect has

been observed in *vps35b-2 vps35c-1* double-mutant line, thus implying a dosage-dependent regulation role of VPS35B/C (Yamazaki et al., 2008). In retromer-deficient mutants, 12S seed storage proteins are secreted out and accumulate in the extracellular matrix. Meanwhile, protein storage vesicles show a defect with a reduction of size and increase on number (Yamazaki et al., 2008). Differently, with a single copy in *Arabidopsis* genome, depletion of VPS29 is more severe when compared to other retromer mutants. *vps29* mutant exhibits the dwarfism (Shimada et al., 2006) and abnormal cotyledons in shape and size (Jaillais et al., 2007). The core retromer subunits have been shown to participate in the sorting and recycling of PIN1, an important regulator for polar auxin transport in plants (Jaillais et al., 2007). As a result, defects including reduced gravity sensitivity as seen in *pin1* mutant are also observed in retromer mutant *vps29* (Jaillais et al., 2007).

In addition, SNX proteins have long been considered as an adaptor in retromer-mediated retrograde trafficking. Previous studies suggested that the cargo sorting specificity is mediated by the core retromer subunit, but recent studies showed that SNX partners also participate in cargo recognition and membrane binding (Leneva et al., 2021). In human, retromer complex cooperates with SNX3, SNX27, and SNX17 respectively for different cargoes (Mcnally et al., 2017; Healy et al., 2021). For example, retromer-SNX3 recognizes the cargo through a Øx(L/M/V) motif, whereas retromer-SNX27 binds to the PDZ domain in β2-adrenoreceptor (Lauffer et al., 2010). Differently, a NxxY motif in α5β1-integrin is recognized by retriever-SNX17 (Mcnally et al., 2017). However, some cargoes are also mediated by both retromer-SNX27 and retriever-SNX17 subcomplexes. Recently, a viral protein HPV-16 L2 has been reported to perform dual recruitment of retromer and retriever complexes simultaneously to assist the infection process, which provides a novel insight on how the two systems cooperate during infection (Pim et al., 2021). In *Arabidopsis thaliana*, counterparts for SNX3 have been recently reported, but whether they perform a similar function in plants is still unclear. In addition, no SNX27 and SNX17 homologs have been identified yet (Healy et al., 2021).

Besides SNX proteins, WASH complex is also reported as an accessory protein in retromer-dependent trafficking in animal cell. VPS35 would recruit WASH complex to the tubulation site through the direct interaction with FAM21, a subunit of WASH complex. The ability to recruit actin polymerization machineries for WASH complex would provide an additional mechanical force to facilitate the tethering of cargo from and out of the endosome (Jia et al., 2012). However, the WASH complex has not been discovered in plant and yeast (Jia et al., 2012; Wang et al., 2018).

Retriever

Retriever was first discovered in 2017 by searching SNX17-interacting proteins using proteomic method (Mcnally et al., 2017). It was found that the recycling of α5β1-integrin on the cell surface from being degraded in the lysosome in mammalian cell requires the retriever subcomplex, but independent of the core retromer complex. Similar to retromer, retriever is a heterotrimeric complex composed of three subunits, namely VPS29, VPS35L, and VPS26C, which are conserved across most eukaryotes including plants, but absent in yeast (Mcnally et al., 2017). Meanwhile, more than 120 cell surface proteins were identified as retriever-dependent cargoes (Mcnally et al., 2017).

A counterpart of retriever complex in plants was also suggested very recently (Jha et al., 2018). It was shown that VPS26C interacts with VPS35A but not with VPS35B, and residents on BFA-insensitive compartments (Jha et al., 2018). Furthermore, loss-of-function analysis showed that deficiency of VPS26C, VPS29, or VPS35A affects root hair length after mannitol treatment, but no obvious changes were detected between wild type and other retromer single mutants (*vps26a, vps26b, vps35b,* and *vps35c*). This study provides the first evidence that VPS26C-VPS35A and VPS26/B-VPS35B/C might form distinct subcomplexes with differential functions in root length growth in *Arabidopsis*. Of note, a previous study also reported a possible divergent role of different retromer subunits in mediating PIN1 recycling (Nodzynski et al., 2013). Malfunction of VPS35a leads to a greater accumulation of PIN1-GFP aggregates and a stronger defect in vacuole morphology in *Arabidopsis* roots. Such defects were not evident when both *vps35b* and *vps35c* were knockout, although VPS35C has a higher expression in the root tissues. Therefore, further efforts are required to test whether VPS35A-VPS26C and VPS35B/C-VPS26A/B function in plant "retromer" or "retriever" subcomplex for the recycling of different cargos.

Another subcomplex called Commd/CCDC22/CCDC93 (CCC) complex also binds to SNX17 and retriever for the assembly of the commander complex. In mammals, it is found that CCC complex interacts with WASH complex on the endosomes to the recruitment of retriever to the endosomes (Bartuzi et al., 2016). Subunits of the CCC complex in *Arabidopsis* genome have also been identified, including coiled-coil domain-containing protein 22 (CCDC22) and coiled-coil domain-containing protein 93 (CCDC93). However, it awaits further study to reveal whether they function together with plant "retriever" in endosome sorting (Healy et al., 2021). Particularly, in human, commander complex also consists of 7 Commd proteins, but no homologs of these proteins can be found in *Arabidopsis thaliana* (Healy et al., 2021).

SNX-BAR

The SNX-BAR subfamily has previous been considered as a part of retromer complex. SNX-BAR subfamily is featured with a structural BAR domain, and the SNX complex may utilize the BAR domain for endosome tubulation (Peter et al., 2004). However, accumulating evidence in both animals and plants suggested that SNX-BAR proteins themselves function independently of the core retromer complex, and there is still no evidence showing a interaction between SNX and retromer in plants yet (Nisar et al., 2010; Pourcher et al., 2010). A retromer-independent role of SNX-BAR is further supported by the evidence that CI-MRP (cation-independent mannose-6-phosphate receptor) requires SNX-BAR for its recycling, but retains its normal localization in retromer-depleted cells

(Kvainickas et al., 2017). Similarly, it has also been suggested that retromer in plants might function independent of SNX proteins (Heucken and Ivanov, 2018), as triple mutant *snx1/snx2a/snx2b* only shows minor developmental defect (Pourcher et al., 2010), whereas *vps35a/vps35b/vps35c* mutation leads to a severe defect or even embryo lethal (Yamazaki et al., 2008). SNX1 either forms a homodimer or heterodimer with SNX2 for different cargoes. For example, SNX1-containing endosomes are specific for PIN2 recycling (Jaillais et al., 2006). In addition, SNX1 homodimer interacts with biogenesis of lysosome-related organelle complex subunits, BLOS1 and BLOS2, for their endosome to vacuole trafficking (Cui et al., 2010), whereas SNX1-SNX2B heterodimer regulates recycling of an iron transporter IRT1 in TGN (Ivanov et al., 2014).

It has also been reported that SNX-BAR proteins coordinate with CLASP, a microtubule-associated protein and FAB1 (formation of aploid and binucleate cells1), to link endosome with microtubule (Ambrose et al., 2013; Hirano et al., 2015). In both *clasp* and *fab1* mutants, SNX1-positive endosomes displayed an altered morphology, which support that microtubule is essential for SNX1 endosome formation. It is also noted that *clasp* null mutant only affects PIN2 transport as SNX1, but deficiency of FAB1 leads to mislocalization of both PIN1 and PIN2. Thus, FAB1 might perform additional function to regulate PIN proteins independent of SNX1 and CLASP.

SUMMARY

The cumulative knowledge of anterograde and retrograde trafficking in other eukaryotic systems has been made in recent years. Yet, the molecular mechanism for different sorting machineries in plants is still less well understood. Plants have evolved distinct trafficking machineries for sorting plant-specific proteins for different developmental processes. For example, the TPC has been demonstrated to participate in plant hormone regulation, cell wall proteins, or cell plate proteins trafficking (Van Damme et al., 2006; Wang et al., 2016). Moreover, AP1 and AP4 are both localized on TGN/EE, but very recently, with the advancement of high-resolution imaging technology, EPSIN1/AP1 and MTV1/AP4 subcomplexes were resolved to operate on distinct TGN/EE subdomains (Heinze et al., 2020). This raises out another question: how do AP1 and AP4 distinguish their specific cargoes on TGN/EE in two independent pathways or whether they function in parallel with overlapping cargos? In another finding using tandem mass spectrometry analysis, only AP1, AP2, and AP4 subunits were identified in enriched CCV proteome in Arabidopsis (Dahhan et al., 2021). It is possible that other accessory proteins might be involved to assemble as coatomer with similar function as the clathrin cage in AP3 vesicles. Therefore, searching the AP3 interactome would provide more insights for the assembly of AP3 vesicles.

In comparison with the well-characterized AP subcomplexes, our understanding for sorting mechanisms of the retromer and retriever complexes is still very limited. Many questions await further study: Whether retromer and retriever function redundantly or operate separately in plant systems? Are they distributed on the separate subdomains of endosomes and how they are recruited? What are the sorting motifs specific to retromer or retriever in plants? What are the plant cargoes mediated by retriever?

Understanding the trafficking system in cells would provide a new tool to engineer protein sorting and secretion pathway for future application. For example, by engineering the sorting mechanism, plant growth signals or cargoes can be properly sorted to achieve a higher growth rate and stress tolerance, or by sorting the important cargo proteins to plant storage vacuole, it would increase the yields and quality for the development of plant-based bioreactor. Further investigations into the sorting mechanism and corresponding cargoes in plants are certainly required, which would greatly pave the way for future applications.

AUTHOR CONTRIBUTIONS

XZ designed the concept of the manuscript. KL, KC, and XZ wrote and edited the manuscript. All authors contributed to the article and approved the submitted version.

FUNDING

This work was supported by grants from the Research Grants Council of Hong Kong (24108820, N_CUHK405/20, G-CUHK404/18, C4002-20WF, R4005-18F, AoE/M-05/12, and AoE/M-403/16) and CUHK Research Committee.

ACKNOWLEDGMENTS

We apologize to researchers whose work has not been included in this manuscript owing to space limit.

REFERENCES

Ambrose, C., Ruan, Y., Gardiner, J., Tamblyn, L. M., Catching, A., Kirik, V., et al. (2013). CLASP interacts with sorting nexin 1 to link microtubules and auxin transport via PIN2 recycling in Arabidopsis thaliana. *Dev. Cell* 24, 649–659. doi: 10.1016/j.devcel.2013.02.007

Arora, D., and Van Damme, D. (2021). Motif-based endomembrane trafficking. *Plant Physiol.* 186, 221–238. doi: 10.1093/plphys/kiab077

Banfield, D. K. (2011). Mechanisms of protein retention in the Golgi. *Cold Spring Harb. Perspect. Biol.* 3:a005264. doi: 10.1101/cshperspect.a005264

Banta, L. M., Robinson, J. S., Klionsky, D. J., and Emr, S. D. (1988). Organelle assembly in yeast: characterization of yeast mutants defective in vacuolar biogenesis and protein sorting. *J. cell biol.* 107, 1369–1383. doi: 10.1083/jcb.107.4.1369

Bartuzi, P., Billadeau, D. D., Favier, R., Rong, S., Dekker, D., Fedoseienko, A., et al. (2016). CCC- and WASH-mediated endosomal sorting of LDLR is required for normal clearance of circulating LDL. *Nat. Commun.* 7:10961. doi: 10.1038/ncomms10961

Bonifacino, J. S., and Traub, L. M. (2003). Signals for sorting of transmembrane proteins to endosomes and lysosomes. *Annu. Rev. Biochem.* 72, 395–447.

Brandizzi, F., and Barlowe, C. (2013). Organization of the ER–Golgi interface for membrane traffic control. *Nat. Rev. Mol. Cell Biol.* 14, 382–392. doi: 10.1038/nrm3588

Chen, K. E., Healy, M. D., and Collins, B. M. (2019). Towards a molecular understanding of endosomal trafficking by Retromer and Retriever. *Traffic* 20, 465–478. doi: 10.1111/tra.12649

Cui, Y., Li, X., Chen, Q., He, X., Yang, Q., Zhang, A., et al. (2010). BLOS1, a putative BLOC-1 subunit, interacts with SNX1 and modulates root growth in *Arabidopsis*. *J. Cell Sci.* 123, 3727–3733. doi: 10.1242/jcs.069732

Dahhan, D. A., Reynolds, G. D., Cárdenas, J. J., Eeckhout, D., Johnson, A., Yperman, K., et al. (2021). Proteomic Characterization of Isolated Arabidopsis Clathrin-Coated Vesicles Reveals Evolutionarily Conserved and Plant Specific Components. *bioRxiv* [preprint] doi: 10.1101/2021.09.16.460678

Di Rubbo, S., Irani, N. G., Kim, S. Y., Xu, Z. Y., Gadeyne, A., Dejonghe, W., et al. (2013). The clathrin adaptor complex AP-2 mediates endocytosis of brassinosteroid INSENSITIVE1 in *Arabidopsis*. *Plant Cell* 25, 2986–2997. doi: 10.1105/tpc.113.114058

Diane, C. B., Federica, B., Marisa, S. O., and Anton, A. S. (2008). The secretory system of *Arabidopsis*. *Arabidopsis Book* 6:e0116. doi: 10.1199/tab.0116

Fan, L., Hao, H., Xue, Y., Zhang, L., Song, K., Ding, Z., et al. (2013). Dynamic analysis of Arabidopsis AP2 σ subunit reveals a key role in clathrin-mediated endocytosis and plant development. *Development* 140, 3826–3837. doi: 10.1242/dev.095711

Feng, Q.-N., Liang, X., Li, S., and Zhang, Y. (2018). The ADAPTOR PROTEIN-3 complex mediates pollen tube growth by coordinating vacuolar targeting and organization. *Plant Physiol.* 177, 216–225. doi: 10.1104/pp.17.01722

Feng, Q. N., Song, S. J., Yu, S. X., Wang, J. G., Li, S., and Zhang, Y. (2017). Adaptor Protein-3-dependent vacuolar trafficking involves a subpopulation of COPII and HOPS tethering proteins. *Plant Physiol.* 174, 1609–1620. doi: 10.1104/pp.17.00584

Feraru, E., Paciorek, T., Feraru, M. I., Zwiewka, M., De Groodt, R., De Rycke, R., et al. (2010). The AP-3 β adaptin mediates the biogenesis and function of lytic vacuoles in *Arabidopsis*. *Plant Cell* 22, 2812–2824. doi: 10.1105/tpc.110.075424

Fuji, K., Shirakawa, M., Shimono, Y., Kunieda, T., Fukao, Y., Koumoto, Y., et al. (2016). The adaptor complex AP-4 regulates vacuolar protein sorting at the trans-golgi network by interacting with VACUOLAR SORTING RECEPTOR11. *Plant Physiol.* 170, 211–219. doi: 10.1104/pp.15.00869

Gadeyne, A., Sánchez-Rodríguez, C., Vanneste, S., Di Rubbo, S., Zauber, H., Vanneste, K., et al. (2014). The TPLATE adaptor complex drives clathrin-mediated endocytosis in plants. *Cell* 156, 691–704. doi: 10.1016/j.cell.2014.01.039

Hatsugai, N., Hillmer, R., Yamaoka, S., Hara-Nishimura, I., and Katagiri, F. (2016). The μ subunit of Arabidopsis adaptor protein-2 is involved in effector-triggered immunity mediated by membrane-localized resistance proteins. *Mol. Plant Microbe Interact.* 29, 345–351. doi: 10.1094/MPMI-10-15-0228-R

Hatsugai, N., Nakatsuji, A., Unten, O., Ogasawara, K., Kondo, M., Nishimura, M., et al. (2018). Involvement of adapter protein complex 4 in hypersensitive cell death induced by avirulent bacteria. *Plant Physiol.* 176, 1824–1834. doi: 10.1104/pp.17.01610

Healy, M. D., Sacharz, J., Mcnally, K. E., Mcconville, C., Hall, R. J., Chilton, M., et al. (2021). Proteomic Identification and Structural Basis for the Interaction between Sorting Nexin Snx17 and Pdlim Family Proteins. *bioRxiv* [preprint] doi: 10.1101/2021.07.29.454387

Heinze, L., Freimuth, N., Rößling, A. K., Hahnke, R., Riebschläger, S., Fröhlich, A., et al. (2020). EPSIN1 and MTV1 define functionally overlapping but molecularly distinct trans-Golgi network subdomains in Arabidopsis. *Proc. Nat. Acad. Sci. U S A* 117, 25880–25889. doi: 10.1073/pnas.2004822117

Heucken, N., and Ivanov, R. (2018). The retromer, sorting nexins and the plant endomembrane protein trafficking. *J. Cell Sci.* 131:jcs203695. doi: 10.1242/jcs.203695

Hirano, T., Munnik, T., and Sato, M. H. (2015). Phosphatidylinositol 3-Phosphate 5-Kinase, FAB1/PIKfyve Kinase Mediates Endosome Maturation to Establish Endosome-Cortical Microtubule Interaction in Arabidopsis. *Plant Physiol.* 169, 1961–1974. doi: 10.1104/pp.15.01368

Hirst, J., Barlow, L. D., Francisco, G. C., Sahlender, D. A., Seaman, M. N., Dacks, J. B., et al. (2011). The fifth adaptor protein complex. *PLoS Biol.* 9:e1001170. doi: 10.1371/journal.pbio.1001170

Hirst, J., Bright, N. A., Rous, B., and Robinson, M. S. (1999). Characterization of a fourth adaptor-related protein complex. *Mol. Biol. Cell* 10, 2787–2802. doi: 10.1091/mbc.10.8.2787

Hirst, J., Schlacht, A., Norcott, J. P., Traynor, D., Bloomfield, G., Antrobus, R., et al. (2014). Characterization of TSET, an ancient and widespread membrane trafficking complex. *eLife* 3:e02866. doi: 10.7554/eLife.02866

Ivanov, R., Brumbarova, T., Blum, A., Jantke, A. M., Fink-Straube, C., and Bauer, P. (2014). SORTING NEXIN1 is required for modulating the trafficking and stability of the Arabidopsis IRON-REGULATED TRANSPORTER1. *Plant Cell* 26, 1294–1307. doi: 10.1105/tpc.113.116244

Jackson, L. P., Kelly, B. T., Mccoy, A. J., Gaffry, T., James, L. C., Collins, B. M., et al. (2010). A large-scale conformational change couples membrane recruitment to cargo binding in the AP2 clathrin adaptor complex. *Cell* 141, 1220–1229.

Jaillais, Y., Fobis-Loisy, I., Miege, C., Rollin, C., and Gaude, T. (2006). AtSNX1 defines an endosome for auxin-carrier trafficking in Arabidopsis. *Nature* 443, 106–109. doi: 10.1038/nature05046

Jaillais, Y., Santambrogio, M., Rozier, F., Fobis-Loisy, I., Miège, C., and Gaude, T. (2007). The Retromer Protein VPS29 Links Cell Polarity and Organ Initiation in Plants. *Cell* 130, 1057–1070. doi: 10.1016/j.cell.2007.08.040

Jha, S. G., Larson, E. R., Humble, J., Domozych, D. S., Barrington, D. S., and Tierney, M. L. (2018). Vacuolar Protein Sorting 26C encodes an evolutionarily conserved large retromer subunit in eukaryotes that is important for root hair growth in *Arabidopsis thaliana*. *Plant J.* 94, 595–611. doi: 10.1111/tpj.13880

Jia, D., Gomez, T. S., Billadeau, D. D., and Rosen, M. K. (2012). Multiple repeat elements within the FAM21 tail link the WASH actin regulatory complex to the retromer. *Mol. Biol. Cell* 23, 2352–2361. doi: 10.1091/mbc.E11-12-1059

Johnson, A., Dahhan, D. A., Gnyliukh, N., Kaufmann, W. A., Zheden, V., Costanzo, T., et al. (2021). The TPLATE complex mediates membrane bending during plant clathrin-mediated endocytosis. *Proc. Natl. Acad. Sci. U S A.* 118:e2113046118. doi: 10.1073/pnas.2113046118

Kansup, J., Tsugama, D., Liu, S., and Takano, T. (2013). The *Arabidopsis* adaptor protein AP-3μ interacts with the G-protein β subunit AGB1 and is involved in abscisic acid regulation of germination and post-germination development. *J. Exp. Bot.* 64, 5611–5621. doi: 10.1093/jxb/ert327

Kim, S. Y., Xu, Z. Y., Song, K., Kim, D. H., Kang, H., Reichardt, I., et al. (2013). Adaptor protein complex 2-mediated endocytosis is crucial for male reproductive organ development in Arabidopsis. *Plant Cell* 25, 2970–2985. doi: 10.1105/tpc.113.114264

Koumandou, V. L., Klute, M. J., Herman, E. K., Nunez-Miguel, R., Dacks, J. B., and Field, M. C. (2011). Evolutionary reconstruction of the retromer complex and its function in *Trypanosoma brucei*. *J. Cell Sci.* 124, 1496–1509. doi: 10.1242/jcs.081596

Kural, C., Tacheva-Grigorova, S. K., Boulant, S., Cocucci, E., Baust, T., Duarte, D., et al. (2012). Dynamics of intracellular clathrin/AP1- and clathrin/AP3-containing carriers. *Cell Rep.* 2, 1111–1119. doi: 10.1016/j.celrep.2012.09.025

Kvainickas, A., Jimenez-Orgaz, A., Nägele, H., Hu, Z., Dengjel, J., and Steinberg, F. (2017). Cargo-selective SNX-BAR proteins mediate retromer trimer independent retrograde transport. *J. Cell Biol.* 216, 3677–3693. doi: 10.1083/jcb.201702137

Lauffer, B. E. L., Melero, C., Temkin, P., Lei, C., Hong, W., Kortemme, T., et al. (2010). SNX27 mediates PDZ-directed sorting from endosomes to the plasma membrane. *J. Cell Biol.* 190, 565–574. doi: 10.1083/jcb.201004060

Leneva, N., Kovtun, O., Morado, D. R., Briggs, J. A. G., and Owen, D. J. (2021). Architecture and mechanism of metazoan retromer:SNX3 tubular coat assembly. *Sci. Adv.* 7:eabf8598. doi: 10.1126/sciadv.abf8598

Mattera, R., Boehm, M., Chaudhuri, R., Prabhu, Y., and Bonifacino, J. S. (2011). Conservation and diversification of dileucine signal recognition by adaptor protein (AP) complex variants. *J. Biol. Chem.* 286, 2022–2030. doi: 10.1074/jbc.M110.197178

Mcmahon, H. T., and Boucrot, E. (2011). Molecular mechanism and physiological functions of clathrin-mediated endocytosis. *Nat. Rev. Mol. Cell Biol.* 12, 517–533.

Mcnally, K. E., Faulkner, R., Steinberg, F., Gallon, M., Ghai, R., Pim, D., et al. (2017). Retriever is a multiprotein complex for retromer-independent endosomal cargo recycling. *Nat. Cell Biol.* 19, 1214–1225. doi: 10.1038/ncb3610

Müdsam, C., Wollschläger, P., Sauer, N., and Schneider, S. (2018). Sorting of Arabidopsis NRAMP3 and NRAMP4 depends on adaptor protein complex AP4 and a dileucine-based motif. *Traffic* 19, 503–521. doi: 10.1111/tra.12567

Muhammad, A., Flores, I., Zhang, H., Yu, R., Staniszewski, A., Planel, E., et al. (2008). Retromer deficiency observed in Alzheimer's disease causes hippocampal dysfunction, neurodegeneration, and Aβ accumulation. *Proc. Natl. Acad. Sci. U S A.* 105, 7327–7332. doi: 10.1073/pnas.0802545105

Nisar, S., Kelly, E., Cullen, P. J., and Mundell, S. J. (2010). Regulation of P2Y1 receptor traffic by sorting Nexin 1 is retromer independent. *Traffic* 11, 508–519. doi: 10.1111/j.1600-0854.2010.01035.x

Nishimura, K., Matsunami, E., Yoshida, S., Kohata, S., Yamauchi, J., Jisaka, M., et al. (2016). The tyrosine-sorting motif of the vacuolar sorting receptor VSR4 from *Arabidopsis thaliana*, which is involved in the interaction between VSR4 and AP1M2, μ1-adaptin type 2 of clathrin adaptor complex 1 subunits, participates in the post-Golgi sorting of VSR4. *Biosci. Biotechnol. Biochem.* 80, 694–705. doi: 10.1080/09168451.2015.1116925

Nodzynski, T., Feraru, M. I., Hirsch, S., De Rycke, R., Niculaes, C., Boerjan, W., et al. (2013). Retromer subunits VPS35A and VPS29 mediate prevacuolar compartment (PVC) function in arabidopsis. *Mol. Plant* 6, 1849–1862. doi: 10.1093/mp/sst044

Oliviusson, P., Heinzerling, O., Hillmer, S., Hinz, G., Tse, Y. C., Jiang, L., et al. (2006). Plant retromer, localized to the prevacuolar compartment and microvesicles in Arabidopsis, may interact with vacuolar sorting receptors. *Plant Cell* 18, 1239–1252. doi: 10.1105/tpc.105.035907

Park, M., Song, K., Reichardt, I., Kim, H., Mayer, U., Stierhof, Y. D., et al. (2013). Arabidopsis mu-adaptin subunit AP1M of adaptor protein complex 1 mediates late secretory and vacuolar traffic and is required for growth. *Proc. Natl. Acad. Sci. U S A.* 110, 10318–10323. doi: 10.1073/pnas.1300460110

Paul, M. J., and Frigerio, L. (2007). Coated vesicles in plant cells. *Semin. Cell Dev. Biol.* 18, 471–478.

Peter, B. J., Kent, H. M., Mills, I. G., Vallis, Y., Butler, P. J., Evans, P. R., et al. (2004). BAR domains as sensors of membrane curvature: the amphiphysin BAR structure. *Science* 303, 495–499. doi: 10.1126/science.1092586

Pim, D., Broniarczyk, J., Siddiqa, A., Massimi, P., and Banks, L. (2021). Human Papillomavirus 16 L2 Recruits both Retromer and Retriever Complexes during Retrograde Trafficking of the Viral Genome to the Cell Nucleus. *J. Virol.* 95, e2068–e2020. doi: 10.1128/JVI.02068-20

Pourcher, M., Santambrogio, M., Thazar, N., Thierry, A. M., Fobis-Loisy, I., Miege, C., et al. (2010). Analyses of sorting nexins reveal distinct retromer-subcomplex functions in development and protein sorting in Arabidopsis thaliana. *Plant Cell* 22, 3980–3991. doi: 10.1105/tpc.110.078451

Robinson, M. S. (2004). Adaptable adaptors for coated vesicles. *Trends Cell Biol.* 14, 167–174.

Sauer, M., Delgadillo, M. O., Zouhar, J., Reynolds, G. D., Pennington, J. G., Jiang, L., et al. (2013). mtv1 and mtv4 encode plant-specific ENTH and ARF GAP proteins that mediate clathrin-dependent trafficking of vacuolar cargo from the trans-Golgi network. *Plant Cell* 25, 2217–2235. doi: 10.1105/tpc.113.111724

Seaman, M. N. J., Mccaffery, J. M., and Emr, S. D. (1998). A membrane coat complex essential for endosome-to-Golgi retrograde transport in yeast. *J. Cell Biol.* 142, 665–681. doi: 10.1083/jcb.142.3.665

Shimada, T., Koumoto, Y., Li, L., Yamazaki, M., Kondo, M., Nishimura, M., et al. (2006). AtVPS29, a putative component of a retromer complex, is required for the efficient sorting of seed storage proteins. *Plant Cell Physiol.* 47, 1187–1194. doi: 10.1093/pcp/pcj103

Shimizu, Y., Takagi, J., Ito, E., Ito, Y., Ebine, K., Komatsu, Y., et al. (2021). Cargo sorting zones in the trans-Golgi network visualized by super-resolution confocal live imaging microscopy in plants. *Nat. Commun.* 12:1901. doi: 10.1038/s41467-021-22267-0

Steinfeld, N., Lahiri, V., Morrison, A., Metur, S. P., Klionsky, D. J., and Weisman, L. S. (2021). Elevating PI3P drives select downstream membrane trafficking pathways. *Mol. Biol. Cell* 32, 143–156. doi: 10.1091/mbc.E20-03-0191

Sullivan, C. P., Jay, A. G., Stack, E. C., Pakaluk, M., Wadlinger, E., Fine, R. E., et al. (2011). Retromer disruption promotes amyloidogenic APP processing. *Neurobiol. Dis.* 43, 338–345. doi: 10.1016/j.nbd.2011.04.002

Teh, O. K., Shimono, Y., Shirakawa, M., Fukao, Y., Tamura, K., Shimada, T., et al. (2013). The AP-1 μ adaptin is required for KNOLLE localization at the cell plate to mediate cytokinesis in arabidopsis. *Plant Cell Physiol.* 54, 838–847. doi: 10.1093/pcp/pct048

Van Damme, D., Coutuer, S., De Rycke, R., Bouget, F. Y., Inzé, D., and Geelen, D. (2006). Somatic cytokinesis and pollen maturation in Arabidopsis depend on TPLATE, which has domains similar to coat proteins. *Plant Cell* 18, 3502–3518. doi: 10.1105/tpc.106.040923

Wang, C., Hu, T., Yan, X., Meng, T., Wang, Y., Wang, Q., et al. (2016). Differential regulation of clathrin and its adaptor proteins during membrane recruitment for endocytosis. *Plant Physiol.* 171, 215–229. doi: 10.1104/pp.15.01716

Wang, J., Fedoseienko, A., Chen, B., Burstein, E., Jia, D., and Billadeau, D. D. (2018). Endosomal receptor trafficking: retromer and beyond. *Traffic* 19, 578–590. doi: 10.1111/tra.12574

Wang, J. G., Li, S., Zhao, X. Y., Zhou, L. Z., Huang, G. Q., Feng, C., et al. (2013). HAPLESS13, the Arabidopsis μ1 adaptin, is essential for protein sorting at the trans-Golgi network/early endosome. *Plant Physiol.* 162, 1897–1910. doi: 10.1104/pp.113.221051

Wang, X., Cai, Y., Wang, H., Zeng, Y., Zhuang, X., Li, B., et al. (2014). Trans-Golgi network-located AP1 gamma adaptins mediate dileucine motif-directed vacuolar targeting in Arabidopsis. *Plant Cell* 26, 4102–4118. doi: 10.1105/tpc.114.129759

Yamaoka, S., Shimono, Y., Shirakawa, M., Fukao, Y., Kawase, T., Hatsugai, N., et al. (2013). Identification and dynamics of *Arabidopsis* adaptor protein-2 complex and its involvement in floral organ development. *Plant Cell* 25, 2958–2969. doi: 10.1105/tpc.113.114082

Yamazaki, M., Shimada, T., Takahashi, H., Tamura, K., Kondo, M., Nishimura, M., et al. (2008). Arabidopsis VPS35, a retromer component, is required for vacuolar protein sorting and involved in plant growth and leaf senescence. *Plant Cell Physiol.* 49, 142–156. doi: 10.1093/pcp/pcn006

Yan, X., Wang, Y., Xu, M., Dahhan, D. A., Liu, C., Zhang, Y., et al. (2021). Cross-talk between clathrin-dependent post-Golgi trafficking and clathrin-mediated endocytosis in Arabidopsis root cells. *Plant Cell* 33, 3057–3075. doi: 10.1093/plcell/koab180

Yperman, K., Wang, J., Eeckhout, D., Winkler, J., Vu, L. D., Vandorpe, M., et al. (2021). Molecular architecture of the endocytic TPLATE complex. *Sci. Adv.* 7:eabe7999. doi: 10.1126/sciadv.abe7999

Zelazny, E., Santambrogio, M., Pourcher, M., Chambrier, P., Berne-Dedieu, A., Fobis-Loisy, I., et al. (2013). Mechanisms governing the endosomal membrane recruitment of the core retromer in Arabidopsis. *J. Biol. Chem.* 288, 8815–8825. doi: 10.1074/jbc.M112.440503

Zhang, Y., Persson, S., Hirst, J., Robinson, M. S., Van Damme, D., and Sánchez-Rodríguez, C. (2015). Change your Tplate, change your fate: plant CME and beyond. *Trends Plant Sci.* 20, 41–48. doi: 10.1016/j.tplants.2014.09.002

Zwiewka, M., Feraru, E., Möller, B., Hwang, I., Feraru, M. I., Kleine-Vehn, J., et al. (2011). The AP-3 adaptor complex is required for vacuolar function in *Arabidopsis*. *Cell Res.* 21, 1711–1722. doi: 10.1038/cr.2011.99

Zysnarski, C. J., Lahiri, S., Javed, F. T., Martinez-Marquez, J. Y., Trowbridge, J. W., and Duncan, M. C. (2019). Adaptor protein complex-1 (AP-1) is recruited by the HEATR5 protein Laa1 and its co-factor Laa2 in yeast. *J. Biol. Chem.* 294, 1410–1419. doi: 10.1074/jbc.RA118.005253

Conflict of Interest: The authors declare that the research was conducted in the absence of any commercial or financial relationships that could be construed as a potential conflict of interest.

Publisher's Note: All claims expressed in this article are solely those of the authors and do not necessarily represent those of their affiliated organizations, or those of the publisher, the editors and the reviewers. Any product that may be evaluated in this article, or claim that may be made by its manufacturer, is not guaranteed or endorsed by the publisher.

frontiers in Plant Science

ORIGINAL RESEARCH
published: 24 February 2022
doi: 10.3389/fpls.2022.817251

ROOT HAIR DEFECTIVE3 Is a Receptor for Selective Autophagy of the Endoplasmic Reticulum in *Arabidopsis*

*Jiaqi Sun, Weina Wang and Huanquan Zheng**

Department of Biology, McGill University, Montreal, QC, Canada

ROOT HAIR DEFECTIVE3 (RHD3) is a plant member of atlastin GTPases, which belong to an evolutionally conserved family of proteins that mediate the homotypic fusion of the endoplasmic reticulum (ER). An atlastin in mammalian cells has recently been shown to act as an ER-phagy receptor for selective autophagy of the ER (ER-phagy) during nutrient starvation. Although RHD3 has been indicated to play a role in ER stress response, it is not very clear how RHD3 is involved in the process. In this study, we showed that the *rhd3* mutant is hyposensitive to ER as well as salt stress. We employed an YFP-tagged ER membrane marker YFP-TMC to monitor the efficiency of ER-phagy microscopically and biochemically. We found that *rhd3* is defective in ER-phagy under ER stress. Furthermore, there is an increased association of YFP-RHD3 with ATG8e-marked autophagosomes. YFP-RHD3 is also visible with ATG8e in the vacuole, and there is a breakdown of YFP-RHD3 under ER stress. RHD3 has two putative ATG8 interaction motifs (AIM1-2). We revealed that RHD3 but not RHD3(ΔAIM1) physically interacts with ATG8, a core autophagosomal component that interacts with various receptor proteins to recruit cargos for degradation by selective autophagy. Furthermore, their interaction is enhanced under ER stress. We thus propose that RHD3 acts as an ER-phagy receptor under ER stress to promote ER-phagy in *Arabidopsis*.

Keywords: ER, ER stress, ER-phagy, RHD3, Atg8, autophagosomes

OPEN ACCESS

Edited by:
Ruixi Li,
Southern University of Science and Technology, China

Reviewed by:
Xiaohong Zhuang,
The Chinese University of Hong Kong, China
Pengwei Wang,
Huazhong Agricultural University, China

***Correspondence:**
Huanquan Zheng
hugo.zheng@mcgill.ca

Specialty section:
This article was submitted to Plant Physiology, a section of the journal Frontiers in Plant Science

Received: *17 November 2021*
Accepted: *17 January 2022*
Published: *24 February 2022*

Citation:
Sun J, Wang W and Zheng H (2022) ROOT HAIR DEFECTIVE3 Is a Receptor for Selective Autophagy of the Endoplasmic Reticulum in Arabidopsis. Front. Plant Sci. 13:817251. doi: 10.3389/fpls.2022.817251

INTRODUCTION

The endoplasmic reticulum (ER) is the largest cellular organelle consisting of interconnected tubules and flattened cisternae that stretch throughout the cytoplasm. Highly conserved across the fungal, plant, and animal kingdoms, the ER is the primary site of protein synthesis, translocation, and modification in all eukaryotic cells. Many other cellular organelles are also physically and functionally linked with the ER. During cell development, the ER remodels its shape continuously to achieve its optical quantity and quality (Brandizzi, 2021). In addition, plants are sessile organisms that live under prevailing environmental conditions. At the cellular level, many environmental stresses can disrupt protein folding in the ER leading to ER stress that is potentially lethal to plant growth (Howell, 2013; Afrin et al., 2020). To alleviate ER stress, plant cells use unfolded

protein response (UPR), ER-associated degradation (ERAD), and selective autophagy of the ER (ER-phagy). When the ER is under stress, UPR increases and expanses the size of the ER and the capacity of protein folding in the ER (Bernales et al., 2006), meanwhile, ERAD and ER-phagy become very active (Sun et al., 2021). ERAD recognizes and translocates misfolded proteins into the cytosol for degradation (Sun et al., 2021), while ER-phagy selectively transports *via* autophagosomes and degrades unnecessary or dysfunctional ER domains in the lysosome/vacuole to maintain ER homeostasis (Bernales et al., 2006).

Endoplasmic reticulum-phagy is selective and relies on the binding of specific ER-phagy receptors and autophagy modifier proteins such as ATG8 proteins (Stolz et al., 2014), a family of ubiquitin-like proteins required for the formation of autophagosomes. In recent years, several receptors that mediate ER-phagy have been identified in mammalian cells. For example, Sec62, a constituent of the protein translocon acts in the ER-phagy during stress recovery, and CCPG1, an ER-resident Cell-Cycle Progression Gene 1 protein, can serve as an ER-phagy receptor under ER stress (Fumagalli et al., 2016; Smith et al., 2018). FAM134B, a reticulon-like protein, is also described as an ER-phagy receptor specific for ER sheet degradation (Khaminets et al., 2015; Bhaskara et al., 2019; Jiang et al., 2020). Most recently, RTN3, a reticulon that shapes tubular domains of the ER, and ATL3, an atlastin that mediates ER membrane fusion, have been identified as ER-phagy receptors that target ER tubules for degradation (Grumati et al., 2017; Chen et al., 2019) during nutrient starvation.

In plants, a few ER-phagy receptors have also been currently reported. ATG8 interaction protein 1 (ATI1) and 2 (ATI2) can serve as the starvation-specific ER-phagy receptors in *Arabidopsis* (Honig et al., 2012; Wu et al., 2021). AtSec62 (Hu et al., 2020), C53 (a cytosolic ATG8 interactor in *Arabidopsis*) (Stephani et al., 2020), and RTN1 and RTN2 (two reticulons in maize) (Zhang et al., 2020) have also been reported to modulate ER-phagy in plant cells under ER stress. ROOT HAIR DEFECTIVE3 (RHD3) is a plant member of atlastins (Sun and Zheng, 2018). Similar to its mammalian counterparts, RHD3 mediates the homotypic fusion of ER membranes (Hu et al., 2009; Zhang et al., 2013; Qi et al., 2016). Although it has been suggested that RHD3 plays a role in plant response to ER stress (Lai et al., 2014), it is not clear how RHD3 is involved in ER stress response. In this report, we showed that, by using a combined approach of ER-phagy marker-based imaging, biochemistry, and protein-protein interaction, RHD3 acts as an ER-phagy receptor under ER stress to promote ER-phagy in *Arabidopsis*.

MATERIALS AND METHODS

Plant Growth Conditions, Drug, and Salt Treatment

All mutant seeds, including characterized *rhd3-8* (SALK_025215) (Sun et al., 2020b) and *atg5-1* (SAIL_129_B07) (Le Bars et al., 2014), were obtained from the Arabidopsis Biological Resource Center and then genotyped and propagated. Col.0 (*35Spro:YFP-TMC*) and *rhd3-8* (*RHD3pro:YFP-RHD3*) transgenic line was generated as previously described (Sun and Zheng, 2018; Sun et al., 2020b). *rhd3-8* (*35Spro:YFP-TMC*) and *atg5-1* (*35Spro:YFP-TMC*) plants were created by crossing *rhd3-8* and *atg5-1* mutants with Col.0 (*35Spro:YFP-TMC*), respectively. For ER stress analysis, Col.0 and *rhd3-8* seeds were directly sown on the 1/2 MS medium with or without 2 mM dithiothreitol (DTT). For salt treatment, Col.0 and *rhd3-8* seeds were directly sown on the 1/2 MS medium, and the 6-day-old seedlings of Col.0 and *rhd3-8* were then moved and grown for 5 days on the 1/2 MS medium with or without 150 mM NaCl. The survival rate was quantified based on the color of seedlings. Yellow-colored seedlings were deemed dead. For ER-phagy induction, the 7-day-old seedlings of Col.0, *rhd3-8*, and *atg5-1* were moved to the 1/2 MS liquid medium with 10 mM DTT or with the same concentration of DMSO as control for different hours. For the confocal imaging of YFP-TMC and YFP-RHD3 in the vacuole, 0.1 μM ConcA was added.

Molecular Cloning

The cloning of the entry vector pCR8-RHD3 was described previously (Sun and Zheng, 2018). pCR8-RHD3(ΔAIM1) was cloned through overlap PCR. The coding sequence of ATG8e was cloned into the pGEM-Gate entry vector. The YFP fragment of pEarleyGate 104 was replaced by mNeonGreen or mCherry to generate pEarleyGate 104-mNeonGreen and pEarleyGate 104-mCherry, respectively, with the AQUA cloning assay (Beyer et al., 2015). Through gateway reaction, pCR8-RHD3 and pGEM-ATG8e were cloned into pEarleyGate 104-mNeonGreen and pEarleyGate 104-mCherry to generate mNeonGreen-RHD3 and mCherry-ATG8e, respectively. For split ubiquitin system (SUS)-based yeast two-hybrid (Y2H) constructs, pCR8-RHD3(ΔAIM1) and pGEM-ATG8e were cloned into pNCW-GWRFC and pNX32-DEST to generate Cub-RHD3(ΔAIM1) and NubG-ATG8e, respectively.

Confocal Microscopy

Microscopy images were acquired with a Leica SP8 point-scanning confocal system equipped with a × 63 oil objective and using 488- (mNeonGreen/YFP) and 552-nm (mCherry) lasers. Two channels were excited sequentially. The emission filter of mNeonGreen/YFP was 490–560 nm, and the emission filter of mCherry was 580–660 nm.

Protein Interaction Assays

For bimolecular fluorescence complementation (BiFC) assay, RHD3, RHD3(ΔAIM1), ATG8e, and p24 were cloned into the 3-in-1 BiFC vector (Sun et al., 2020b) with the AQUA cloning method (Beyer et al., 2015). Then, agrobacteria containing different constructs were infiltrated into *Nicotiana benthamiana* leaves with OD_{600} = 0.01. Notably, 72 h later, images were captured by the confocal microscope.

The SUS-based Y2H was performed as previously described (Sun et al., 2020a). The AP4 cells expressing Cub-tagged proteins as indicated and the AP5 cells expressing NubG-tagged proteins as indicated were inoculated in Synthetic Complete (SC) selection liquid medium (-Leu for AP4 and -Trp for AP5) overnight at

30°C. Then, AP4 and AP5 cells were mixed and plated on YPD plates for mating. After 6 h, mated cells were streaked on the -LT selection medium and incubated at 28°C for 2 days. The diploid cells (mated cells) were collected, inoculated in the -LT liquid medium, and incubated overnight at 30°C. Then, the cells were collected and resuspended in water. The optical density (OD) values of all the suspensions were adjusted to 1, 0.1, and 0.01 with water. Then, 10 μl per spot was dropped on -LT or -LTH plates for the interaction test. The plates were incubated at 30°C for 3 days.

Co-immunoprecipitation (Co-IP) was performed as previously described (Sun et al., 2020b). The infiltrated *N. benthamiana* leaves were grinded with the extraction buffer [50 mM Tris–HCl pH 7.5, 150 mM NaCl, 10% (v/v) glycerol, and 0.5% IGEPAL® CA-630 (#I8896, Sigma), 1/100 volume of Protease Inhibitor Cocktail (#P9599, Sigma)]. The extract was centrifuged at 17,000 × *g* for 10 min at 4°C, and the supernatant was collected and incubated with green fluorescent protein (GFP)-Trap beads (Chromotek) for 1 h at 4°C. Then, the beads were washed three times, resuspended in 50 μl 2 × SDS-loading buffer, and boiled for 10 min. The solution was centrifuged, and the supernatant was used for Western blot.

Western Blot

The total protein was extracted with 1 × SDS loading buffer and boiled for 5 min. The samples were loaded on 10% SDS-PAGE gel and transferred to a polyvinylidene difluoride (PVDF) membrane. Western blot was carried out with anti-GFP antibody (Sigma-Aldrich, G1544) at 1:5,000, anti-mCherry (Sigma-Aldrich, AB356482) at 1:5,000, and anti-tubulin (T6074; Sigma-Aldrich; 1:5,000). The secondary goat anti-rabbit IgG-peroxidase (Sigma–Aldrich, A4914-1ML) was used at 1:5,000 dilution, and goat anti-mouse (A4914-1ML; Sigma–Aldrich) was used at 1:10,000 dilution.

RESULTS

rhd3 Mutant Is Defective in Endoplasmic Reticulum-Phagy Under Endoplasmic Reticulum Stress

To understand how RHD3 may be involved in plant response to ER stress, we first treated seedlings of wild type (WT) and *rhd3-8* mutant with DTT, a reducing agent that blocks disulfide-bond formation in protein folding, thus leading to ER stress. We found that the seedlings of *rhd3-8* were hyposensitive to the treatment of 2 mM DTT, when compared to WT seedlings (**Figure 1A**). The quantification of the survival rate in the 10-day-old seedlings indicated that the survival rate of *rhd3-8* seedlings was ∼45%, while that of WT was ∼65% (**Figure 1B**). In addition, the seedlings of *rhd3-8* were also hyposensitive to the treatment of 150 mM NaCl (**Figure 2A**). The survival rate of *rhd3-8* was ∼20%, while that of WT was above 75% (**Figure 2B**). These results suggested that the *rhd3* mutant is defective in resolving ER as well as salt stress.

A strategy that eukaryotic cells use to alleviate ER and other stresses is to activate ER-phagy (Howell, 2013). Therefore, we wondered if the *rhd3-8* mutant is defective in ER-phagy. To test this, we utilized YFP-TMC as a marker to monitor the efficiency of ER-phagy. TMC is composed of the transmembrane (TM) domain and C-terminus of Sey1p (682–766), a yeast homolog of atlastins. When expressed in plant cells, YFP-TMC labels ER membranes without altering the ER morphology and plant growth (Stefano and Brandizzi, 2014; Sun et al., 2020b). It is known that it is difficult to use endogenous ER proteins to monitor ER-phagy as many endogenous ER markers do not change much during ER-phagy, and some ER proteins, e.g., BIP2 and Calreticulin2, are in fact transcriptionally upregulated under ER stress (Srivastava et al., 2018) even they are being degraded by ER-phagy. Exogenously expressed YFP-fused ER proteins do not change their expression significantly, and the cleavage of free fluorescent protein has been utilized as a good biochemical indicator of ER-phagy (Liang et al., 2018). We first monitored the transport of YFP-TMC to the vacuole in the presence of 2 mM DTT with ConcA, a V-ATPase inhibitor that raises the vacuolar pH to stabilize YFP-labeled autophagosomes transported to the vacuole (Liu et al., 2012). As indicated in **Figure 3A**, in the absence of DTT, there was no much difference between WT, *rhd3-8*, and *atg5-1* mutant cells when the central part of cells was scanned (**Figure 3A**, the left panel). ATG5 is known to be essential for autophagosome formation and maturation (Le Bars et al., 2014). In 4 h of the presence of DTT, a large number of YFP-TMC bodies were observed in the vacuole of WT plant cells, while no and a few were visible in *atg5-1* and *rhd3-8* mutant cells (**Figure 3A**, the right panel), respectively. We then examined the cleavage of YFP in YFP-TMC in *rhd3-8* in the absence and presence of DTT by Western blot. As expected, free YFP was detected in WT plants treated with DTT, but no such cleavage was yet detectable in *rhd3-8* plants treated with DTT for 4 h (**Figure 3B**), although at this time point, there were some visible YFP-TMC punctae in *rhd3-8* under the same conditions (**Figure 3A**). This indicated that the cleavage of free YFP was compromised in *rhd3-8* plants. Taken all together, we concluded that the *rhd3* mutant is defective in ER-phagy under ER stress.

ROOT HAIR DEFECTIVE3 Is Increasingly Associated With Autophagosomes Under Endoplasmic Reticulum Stress

If RHD3 is involved in ER-phagy, there should be an increased association of RHD3 with autophagosomes under ER stress. To test this notion, we transiently co-expressed mNeonGreen-RHD3 and mCherry-ATG8e in tobacco epidermal leaf cells. ATG8e has been widely used as an autophagosomal marker in plants (Zhuang et al., 2017). In cells without DTT, mCherry-ATG8e was largely cytosolic, but mCherry-ATG8e-positive dot-like structures were occasionally observed in close proximity to mNeonGreen-RHD3, which marked ER membranes (**Figure 4A**, arrow in the upper panel). In cells treated with DTT, however, more mCherry-ATG8e-positive dot-like structures were observed. Many of them were colocalized with mNeonGreen-RHD3 (**Figure 4A**, white arrowheads in the middle panel). This suggested that RHD3 travels to autophagosomes under ER stress. Furthermore, in the central section of cells treated with

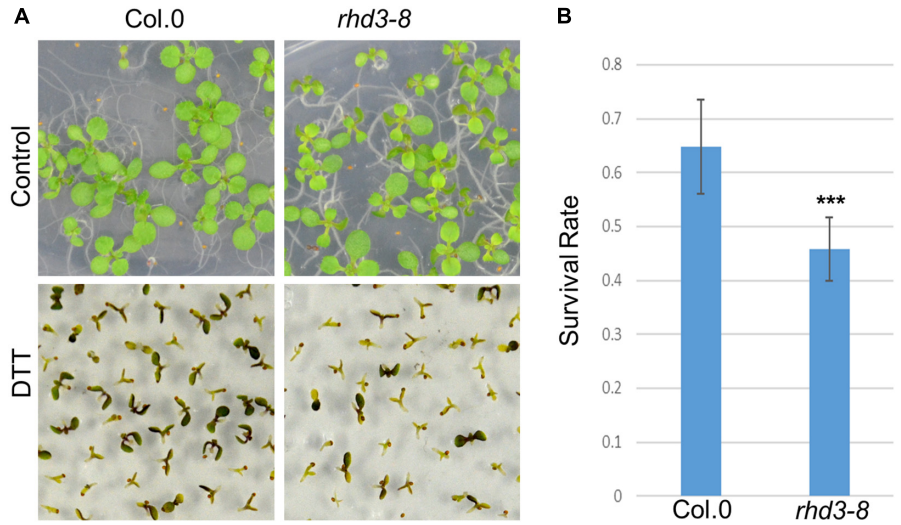

FIGURE 1 | *rhd3* mutant is sensitive to endoplasmic reticulum (ER) stress. **(A)** Ten-day old seedlings of wild type (WT) and *rhd3-8* grown on 1/2 MS in the absence (control) and presence of 2 mM dithiothreitol (DTT). **(B)** Quantification of survival rate of seedlings of WT ($n = 6$, each time with 100–200 seedlings) and *rhd3-8* ($n = 6$, each time with 100–200 seedlings) grown under 2 mM DTT. Error bars represent SD, *** represents significant difference (P-value < 0.001, t-test).

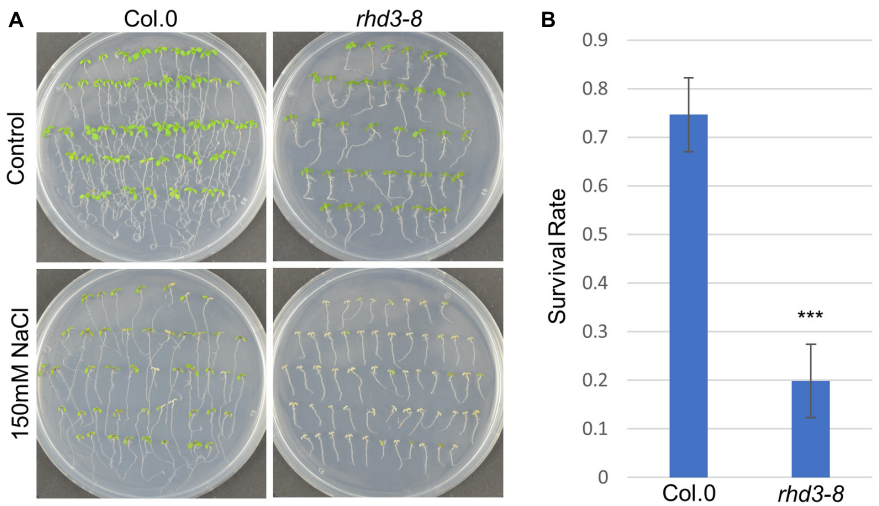

FIGURE 2 | *rhd3* mutant is sensitive to salt stress. **(A)** Six-day old seedlings of WT and *rhd3-8* grown on 1/2 MS for 5 days in the absence (control) and presence of 150 mM NaCl. **(B)** Quantification of survival rate of seedlings of WT ($n = 4$, each time with 40–60 seedlings) and *rhd3-8* ($n = 4$, each time with 40–60 seedlings) grown on 1/2 MS with 150 mM NaCl. Error bars represent SD, *** represents significant difference (P-value < 0.001, t-test).

DTT and ConcA, mNeonGreen-RHD3 was visible together with mCherry-ATG8e (**Figure 4A**, yellow arrowheads in the lower panel), indicating that the final destination of mNeonGreen-RHD3 + mCherry-ATG8e is likely the vacuole. We then wondered if there is an increased fluorescent protein breakdown when RHD3 is fused with a fluorescent protein under ER stress. When YFP-RHD3 driven by the RHD3 native promoter (RHD3pro:YFP-RHD3) was expressed in *rhd3-8*, we did not observe any breakdown of YFP-RHD3 in the absence of DTT (**Figure 4B**, lane 1). However, when *rhd3-8*:RHD3pro:YFP-RHD3 plants were treated with 10 mM DTT, we started to observe a breakdown in 2 h (**Figure 4B**, lane 2) and a clear breakdown of YFP-RHD3 in 6 h (**Figure 4B**, lane 3). Taken all together, RHD3 travels together with autophagosomes to the vacuole for degradation under ER stress.

ROOT HAIR DEFECTIVE3 But Not RHD3(ΔAIM1) Physically Interacts With ATG8, and Such Interaction Is Enhanced Under Endoplasmic Reticulum Stress

ATL3 in mammalian cells has been recognized as an ER-phagy receptor by its interaction with ATG8 (Chen et al., 2019; Molinari, 2021). We thus wondered if RHD3 also acts as an ER-phagy

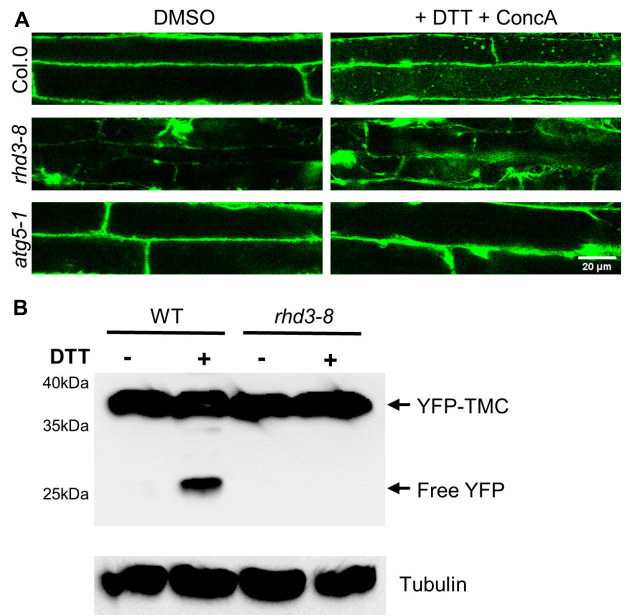

FIGURE 3 | Endoplasmic reticulum (ER)-phagy in *rhd3* mutant is defective. **(A)** Confocal microscopic images of root cells of WT, *rhd3-8*, and *atg5-1* plants expressing YFP-TMC in the absence (DMSO) and presence of 10 mM DTT with ConcA. Scale bars = 20 μm. **(B)** Western blot of YFP-TMC expressed in WT and *rhd3-8* seedlings treated with or without 10 mM DTT for 4 h. Tubulin was used as the loading control.

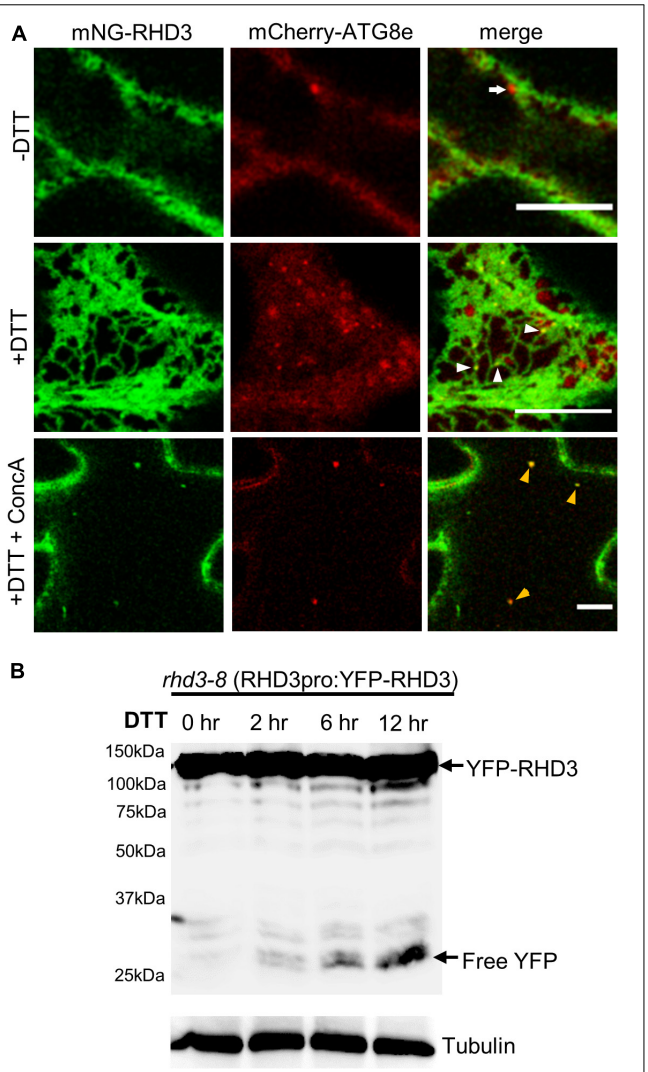

FIGURE 4 | ROOT HAIR DEFECTIVE3 (RHD3) is increasingly associated with autophagosomes under ER stress. **(A)** The association between RHD3 and mCherry-ATG8e-labeled autophagosomes without or with 10 mM DTT treatment. The arrow in the upper panel points to an autophagosome adjacent to mNeonGreen-RHD3 in a cell without the DTT treatment, while the arrowheads in the middle panel point to the increased association of mNeonGreen-RHD3 with autophagosomes in a cell treated with DTT. Yellow arrowheads in the lower panel point to mNeonGreen-RHD3 together with mCherry-ATG8e-labeled autophagosomes in the vacuole. Scale bars = 10 μm. **(B)** Western blot of YFP-RHD3 in *rhd3-8* plants expressing YFP-RHD3 driven by the RHD3 native promoter treated with 10 mM DTT for different hours indicated.

receptor in plants. To investigate this, we examined if RHD3 interacts with ATG8e. In the SUS-based Y2H assay, we found that Cub-RHD3 interacted with NubG-RHD3 (Sun and Zheng, 2018; **Figure 5A**, the first row, positive control) and NubG-ATG8e (**Figure 5A**, the third row) but not with NubG (**Figure 5A**, the second row, negative control). Based on hfAIM, which is a software for the identification of autophagy-associated Atg8-interacting motifs (AIMs) (Xie et al., 2016), RHD3 has two putative AIMs: AIM1 is within the GTPase domain and AIM2 is within the third 3HB in the middle domain (**Figure 5B**). Because the third 3HB is critical for the stability of RHD3 (Sun and Zheng, 2018), an AIM2 deletion in the 3HB may influence the stability of the protein. We, therefore, tested if RHD3 without AIM1 [RHD3(ΔAIM1)] interacts with ATG8e or not. As indicated, Cub-RHD3(ΔAIM1) did not interact with NubG-ATG8e (**Figure 5A**, the fourth row). Moreover, in our 3-in-1-based BiFC analysis (Sun et al., 2020a), RHD3, but not RHD3(ΔAIM1), was found to interact with ATG8e on the ER membrane marked by mCherry-HDEL (**Figure 5C**, the first and fourth panels, respectively). Neither RHD3 nor ATG8e interacted with p24, an ER membrane protein (Chen et al., 2012; **Figure 5C**, negative controls, the second, and third panels). To further confirm that RHD3 interacts with ATG8 by Co-IP, we transiently co-expressed YFP-RHD3 with mCherry-ATG8e or mCherry in *N. benthamiana* leaves. When YFP-RHD3 was purified by using GFP-Trap beads, mCherry-ATG8e but not mCherry was copurified (**Figure 6**, compare lane 2 with lane 1). Interestingly, an increased amount of mCherry-ATG8e was copurified when cells were treated with DTT (**Figure 6**, compare lane 3 with lane 2), suggesting that the DTT treatment enhances the interaction of RHD3 with ATG8 under ER stress.

DISCUSSION

In this study, we reported that *Arabidopsis* RHD3 can act as an ER-phagy receptor under ER stress and likely under

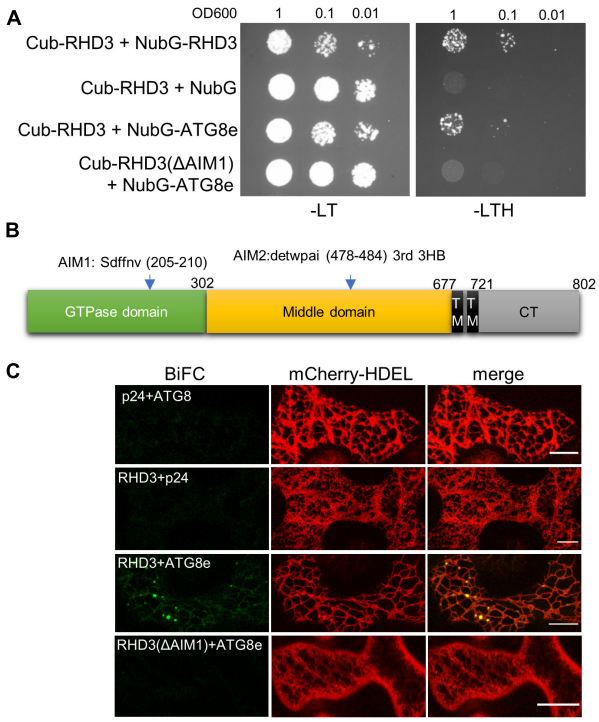

FIGURE 5 | ROOT HAIR DEFECTIVE3 (RHD3) but not RHD3(ΔAIM1) interacts with ATG8. **(A)** The interaction between RHD3/RHD3(ΔAIM1) and ATG8e revealed by the split ubiquitin system (SUS) of yeast two-hybrid (Y2H). RHD3 (row 1) but not RHD3(ΔAIM1) (row 4) interacted with ATG8e. **(B)** The schematic presentation of the locations of two putative AIMs in RHD3 predicted by hfAIM. **(C)** The interaction of RHD3 RHD3(ΔAIM1) and ATG8e in the bimolecular fluorescence complementation (BiFC) system. RHD3 (panel 3) but not RHD3(ΔAIM1) (panel 4) interacted with ATG8e on the ER indicated by mCherry-HDEL. Scale bars = 10 μm.

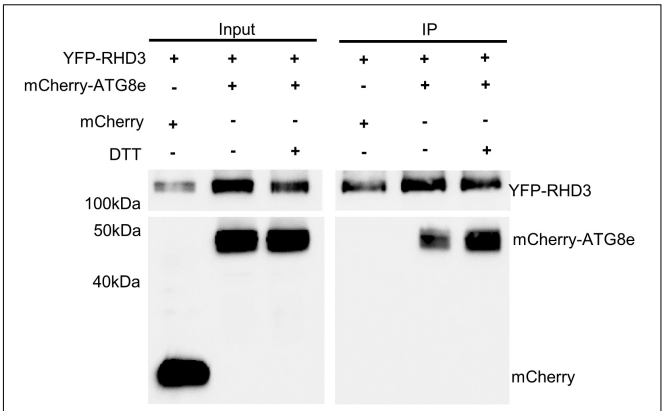

FIGURE 6 | Co-immunoprecipitation (Co-IP) assay of the interaction between RHD3 and ATG8e. mCherrry-ATG8e (lane 2), but not mCherry (lane 1), was copurified by YFP-RHD3. Notably, the increased amount of mCherry-ATG83e was copurified by YFP-RHD3 in the presence of 10 mM DTT (in comparison of lane 3 with lane 2).

salt stress to promote selective ER degradation by directly interacting with ATG8 *via* its AIM domain. Similarly, atlastin proteins in mammalian cells have been found to act as ER-phagy receptors to regulate ER turnover during nutrient starvation (Liang et al., 2018; Chen et al., 2019). It is interesting to note that mammalian atlastin knockout cell lines are also hyposensitive to ER stress induced by Tunicamycin, a chemical that inhibits protein glycosylation (Zhao et al., 2016), although it has not been reported if atlastins also act as ER-phagy receptors under ER stress. Given what we reported here, it is highly likely that all atlastin proteins can serve as an ER-phagy receptor for the selective degradation of the ER in multiple stress conditions, such as nutrient starvation, salt stress, and ER stress. In plants, it has been found that ATI1 and ATI2 act as ER-phagy receptors in a carbon starvation-induced ER-phagy, and they are highly cargo-specific in the process (Wu et al., 2021). Thus, it will be interesting to examine (1) if RHD3 can serve as an ER-phagy receptor in carbon starvation and/or other environmental stresses such as drought and heat and (2) if RHD3 has its own specific cargos in ER-phagy, and perhaps even its own specific set of different cargos under different environmental stress conditions.

The interaction with ATG8 is one of the key criteria for a protein to be considered as an ER-phagy receptor (Molinari, 2021). Interestingly, RHD3 interacts with ATG8 in the absence of DTT, although the treatment of DTT can enhance the interaction between the two. We attempt to suggest here that RHD3 may also be an ER-phagy receptor for basal ER-phagy. It is known that ER-phagy occurs constitutively at a low level under basal conditions for the turnover of the ER (Khaminets et al., 2015; Wilkinson, 2019).

The RHD3 is known to mediate the homotypic fusion of ER membranes (Hu et al., 2009; Zhang et al., 2013; Qi et al., 2016). How could it also serve as an ER-phagy receptor? In other words, what could turn the action of RHD3 as an ER fusogen to an ER-phagy receptor? In this regard, it is worth noting that the action of C53 as an ER-phagy receptor under ER stress is promoted by an UFMylation E3 ligase UFL1 (Stephani et al., 2021), although the detailed mechanism is not clear. It has been reported that RHD3 interacts with a novel ubiquitination E3 ligase LUNAPARK (LNP) in *Arabidopsis* (Sun et al., 2020a). RHD3 can be ubiquitinated by LNPs (Sun et al., 2020a). It may be that LNPs will sense ER stress and then ubiquitinate RHD3 to promote its action in ER-phagy. It is worth examining (1) if ER stress could promote the ubiquitination of RHD3 by LNPs and (2) if LNP could regulate/enhance the interaction between RHD3 and ATG8. RHD3 is also known to be phosphorylated, i.e., important for the oligomerization of RHD3 (Ueda et al., 2016). This modification could also be a potential regulation in the action of RHD3 in ER-phagy, as the super-assembly of Atg40 (a yeast reticulon-like protein that can serve as an ER-phagy receptor) could induce local ER remodeling to facilitate the autophagosome formation (Mochida et al., 2020).

Finally, it is reported recently that ATL2 and ATL3 in mammalian cells also regulate autophagosome initiation. ATL2 and ATL3 facilitate the recruitment and stabilization of the ULK1 complex onto the ER and tether isolation membranes (an autophagosomal precursor in mammalian cells) with the ER

(Liu et al., 2021). The ULK1 complex is crucial for initiating autophagosome formation. Does RHD3 play a similar role in autophagosome initiation in plant cells as well? This can be tested by investigating the action of ATG1 in the *rhd3* mutant. ATG1 (a homolog of ULK1 in *Arabidopsis*) plays a role in autophagy under nitrogen deprivation and short-term carbon starvation (Huang et al., 2019).

DATA AVAILABILITY STATEMENT

The raw data supporting the conclusions of this article will be made available by the authors, without undue reservation.

AUTHOR CONTRIBUTIONS

JS designed and performed all experiments excepting Y2H, collected the data, and wrote the first draft of the manuscript. WW performed the Y2H experiment. HZ conceived the project, analyzed the data, and revised the manuscript. All authors read and approved the final manuscript.

FUNDING

This study was supported by a grant from the National Science and Engendering Research Council of Canada to HZ.

REFERENCES

Afrin, T., Diwan, D., Sahawneh, K., and Pajerowska-Mukhtar, K. (2020). Multilevel regulation of endoplasmic reticulum stress responses in plants: where old roads and new paths meet. *J. Exp. Bot.* 71, 1659–1667. doi: 10.1093/jxb/erz487

Bernales, S., Mcdonald, K. L., and Walter, P. (2006). Autophagy counterbalances endoplasmic reticulum expansion during the unfolded protein response. *PLoS Biol.* 4:e423. doi: 10.1371/journal.pbio.0040423

Beyer, H. M., Gonschorek, P., Samodelov, S. L., Meier, M., Weber, W., and Zurbriggen, M. D. (2015). AQUA cloning: a versatile and simple enzyme-free cloning approach. *PLoS One* 10:e0137652. doi: 10.1371/journal.pone.0137652

Bhaskara, R. M., Grumati, P., Garcia-Pardo, J., Kalayil, S., Covarrubias-Pinto, A., Chen, W., et al. (2019). Curvature induction and membrane remodeling by FAM134B reticulon homology domain assist selective ER-phagy. *Nat. Commun.* 10:2370. doi: 10.1038/s41467-019-10345-3

Brandizzi, F. (2021). Maintaining the structural and functional homeostasis of the plant endoplasmic reticulum. *Dev. Cell* 56, 919–932. doi: 10.1016/j.devcel.2021.02.008

Chen, J., Qi, X., and Zheng, H. (2012). Subclass-specific localization and trafficking of *Arabidopsis* p24 proteins in the ER-Golgi interface. *Traffic* 13, 400–415. doi: 10.1111/j.1600-0854.2011.01317.x

Chen, Q., Xiao, Y., Chai, P., Zheng, P., Teng, J., and Chen, J. (2019). ATL3 is a tubular ER-Phagy receptor for GABARAP-mediated selective autophagy. *Curr. Biol.* 29, 846–855. doi: 10.1016/j.cub.2019.01.041

Fumagalli, F., Noack, J., Bergmann, T. J., Cebollero, E., Pisoni, G. B., Fasana, E., et al. (2016). Translocon component Sec62 acts in endoplasmic reticulum turnover during stress recovery. *Nat. Cell Biol.* 18, 1173–1184. doi: 10.1038/ncb3423

Grumati, P., Morozzi, G., Holper, S., Mari, M., Harwardt, M. I., Yan, R., et al. (2017). Full length RTN3 regulates turnover of tubular endoplasmic reticulum via selective autophagy. *eLife* 6:e25555. doi: 10.7554/eLife.25555

Honig, A., Avin-Wittenberg, T., Ufaz, S., and Galili, G. (2012). A new type of compartment, defined by plant-specific Atg8-interacting proteins, is induced upon exposure of *Arabidopsis* plants to carbon starvation. *Plant Cell* 24, 288–303. doi: 10.1105/tpc.111.093112

Howell, S. H. (2013). Endoplasmic reticulum stress responses in plants. *Annu. Rev. Plant Biol.* 64, 477–499. doi: 10.1146/annurev-arplant-050312-120053

Hu, J., Shibata, Y., Zhu, P. P., Voss, C., Rismanchi, N., Prinz, W. A., et al. (2009). A class of dynamin-like GTPases involved in the generation of the tubular ER network. *Cell* 138, 549–561. doi: 10.1016/j.cell.2009.05.025

Hu, S., Ye, H., Cui, Y., and Jiang, L. (2020). AtSec62 is critical for plant development and is involved in ER-phagy in *Arabidopsis thaliana*. *J. Integr. Plant Biol.* 62, 181–200. doi: 10.1111/jipb.12872

Huang, X., Zheng, C., Liu, F., Yang, C., Zheng, P., Lu, X., et al. (2019). Genetic analyses of the *Arabidopsis* ATG1 kinase complex reveal both kinase-dependent and independent autophagic routes during fixed-carbon starvation. *Plant Cell* 31, 2973–2995. doi: 10.1105/tpc.19.00066

Jiang, X., Wang, X., Ding, X., Du, M., Li, B., Weng, X., et al. (2020). FAM134B oligomerization drives endoplasmic reticulum membrane scission for ER-phagy. *EMBO J.* 39:e102608. doi: 10.15252/embj.2019102608

Khaminets, A., Heinrich, T., Mari, M., Grumati, P., Huebner, A. K., Akutsu, M., et al. (2015). Regulation of endoplasmic reticulum turnover by selective autophagy. *Nature* 522, 354–358. doi: 10.1038/nature14498

Lai, Y. S., Stefano, G., and Brandizzi, F. (2014). ER stress signaling requires RHD3, a functionally conserved ER-shaping GTPase. *J. Cell Sci.* 127, 3227–3232. doi: 10.1242/jcs.147447

Le Bars, R., Marion, J., Le Borgne, R., Satiat-Jeunemaitre, B., and Bianchi, M. W. (2014). ATG5 defines a phagophore domain connected to the endoplasmic reticulum during autophagosome formation in plants. *Nat. Commun.* 5:4121. doi: 10.1038/ncomms5121

Liang, J. R., Lingeman, E., Ahmed, S., and Corn, J. E. (2018). Atlastins remodel the endoplasmic reticulum for selective autophagy. *J. Cell Biol.* 217, 3354–3367.

Liu, N., Zhao, H., Zhao, Y. G., Hu, J., and Zhang, H. (2021). Atlastin 2/3 regulate ER targeting of the ULK1 complex to initiate autophagy. *J. Cell Biol.* 220:e202012091. doi: 10.1083/jcb.202012091

Liu, Y., Burgos, J. S., Deng, Y., Srivastava, R., Howell, S. H., and Bassham, D. C. (2012). Degradation of the endoplasmic reticulum by autophagy during endoplasmic reticulum stress in *Arabidopsis*. *Plant Cell* 24, 4635–4651. doi: 10.1105/tpc.112.101535

Mochida, K., Yamasaki, A., Matoba, K., Kirisako, H., Noda, N. N., and Nakatogawa, H. (2020). Super-assembly of ER-phagy receptor Atg40 induces local ER remodeling at contacts with forming autophagosomal membranes. *Nat. Commun.* 11:3306. doi: 10.1038/s41467-020-17163-y

Molinari, M. (2021). ER-phagy responses in yeast, plants, and mammalian cells and their crosstalk with UPR and ERAD. *Dev. Cell* 56, 949–966. doi: 10.1016/j.devcel.2021.03.005

Qi, X. Y., Sun, J. Q., and Zheng, H. Q. (2016). A GTPase-Dependent Fine ER is required for localized secretion in polarized growth of root hairs. *Plant Physio.* 171, 1996–2007. doi: 10.1104/pp.15.01865

Smith, M. D., Harley, M. E., Kemp, A. J., Wills, J., Lee, M., Arends, M., et al. (2018). ccpg1 is a non-canonical autophagy cargo receptor essential for ER-Phagy and pancreatic ER proteostasis. *Dev. Cell* 44, 217.e11–232.e11. doi: 10.1016/j.devcel.2017.11.024

Srivastava, R., Li, Z., Russo, G., Tang, J., Bi, R., Muppirala, U., et al. (2018). Response to persistent er stress in plants: a multiphasic process that transitions cells from prosurvival activities to cell death. *Plant Cell* 30, 1220–1242. doi: 10.1105/tpc.18.00153

Stefano, G., and Brandizzi, F. (2014). Unique and conserved features of the plant ER-shaping GTPase RHD3. *Cell Logist.* 4:e28217. doi: 10.4161/cl.28217

Stephani, M., Picchianti, L., and Dagdas, Y. (2021). C53 is a cross-kingdom conserved reticulophagy receptor that bridges the gap betweenselective autophagy and ribosome stalling at the endoplasmic reticulum. *Autophagy* 17, 586–587. doi: 10.1080/15548627.2020.1846304

Stephani, M., Picchianti, L., Gajic, A., Beveridge, R., Skarwan, E., Sanchez De Medina Hernandez, V., et al. (2020). A cross-kingdom conserved ER-phagy receptor maintains endoplasmic reticulum homeostasis during stress. *eLife* 9:e58396. doi: 10.7554/eLife.58396

Stolz, A., Ernst, A., and Dikic, I. (2014). Cargo recognition and trafficking in selective autophagy. *Nat. Cell Biol.* 16, 495–501. doi: 10.1038/ncb2979

Sun, J., Zhang, M., Qi, X., Doyle, C., and Zheng, H. (2020b). Armadillo-repeat kinesin1 interacts with *Arabidopsis atlastin* RHD3 to move ER with plus-end of microtubules. *Nat. Commun.* 11:5510. doi: 10.1038/s41467-020-19343-2

Sun, J., Movahed, N., and Zheng, H. (2020a). LUNAPARK Is an E3 ligase that mediates degradation of ROOT HAIR DEFECTIVE3 to maintain a tubular ER network in *Arabidopsis*. *Plant Cell* 32, 2964–2978. doi: 10.1105/tpc.18.00937

Sun, J., and Zheng, H. (2018). Efficient ER fusion requires a dimerization and a C-Terminal tail mediated membrane anchoring of RHD3. *Plant Physiol.* 176, 406–417. doi: 10.1104/pp.17.01411

Sun, J. L., Li, J. Y., Wang, M. J., Song, Z. T., and Liu, J. X. (2021). Protein quality control in plant organelles: current progress and future perspectives. *Mol. Plant* 14, 95–114. doi: 10.1016/j.molp.2020.10.011

Ueda, H., Yokota, E., Kuwata, K., Kutsuna, N., Mano, S., Shimada, T., et al. (2016). Phosphorylation of the C terminus of RHD3 Has a critical role in homotypic ER membrane fusion in *Arabidopsis*. *Plant Physiol.* 170, 867–880. doi: 10.1104/pp.15.01172

Wilkinson, S. (2019). ER-phagy: shaping up and destressing the endoplasmic reticulum. *FEBS J.* 286, 2645–2663. doi: 10.1111/febs.14932

Wu, J., Michaeli, S., Picchianti, L., Dagdas, Y., Galili, G., and Peled-Zehavi, H. (2021). ATI1 (ATG8-interacting protein 1) and ATI2 define a plant starvation-induced reticulophagy pathway and serve as MSBP1/MAPR5 cargo receptors. *Autophagy* 17, 3375–3388. doi: 10.1080/15548627.2021.1872886

Xie, Q., Tzfadia, O., Levy, M., Weithorn, E., Peled-Zehavi, H., Van Parys, T., et al. (2016). hfAIM: a reliable bioinformatics approach for in silico genome-wide identification of autophagy-associated Atg8-interacting motifs in various organisms. *Autophagy* 12, 876–887. doi: 10.1080/15548627.2016.1147668

Zhang, M., Wu, F., Shi, J., Zhu, Y., Zhu, Z., Gong, Q., et al. (2013). RHD3 family of dynamin-like GTPases mediates homotypic endoplasmic reticulum fusion and is essential for *Arabidopsis* development. *Plant Physiol.* 163, 713–720. doi: 10.1104/pp.113.224501

Zhang, X., Ding, X., Marshall, R. S., Paez-Valencia, J., Lacey, P., Vierstra, R. D., et al. (2020). Reticulon proteins modulate autophagy of the endoplasmic reticulum in maize endosperm. *eLife* 9:e51918. doi: 10.7554/eLife.51918

Zhao, G., Zhu, P. P., Renvoise, B., Maldonado-Baez, L., Park, S. H., and Blackstone, C. (2016). Mammalian knock out cells reveal prominent roles for atlastin GTPases in ER network morphology. *Exp. Cell Res.* 349, 32–44. doi: 10.1016/j.yexcr.2016.09.015

Zhuang, X., Chung, K. P., Cui, Y., Lin, W., Gao, C., Kang, B. H., et al. (2017). ATG9 regulates autophagosome progression from the endoplasmic reticulum in *Arabidopsis*. *Proc. Natl. Acad. Sci. U.S..A.* 114, E426–E435. doi: 10.1073/pnas.1616299114

Conflict of Interest: The authors declare that the research was conducted in the absence of any commercial or financial relationships that could be construed as a potential conflict of interest.

Publisher's Note: All claims expressed in this article are solely those of the authors and do not necessarily represent those of their affiliated organizations, or those of the publisher, the editors and the reviewers. Any product that may be evaluated in this article, or claim that may be made by its manufacturer, is not guaranteed or endorsed by the publisher.

frontiers | Frontiers in Plant Science

ORIGINAL RESEARCH
published: 25 April 2022
doi: 10.3389/fpls.2022.866367

Monitoring Autophagy in Rice With GFP-ATG8 Marker Lines

Rui Liu[1], Rongxue Zhang[2], Yi Yang[3], Xuejun Liu[2] and Qingqiu Gong[1]**

[1]State Key Laboratory of Microbial Metabolism, Joint International Research Laboratory of Metabolic and Developmental Sciences, School of Life Sciences and Biotechnology, Shanghai Jiao Tong University, Shanghai, China, [2]Tianjin Key Laboratory of Crop Genetics and Breeding, Tianjin Agricultural University, Tianjin, China, [3]College of Life Sciences, Nankai University, Tianjin, China

Autophagy is a conserved intracellular trafficking pathway for bulk degradation and recycling of cellular components in eukaryotes. The hallmark of autophagy is the formation of double-membraned vesicles termed autophagosomes, which selectively or non-selectively pack up various macromolecules and organelles and deliver these cargoes into the vacuole/lysosome. Like all other membrane trafficking pathways, the observation of autophagy is largely dependent on marker lines. ATG8/LC3 is the only autophagy-related (ATG) protein that, through a covalent bond to phosphatidylethanolamine (PE), associates tightly with the isolation membrane/pre-autophagosomal structure (PAS), the growing phagophore, the mature autophagosome, and the autophagic bodies. Therefore, fluorescent protein (FP)-tagged ATG8 had been widely used for monitoring autophagosome formation and autophagic flux. In rice (*Oryza sativa*), FP-OsATG8 driven by Cauliflower mosaic virus (CaMV) 35S promoter had been used for imaging autophagosome and autophagic bodies. Here, we constructed three vectors carrying *GFP-OsATG8a*, driven by *35S*, *ubiquitin*, and the endogenous *ATG8a* promoter, individually. Then, we compared them for their suitability in monitoring autophagy, by observing GFP-ATG8a puncta formation in transiently transformed rice protoplasts, and by tracking the autophagic flux with GFP-ATG8 cleavage assay in rice stable transgenic lines. GFP-Trap immunoprecipitation and mass spectrometry were also performed with the three marker lines to show that they can be used reliably for proteomic studies. We found out that the ubiquitin promoter is the best for protoplast imaging. Transgenic rice seedlings of the three marker lines showed comparable performance in autophagic flux measurement using the GFP-ATG8 cleavage assay. Surprisingly, the levels of GFP-ATG8a transcripts and protein contents were similar in all marker lines, indicating post-transcriptional regulation of the transgene expression by a yet unknown mechanism. These marker lines can serve as useful tools for autophagy studies in rice.

Keywords: autophagy, ATG8, rice, autophagic flux, post-transcriptional regulation

OPEN ACCESS

Edited by:
Ruixi Li,
Southern University of Science and Technology, China

Reviewed by:
Jinbo Shen,
Zhejiang Agriculture and Forestry University, China
Olga V. Voitsekhovskaja,
Komarov Botanical Institute (RAS), Russia

****Correspondence:***
Xuejun Liu
goodrice@263.net
Qingqiu Gong
gongqingqiu@sjtu.edu.cn

Specialty section:
This article was submitted to Plant Physiology, a section of the journal Frontiers in Plant Science

Received: *31 January 2022*
Accepted: *28 March 2022*
Published: *25 April 2022*

Citation:
Liu R, Zhang R, Yang Y, Liu X and Gong Q (2022) Monitoring Autophagy in Rice With GFP-ATG8 Marker Lines. Front. Plant Sci. 13:866367. doi: 10.3389/fpls.2022.866367

INTRODUCTION

Plants are constantly in need of nutrient reallocation during growth and development, yet they are continuously challenged by nutrient limitation and stresses. To combat starvation, biotic, and abiotic stresses while maintaining growth, plants have to efficiently remobilize and reallocate nutrients and clear up pathogens, damaged proteins, and even organelles. Among the degradation/remobilization pathways employed by plants, an intracellular trafficking pathway termed autophagy is particularly important, and the defects in autophagy strongly compromise biomass production and yield (Li et al., 2015; Wada et al., 2015; Have et al., 2017; Avin-Wittenberg et al., 2018; Signorelli et al., 2019; Cao et al., 2020; McLoughlin et al., 2020; Su et al., 2020).

Autophagy is an evolutionarily conserved, bulk degradation pathway of eukaryotic cells that can eliminate and recycle damaged or obsolete proteins and organelles (Nakatogawa, 2020; Zhang et al., 2021). In this pathway, the cargoes, either recognized selectively or non-selectively (Floyd et al., 2012; Farre and Subramani, 2016), are firstly sequestered to a double-membraned vesicle termed isolation membrane (IM) or phagophore, at a specific site termed phagophore assembly site (PAS) usually close by the endoplasmic reticulum (ER; Hollenstein and Kraft, 2020; Wun et al., 2020). Then, the phagophore expands and eventually seals to form an autophagosome. The autophagosome fuses with the tonoplast, and the cargoes, together with the inner membrane (termed autophagic bodies), are released into the vacuole for degradation (Yim and Mizushima, 2020). Through transporters yet unidentified in plants, the amino acids and other macromolecules are transported back into the cytoplasm. Clearly, to monitor the entire process, a marker protein that labels the isolation membrane, autophagosome, and autophagic bodies is essential. ATG8 is the protein (Contento et al., 2005).

ATG8 of yeasts and plants, and LC3/GABARAP of animals, was firstly discovered in the budding yeast (*Saccharomyces cerevisiae*), through the screen for autophagy (as APG8; Tsukada and Ohsumi, 1993), cytoplasm to vacuole targeting (Cvt; as CVT5; Harding et al., 1995), and pexophagy (as AUT7) mutants (Harding et al., 1996). ATG8 is an ubiquitin-like (Ubl) protein that scaffolds the expanding phagophore and autophagosome (Nakatogawa et al., 2007; Xie et al., 2008). After processing by the cysteine protease ATG4, a C-terminal glycine residue of ATG8 is exposed and gets conjugated to the lipid phosphatidylethanolamine (PE) by the ATG8 conjugation system composed of ATG7 as the E1 activating enzyme, ATG3 as the E2 conjugating enzyme, and ATG12-ATG5 complex as the E3 ligase (Mizushima et al., 1998). PE-conjugated ATG8 stays on the expanding phagophore and the mature autophagosome. Then, ATG4 cleaves PE-conjugated ATG8 off the outer membrane of autophagosome before it fuses with the vacuole (Yu et al., 2012). Since it is attached to both sides of the phagophore, upon autophagosome closure, approximately one-third of ATG8 molecules are trapped on the inner membrane of autophagosome along with the cargoes (Nair et al., 2012), thus gets degraded in the vacuole. The fact that ATG8 cannot be fully recycled before autophagosome-vacuole fusion may explain why it is strongly transcriptionally upregulated by autophagy-inducing conditions (Yoshimoto et al., 2004; Nair et al., 2012).

ATG8 not only controls phagophore expansion but is a key element in cargo sequestration. Using their ATG8-interacting motif (AIM)/LC3-interacting region (LIR), ULK1/ATG1 and ATG13 bind ATG8 to regulate autophagosome formation (Wild et al., 2014). Autophagy receptors, adaptors, and cargoes bind ATG8 with AIM/LIR or the ubiquitin-interacting motif (UIM) to get packed into the expanding phagophore (Marshall et al., 2019; Johansen and Lamark, 2020). Possibly for this reason, ATG8 has become arguably the most frequently studied ATG protein. Screens that designed to identify new players in autophagy generally centered on ATG8 (Honig et al., 2012; Zeng et al., 2021). In the autophagy protein–protein interaction network, ATG8 is always a node (Behrends et al., 2010; Tu et al., 2021).

Apart from the shared characteristics with the yeast and animal ATG8s, the plant ATG8s have unique properties (Bu et al., 2020). Arabidopsis has nine ATG8s (ATG8a-i; Yoshimoto et al., 2004), maize has five, and rice has seven that can be mapped (Chung et al., 2009; Xia et al., 2011). The plant ATG8s are categorized into three sub-families and the expansion of the ATG8 family was thought to take place early in the green lineage (Kellner et al., 2017; Zhang et al., 2021). Transcriptome data gave diverse expression patterns of ATG8s of Arabidopsis, indicative of their tissue specific roles (Thompson et al., 2005). Master regulator that governs autophagosome and lysosome biogenesis, such as transcription factor EB (TFEB; Settembre et al., 2011), has not been identified in plants, yet searches for plant-specific transcription regulators led to the discovery of TGACG (TGA) motif-binding protein 9 (TGA9) as a positive regulator of autophagy (Wang et al., 2020). ELONGATED HYPOCOTYL 5 (HY5), along with HISTONE DEACETYLASE 9 (HDA9), was discovered to repress the transcription of autophagy genes such as ATG8e and ATG5 during light-to-dark transition (Yang et al., 2020), thus providing an answer for an open question in plant autophagy.

The way ATG8 is used as a marker for autophagy is also unique in plants. Firstly, the fact that plants have many ATG8s with different molecular weights prevented us from using one anti-ATG8 antibody to examine the autophagic flux, for it is futile to separate different ATG8 isoforms from the PE-conjugated ATG8s. Secondly, the plant vacuole (pH 5.4–5.8) is not as acidic as the lysosome (pH 4.5); hence, the acid-sensitive GFP tag is not promptly degraded in the vacuole. For this reason, it is not possible to use a double tagged ATG8, such as mCherry-GFP-LC3, and take the fluorescent color change as an indicator for autophagic flux (Kaizuka et al., 2016). So far, the relatively reliable way is to use FP-ATG8 transgenic lines and a FP antibody, and to treat the plants with or without V-ATPase inhibitors, such as Concanamycin A (ConA), to distinguish the free FP band (presumably residing in the lytic vacuole as a consequence of autophagy, more resistant to vacuolar hydrolases than ATG8 due to its structural feature) from the FP-ATG8 band (presumably outside the vacuole).

Abbreviations: ATG, Autophagy-related; ConA, Concanamycin A; ER, Endoplasmic reticulum; GFP, Green fluorescent protein; LSCM, Laser Scanning Confocal Microscopy; WT, Wild type.

This method is termed FP-ATG8 cleavage assay. Selection of a proper promoter for the GFP-ATG8 transgenic line is also important, for ectopic expression of ATG8 often promotes transition into flowering, improves nitrogen use efficiency, and increases yield (Chen et al., 2019; Yu et al., 2019), and thus could be unsuitable for stress and developmental studies.

For autophagy studies in rice, *35S:mRFP-OsATG8a* and *35S:mRFP-OsATG8d* lines were firstly generated and imaged for autophagosome accumulation upon ConA treatments (Izumi et al., 2015). Recently, *35S:GFP-OsATG8a* and *35S:GFP-OsATG8b* lines have been generated, and both were reported to increase yield (Yu et al., 2019; Fan et al., 2020). The lack of a comparison between different *GFP-OsATG8* constructs prompted us to generate OsATG8 monitoring lines with *35S*, *ubiquitin*, and endogenous promoters, and to compare their performance under autophagy-inducing conditions. We aimed to pin down specific constructs and lines that are suitable for documenting autophagy, *via* imaging or immunoblotting. We also wanted to evaluate the potential of GFP-OsATG8 in protein–protein interaction screen, which have been a powerful tool in the identification of new players in plant autophagy (Honig et al., 2012; Han et al., 2015; Zeng et al., 2021).

MATERIALS AND METHODS

Plasmids Construction

In this study, the *pCAMBIA1302* vector was used for generating transgenic rice lines. The coding sequence of *OsATG8a* (*Os07g0512200*; 360 bp in length) was amplified from rice cDNA and inserted at the *Eco91*I site through homologous recombination as described (Luo et al., 2017). To generate *ProUBQ10:GFP-OsATG8a* and *ProATG8a:GFP-OsATG8a* plasmids, the *35S* promoter was replaced with the *ubiquitin* promoter and the *OsATG8a* promoter, respectively, and inserted between HindIII and NcoI sites. All constructs were verified by DNA sequencing. The primers used for cloning, plasmid construction, and sequencing are listed in **Supplementary Table S1**.

Generation of Transgenic Rice Lines and Plant Growth Conditions

Transgenic rice lines were generated similarly to a previous report on OsATG8s (Izumi et al., 2015). Briefly, sterilized rice seeds (japonica rice cultivar Jinjing 818) were used for callus induction. The vectors were transformed into mature seed-derived rice calli by Agrobacterium-mediated transformation. Transgenic rice plants (T1) were obtained through several rounds of differentiation inductions and selected on medium containing Hygromycin B. These T1 transgenic rice lines were selected by liquid medium containing 50 mg/L Hygromycin B for 3 days. After germinating in plates containing water for 5–6 days, the seedlings were grown in the modified Hoagland's solution (5 mM KNO_3, 2 mM $MgSO_4{\cdot}7H_2O$, 5 mM $Ca(NO_3)_2{\cdot}4H_2O$, 1 mM KH_2PO_4, 0.05 mM $FeSO_4{\cdot}7H_2O$, 0.05 mM Na_2EDTA, 46 nM H_2BO_3, 9 nM $MnCl_2{\cdot}4H_2O$, 0.3 nM $CuSO_4{\cdot}5H_2O$, and 0.8 nM $ZnSO_4{\cdot}7H_2O$) at 28°C/24°C, 14 h light/10 h dark in a growth chamber. Transgenic rice was cultivated in paddy fields in growth seasons of 2019 to 2021 in Tianjin, Jiangsu, and Hainan provinces of China.

Transient Transformation of Tobacco Leaves

GFP-OsATG8a driven by three different promoters were transiently expressed in tobacco leaves as described (Luo et al., 2017). Soil grown, 4-week-old *N. benthamiana* leaves were used for Agrobacterium infiltration. After 2 days of inoculation, leaves were collected and cut into small squares for confocal microscopy.

Rice Protoplast Transformation

Sterilized rice seeds (japonica rice cultivar Jinjing 818) were germinated on 1/2 Murashige and Skoog (MS) medium with a photoperiod of 14 h light and 10 h dark at 26°C for 5–6 days, then moved to the dark for another 5–6 days. The etiolated stem and sheath of rice seedlings were cut into pieces of approximately 0.5 mm with sharp razors. These pieces were immediately transferred into 20 ml enzyme solution (1.5% Cellulase RS, 0.75% Macerozyme R-10, 0.6 M mannitol, 10 mM MES at pH 5.7, 10 mM $CaCl_2$, and 0.1% BSA), vacuum infiltrated for 30 min, and further digested in the dark for 4–5 h with gentle shaking. After enzyme digestion, protoplasts were released by adding an equal volume of W5 solution (154 mM NaCl, 125 mM $CaCl_2$, 5 mM KCl, and 2 mM MES at pH 5.7) and gentle shaking by hand for 2 min. Then, the protoplasts were filtered through a 40 μm-gauge nylon mesh with 3–5 washes using W5 solution and collected by spinning at 100 g for 3 min. After protoplasts were re-suspended and washed once with W5 solution, MMG solution (0.4 M mannitol, 15 mM $MgCl_2$, and 4 mM MES at pH 5.7) was used to re-suspend the pellets at a concentration of 2×10^6 cells ml^{-1}. For each transformation, 6–8 μg of freshly prepared plasmid DNA and 200 μl protoplasts (about 4×10^5 cells) were mixed with 220 μl freshly prepared PEG solution [40% (w/v) PEG 4000, 0.4 M mannitol, and 0.1 M $CaCl_2$] and were incubated at room temperature for 30 min in the dark. After incubation, the protoplasts were mixed with 1 ml W5 solution and incubated at 28°C for 12–15 h in the dark before imaging.

Laser Scanning Confocal Microscopy

Transiently transformed tobacco leaves (lower epidermis) and rice protoplasts were observed with a Ni-E A1 HD25 confocal microscope (Nikon, Japan). Prior to image collection, the background auto-fluorescence was eliminated using untransformed tobacco leaves or rice protoplasts. The GFP fluorescence signal was exited at 488 nm and emission was collected at 500–550 nm. The chlorophyll auto-fluorescence was exited with 561 nm laser and emission was collected at 600–700 nm. For NaCl treatments, protoplasts were incubated in W5 solution with 250 mM NaCl, or 50 μM E-64d, or both NaCl and E-64d, for 30 min at room temperature. For inhibitor treatments, transformed protoplasts were incubated in W5 solution containing 200 nM AZD8055, or 1 μM ConA, or both AZD8055 and ConA, for 3 h at room temperature.

Quantitative Real-Time RT-PCR

Leaves from 14-day-old seedlings were used for RNA extraction, cDNA synthesis, and quantitative real-time RT-PCR (qRT-PCR) as described (Luo et al., 2017). Transcript levels of *GFP* and *OsATG8a* were normalized to *OsEF1a (LOC_Os03g08020)* with three biological replicates consisting of four technical repeats. Specific amplification was verified by a melt curve analysis following the completion of the PCR cycles. Each PCR product generated a single peak in melt curve analysis, indicating specific amplification. The $2^{-\Delta\Delta CT}$ method was used for relative quantification of qRT-PCR data. Primers used are listed in **Supplementary Table S1**.

Immunoblotting

Two-week-old seedlings were used for autophagic flux measurement. Excised leaves were incubated in the Hoagland's solution with 0.01% Tween-20, and stirred and vacuumed to make sure the leaves were completely soaked in the solution. For NaCl treatments, excised leaves were incubated in the Hoagland's solution plus 150 mM NaCl, or 100 μM E-64d, or both NaCl and E-64d, for 1 h at room temperature. Alternatively, 250 mM NaCl was used. For inhibitor treatments, excised leaves were incubated in the Hoagland's solution containing 2 μM AZD8055, or 1 μM ConA, or both AZD8055 and ConA, for 6 h at room temperature. In addition, 6 h with 200 μM BTH plus 100 μM E-64d treatment and 4 h with 2 mM DTT plus 100 μM E-64d treatment were used to induce autophagy. Protein extraction and immunoblotting were done as described (Luo et al., 2017). Semi-quantification of the protein levels was performed with ImageJ[1] and protein levels were normalized to Coomassie brilliant blue R-250-stained band of the RuBisCO large subunit (RbcL). For immunoblotting, mouse anti-GFP (1:5,000 dilution, Utibody, China), rabbit anti-H3 (1:8,000 dilution, ABclonal, China), and the appropriate IgG-HRP conjugated secondary antibody (1:5,000; ZSGB-Bio, China) were used. The signal was developed using High-sensitivity ECL chemiluminescence detection kit (Vazyme, China) and chemiluminescence was detected using a chemiluminescent Western Blot scanner (ChemiScope 6100T, Clinx, China). All experiments were repeated for three to five times, and one representative result was shown.

GFP-Trap and Mass Spectrometry

Transgenic rice seedlings were frozen and ground in liquid nitrogen, and protein extraction buffer (50 mM Tris–HCl, pH 7.5, 150 mM NaCl, 20% Glycerol, 1 mM $MgCl_2$, 0.2% NP-40, and 1% Protease Inhibitor Cocktail) was added at a proportion of 1:2 (m:v). Extracts were centrifuged at 12,000 rpm for 15 min at 4°C. Then, the supernatants were collected and centrifuged again at 12,000 rpm for 5 min at 4°C. The supernatants (1 ml to 10 μl bead volume) were incubated with GFP-Trap A beads pre-equilibrated in wash buffer (50 mM Tris–HCl, pH 7.5, 150 mM NaCl, 20% Glycerol, 1 mM $MgCl_2$, and 0.1% NP-40) at 4°C for 2–3 h. The beads were washed 3–4 times with wash buffer and were re-suspended in 100 μl wash buffer. Samples were verified by Western blotting; the corresponding gels were cut and sent for mass spectrometry analysis at the Instrumental Analysis Center of Shanghai Jiao Tong University.

[1]https://imagej.nih.gov/

RESULTS

The Ubiquitin Promoter Is More Suitable for the Observation of Transiently Expressed *GFP-OsATG8a*

We cloned OsATG8s from an herbicide-resistant japonica rice cultivar Jinjing 818 and examined their transcript levels. Consistent with previous reports (Xia et al., 2011; Izumi et al., 2015), OsATG8a was the most highly expressed isoform. Hence, it was selected for vector construction (**Figure 1A**). OsATG8d was also selected (**Supplementary Figure S2**); however, we were unable to obtain transgenic lines carrying *ProATG8d:GFP-OsATG8d*, and it was eventually left out.

Expression of *GFP-OsATG8a* driven by *35S*, *ubiquitin*, and *OsATG8a* (endogenous) promoters was firstly examined in transiently transformed *N. benthamiana* leaf epidermal cells. *Pro35S:GFP* gave typical, strong nuclear, and cytoplasmic GFP signals. *Pro35S:GFP-OsATG8a* gave relatively weak cytoplasmic signals and punctate signals that likely represent autophagosomes. Strong cytoplasmic/endoplasmic reticulum and punctate signals were observed from cells transformed with *ProUBQ10:GFP-OsATG8a* (**Figure 1B**). *ProATG8a:GFP-OsATG8a* had the lowest expression level, with puncta representing autophagosomes observed (**Figure 1B**).

We then examined the expression levels of the three constructs in transiently transformed rice protoplasts (**Figure 1C**). Again, *ProUBQ10:GFP* gave cytoplasmic signals, whereas the *GFP-ATG8a* constructs gave both cytoplasmic and punctate signals. Similar to our observation in tobacco leaves, *ProUBQ10:GFP-ATG8a* gave strong and clear signals, and signal from *GFP-ATG8a* driven by the endogenous promoter was very weak.

We had previously shown that the autophagic flux can be induced by salt stress within 30 min in Arabidopsis (Luo et al., 2017). Here, we also treated the transformed rice protoplasts with 250 mM NaCl in the presence of a lysosomal cysteine protease inhibitor E-64d to see if autophagic flux could be induced by salt treatment (**Figure 2**). GFP-OsATG8a driven by all three promoters responded to salt treatment, as NaCl plus E-64d significantly induced GFP-OsATG8a accumulation (**Figures 2A–C**).

Since inhibition of Target of Rapamycin (TOR) can reliably induce autophagy, we treated the protoplasts with 200 nM AZD8055, a potent TOR inhibitor (Chresta et al., 2010), in the presence of the V-ATPase inhibitor ConA (Huss et al., 2002), to further validate the constructs. *GFP-OsATG8a* driven by *UBQ10* and *ATG8a* promoters both responded to TOR inhibition (**Supplementary Figure S1**).

Inferring from the expression intensities, the ubiquitin promoter is a good choice for the transient expression of OsATG8a.

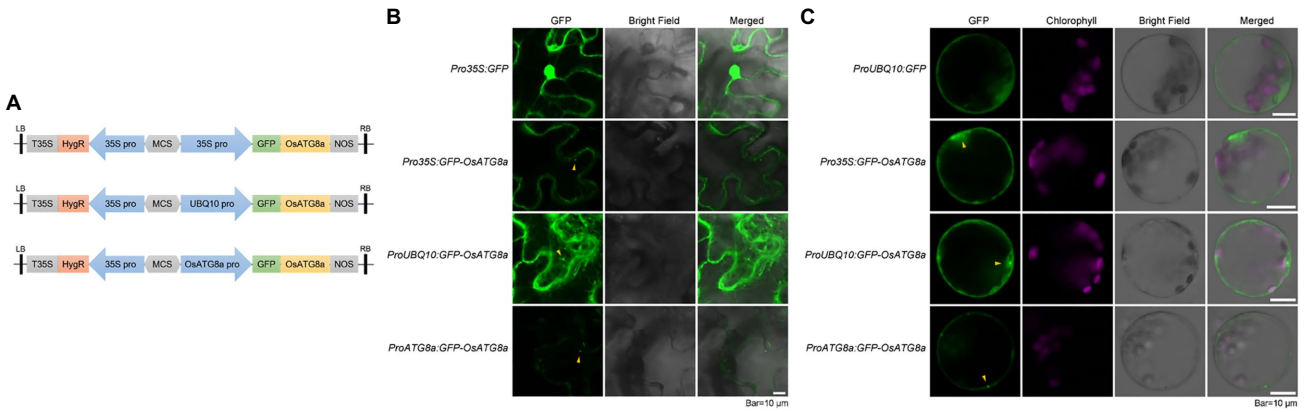

FIGURE 1 | Transient expression of constructs carrying *GFP-OsATG8a*. **(A)** Schematic representation of the *GFP-OsATG8a* fusion gene constructs. Three promoters—the *CaMV35S* promoter, the *ubiquitin* (*UBQ10*) promoter, and the endogenous (*OsATG8a*) promoter—are used for the constructs. **(B)** LSCM of tobacco leaf epidermal cells transiently expressing GFP and GFP-OsATG8a. **(C)** Transient expression of GFP and GFP-OsATG8a in rice protoplasts. Puncta representing autophagosomes are indicated by yellow arrowheads in **(B,C)**. Bar = 10 μm in **(B,C)**.

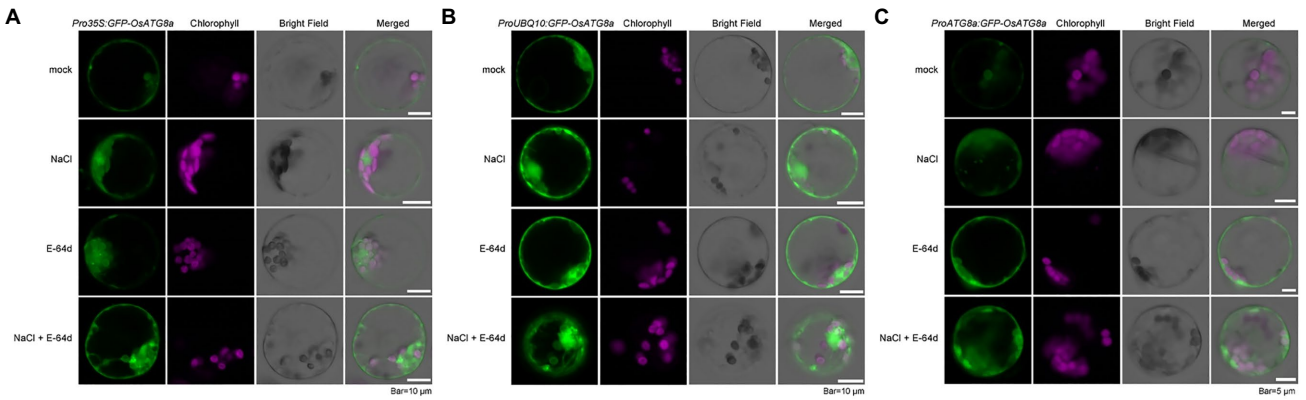

FIGURE 2 | Visualization of autophagic body accumulation in rice protoplasts. Rice protoplasts expressing *GFP-OsATG8a* driven by **(A)** *35S* promoter, **(B)** *UBQ10* promoter, and **(C)** *OsATG8a* promoter were observed with LSCM after treatment with 250 mM NaCl, or 50 μM E-64d, or NaCl plus E-64d for 30 min. Accumulation of GFP signals, indicative of autophagosome and autophagic bodies, can be seen in protoplasts treated with NaCl plus E-64d. Bar = 10 μm in **(A,B)**; 5 μm in **(C)**.

Stable Transgenic Lines Carrying *GFP-OsATG8a* Are Comparable for Immunoblotting

After validating and comparing the three constructs in transient expression systems, transgenic rice carrying these constructs were generated. T1 transgenic lines regenerated from the transformed calli were firstly validated with genomic PCR and immunoblotting (**Supplementary Figures S2A,B**). Then, the plants were grown in the paddy fields and measured for their heights and the number of tillers before harvesting. Consistent with a recent report (Fan et al., 2020), the transgenic lines were not very different among themselves in their heights (**Supplementary Figure S3A**). The numbers of tillers were not very different either (**Supplementary Figure S3B**). No significant change in phenotype was observed at the seedling stage in the T3 transgenic lines (**Supplementary Figure S3C**).

The T3 transgenic seedlings carrying *Pro35S:GFP-OsATG8a*, *ProUBQ10:GFP-OsATG8a*, and *ProOsATG8a:GFP-OsATG8a* were evaluated for their suitability in measuring autophagic flux. The autophagic flux was measured with the GFP-ATG8 cleavage assay, in which the flux is represented by the ratio of the amount of cleaved GFP (27 kD) to total GFP in the lane (40 kD plus 27 kD), i.e., GFP/(GFP + GFP-ATG8a). Firstly, GFP-OsATG8a (40kD) and free GFP (27kD) bands were readily detected in the transgenic lines (**Figure 3**). Since one or two bands were detected for GFP-OsATG8a on immunoblots, we validated the bands by running the samples along with recombinant GFP-OsATG8s purified from *E.coli*. Two bands of similar sizes were seen for the recombinant proteins GFP-OsATG8a and GFP-OsATG8d (**Supplementary Figure S2C**). Such observation indicated that both bands correspond to GFP-ATG8, and the amount of GFP-ATG8 should be measured as the sum of the two.

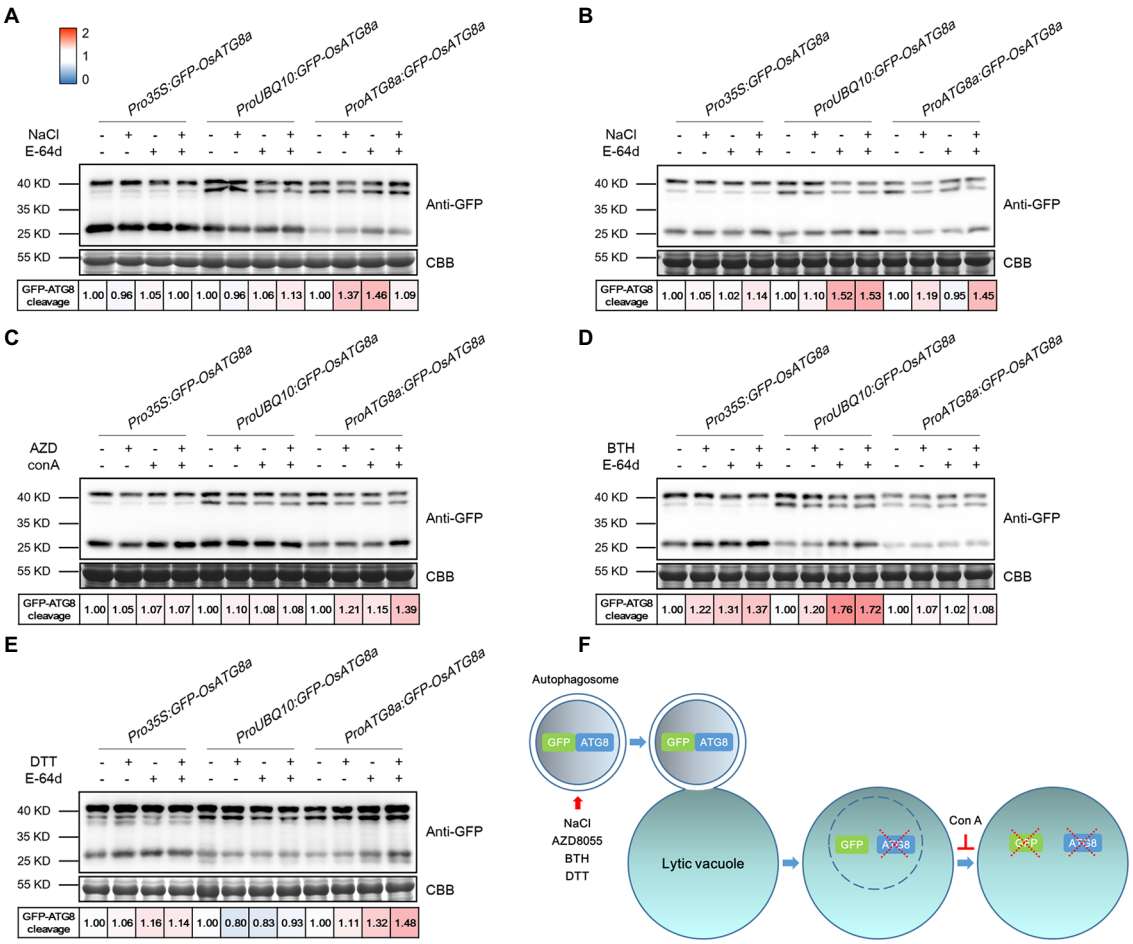

FIGURE 3 | Measuring autophagic flux in *GFP-OsATG8a* marker lines. The level of autophagic flux is represented by the difference of the GFP-ATG8 cleavage between control and treatment. GFP-ATG8 cleavage was calculated as the ratio of the free GFP band (27 kD) to the total GFP signal in the lane (40kD plus 27 kD), then normalized to the respective control (no treatment, no E-64d or ConA; set as 1.00). A color scale (Blue for 0, white for 1, and red for 2) was used to illustrate the semi-quantified values of GFP-ATG8 cleavage. Coomassie Brilliant Blue (CBB) staining of RuBisCO large subunit was used as loading control. **(A)** For moderate salt stress-induced autophagy, excised leaves from 14-day-old rice seedlings were incubated in the Hoagland's solution plus 150 mM NaCl, or 100 μM E-64d, or both NaCl and E-64d for 1 h. **(B)** For severe salt stress-induced autophagy, leaves were incubated in 250 mM NaCl and 100 μM E-64d for 1 h. **(C)** For TOR inhibition-induced autophagy, leaves were incubated in 2 μM AZD8055 and 1 μM Concanamycin A for 6 h. **(D)** For BTH-induced autophagy, 200 μM BTH and 100 μM E-64d for 6 h were used. **(E)** For ER stress-induced autophagy, 2 mM DTT and 100 μM E-64d for 4 h were used. At least three biological replicates were done for each treatment, and one representative replicate is shown. **(F)** A diagram illustrating the GFP cleavage assay and the chemicals used.

For autophagy induction, rice seedlings were treated with NaCl, AZD8055, BTH, and DTT (**Figures 3A–E**). Benzo-(1,2,3)-thiadiazole-7-carbothioic acid (BTH), a salicylic acid agonist, has been used to induce autophagy (Yoshimoto et al., 2009; Zeng et al., 2021). DTT is known to induce ER stress-elicited autophagy (Liu et al., 2012). In general, GFP-OsATG8a driven by all three promoters responded mildly to the treatments and chemicals. A possible explanation is that the basal level autophagy is relatively high already in rice. Specifically, *Pro35S:GFP-OsATG8a* responded relatively strongly to 200 μM BTH. *ProUBQ10:GFP-OsATG8a* responded well to 250 mM NaCl and BTH, but not to 2 mM DTT. *ProOsATG8a:GFP-OsATG8a* responded nicely to moderate and severe salt stress, AZD8055, and DTT. A diagram illustrating the GFP cleavage assay and the chemicals used is presented (**Figure 3F**). E-64d is omitted from the diagram because its precise role in preserving GFP, or even GFP-ATG8, is currently unknown.

At this point, we noticed an interesting phenomenon. The T3 transgenic lines carrying *35S:GFP* and *Ubiquitin:GFP* gave strong GFP bands (**Figure 4A**; **Supplementary Figure S2B**), validating the strength of the promoters. However, lines carrying *GFP-OsATG8a* driven by *35S*, *ubiquitin*, or *OsATG8a* promoters had comparable protein levels of GFP-OsATG8a among themselves (**Figure 4A, Supplementary Figure S2B**). We then examined the transcript levels of the *GFP-OsATG8a* fusion gene and the endogenous *OsATG8a* with qRT-PCR (**Figures 4B–E**). To distinguish ectopic *OsATG8a* from the endogenous transcript, two pairs of primers were used for *OsATG8a*, with one targeting the coding sequence and the

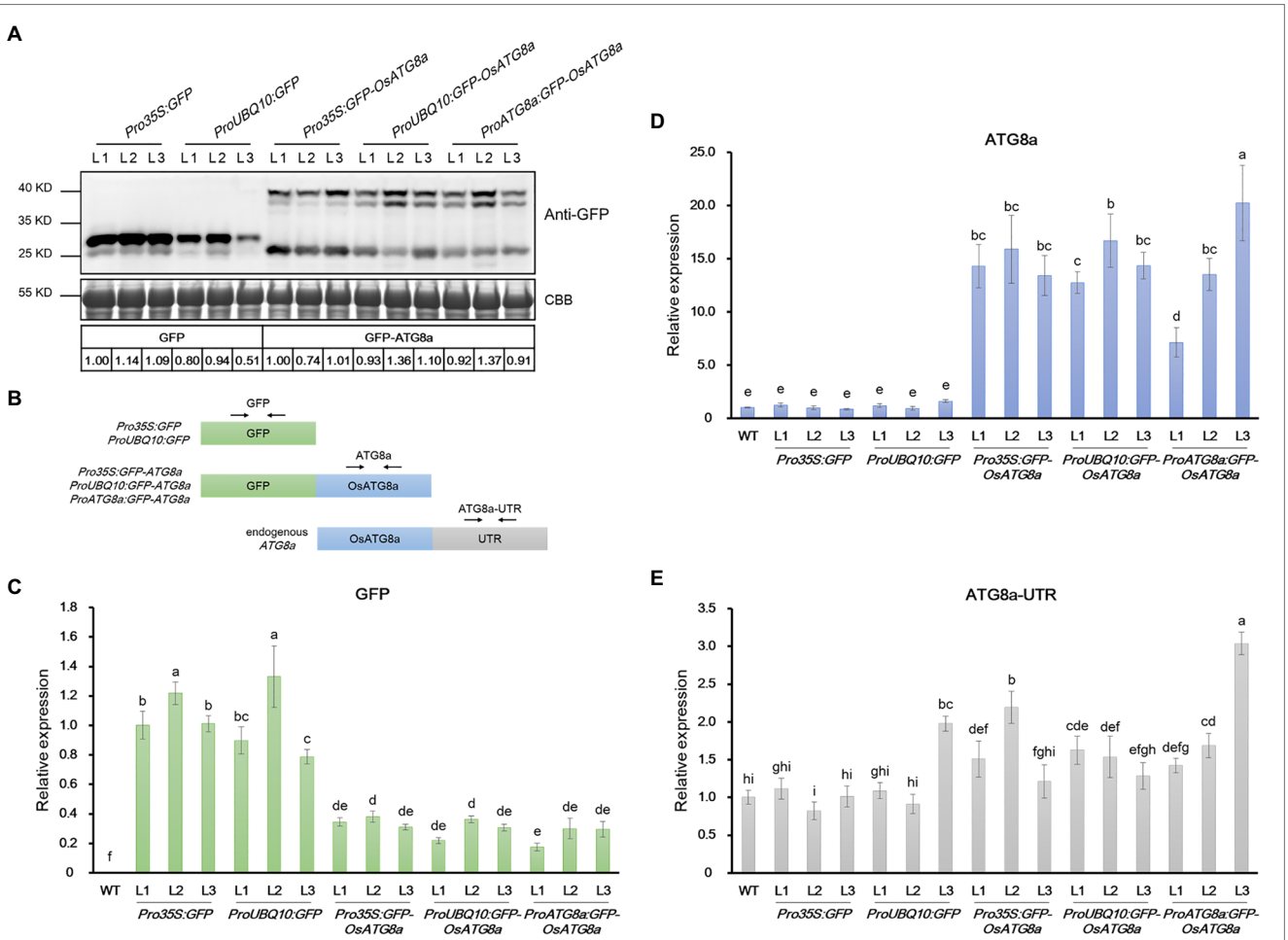

FIGURE 4 | mRNA and protein levels of GFP and GFP-OsATG8a in rice transgenic lines. **(A)** Expression of GFP (27 kD) and GFP-OsATG8a (40 kD, one or two bands) were detected by immunoblotting and quantified by ImageJ. The protein level of GFP was normalized to *Pro35S:GFP*—L1 (set as 1), and the level of GFP-OsATG8a was normalized to *Pro35S:GFP-OsATG8a*—L1 (set as 1). Three T2 transgenic lines for each construct were shown. Coomassie Blue staining of RuBisCO large subunit was used as loading control. Three biological replicates were done, and one representative replicate is shown. **(B)** Schematic representation of the primers designed for qRT-PCR in **(C–E)**. **(C–E)** qRT-PCR analysis of transgenic seedlings. Transcript levels of **(C)** *GFP*, **(D)** *OsATG8a*, and **(E)** *OsATG8a-UTR* were profiled and normalized to the *Pro35S:GFP*—L1 **(C)** or the wild-type control **(D,E)**. Data are means ± SD ($n = 4$), one-way ANOVA followed by Tukey B test; $p = 0.05$. Different letters denote significant differences. Three biological replicates, each consisting of four technical repeats, were done, and one representative replicate is shown.

other targeting the 3'-UTR (**Figure 4B**). Consistent with the protein levels (**Figure 4A**), when expressed alone, the *GFP* transcript can accumulate to high levels if driven by 35S or ubiquitin promoters (**Figure 4C**). In contrast, when expressed as *GFP-OsATG8a*, the transcript level of *GFP*, representing the fusion gene, was clearly repressed (**Figure 4C**), indicative of transcriptional regulation. *OsATG8a* transcripts, representing both endogenous and ectopic *OsATG8a*, accumulated in all *GFP-ATG8s* lines carrying the three constructs, however not very differently except for one line (**Figure 4D**), yet again suggesting a regulation at the transcription level. Judging from the levels of the *OsATG8a-UTR*, the endogenous expression of *OsATG8a* was not very different in all lines including the wild type, suggesting that it is the transcription of the fusion gene that gets regulated (**Figure 4E**). Therefore, both transcriptional and post-transcriptional regulation of ATG8a have taken place in the transgenic lines carrying *GFP-ATG8a*, especially in *Pro35S:GFP-OsATG8a* and *ProUBQ10:GFP-OsATG8a*, resulting in comparable *GFP-OsATG8a* protein levels. The mechanism is currently unknown and awaits further study.

Immunoprecipitation-Mass Spectrometry Analyses on the Three *GFP-OsATG8a* Transgenic Lines

ATG8 is a star molecule in proteomic studies of autophagy. To see if the *GFP-OsATG8a* transgenic lines could be used for protein–protein interaction studies, GFP-Trap immunoprecipitation was performed using seedlings from three transgenic lines along with GFP control plants grown under control conditions (mock = Hoagland's solution) or treated with

Hoagland's solution containing 150 mM NaCl for 1 h. The immuno-precipitated proteins were verified with SDS-PAGE and sent for mass spectrometry analyses.

From the eight conditions, 2,244 proteins from 8,120 peptides altogether were obtained. After subtracting the proteins identified in GFP control, 56, 97, and 86 proteins remained for *Pro35S:GFP-OsATG8a*, *ProUBQ10:GFP-OsATG8a*, and *ProOsATG8a:GFP-OsATG8a* under control conditions (**Figure 5A**). With salt treatment, 54, 106, and 97 proteins were identified as interacting partners for OsATG8a in the three lines, respectively (**Figure 5B**). The numbers of shared target proteins between different transgenic lines were also shown in the Venn diagrams (**Figures 5A,B**). To better describe the OsATG8a-interacting protein landscape, we mapped the proteins to the Arabidopsis proteome by batch BLAST and used the Arabidopsis protein with the lowest e-value to represent the rice protein. Then, we combined all target proteins identified from mock or NaCl treatment for Gene Ontology (GO) analysis using Cytoscape as described (Wu et al., 2022). Under controlled (mock) conditions, most enriched GO terms are tryptophan metabolic processes, indolalkylamine metabolic processes, photosynthesis, and starch biosynthesis, indicative of growth-related processes like auxin biosynthesis and photosynthesis (**Figure 5C**). Such categorization is consistent with the knowledge that basal level autophagy constitutively recycles damaged and obsolete proteins. With salt stress, GO terms related to the amino acid metabolic processes, especially serine, aspartate, and cysteine metabolic processes overwhelmingly enriched (**Figure 5D**). Energy reserve and starch metabolic processes were also enriched (**Figure 5D**).

We also randomly generated a list of cytoplasmic proteins that have not been reported to interact with ATG8 (**Supplementary Table S4**) and searched their protein sequences to see whether they have LIR/AIM. All selected proteins indeed have one or more LIR/AIM, suggesting that they may be ATG8-interating partners.

Apart from the GO analysis, we manually examined the list of potential ATG8-interacting proteins and spotted some very interesting proteins. A manually annotated list is shown in **Figure 5E**. First of all, like all other ATG8/LC3 interactomes, essential membrane trafficking regulators were identified. These include SH3P2, the ATG8-, and PI3P-binding protein that regulates autophagosome formation; the COPII coat proteins SEC13 and SEC24—COPII vesicles have been revealed to participate in autophagosome formation; EXO70A1, the Exocyst component that had been reported to regulate root growth; Rab2, the Rab GTPase whose mammalian homolog have been reported to regulate autophagy; the Guanosine nucleotide diphosphate dissociation inhibitor GDI1, which is general to Rab GTPases and ROP GTPases; TRS120, the TRAPPII component that is required for cell plate formation; and CLASP, the microtubule-associated protein that regulates both cell division and cell expansion. Plasma membrane- and tonoplast-localized proteins, such as the P-ATPase AHA6, the sodium transporter HKT1, and the Vacuolar H^+-Pyrophosphatase AVP1, were also identified. Furthermore, kinase and phosphatases that have been reported to regulate autophagy or stress response were seen in the list. These include the catalytic and regulatory subunits of the plant AMPK, SnRK1/KIN10, the key regulator in autophagy, response to carbon limitation, and circadian clock; Casein kinase 1, an ancient protein kinase that had been reported to regulate selective autophagy; PHOT2, a key blue light receptor and kinase that regulate response to high light; stress responsive kinases ABC1K10A and LECRK-IV.1; TOPP4, an evolutionarily conserved PP1 phosphatase that regulates plant growth and immune response; and ATB'GAMMA, a regulatory subunit of the PP2A phosphatase that is known to balance growth and defense. Other stress response proteins identified include UBP1B, a marker protein for stress granules that stores mRNA during stress conditions, as well as FIERY1/HOS2, SAD2, ADH1, RPM1/RPS3, and PUP1 and PUP3, two purple acid phosphatases that function in response to low phosphate. We concluded that the potential OsATG8a-interacting proteins are worthy of further exploration, and the transgenic lines that we generated can be used by the community in future to identify new OsATG8a-interacting proteins under various developmental and stress conditions.

DISCUSSION

In this study, we validated that transgenic lines carrying *GFP-OsATG8a*, either driven by the *35S*, the *ubiquitin*, or the endogenous promoter, are suitable for monitoring autophagy in rice. An accidental yet interesting finding is that transcriptional and post-transcriptional regulation occurred when *GFP-OsATG8a* is ectopically expressed in rice (**Figure 4**). Firstly, both the *35S* and the *ubiquitin* promoter can strongly and effectively drive the expression of GFP. However, the expression levels of *GFP-ATG8a*, driven by the three promoters, are more or less comparable. We analyzed approximately a hundred lines carrying the three constructs with immunoblotting, yet a *GFP-ATG8a* line with the level of GFP-ATG8a comparable to GFP driven by *35S* or *ubiquitin* promoters was not found. For this reason, the promoter selection for the rice GFP-ATG8 marker line may not be as important as for the Arabidopsis GFP-ATG8 markers. It is likely that over-accumulation of the ATG8a protein could exert an adverse effect on reproduction and that a feed-back regulation likely exists for *ATG8a* to maintain a not-too-high level of the ATG8a protein. The detailed mechanism remains to be discovered. The transcription factors that may regulate the expression of *OsATG8a* remains unidentified; checking the rice homologs of the relevant Arabidopsis transcription factors may help to answer the question. A few transcription factors were identified from the IP-MS, and they are also worthy of further examination. Another possibility is through a miRNA that targets ATG8a. In animals, for instance, MIR204 and MIR33 have been reported to target LC3B to suppress autophagy; MIR143 and MIR133A-3p have been reported to target GABARAPL1 to induce autophagy, and MIR195 targets GABARAPL1 to repress autophagy (Akkoc and Gozuacik, 2020). Whether similar mechanism may exist in rice remains to be discovered.

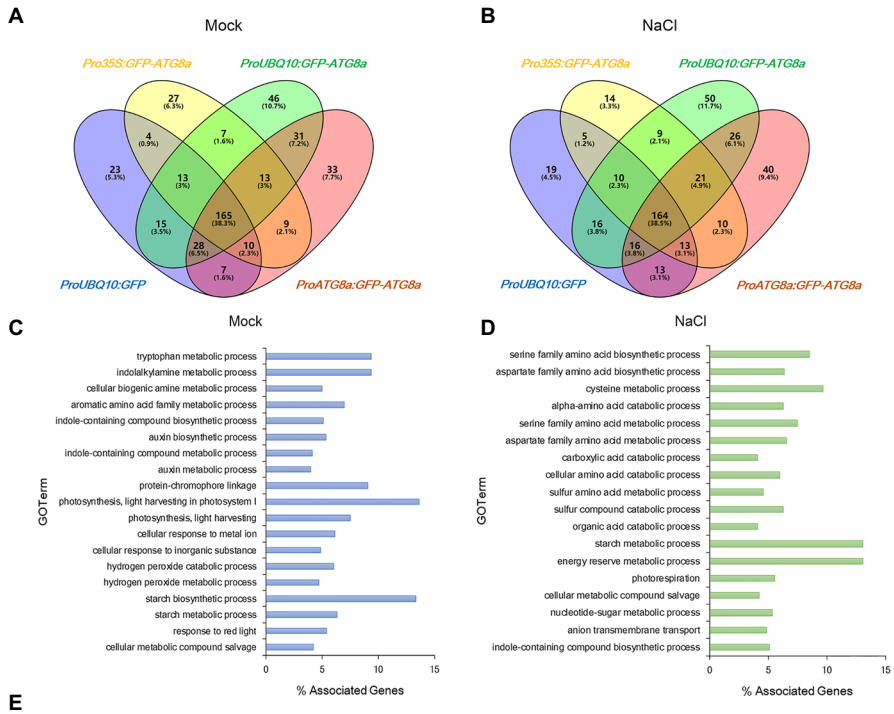

E

Uniprot ID	Description	Arabidopsis homolog	Gene names	Functional category
Q710Q4	Autophagy protein ATG8	AT1G62040	ATG8D	Autophagy; Membrane trafficking
Q01IQ0	SH3 domain-containing protein, binds PI3P and ATG8 and regulates autophagosome formation	AT4G34660	SH3P2	
Q8W403	COPII component SEC13	AT2G30050	SEC13	
Q01MT8	COPII component SEC24a/ERMO2, required for endoplasmic reticulum morphology	AT3G07100	SEC24A, ERMO2	
Q259N6	Exocyst subunit EXO70A1	AT5G03540	EXO70A1	
Q01JN3	RAB GTPASE HOMOLOG B1C	AT4G17170	RAB2A, RABB1C	
O22470	GDP dissociation inhibitor OsGDI1	AT2G44100	GDI1	
Q01I83	Tethering factor required for cell plate biogenesis	AT5G11040	TRS120, VAN4	
Q01IV2	Microtubule-associated protein, involved in both cell division and cell expansion	AT2G20190	CLASP	
Q8RW29	Plasma membrane H[+]-ATPase	AT2G07560	AHA6	Transporters
A0A6F8FJD4	High-affinity K+ transporter 2	AT4G10310	HKT1	
P93409	Vacuolar membrane H(+)-Ppase, regulator of apoplastic pH and auxin transport	AT1G15690	AVP1,FUGU5	
Q40740	SNF1-related protein kinase 1, activator of autophagy	AT3G01090	KIN10, SNRK1	Protein kinases and phosphatases
Q01LJ2	SNF1-related protein kinase regulatory subunit gamma 1	AT3G48530	KINgamma, KING1	
Q01I14	CASEIN KINASE I	AT4G14340	CK1, CKL11	
Q01ME5	PHOTOTROPIN 2, membrane-bound protein kinase that functions redundantly with PHOT1 as blue light photoreceptor	AT5G58140	PHOT2, NPL1	
Q01JL8	Atypical kinase which functions in salt stress tolerance by regulating reactive oxygen species (ROS)	AT1G11390	ABC1K10A	
Q00RH9	L-TYPE LECTIN RECEPTOR KINASE IV.1, induced in response to Salicylic acid	AT2G37710	LECRK-IV.1	
Q94F84	Type 1 phosphoprotein Ser/Thr phosphatase (PP1), catalytic subunit	AT2G39840	TOPP4	
Q01IF6	B' regulatory subunit of PP2A (AtB'gamma)	AT4G15415	ATB' GAMMA	
Q84V55	Purple acid phosphatase Ossap2, involved in extracellular phosphate-scavenging	AT2G16430	PUP1, PAP10	Other regulators of stress responses
Q8S505	Purple acid phosphatase, involved in extracellular phosphate-scavenging	AT5G34850	PUP3, PAP26	
P0C5A3	Bifunctional stress regulator with 3'(2'),5'-bisphosphate nucleotidase and inositol polyphosphate 1-phosphatase activities	AT5G63980	FIERY1, RON1, SUPO1,HOS2	
Q01KY9	Importin beta-domain family protein, likely involved in nuclear transport in ABA signaling	AT2G31660	SAD2, GIR1, EMA1, URM9	
D7PPK2	Alcohol dehydrogenase 1, catalyzes the reduction of acetaldehyde using NADH as reductant	AT1G77120	ADH1	
Q9XEV3	OLIGOURIDYLATE BINDING PROTEIN 1B, RNA-binding protein involved in stress granule formation	AT1G17370	UBP1B	
A0A0U2SCX6	NBS-LRR-like resistance protein, confers resistance to Pseudomonas syringae strains carrying the avirulence genes avrB and avrRpm1	AT3G07040	RPM1, RPS3	

FIGURE 5 | Identification of new ATG8-interacting proteins with immunoprecipitation-mass spectrometry analyses on GFP-OsATG8a marker lines. **(A)** Venn diagram showing the overlap in the number of proteins identified from three GFP-OsATG8a lines and the GFP control line, under normal growth condition (Mock). **(B)** Venn diagram showing the overlap in the number of proteins identified from three *GFP-OsATG8a* lines and the *GFP* control line, treated with 150 mM NaCl for 1 h (NaCl). **(C)** Gene Ontology (GO)-Biological Process (BP) enriched in all OsATG8a-interacting proteins (166 in total) identified from the three transgenic lines under normal growth condition (Mock). **(D)** GO-BP enriched in all 170 OsATG8a-interacting proteins identified after salt stress (NaCl). **(E)** Selected OsATG8a-interacting proteins, including regulators of autophagy and other trafficking routes, plasma membrane and tonoplast transporters, protein kinases and phosphatases, and other regulators of stress responses.

The transcriptional and post-transcriptional regulation on ATG8a could also explain why the three GFP-Trap/Mass Spectrometry experiments generated similar lists of proteins (**Figure 5**). Repeated identification of the same proteins actually added more confidence to the IP-MS study. A number of proteins identified are worthy of further study and may help answer some existing questions in plant autophagy, such as which membranes or vesicles, apart from COPII vesicles (Zeng et al., 2021; Kim et al., 2022), may contribute to autophagosome formation. Early studies for plant autophagy had identified ATI1 and ATI2 as plant-specific ATG8-interacting proteins; both were uncovered through an Y2H screen (Honig et al., 2012). Both ATIs have recently been characterized as starvation-induced ER-phagy receptors for MSBP1 (Wu et al., 2021). We have recently reported a non-autophagy role for ScATG8 in promoting the degradation of vacuolar membrane proteins when the yeast cells approach the stationary phase (He et al., 2021). A similar process had previously been reported for the fission yeast (Liu et al., 2018), suggesting non-autophagy functions of ATG8 could be widespread. Interestingly, in this process, the vacuolar membrane protein that recruits ATG8 to the vicinity of tonoplast, Hfl1, was homologs to lazarus 1(LAZ1) of Arabidopsis, which was initially identified as a suppressor of *acd11*-related cell death (Malinovsky et al., 2010). The transgenic lines generated in this study, with other screening methods, can be used to identify new OsATG8a-interacting proteins and even non-autophagy functions of plant ATG8s. We hope these rice autophagy marker lines will facilitate both the research and the applications of plant autophagy.

DATA AVAILABILITY STATEMENT

The original contributions presented in the study are included in the article/**Supplementary Material**, and further inquiries can be directed to the corresponding authors.

AUTHOR CONTRIBUTIONS

QG: conceptualization and writing—review and editing. RL, RZ, and QG: methodology. RL and YY: investigation. RL and QG: writing—original draft. XL and QG: funding acquisition. RZ, XL, and QG: supervision. All authors contributed to the article and approved the submitted version.

FUNDING

This work is supported by the National Natural Science Foundation of China (91954102 and 31871355) to QG.

ACKNOWLEDGMENTS

The authors thank Gaosong Huang, Mingxing Xin, Yong Peng, Xueyong Liu, Dekuan Zhang, and Kai Zhao for help with growing rice. The authors thank the Gong lab members Liming Luo for help with protein annotation, Pingping Zhang for help with tobacco transient expression and insightful suggestions, Xinjing Li for discussions, and Taotao Wang for critical reading of the manuscript.

SUPPLEMENTARY MATERIAL

The Supplementary Material for this article can be found online at: https://www.frontiersin.org/articles/10.3389/fpls.2022.866367/full#supplementary-material

Supplementary Figure S1 | Visualization of accumulation of autophagic bodies in rice protoplasts. Rice protoplasts expressing *GFP-OsATG8a* driven by **(A)** *UBQ10* promoter, **(B)** *OsATG8a* promoter was observed with LSCM after treatment with 200 nM AZD8055 or 1 μM ConA, or AZD8055 plus ConA, for 3 h. Bar = 7.5 μm.

Supplementary Figure S2 | Verification of *GFP* and *GFP-OsATG8a* transgenic lines. T1 transgenic lines regenerated from the transformed rice calli were verified with **(A)** genomic PCR and **(B)** immunoblotting. GFP antibody recognizes GFP-ATG8 bands (40 kD) and free GFP (27 kD). **(C)** GFP-OsATG8a and GFP-OsATG8d from rice transgenic lines (P for plant) or prokaryotically expressed (E for *E.coli*) were detected with a GFP antibody. Primers used in **(A)** are listed in **Supplementary Table S1**. Anti-histone H3 was used as an internal control in **(B)**.

Supplementary Figure S3 | Growth parameters of rice transgenic lines carrying *GFP-OsATG8a*. **(A,B)** T1 transgenic rice plants grown in the paddy field were measured before harvesting. **(A)** Plant height and **(B)** tiller number were measured. Data are means ± SD ($n = 7–15$), one-way ANOVA followed by a Duncan test; $p = 0.05$. Different letters denote significant differences. **(C)** Phenotypes of 16-day-old transgenic rice seedlings. Three T3 lines for each construct were shown. Bar = 3 cm.

REFERENCES

Akkoc, Y., and Gozuacik, D. (2020). MicroRNAs as major regulators of the autophagy pathway. *Biochim. Biophys. Acta, Mol. Cell Res.* 1867:118662. doi: 10.1016/j.bbamcr.2020.118662

Avin-Wittenberg, T., Baluska, F., Bozhkov, P. V., Elander, P. H., Fernie, A. R., Galili, G., et al. (2018). Autophagy-related approaches for improving nutrient use efficiency and crop yield protection. *J. Exp. Bot.* 69:3173. doi: 10.1093/jxb/ery113

Behrends, C., Sowa, M. E., Gygi, S. P., and Harper, J. W. (2010). Network organization of the human autophagy system. *Nature* 466, 68–76. doi: 10.1038/nature09204

Bu, F., Yang, M., Guo, X., Huang, W., and Chen, L. (2020). Multiple functions of ATG8 family proteins in plant autophagy. *Front. Cell Dev. Biol.* 8:466. doi: 10.3389/fcell.2020.00466

Cao, J. J., Liu, C. X., Shao, S. J., and Zhou, J. (2020). Molecular mechanisms of autophagy regulation in plants and their applications in agriculture. *Front. Plant Sci.* 11:618944. doi: 10.3389/fpls.2020.618944

Chen, Q., Soulay, F., Saudemont, B., Elmayan, T., Marmagne, A., and Masclaux-Daubresse, C. L. (2019). Overexpression of ATG8 in Arabidopsis stimulates autophagic activity and increases nitrogen remobilization efficiency and grain filling. *Plant Cell Physiol.* 60, 343–352. doi: 10.1093/pcp/pcy214

Chresta, C. M., Davies, B. R., Hickson, I., Harding, T., Cosulich, S., Critchlow, S. E., et al. (2010). AZD8055 is a potent, selective, and orally bioavailable ATP-competitive mammalian target of rapamycin kinase inhibitor with *in vitro*

and *in vivo* antitumor activity. *Cancer Res.* 70, 288–298. doi: 10.1158/0008-5472.CAN-09-1751

Chung, T., Suttangkakul, A., and Vierstra, R. D. (2009). The ATG autophagic conjugation system in maize: ATG transcripts and abundance of the ATG8-lipid adduct are regulated by development and nutrient availability. *Plant Physiol.* 149, 220–234. doi: 10.1104/pp.108.126714

Contento, A. L., Xiong, Y., and Bassham, D. C. (2005). Visualization of autophagy in Arabidopsis using the fluorescent dye monodansylcadaverine and a GFP-AtATG8e fusion protein. *Plant J.* 42, 598–608. doi: 10.1111/j.1365-313X.2005.02396.x

Fan, T., Yang, W., Zeng, X., Xu, X., Xu, Y., Fan, X., et al. (2020). A rice autophagy gene OsATG8b is involved in nitrogen remobilization and control of grain quality. *Front. Plant Sci.* 11:588. doi: 10.3389/fpls.2020.00588

Farre, J. C., and Subramani, S. (2016). Mechanistic insights into selective autophagy pathways: lessons from yeast. *Nat. Rev. Mol. Cell Biol.* 17, 537–552. doi: 10.1038/nrm.2016.74

Floyd, B. E., Morriss, S. C., Macintosh, G. C., and Bassham, D. C. (2012). What to eat: evidence for selective autophagy in plants. *J. Integr. Plant Biol.* 54, 907–920. doi: 10.1111/j.1744-7909.2012.01178.x

Han, S., Wang, Y., Zheng, X., Jia, Q., Zhao, J., Bai, F., et al. (2015). Cytoplastic glyceraldehyde-3-phosphate dehydrogenases interact with ATG3 to negatively regulate autophagy and immunity in *Nicotiana benthamiana*. *Plant Cell* 27, 1316–1331. doi: 10.1105/tpc.114.134692

Harding, T. M., Hefner-Gravink, A., Thumm, M., and Klionsky, D. J. (1996). Genetic and phenotypic overlap between autophagy and the cytoplasm to vacuole protein targeting pathway. *J. Biol. Chem.* 271, 17621–17624. doi: 10.1074/jbc.271.30.17621

Harding, T. M., Morano, K. A., Scott, S. V., and Klionsky, D. J. (1995). Isolation and characterization of yeast mutants in the cytoplasm to vacuole protein targeting pathway. *J. Cell Biol.* 131, 591–602. doi: 10.1083/jcb.131.3.591

Have, M., Marmagne, A., Chardon, F., and Masclaux-Daubresse, C. (2017). Nitrogen remobilization during leaf senescence: lessons from Arabidopsis to crops. *J. Exp. Bot.* 68, 2513–2529. doi: 10.1093/jxb/erw365

He, C. W., Cui, X. F., Ma, S. J., Xu, Q., Ran, Y. P., Chen, W. Z., et al. (2021). Membrane recruitment of Atg8 by Hfl1 facilitates turnover of vacuolar membrane proteins in yeast cells approaching stationary phase. *BMC Biol.* 19:117. doi: 10.1186/s12915-021-01048-7

Hollenstein, D. M., and Kraft, C. (2020). Autophagosomes are formed at a distinct cellular structure. *Curr. Opin. Cell Biol.* 65, 50–57. doi: 10.1016/j.ceb.2020.02.012

Honig, A., Avin-Wittenberg, T., Ufaz, S., and Galili, G. (2012). A new type of compartment, defined by plant-specific Atg8-interacting proteins, is induced upon exposure of Arabidopsis plants to carbon starvation. *Plant Cell* 24, 288–303. doi: 10.1105/tpc.111.093112

Huss, M., Ingenhorst, G., Konig, S., Gassel, M., Drose, S., Zeeck, A., et al. (2002). Concanamycin A, the specific inhibitor of V-ATPases, binds to the V(o) subunit c. *J. Biol. Chem.* 277, 40544–40548. doi: 10.1074/jbc.M207345200

Izumi, M., Hidema, J., Wada, S., Kondo, E., Kurusu, T., Kuchitsu, K., et al. (2015). Establishment of monitoring methods for autophagy in rice reveals autophagic recycling of chloroplasts and root plastids during energy limitation. *Plant Physiol.* 167, 1307–1320. doi: 10.1104/pp.114.254078

Johansen, T., and Lamark, T. (2020). Selective autophagy: ATG8 family proteins, LIR motifs and cargo receptors. *J. Mol. Biol.* 432, 80–103. doi: 10.1016/j.jmb.2019.07.016

Kaizuka, T., Morishita, H., Hama, Y., Tsukamoto, S., Matsui, T., Toyota, Y., et al. (2016). An autophagic flux probe that releases an internal control. *Mol. Cell* 64, 835–849. doi: 10.1016/j.molcel.2016.09.037

Kellner, R., De la Concepcion, J. C., Maqbool, A., Kamoun, S., and Dagdas, Y. F. (2017). ATG8 expansion: A driver of selective autophagy diversification? *Trends Plant Sci.* 22, 204–214. doi: 10.1016/j.tplants.2016.11.015

Kim, J. H., Lee, H. N., Huang, X., Jung, H., Otegui, M. S., Li, F., et al. (2022). FYVE2, a phosphatidylinositol 3-phosphate effector, interacts with the COPII machinery to control autophagosome formation in Arabidopsis. *Plant Cell* 34, 351–373. doi: 10.1093/plcell/koab263

Li, F., Chung, T., Pennington, J. G., Federico, M. L., Kaeppler, H. F., Kaeppler, S. M., et al. (2015). Autophagic recycling plays a central role in maize nitrogen remobilization. *Plant Cell* 27, 1389–1408. doi: 10.1105/tpc.15.00158

Liu, Y., Burgos, J. S., Deng, Y., Srivastava, R., Howell, S. H., and Bassham, D. C. (2012). Degradation of the endoplasmic reticulum by autophagy during endoplasmic reticulum stress in Arabidopsis. *Plant Cell* 24, 4635–4651. doi: 10.1105/tpc.112.101535

Liu, X. M., Yamasaki, A., Du, X. M., Coffman, V. C., Ohsumi, Y., Nakatogawa, H., et al. (2018). Lipidation-independent vacuolar functions of Atg8 rely on its noncanonical interaction with a vacuole membrane protein. *elife* 7:e41237. doi: 10.7554/eLife.41237

Luo, L., Zhang, P., Zhu, R., Fu, J., Su, J., Zheng, J., et al. (2017). Autophagy is rapidly induced by salt stress and is required for salt tolerance in Arabidopsis. *Front. Plant Sci.* 8:1459. doi: 10.3389/fpls.2017.01459

Malinovsky, F. G., Brodersen, P., Fiil, B. K., McKinney, L. V., Thorgrimsen, S., Beck, M., et al. (2010). Lazarus1, a DUF300 protein, contributes to programmed cell death associated with Arabidopsis acd11 and the hypersensitive response. *PLoS One* 5:e12586. doi: 10.1371/journal.pone.0012586

Marshall, R. S., Hua, Z., Mali, S., McLoughlin, F., and Vierstra, R. D. (2019). ATG8-binding UIM proteins define a new class of autophagy adaptors and receptors. *Cell* 177:e724, 766.e24–781.e24. doi: 10.1016/j.cell.2019.02.009

McLoughlin, F., Marshall, R. S., Ding, X., Chatt, E. C., Kirkpatrick, L. D., Augustine, R. C., et al. (2020). Autophagy plays prominent roles in amino acid, nucleotide, and carbohydrate metabolism during fixed-carbon starvation in maize. *Plant Cell* 32, 2699–2724. doi: 10.1105/tpc.20.00226

Mizushima, N., Noda, T., Yoshimori, T., Tanaka, Y., Ishii, T., George, M. D., et al. (1998). A protein conjugation system essential for autophagy. *Nature* 395, 395–398. doi: 10.1038/26506

Nair, U., Yen, W. L., Mari, M., Cao, Y., Xie, Z., Baba, M., et al. (2012). A role for Atg8-PE deconjugation in autophagosome biogenesis. *Autophagy* 8, 780–793. doi: 10.4161/auto.19385

Nakatogawa, H. (2020). Mechanisms governing autophagosome biogenesis. *Nat. Rev. Mol. Cell Biol.* 21, 439–458. doi: 10.1038/s41580-020-0241-0

Nakatogawa, H., Ichimura, Y., and Ohsumi, Y. (2007). Atg8, a ubiquitin-like protein required for autophagosome formation, mediates membrane tethering and hemifusion. *Cell* 130, 165–178. doi: 10.1016/j.cell.2007.05.021

Settembre, C., Di Malta, C., Polito, V. A., Garcia Arencibia, M., Vetrini, F., Erdin, S., et al. (2011). TFEB links autophagy to lysosomal biogenesis. *Science* 332, 1429–1433. doi: 10.1126/science.1204592

Signorelli, S., Tarkowski, L. P., Van den Ende, W., and Bassham, D. C. (2019). Linking autophagy to abiotic and biotic stress responses. *Trends Plant Sci.* 24, 413–430. doi: 10.1016/j.tplants.2019.02.001

Su, T., Li, X., Yang, M., Shao, Q., Zhao, Y., Ma, C., et al. (2020). Autophagy: an intracellular degradation pathway regulating plant survival and stress response. *Front. Plant Sci.* 11:164. doi: 10.3389/fpls.2020.00164

Thompson, A. R., Doelling, J. H., Suttangkakul, A., and Vierstra, R. D. (2005). Autophagic nutrient recycling in Arabidopsis directed by the ATG8 and ATG12 conjugation pathways. *Plant Physiol.* 138, 2097–2110. doi: 10.1104/pp.105.060673

Tsukada, M., and Ohsumi, Y. (1993). Isolation and characterization of autophagy-defective mutants of *Saccharomyces cerevisiae*. *FEBS Lett.* 333, 169–174. doi: 10.1016/0014-5793(93)80398-E

Tu, Y. X. I., Sydor, A. M., Coyaud, E., Laurent, E. M. N., Dyer, D., Mellouk, N., et al. (2021). Global proximity Interactome of the human macroautophagy pathway. *Autophagy*, 1–13. doi: 10.1080/15548627.2021.1965711 [Epub ahead of print]

Wada, S., Hayashida, Y., Izumi, M., Kurusu, T., Hanamata, S., Kanno, K., et al. (2015). Autophagy supports biomass production and nitrogen use efficiency at the vegetative stage in rice. *Plant Physiol.* 168, 60–73. doi: 10.1104/pp.15.00242

Wang, P., Nolan, T. M., Yin, Y., and Bassham, D. C. (2020). Identification of transcription factors that regulate ATG8 expression and autophagy in Arabidopsis. *Autophagy* 16, 123–139. doi: 10.1080/15548627.2019.1598753

Wild, P., McEwan, D. G., and Dikic, I. (2014). The LC3 interactome at a glance. *J. Cell Sci.* 127, 3–9. doi: 10.1242/jcs.140426

Wu, Y., Chang, Y., Luo, L., Tian, W., Gong, Q., and Liu, X. (2022). Abscisic acid employs NRP-dependent PIN2 vacuolar degradation to suppress auxin-mediated primary root elongation in Arabidopsis. *New Phytol.* 233, 297–312. doi: 10.1111/nph.17783

Wu, J., Michaeli, S., Picchianti, L., Dagdas, Y., Galili, G., and Peled-Zehavi, H. (2021). ATI1 (ATG8-interacting protein 1) and ATI2 define a plant starvation-induced reticulophagy pathway and serve as MSBP1/MAPR5 cargo receptors. *Autophagy* 17, 3375–3388. doi: 10.1080/15548627.2021.1872886

Wun, C. L., Quan, Y., and Zhuang, X. (2020). Recent advances in membrane shaping for plant autophagosome biogenesis. *Front. Plant Sci.* 11:565. doi: 10.3389/fpls.2020.00565

Xia, K., Liu, T., Ouyang, J., Wang, R., Fan, T., and Zhang, M. (2011). Genome-wide identification, classification, and expression analysis of autophagy-associated gene homologues in rice (*Oryza sativa* L.). *DNA Res.* 18, 363–377. doi: 10.1093/dnares/dsr024

Xie, Z., Nair, U., and Klionsky, D. J. (2008). Atg8 controls phagophore expansion during autophagosome formation. *Mol. Biol. Cell* 19, 3290–3298. doi: 10.1091/mbc.e07-12-1292

Yang, C., Shen, W., Yang, L., Sun, Y., Li, X., Lai, M., et al. (2020). HY5-HDA9 module transcriptionally regulates plant autophagy in response to light-to-dark conversion and nitrogen starvation. *Mol. Plant* 13, 515–531. doi: 10.1016/j.molp.2020.02.011

Yim, W. W., and Mizushima, N. (2020). Lysosome biology in autophagy. *Cell Discov.* 6:6. doi: 10.1038/s41421-020-0141-7

Yoshimoto, K., Hanaoka, H., Sato, S., Kato, T., Tabata, S., Noda, T., et al. (2004). Processing of ATG8s, ubiquitin-like proteins, and their deconjugation by ATG4s are essential for plant autophagy. *Plant Cell* 16, 2967–2983. doi: 10.1105/tpc.104.025395

Yoshimoto, K., Jikumaru, Y., Kamiya, Y., Kusano, M., Consonni, C., Panstruga, R., et al. (2009). Autophagy negatively regulates cell death by controlling NPR1-dependent salicylic acid signaling during senescence and the innate immune response in Arabidopsis. *Plant Cell* 21, 2914–2927. doi: 10.1105/tpc.109.068635

Yu, Z. Q., Ni, T., Hong, B., Wang, H. Y., Jiang, F. J., Zou, S., et al. (2012). Dual roles of Atg8-PE deconjugation by Atg4 in autophagy. *Autophagy* 8, 883–892. doi: 10.4161/auto.19652

Yu, J., Zhen, X., Li, X., Li, N., and Xu, F. (2019). Increased autophagy of rice can increase yield and nitrogen use efficiency (NUE). *Front. Plant Sci.* 10:584. doi: 10.3389/fpls.2019.00584

Zeng, Y., Li, B., Ji, C., Feng, L., Niu, F., Deng, C., et al. (2021). A unique AtSar1D-AtRabD2a nexus modulates autophagosome biogenesis in *Arabidopsis thaliana*. *Proc. Natl. Acad. Sci. U. S. A.* 118:e2021293118. doi: 10.1073/pnas.2021293118

Zhang, S., Hama, Y., and Mizushima, N. (2021). The evolution of autophagy proteins—diversification in eukaryotes and potential ancestors in prokaryotes. *J. Cell Sci.* 134:jcs233742. doi: 10.1242/jcs.233742

Conflict of Interest: The authors declare that the research was conducted in the absence of any commercial or financial relationships that could be construed as a potential conflict of interest.

Publisher's Note: All claims expressed in this article are solely those of the authors and do not necessarily represent those of their affiliated organizations, or those of the publisher, the editors and the reviewers. Any product that may be evaluated in this article, or claim that may be made by its manufacturer, is not guaranteed or endorsed by the publisher.

frontiers | Frontiers in Plant Science

MINI REVIEW
published: 07 June 2022
doi: 10.3389/fpls.2022.863389

Vacuoles in Bryophytes: Properties, Biogenesis, and Evolution

*Hao-ran Liu[1], Chao Shen[1], Danial Hassani[1], Wan-qi Fang[1], Zhi-yi Wang[1], Yi Lu[1], Rui-liang Zhu[1] and Qiong Zhao[1,2]**

[1] School of Life Sciences, East China Normal University, Shanghai, China, [2] Institute of Eco-Chongming, Shanghai, China

Vacuoles are the most conspicuous organelles in plants for their indispensable functions in cell expansion, solute storage, water balance, etc. Extensive studies on angiosperms have revealed that a set of conserved core molecular machineries orchestrate the formation of vacuoles from multiple pathways. Usually, vacuoles in seed plants are classified into protein storage vacuoles and lytic vacuoles for their distinctive morphology and physiology function. Bryophytes represent early diverged non-vascular land plants, and are of great value for a better understanding of plant science. However, knowledge about vacuole morphology and biogenesis is far less characterized in bryophytes. In this review, first we summarize known knowledge about the morphological and metabolic constitution properties of bryophytes' vacuoles. Then based on known genome information of representative bryophytes, we compared the conserved molecular machinery for vacuole biogenesis among different species including yeast, mammals, *Arabidopsis* and bryophytes and listed out significant changes in terms of the presence/absence of key machinery genes which participate in vacuole biogenesis. Finally, we propose the possible conserved and diverged mechanism for the biogenesis of vacuoles in bryophytes compared with seed plants.

Keywords: bryophyte, endomembrane system, vacuole, biogenesis, regulator, evolution

OPEN ACCESS

Edited by:
Xiaojuan Li,
Beijing Forestry University, China

Reviewed by:
Shutang Tan,
University of Science and Technology of China, China
David Scheuring,
University of Kaiserslautern, Germany

***Correspondence:**
Qiong Zhao
qzhao@bio.ecnu.edu.cn

Specialty section:
This article was submitted to Plant Physiology, a section of the journal Frontiers in Plant Science

Received: *27 January 2022*
Accepted: *02 May 2022*
Published: *07 June 2022*

Citation:
Liu H-r, Shen C, Hassani D, Fang W-q, Wang Z-y, Lu Y, Zhu R-l and Zhao Q (2022) Vacuoles in Bryophytes: Properties, Biogenesis, and Evolution. Front. Plant Sci. 13:863389. doi: 10.3389/fpls.2022.863389

INTRODUCTION

The endomembrane system (ES), which is composed of organelles and their connections termed as membrane trafficking, is found only in eukaryotes. This remarks its evolutionary and functional importance to eukaryotic life. Based on the type of eukaryotic cells, the endomembrane trafficking pathway, engage various organelles including, endoplasmic reticulum (ER), Golgi, *trans*-Golgi network/early endosome (TGN/EE), multivesicular body/late endosome (MVB/LE), and lysosome/vacuole (Cui et al., 2020; Hu et al., 2020). Extant eukaryotes, as descendants from the last eukaryotic common ancestor (LECA), although exhibit enormous distinctions, share several sets of conserved-core molecular machineries (CCMMs) which orchestrate the basic ES-related cellular events. Here in this review, we mainly focus on the CCMMs orchestrating vacuole biogenesis across kingdoms.

Different from animal cells, plant cells have evolved several fundamental unique cellular structures, such as cell wall, chloroplast, central vacuole, and plasmodesmata to cope with changing signals from internal and external stimuli. The membrane trafficking pathway in plants is mainly divided into the biosynthetic secretory pathway, the endocytic pathway, and the vacuole

trafficking pathway (Aniento et al., 2022). In plant cells, the vacuole is an important part of the vacuole trafficking pathway. Except for protein storage and degradation, vacuoles store water, accommodate many other metabolites, and maintain the basic cell physiological activities such as pH and turgor pressure (Wolf et al., 2010; Shimada et al., 2018; Tan et al., 2019). In addition, vacuoles play significant roles in plant protection against biotic and abiotic stress. Tracheophytes and bryophytes share a common ancestor about 500 million years ago and constitute the two deeply diverged land plant groups. Therefore, it is of great importance to characterize plant-unique membrane-related regulatory paradigm by referring to bryophyte plant species.

Bryophytes are a group of terrestrial, non-vascular plant species, which represent early-diverging embryophytes. In bryophytes, for instance, storage of heavy metals such as Fe, Al, and Cd in vacuoles is a protective strategy to reduce their adverse effect (Thiébaut et al., 2008; Zhang et al., 2018; Tan et al., 2019). Similarly, under intense UV-B conditions, vacuoles accumulate UV-absorbing compounds, mostly phenolic, in both angiosperms and bryophytes (Wolf et al., 2010; Fabón et al., 2012). These indeed highlight the importance of vacuoles and their conserved evolutionary biogenesis among various plant species.

Here, by referring to vacuole-related research on bryophytes, including both experimental studies and our own phylogenetic studies with comparative genomic approaches, we first highlighted the most current morphological and metabolic constitution properties of bryophytes' vacuoles; and then we compared the conserved molecular machinery for vacuole biogenesis among different bryophytes species with *Arabidopsis*, and listed out important presence/absence events of key proteins which participate in vacuole biogenesis; finally we propose possible interpretations of conserved and diverse vacuole biogenesis and function in bryophytes compared with seed plants.

BRYOPHYTES' MORPHOLOGY AND LIFE CYCLE

Bryophytes are divided into three types, namely, *Hepaticopsida* (Liverworts), *Bryopsida* (Mosses), and *Anthocerotopsida* (Hornworts) (Klips, 2016). They lack flowers, seeds, and true root systems, which are quite different from the model seed plant *Arabidopsis thaliana* (**Figures 1A–H**).

The life cycle of bryophytes consists of two alternating generations, namely, the haploid gametophyte and the diploid sporophyte, of which the gametophyte is the dominant generation (**Figure 1I**). The haploid gametophyte stage begins from a single cell by spore (single cell) germination, which will be further developed into a 2-D multiple-cell stage termed as protonemata. In mosses, the protonemata are divided into the early stage chloronema and late stage caulonema which possess higher and lower chloroplast density, respectively (Cove et al., 1997). Further in most bryophytes, the 2-D multicellular stage protonema will develop more complicated 3-D multicellular organs including thalloid, rhizoids, and aerial filaments, finally leading to a mature leafy or thallus gametophyte individual (**Figures 1A–D**). Bryophytes reproduce both in sexual and asexual (vegetative) ways. For sexual reproduction, bryophytes use two types of reproductive organs, namely the antheridium for eggs, and the archegonium for sperms. The mixing of genetic material from parental plants is achieved via egg fertilization in the antheridium. The fertilized egg will further develop into the diploid sporophyte stage (Shimamura, 2016) (**Figure 1I**). The continued mitosis division of the embryo will give rise to a mature sporophyte containing foot, seta, and capsule, which will further produce and release haploid spores through meiosis (Frangedakis et al., 2021). For vegetative reproduction, various ways have been reported for different bryophytes species, and almost all bryophytes could reproduce vegetatively.

DIFFERENT POPULATIONS OF VACUOLES IN BRYOPHYTES

It has been known that vacuoles do not have a fixed morphology and size, while its structure varies according to the growth stage or the environmental conditions (Richards et al., 2010; Cao et al., 2020; Cui et al., 2020). In seed plants, like in *A. thaliana*, vacuoles are mainly divided into lytic vacuoles (LVs) and protein storage vacuoles (PSVs) due to their distinctive morphologies and physiology functions (Paris et al., 1996; Feeney et al., 2013; Cui et al., 2020). LVs contain lytic enzymes and keep an acidic pH (Kriegel et al., 2015), while PSVs store lots of proteins in seeds and keep a neutral pH (Isayenkov, 2014; Zhang et al., 2021). LVs and PSVs are interchangeable during different developmental stages (Feeney et al., 2018).

Similar to any plants, the bryophytes cells are of different shapes and sizes with different subcellular structures during the growth, development, and in response to changing environment. Numerous researches with light and electron microscopic images of different bryophyte cells indicate the presence of multiple vacuole populations, including vacuoles of different sizes, vacuoles of different pHs, and vacuoles of different contents, but no PSV is reported.

Vacuoles of different sizes have been reported to different species including both moss and liverwort. During the mature gametophyte stage, several mosses including, *Sphagnum recurvum, Sphagnum cuspidatum*, and *Sphagnum palustre*, bear large central vacuoles in thick walled sterome cells, while the internal thin-walled cells possess abundant number of small vacuoles (Ligrone and Duckett, 1998). In contrast to the gametophyte stage, in some mosses such as *Ephemerum cohaerens* the small vacuole is dominant in basal foot cells, while in *Timmiella barbuloides* big vacuole in the tapetum cells is formed after cytokinesis in sporophyte (Gambardella et al., 1994; Yip and Rushing, 1999). In liverworts, for example, in *Asterella wilmsii*, central large vacuoles are present in the chlorenchyma cells besides air chambers and the young inner thallus cells, while the small vacuoles lay near the fully differentiated thallus apex (Ligrone and Duckett, 1994).

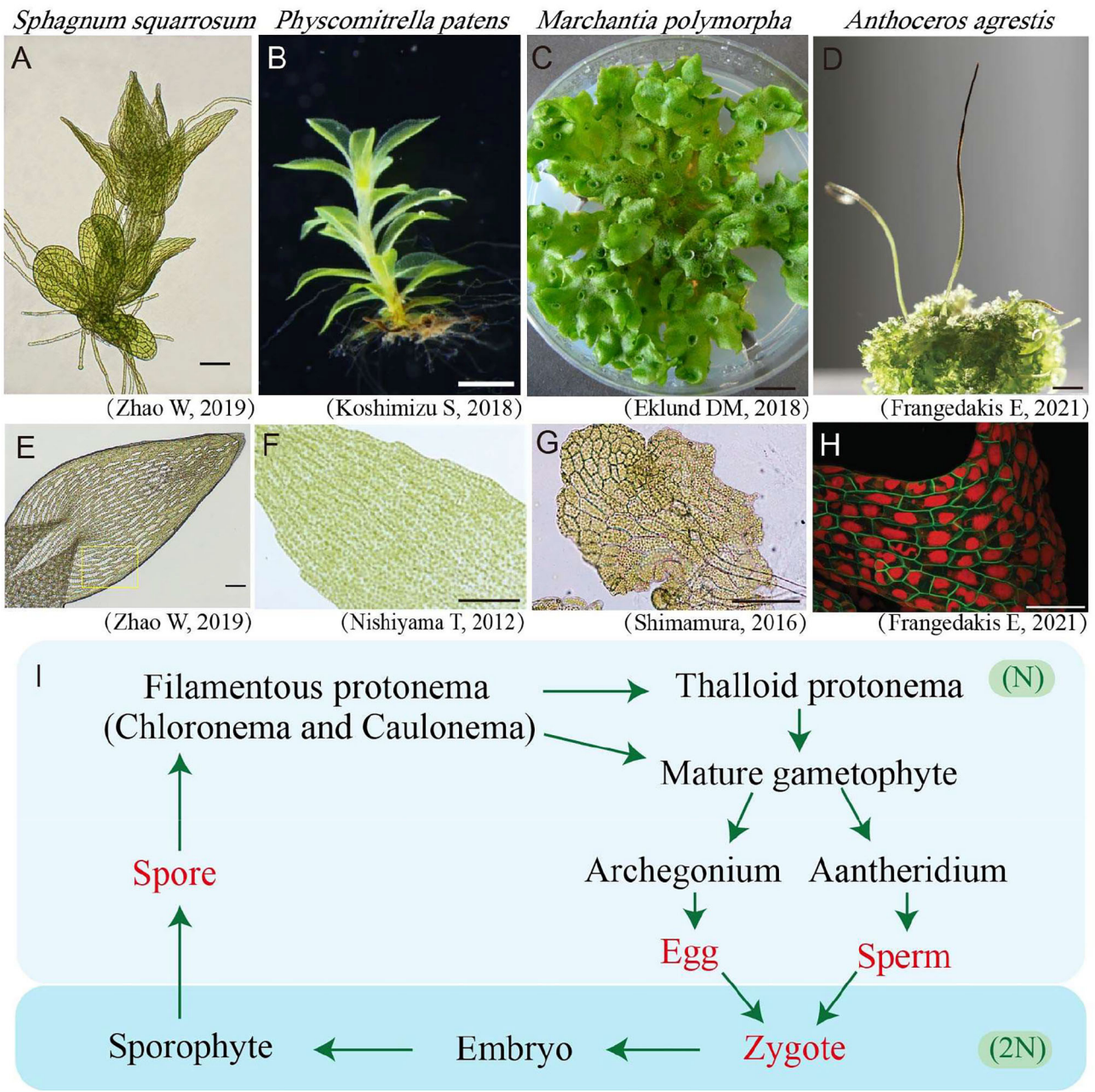

FIGURE 1 | Gametophyte and leaves/thallus cells of bryophytes. **(A)** Light microscopy photos of young *Sphagnum squarrosum* gametophyte. Bar = 100 μm. **(B)** Photo of *Physcomitrella patens's* mature gametophyte (Koshimizu et al., 2018). Bar = 1 mm. **(C)** Photo of *Marchantia polymorpha's* mature gametophyte (Eklund et al., 2018). Bar = 1 mm. **(D)** Photo of *Anthoceros agrestis* gametophyte (the bottom area) and sporophytes (the top slender area). Bar = 3 mm. **(E)** Photo of a leaf with green and white cells in *S. squarrosum* (Li et al., 2019). Bar = 100 μm. **(F)** Light microscopy photo of a leaf in *P. patens* (Nishiyama et al., 2012). Bar = 100 μm. **(G)** Light microscopy photo of young thallus cells of *M. polymorpha* (Shimamura, 2016). Bar = 100 μm. **(H)** Confocal fluorescence microscopy image of *A. agrestis* gametophyte cells in which the plasma membrane is shown in green and the plastid is shown in red (Frangedakis et al., 2021). Bar = 100 μm. **(I)** Life cycle of bryophytes. The words in red denote single cell stages while the words in black denote multicellular stages. The light blue background indicates the haploid (N) stages, while the dark blue background indicates the diploid (2N) stages of bryophytes.

The study in liverwort *Lophozia ventricosa* and *Bazzania trilobata* found that meristematic cells of the shoot apex lacked vacuoles, while the vacuoles in a mature leaf cell were large (Pihakaski, 1968).

Vacuoles maintain the cellular pH via the pumping of protons through the action of V-ATPase into the vacuole lumen, making it acidic (Kriegel et al., 2015). Inside vacuoles, under these acidic conditions, acid hydrolase enzymes break down large molecules

(Rojo et al., 2003). In seed plants, LVs are the most acidic compartment (Shen et al., 2013). In addition to pH adjustment, the V-ATPase is crucial for a plethora of cellular functions including both endocytic and secretory pathways (Dettmer et al., 2006). In bryophytes, vacuoles of similar appearance but different pHs have been reported. For example, large central vacuoles in protonema and rhizoids cells of *P. patens* are acidic vacuoles (AV), while non-acidic vacuoles (NV) coexist in the same protonema apical cell (Ayachi, 2013). This highlights that vacuoles of different pH exist in bryophytes.

Vacuoles are not only on the structure basis of plant cells but also play crucial roles in the transportation and storage of more than 200,000 secondary metabolites, such as phenolic, terpenoids, and alkaloids compounds (Francisco and Martinoia, 2018). Most of these metabolites are considered as a defensive tool against biotic and abiotic stress which are released upon cell destruction. For instance, under UV-B radiation, bryophytes could synthesize and accumulate UV-absorbing compounds (UVAC) to protect themselves. These phenolic compounds include two types, namely, the soluble SUVAC and the cell-wall bound WUVAC. Vacuoles-localized SUVACs are more responsive to the elevation in UV-B level in comparison to WUVACs (Fabón et al., 2012; Hespanhol et al., 2014; Monforte et al., 2015; Soriano et al., 2019).

Besides UV-B absorbing compounds, there are other groups of secondary metabolites which are synthesized and accumulate in bryophytes. Flavonoids and terpenoids are among the most abundant groups of natural bioactive compounds which are not only beneficial for the plant itself but also play a health-promoting role for humans (Hassani et al., 2020). For instance, hundreds of compounds are extracted, and over 40 aromatic compounds and terpenoids have been discovered in *M. polymorpha* (Asakawa and Ludwiczuk, 2013). However, how vacuoles may contribute to these groups of secondary metabolites are largely unknown. Recent studies in *M. polymorpha* highlighted that the secretory pathway of the endomembrane system contributes to the formation of the specialized organelle called the oil body, which is responsible for terpenoid storage in liverwort. The production of secondary metabolites is a crucial evolutionary trait that the plants have adopted to enhance their survival rate against harsh environmental factors. In this regard, the co-evolution of the endomembrane system and their regulatory network with secondary metabolites production and storage is indispensable in plants.

VACUOLE DYNAMICS IN BRYOPHYTES

Plant vacuoles are also highly dynamic, which may undergo continuous coordinated cycles of fusion and fission actions as observed in guard cells, or perform convolution-like actions to transform a large central vacuole into interconnected bubbles or into separated fragmented small vacuoles (Cui et al., 2020). Vacuole dynamics allow vacuoles to change in size, shape, and number during cell division and in response to growth and environmental signals (Kimata et al., 2019). In Arabidopsis, studies have shown that the SNAREs VTI11 and VTI12 are major players in tonoplast remodeling and transport to the vacuole, respectively (Sanmartin et al., 2007). Meanwhile, excellent studies in Arabidopsis have recently demonstrated that vacuole-actin interaction severely impacts vacuole dynamics and vacuole morphologies (Deeks et al., 2012; Scheuring et al., 2016). Also, it has been found that Vacuole-actin adaptors Networked 4 are regulating vacuole size and morphology (Kaiser et al., 2019). The cell wall, as a rigid container outside of protoplast, was recently shown to affect vacuole size and shape through cellular signal communication between cell wall and vacuole (Dunser et al., 2019). In addition, plant hormone auxin has been shown to change vacuole morphology through the regulation of SNARE protein abundance (Lofke et al., 2015). Studies in BY2 cells have also revealed the dynamic change of vacuole size and morphology during different stages of the cell cycle (Kutsuna et al., 2003). Tonoplast localized water channel protein TIPs are traditionally used as markers to distinguish different populations of vacuoles in a variety of seed plants (Gattolin et al., 2009, 2010), but not in bryophytes.

Similar vacuole dynamics have been observed in bryophytes. In moss, for instance, in *P. patens* a large central vacuole occupies the cellular space in apical and subapical cells during chloronema and caulonema stages, respectively, while the large vacuole will transform into several small vacuoles in apical cells during caulonema stage (Jensen and Jensen, 1984; Pressel et al., 2008; Ayachi, 2013; Radin et al., 2021). Pressel et al. reported the presence of a large central vacuole in either undifferentiated or early-stage differentiated caulonema of several mosses, including *Funaria hygrometrica*, *Tortula muralis,* and *Bartramia pomiformi*. However, the presence of cytoplasmic strands in these mosses leads to the separation of large vacuoles into several small vacuoles during late-stage differentiation of caulonema and rhizoid (Pressel et al., 2008). In addition, liverwort *Polytrichum juniperinum* and *Hypnum jutlandicum* possess several transparent vacuoles in younger spermatids and a large vacuole opening (VO) onto the spermatid surface during the spermatogenesis stage (Miller and Duckett, 1986).

In addition to the growth stage, environmental stimuli will greatly influence the shape and structure of vacuoles in bryophytes. For instance, the abscisic acid (ABA) treatment disintegrated large vacuoles into smaller ones in protonema of moss including *P. patens* and *F. hygrometrica* (Schnepf and Reinhard, 1997; Nagao et al., 2005; Arif et al., 2019). In the liverwort *Southbya nigrella,* the large central vacuoles were broken into small vacuoles in dehydrated leaf and cortical stem cells (Pressel et al., 2009). Another research also observed the small vacuoles in moss *D. plumbicola* dehydrated protonema cells and the frozen cells also contain many small vacuoles (Rowntree et al., 2007). Similarly, vacuoles in *M. polymorpha*, cells fragmented into small vacuoles when treated with ABA, and similar phenomena appeared when treated with sucrose (Akter et al., 2014). A similar ABA effect on vacuoles has been observed in moss *Ditrichum plumbicola*, and vacuoles in protonema cells fragmented into small vacuoles under ABA and sucrose treatment (Rowntree et al., 2007). It is worth noting that, however, contradicted effects have been reported in another recent independent study. In M. *polymorpha* cells, the vacuole

volume increased with 1 μM ABA, with water deficit (with relative humidity maintained at 60%), or with NaCl (Godinez-Vidal et al., 2020). The reason why the vacuoles had opposite phenotypes under the similar treatment may be due to different growth and physiological status.

CHANGES IN THE MOLECULAR TOOLKIT CONTROLLING VACUOLE BIOGENESIS IN BRYOPHYTES

Similar to every other mechanism taking place in living organisms, the biogenesis and function of vacuoles are also controlled by the molecular machinery of the cells. In *A. thaliana*, main vacuolar biogenesis pathways are regulated by different functional protein complexes, such as the endosomal sorting complex required for transport (ESCRT) (Gao et al., 2017), adaptor protein complexes (APs) (Zwiewka et al., 2011; Wang et al., 2014), RAB5 (Sohn et al., 2003; Goh et al., 2007), RAB7 (Cui et al., 2014), Phosphoinositide 3-kinase (PI3K), homotypic fusion and protein sorting (HOPS) and soluble NSF attachment protein receptor (SNARE) (Takemoto et al., 2018). In many plants, the ESCRT complex mediates the MVB biogenesis and protein sequestering into intraluminal vesicles (ILVs) (Henne William et al., 2011; Cui et al., 2016), while APs regulate protein trafficking to both LVs and PSVs (Zhang et al., 2021). In contrast, RAB5, RAB7, and SNAREs are involved in vesicles transporting and vesicles fusion with vacuoles, respectively (Wang et al., 2017; Minamino and Ueda, 2019). Most of these regulators are conserved in plants and play key roles in angiosperms and bryophytes' endomembrane trafficking pathways (Kanazawa et al., 2016). For instance, several members of SNAREs family, such as SYP8, SEC20, USE1, and SEC22, are localized to the ER in both *A. thaliana* and *Marchantia polymorpha* (Uemura et al., 2004; Kanazawa et al., 2016). However, some members of SNAREs family including SYP5, SYP2, and VAMP71, which have one copy in *M. polymorpha* are exclusively localized to the vacuole. In turn, *A. thaliana* contains two, three, and four copies of these proteins, which are localized to Golgi or vacuoles, respectively (Kanazawa et al., 2016).

Extensive studies have demonstrated that, similar to in other eukaryotes, the conserved key molecular toolkit belonging to CCMM is in charge of vacuole biogenesis from multiple pathways in plants, mainly including ESCRT mediated MVB pathway (Gao et al., 2014; Kolb et al., 2015), Rab5/Rab7 mediated endosome maturation pathway (Ebine et al., 2014) and AP3-dependent pathway (Uemura and Ueda, 2014; Minamino and Ueda, 2019; Cui et al., 2020) (**Figure 2A**). Through the comparative genomic study of these key molecular toolkit genes in bryophytes, we found that, in line with this hypothesis, orthologs of most vacuole biogenesis genes are present in bryophytes. More notably, we found several significant gene loss events, which may be caused by reductive evolution for niche adaptation (**Supplementary Tables 1, 2**). We classified these gene loss events into four groups according to their molecular and cellular functions, namely the VPS9 protein, AP3 complex, KEG protein, and the MVB-related proteins (**Figure 2B**). In *A. thaliana*, most genes of these highlighted four groups are indispensable for seedling viability. It has been known that gene loss depends on the dispensability of gene function, which is affected by both the mutational robustness and environmental adaptability. Here we review what has been inferred about the molecular toolkit changes that accompanied the evolution of the vacuole biogenesis pathways in bryophytes, aiming to highlight the role that bryophytes could play in better understanding of vacuole biogenesis and function during land plant evolution.

The absence of VPS9 in all sequenced hornwort is of great interest because in *Arabidopsis*, *vps9* null mutants are defective in early embryo development with the fragmented vacuole, which highlights the necessity of its function (Goh et al., 2007). The function of VPS9 was first identified in yeast S. cerevisiae as Rab5 guanidine exchange factors (GEF) to generate an active Rab5-GTP complex (Prag et al., 2003). Rab protein activation by GTP binding via GEF protein is a prerequisite to complete vesicle targeting and fusion. For Rab5 activation, studies in yeast and human identified Vps9p and Rabex-5 as GEFs and found the shared region of homology now known as the Vps9 domain (Carney et al., 2006). From yeast to humans and plants, the small GTPase Rab5/Rab7 switch is crucial for the endosomal maturation pathway. During the maturation process, the early endosomal Rab5 GTPase is replaced with the late endosomal Rab7 GTPase (**Figure 2B**). *Arabidopsis* genome encodes three members of RAB5, and the activation of RAB5 via VPS9a enables subsequent cellular events (Kotzer et al., 2004). The action of the VPS9 protein enhances the RAB5-MON1-CCZ1 complex formation which will further run the pathway with the assistance of RAB7 (Minamino and Ueda, 2019; Cui et al., 2020; Hu et al., 2020). Despite the importance of VPS9a protein in many land plants, there has not been any VPS9a protein in three members of the *Anthoceros* family, including *Anthoceros agrestis*, *Anthoceros angustus*, and *Anthoceros punctants* (**Figure 2B** and **Supplementary Table 1**). This suggests the diverged evolution of VPS9 mediated vacuole biogenesis in hornworts.

Different from RAB5/RAB7 pathway, the adaptor protein complex 3 (AP-3) mediated an independent vacuole trafficking pathway in yeast, flies, mammals, and seed plants (Boehm and Bonifacino, 2002). The transportation of VAMP711 and VAMP713 in *A. thaliana* is carried out through the AP-3 pathway (Feng et al., 2017; Takemoto et al., 2018; Cui et al., 2020). The AP-3 complex comprises four members including, AP-3β, AP-3δ, AP-3μ, and AP-3σ. In particular, *M. polymorpha* lacks the AP-3δ protein, while *A. angustus* lack the AP-3σ. However, AP-3δ or AP-3μ in *A. agrestis* that grown in two different environments show an opposite manner which requires further investigation. Similarly, no VPS16 protein, was identified in *A. agrestis* which indicates the alteration or diversified manner of AP3 pathway in these species (**Figure 2B** and **Supplementary Table 1**).

ESCRT-regulated MVB formation is critical for vacuole biogenesis and function in both yeast and seed plants (Gao et al., 2017). Before being transported to vacuoles, protein cargoes are sequestered into ILVs with the help of ESCRT machinery. Plants contain ESCRT-I, -II, -III, and VPS4 (vacuole protein sorting 4) isoforms as the yeast and mammal, but

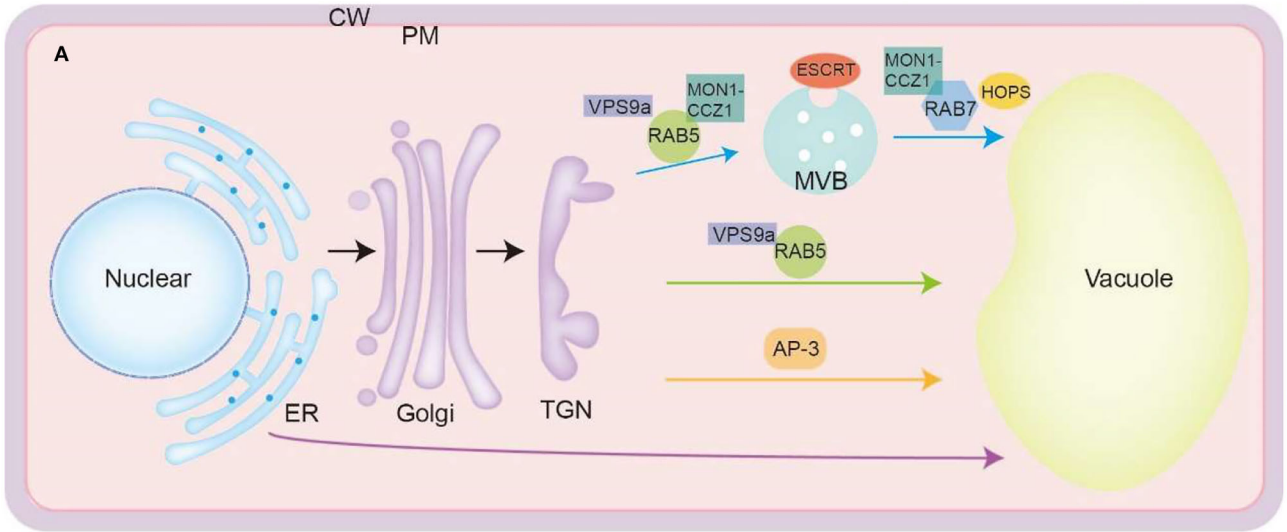

B

		AP-3				MVB-related					
		VPS9	AP-3 δ	AP-3 μ	AP-3 σ	KEG	VPS16	VPS37	LIP5	FYVE4	RST1	
	Yeast	2	1	1	1	0	1	1	1	0	0	
	Human	6	1	1	1	0	1	4	1	0	1	
Angiosperm	*Arabidopsis thaliana*	2	1	1	1	1	1	2	1	1	1	(Lamesch et al., 2011)
Moss	*Sphagnum fallax*	2	1	1	1	1	1	3	2	1	1	DOE-JGI[1]
Moss	*Sphagnum magellanicum*	2	1	1	1	1	1	3	2	1	1	DOE-JGI[1]
Moss	*Physcomitrella patens*	1	1	1	1	0	1	3	1	1	0	(Lang et al., 2018)
Moss	*Ceratodon purpureus* GG1	1	1	1	1	0	1	2	2	1	0	(Carey et al., 2021)
Moss	*Ceratodon purpureus* R40	1	1	1	1	0	1	2	2	1	0	(Carey et al., 2021)
Liverwort	*Marchantia polymorpha*	1	0	1	1	1	1	1	1	1	1	(Bowman et al., 2017)
Hornwort	*Anthoceros agrestis* (BONN)	0	1	0	2	1	0	0	0	0	0	(Li et al., 2020)
Hornwort	*Anthoceros agrestis* (OXF)	0	0	1	2	1	0	0	0	0	0	(Li et al., 2020)
Hornwort	*Antheoceros angustus*	0	1	1	0	1	1	0	0	0	0	(Zhang et al., 2020)
Hornwort	*Anthoceros punctatus*	0	1	1	1	1	1	0	0	0	0	(Li et al., 2020)

FIGURE 2 | (A) Vacuole trafficking pathway in plants. The blue arrows indicate the pathway mediated by RAB5 and RAB7. The green arrows indicate the vacuole trafficking pathway regulated by RAB5 but do not include RAB7. The orange arrows indicate the AP-3-dependent pathway. The purple arrows indicate the ER to vacuole trafficking pathway. ER, endoplasmic reticulum; Golgi, Golgi apparatus; TGN, *trans*-Golgi network; MVB, multivesicular body; PM, plasma membrane; CW, cell wall. **(B)** Some special regulator proteins in bryophytes and species genome databases are used in this article. The complete table was in the **Supplementary Tables**. The numbers represent the quantity of the ortholog proteins in this species. The genome database reference for *Arabidopsis thaliana* (Lamesch et al., 2011), *P. patens* (Lang et al., 2018), *C. purpureus* (Carey et al., 2021), *M. polymorpha* (Bowman et al., 2017), *A. agrestis* (Li et al., 2020), *A. angustus* (Zhang et al., 2020), *A. punctatus* (Li et al., 2020). The *S. fallax* and *S. magellanicum* databases were obtained from DOE-JGI, http://phytozome.jgi.doe.gov/.

no ESCRT-0 subunits VPS27 and Hse1 (Hurley and Hanson, 2010). Instead, there were TOL1-9 (TOM1-like) proteins in *A. thaliana* and bryophytes (Korbei et al., 2013), which function similarly to ESCRT-0. However, we were able to find ISTL1 (Goodman et al., 2021) in *A. thaliana* and yeast, but not in these bryophytes or mammal (**Figure 2B** and **Supplementary Table 2**). Specially, VPS37 (component of ESCRT-I) (Okumura et al., 2013), LIP5 (positive regulator of VPS4/SKD1) (Buono et al., 2016), and FYVE4 (affect the connection of ESCRT-III and VPS4) (Liu et al., 2021) are absent in hornwort. More interestingly, as a suppressor of FREE1 (Gao et al., 2014), RESURRECTION1 (RST1) (Zhao et al., 2019) only exists in *S. fallax*, *S. magellanicum* and *M. polymorpha,* which indicates that this protein may have special functions in these bryophytes (**Figure 2B**).

KEG is a plant-specific RING-type E3 ligase, that localizes on the early endosome, and plays an essential role in multiple endomembrane trafficking processes including vacuole biogenesis (Gu and Innes, 2012). Here we found the specific KEG gene loss in *P. patens* and *C. purpureus,* indicating that KEG mediated pathway can be bypassed in these species.

CONCLUSIONS AND PERSPECTIVES

This review summarized the current understanding of bryophyte vacuole morphology and function. Combining with our comparative phylogenetic analysis of vacuole biogenesis-related CCMM genes, so far, we are sure that bryophytes share key vacuole-related features with seed plants, but with several exceptional innovations.

Similarly like in seed plants, the different populations of vacuoles exist in bryophytes, however, there lack of clear evidence to support the extant of PSV in bryophytes. In addition, similar vacuole fission and fusion dynamics have been observed in both seed plants and bryophytes. The interesting point is the prominent effect of ABA on vacuole dynamics in bryophytes, while the underlying mechanism and the biological significance are still mysterious.

Studies in seed plants, especially in Arabidopsis, have reached several different models for vacuole biogenesis (Cui et al., 2020). Whether a similar different *de-novo* biogenesis model (Cui et al., 2019) and ER-derived model (Viotti et al., 2013) for vacuole formation co-exist in bryophyte still need further research.

Secondary metabolites, especially UVAC, may represent a unique innovation in bryophytes' vacuole function. Under the UV-B radiation, bryophyte vacuoles would accumulate SUVAC, which may protect the plant from UV-B damage (Fabón et al., 2012; Hespanhol et al., 2014; Monforte et al., 2015; Soriano et al., 2019).

Usually one would assume that the propensity for gene loss negatively correlated with the necessity of the function on organism viability. That is to say, if a gene is kept throughout the whole span of evolution, that is because the function of this gene is essential for survival. However, here we found that some essential proteins are absent in *Anthoceros*, such as VPS9a, VPS37, LIP5, FYVE4, and RST1, and some other proteins disappeared in *S. fallax*, *S. magellanicum*, *P. patens,* and *M. polymorpha* (**Figure 2B**). How is the vacuole trafficking and biogenesis running in these plants without these key proteins? Whether there are some alternative proteins to help sort cargoes? It remains to be answered. To answer these questions, we strongly urge that on the basis of further in-depth study of model bryophytes, we also need to pay attention to more evolutionary basal or advanced bryophytes.

AUTHOR CONTRIBUTIONS

H-rL, CS, DH, W-qF, Z-yW, YL, R-lZ, and QZ reviewed literature, formulated ideas, and wrote the manuscript. H-rL and QZ prepared the figures. H-rL, CS, and QZ conducted the bioinformatic analysis. All authors contributed to the article and approved the submitted version.

FUNDING

Sponsored by East China Normal University and Shanghai Pujiang Program 20PJ1403200.

SUPPLEMENTARY MATERIAL

The Supplementary Material for this article can be found online at: https://www.frontiersin.org/articles/10.3389/fpls.2022.863389/full#supplementary-material

REFERENCES

Akter, K., Kato, M., Sato, Y., Kaneko, Y., and Takezawa, D. (2014). Abscisic acid-induced rearrangement of intracellular structures associated with freezing and desiccation stress tolerance in the liverwort Marchantia polymorpha. *J. Plant Physiol.* 171, 1334–1343. doi: 10.1016/j.jplph.2014.05.004

Aniento, F., Sanchez de Medina Hernandez, V., Dagdas, Y., Rojas-Pierce, M., and Russinova, E. (2022). Molecular mechanisms of endomembrane trafficking in plants. *Plant Cell* 34, 146–173. doi: 10.1093/plcell/koab235

Arif, M. A., Hiss, M., Tomek, M., Busch, H., Meyberg, R., Tintelnot, S., et al. (2019). ABA-induced vegetative diaspore formation in physcomitrella patens. *Front. Plant Sci.* 10:315. doi: 10.3389/fpls.2019.00315

Asakawa, Y., and Ludwiczuk, A. (2013). Bryophytes: liverworts, mosses, and hornworts: extraction and isolation procedures. *Methods Mol. Biol.* 1055, 1–20. doi: 10.1007/978-1-62703-577-4_1

Ayachi, S. (2013). Study of moss vacuoles and functional characterization of the putative vacuolar receptors: the RMR proteins. *Free.* 23:911–921.

Boehm, M., and Bonifacino, J. S. (2002). Genetic analyses of adaptin function from yeast to mammals. *Gene* 286, 175–186. doi: 10.1016/S0378-1119(02)00422-5

Bowman, J. L., Kohchi, T., Yamato, K. T., Jenkins, J., Shu, S., Ishizaki, K., et al. (2017). Insights into land plant evolution garnered from the Marchantia polymorpha Genome. *Cell* 171, 287–304.e15. doi: 10.1016/j.cell.2017.09.030

Buono, R. A., Paez-Valencia, J., Miller, N. D., Goodman, K., Spitzer, C., Spalding, E. P., et al. (2016). Role of SKD1 regulators LIP5 and IST1-LIKE1 in endosomal sorting and plant development. *Plant Physiol.* 171, 251–264. doi: 10.1104/pp.16.00240

Cao, Y., Cai, W., Chen, X., Chen, M., Chu, J., Liang, W., et al. (2020). Bright fluorescent vacuolar marker lines allow vacuolar tracing across multiple tissues and stress conditions in rice. *Int. J. Mol. Sci.* 21:4203. doi: 10.3390/ijms21124203

Carey, S. B., Jenkins, J., Lovell, J. T., Maumus, F., Sreedasyam, A., Payton, A. C., et al. (2021). Gene-rich UV sex chromosomes harbor conserved regulators of sexual development. *Sci. Adv.* 7:eabh2488. doi: 10.1126/sciadv.abh2488

Carney, D. S., Davies, B. A., and Horazdovsky, B. F. (2006). Vps9 domain-containing proteins: activators of Rab5 GTPases from yeast to neurons. *Trends Cell Biol.* 16, 27–35. doi: 10.1016/j.tcb.2005.11.001

Cove, D. J., Knight, C. D., and Lamparter, T. (1997). Mosses as model systems. *Trends Plant Sci.* 2, 99–105. doi: 10.1016/S1360-1385(96)10056-X

Cui, Y., Cao, W., He, Y., Zhao, Q., Wakazaki, M., Zhuang, X., et al. (2019). A whole-cell electron tomography model of vacuole biogenesis in Arabidopsis root cells. *Nat. Plants* 5, 95–105. doi: 10.1038/s41477-018-0328-1

Cui, Y., Shen, J., Gao, C., Zhuang, X., Wang, J., and Jiang, L. (2016). Biogenesis of plant prevacuolar multivesicular bodies. *Mol. Plant.* 9, 774–786. doi: 10.1016/j.molp.2016.01.011

Cui, Y., Zhao, Q., Gao, C., Ding, Y., Zeng, Y., Ueda, T., et al. (2014). Activation of the Rab7 GTPase by the MON1-CCZ1 complex is essential for PVC-to-Vacuole trafficking and plant growth in Arabidopsis. *Plant Cell.* 26, 2080–2097. doi: 10.1105/tpc.114.123141

Cui, Y., Zhao, Q., Hu, S., and Jiang, L. (2020). Vacuole biogenesis in plants: how many vacuoles, how many models? *Trends Plant Sci.* 25, 538–548. doi: 10.1016/j.tplants.2020.01.008

Deeks, M. J., Calcutt, J. R., Ingle, E. K., Hawkins, T. J., Chapman, S., Richardson, A. C., et al. (2012). A superfamily of actin-binding proteins at the actin-membrane nexus of higher plants. *Curr Biol.* 22, 1595–1600. doi: 10.1016/j.cub.2012.06.041

Dettmer, J., Hong-Hermesdorf, A., Stierhof, Y. D., and Schumacher, K. (2006). Vacuolar H+-ATPase activity is required for endocytic and secretory trafficking in Arabidopsis. *Plant Cell*. 18, 715–730. doi: 10.1105/tpc.105.037978

Dunser, K., Gupta, S., Herger, A., Feraru, M. I., Ringli, C., and Kleine-Vehn, J. (2019). Extracellular matrix sensing by FERONIA and Leucine-Rich Repeat Extensins controls vacuolar expansion during cellular elongation in *Arabidopsis thaliana*. *EMBO J*. 38:e100353. doi: 10.15252/embj.2018100353

Ebine, K., Inoue, T., Ito, J., Ito, E., Uemura, T., Goh, T., et al. (2014). Plant vacuolar trafficking occurs through distinctly regulated pathways. *Curr. Biol*. 24, 1375–1382. doi: 10.1016/j.cub.2014.05.004

Eklund, D. M., Kanei, M., Flores-Sandoval, E., Ishizaki, K., Nishihama, R., Kohchi, T., et al. (2018). An evolutionarily conserved abscisic acid signaling pathway regulates dormancy in the Liverwort *Marchantia polymorpha*. *Curr. Biol*. 28, 3691–3699.e3. doi: 10.1016/j.cub.2018.10.018

Fabón, G., Monforte, L., Tomás-Las-Heras, R., Martínez-Abaigar, J., and Núñez-Olivera, E. (2012). Cell compartmentation of UV-absorbing compounds in two aquatic mosses under enhanced UV-B. *Cryptogamie Bryol*. 33, 169–184. doi: 10.7872/cryb.v33.iss2.2012.169

Feeney, M., Frigerio, L., Cui, Y., and Menassa, R. (2013). Following vegetative to embryonic cellular changes in leaves of Arabidopsis overexpressing LEAFY COTYLEDON2. *Plant Physiol*. 162, 1881–1896. doi: 10.1104/pp.113.220996

Feeney, M., Kittelmann, M., Menassa, R., Hawes, C., and Frigerio, L. (2018). Protein storage vacuoles originate from remodeled preexisting vacuoles in *Arabidopsis thaliana*. *Plant Physiol*. 177, 241–254. doi: 10.1104/pp.18.00010

Feng, Q. N., Song, S. J., Yu, S. X., Wang, J. G., Li, S., and Zhang, Y. (2017). Adaptor Protein-3-Dependent vacuolar trafficking involves a subpopulation of COPII and HOPS tethering proteins. *Plant Physiol*. 174, 1609–1620. doi: 10.1104/pp.17.00584

Francisco, R. D. B., and Martinoia, E. (2018). The vacuolar transportome of plant specialized metabolites. *Plant Cell Physiol*. 59, 1326–1336. doi: 10.1093/pcp/pcy039

Frangedakis, E., Shimamura, M., Villarreal, J. C., Li, F. W., Tomaselli, M., Waller, M., et al. (2021). The hornworts: morphology, evolution and development. *New Phytol*. 229, 735–754. doi: 10.1111/nph.16874

Gambardella, R., Alfano, F., Gargiulo, M., and Squillacioti, C. (1994). Studies on the sporogenous lineage in the moss *Timmiella barbuloides* IX. Development of the Tapetum. *Ann. Bot*. 73, 369–375. doi: 10.1006/anbo.1994.1046

Gao, C., Luo, M., Zhao, Q., Yang, R., Cui, Y., Zeng, Y., et al. (2014). A unique plant ESCRT component, FREE1, regulates multivesicular body protein sorting and plant growth. *Curr. Biol*. 24, 2556–2563. doi: 10.1016/j.cub.2014.09.014

Gao, C., Zhuang, X., Shen, J., and Jiang, L. (2017). Plant ESCRT complexes: moving beyond endosomal sorting. *Trends Plant Sci*. 22, 986–998. doi: 10.1016/j.tplants.2017.08.003

Gattolin, S., Sorieul, M., and Frigerio, L. (2010). Tonoplast intrinsic proteins and vacuolar identity. *Biochem. Soc. Trans*. 38, 769–773. doi: 10.1042/BST0380769

Gattolin, S., Sorieul, M., Hunter, P. R., Khonsari, R. H., and Frigerio, L. (2009). In vivo imaging of the tonoplast intrinsic protein family in Arabidopsis roots. *BMC Plant Biol*. 9:133. doi: 10.1186/1471-2229-9-133

Godinez-Vidal, D., López-Leal, G., Covarrubias, A. A., and Reyes, J. L. (2020). Early events leading to water deficit responses in the liverwort Marchantia polymorpha. *Environ. Exp. Bot*. 178:104172. doi: 10.1016/j.envexpbot.2020.104172

Goh, T., Uchida, W., Arakawa, S., Ito, E., Dainobu, T., Ebine, K., et al. (2007). VPS9a, the common activator for two distinct types of Rab5 GTPases, is essential for the development of *Arabidopsis thaliana*. *Plant Cell*. 19, 3504–3515. doi: 10.1105/tpc.107.053876

Goodman, K., Paez-Valencia, J., Pennington, J., Sonntag, A., Ding, X., Lee, H. N., et al. (2021). ESCRT components ISTL1 andLIP5 are required for tapetal function and pollen viability. *Plant Cell*. 33, 2850–2868. doi: 10.1093/plcell/koab132

Gu, Y., and Innes, R. W. (2012). The KEEP ON GOING protein of Arabidopsis regulates intracellular protein trafficking and is degraded during fungal infection. *Plant Cell* 24, 4717–4730. doi: 10.1105/tpc.112.105254

Hassani, D., Fu, X., Shen, Q., Khalid, M., Rose, J. K. C., and Tang, K. (2020). Parallel transcriptional regulation of artemisinin and flavonoid biosynthesis. *Trends Plant Sci*. 25, 466–476. doi: 10.1016/j.tplants.2020.01.001

Henne William, M., Buchkovich Nicholas, J., and Emr Scott, D. (2011). The ESCRT pathway. *Dev. Cell* 21, 77–91. doi: 10.1016/j.devcel.2011.05.015

Hespanhol, H., Fabón, G., Monforte, L., Martínez-Abaigar, J., and Núñez-Olivera, E. (2014). Among- and within-genus variability of the UV-absorption capacity in saxicolous mosses. *Bryologist* 117, 1–9. doi: 10.1639/0007-2745-117.1.001

Hu, S., Li, Y., and Shen, J. (2020). A diverse membrane interaction network for plant multivesicular bodies: roles in proteins vacuolar delivery and unconventional secretion. *Front. Plant Sci*. 11:425. doi: 10.3389/fpls.2020.00425

Hurley, J. H., and Hanson, P. I. (2010). Membrane budding and scission by the ESCRT machinery: it's all in the neck. *Nat. Rev. Mol. Cell Biol*. 11, 556–566. doi: 10.1038/nrm2937

Isayenkov, S. V. (2014). Plant vacuoles: Physiological roles and mechanisms of vacuolar sorting and vesicular trafficking. *Cytol. Genet*. 48, 127–137. doi: 10.3103/S0095452714020042

Jensen, L., and Jensen, C. G. (1984). Fine structure of protonemal apical cells of the moss*Physcomitrium turbinatum*. *Protoplasma* 122, 1–10. doi: 10.1007/BF01279432

Kaiser, S., Eisa, A., Kleine-Vehn, J., and Scheuring, D. (2019). NET4 modulates the compactness of vacuoles in *Arabidopsis thaliana*. *Int. J. Mol. Sci*. 20:4752. doi: 10.3390/ijms20194752

Kanazawa, T., Era, A., Minamino, N., Shikano, Y., Fujimoto, M., Uemura, T., et al. (2016). SNARE molecules in Marchantia polymorpha: unique and conserved features of the membrane fusion machinery. *Plant Cell Physiol*. 57, 307–324. doi: 10.1093/pcp/pcv076

Kimata, Y., Kato, T., Higaki, T., Kurihara, D., Yamada, T., Segami, S., et al. (2019). Polar vacuolar distribution is essential for accurate asymmetric division of Arabidopsis zygotes. *Proc. Natl. Acad. Sci. U.S.A*. 116, 2338–2343. doi: 10.1073/pnas.1814160116

Klips, R. (2016). Mosses, liverworts and hornworts: a field guide to common bryophytes of the Northeast. *Castanea* 82, 169–70. doi: 10.2179/17-BR001

Kolb, C., Nagel, M. K., Kalinowska, K., Hagmann, J., Ichikawa, M., Anzenberger, F., et al. (2015). FYVE1 is essential for vacuole biogenesis and intracellular trafficking in Arabidopsis. *Plant Physiol*. 167, 1361–1373. doi: 10.1104/pp.114.253377

Korbei, B., Moulinier-Anzola, J., De-Araujo, L., Lucyshyn, D., Retzer, K., Khan Muhammad, A., et al. (2013). Arabidopsis TOL proteins act as gatekeepers for vacuolar sorting of PIN2 plasma membrane protein. *Curr. Biol*. 23, 2500–2505. doi: 10.1016/j.cub.2013.10.036

Koshimizu, S., Kofuji, R., Sasaki-Sekimoto, Y., Kikkawa, M., Shimojima, M., Ohta, H., et al. (2018). Physcomitrella MADS-box genes regulate water supply and sperm movement for fertilization. *Nat. Plants* 4, 36–45. doi: 10.1038/s41477-017-0082-9

Kotzer, A. M., Brandizzi, F., Neumann, U., Paris, N., Moore, I., and Hawes, C. (2004). AtRabF2b (Ara7) acts on the vacuolar trafficking pathway in tobacco leaf epidermal cells. *J. Cell Sci*. 117, 6377–6389. doi: 10.1242/jcs.01564

Kriegel, A., Andres, Z., Medzihradszky, A., Kruger, F., Scholl, S., Delang, S., et al. (2015). Job sharing in the endomembrane system: vacuolar acidification requires the combined activity of V-ATPase and V-PPase. *Plant Cell*. 27, 3383–3396. doi: 10.1105/tpc.15.00733

Kutsuna, N., Kumagai, F., Sato, M. H., and Hasezawa, S. (2003). Three-dimensional reconstruction of tubular structure of vacuolar membrane throughout mitosis in living tobacco cells. *Plant Cell Physiol*. 44, 1045–1054. doi: 10.1093/pcp/pcg124

Lamesch, P., Berardini, T. Z., Li, D., Swarbreck, D., Wilks, C., Sasidharan, R., et al. (2011). The Arabidopsis Information Resource (TAIR): improved gene annotation and new tools. *Nucleic Acids Res*. 40, D1202–D1210. doi: 10.1093/nar/gkr1090

Lang, D., Ullrich, K. K., Murat, F., Fuchs, J., Jenkins, J., Haas, F. B., et al. (2018). The Physcomitrella patens chromosome-scale assembly reveals moss genome structure and evolution. *Plant J*. 93, 515–533. doi: 10.1111/tpj.13801

Li, F.-W., Nishiyama, T., Waller, M., Frangedakis, E., Keller, J., Li, Z., et al. (2020). Anthoceros genomes illuminate the origin of land plants and the unique biology of hornworts. *Nat. Plants* 6, 259–272. doi: 10.1038/s41477-020-0618-2

Ligrone, R., and Duckett, J. G. (1994). Thallus differentiation in the marchantialean liverwort *Asterella wilmsii* (Steph.) with particular reference to longitudinal arrays of endoplasmic microtubules in the inner cells. *Ann. Bot*. 73, 577–586. doi: 10.1006/anbo.1994.1072

Ligrone, R., and Duckett, J. G. (1998). The leafy stems of Sphagnum (Bryophyta) contain highly differentiated polarized cells with axial arrays of endoplasmic microtubules. *N. Phytol*. 140, 567–579. doi: 10.1046/j.1469-8137.1998.00298.x

Liu, C., Zeng, Y., Li, H., Yang, C., Shen, W., Xu, M., et al. (2021). A plant-unique ESCRT component, FYVE4, regulates multivesicular endosome biogenesis and plant growth. *N. Phytol*. 231, 193–209. doi: 10.1111/nph.17358

Lofke, C., Dunser, K., Scheuring, D., and Kleine-Vehn, J. (2015). Auxin regulates SNARE-dependent vacuolar morphology restricting cell size. *Elife*. 4:e05868. doi: 10.7554/eLife.05868.024

Miller, C. C. J., and Duckett, J. G. (1986). Cytoplasmic deletion processes during spermatogenesis in mosses. *Gamete Res*. 13, 253–270. doi: 10.1002/mrd.1120130308

Minamino, N., and Ueda, T. (2019). RAB GTPases and their effectors in plant endosomal transport. *Curr. Opin. Plant Biol*. 52, 61–68. doi: 10.1016/j.pbi.2019.07.007

Monforte, L., Núñez-Olivera, E., and Martínez-Abaigar, J. (2015). UV radiation biomonitoring using cell compartmentation of UV-absorbing compounds in herbarium samples of a liverwort. *Ecol. Indic*. 52, 48–56. doi: 10.1016/j.ecolind.2014.11.027

Nagao, M., Minami, A., Arakawa, K., Fujikawa, S., and Takezawa, D. (2005). Rapid degradation of starch in chloroplasts and concomitant accumulation of soluble sugars associated with ABA-induced freezing tolerance in the moss *Physcomitrella patens*. *J. Plant Physiol*. 162, 169–180. doi: 10.1016/j.jplph.2004.06.012

Nishiyama, T., Miyawaki, K., Ohshima, M., Thompson, K., Nagashima, A., Hasebe, M., et al. (2012). Digital gene expression profiling by 5′-end sequencing of cdnas during reprogramming in the moss physcomitrella patens. *PLoS ONE*. 7:e36471. doi: 10.1371/journal.pone.0036471

Okumura, M., Katsuyama, A. M., Shibata, H., and Maki, M. (2013). VPS37 isoforms differentially modulate the ternary complex formation of ALIX, ALG-2, and ESCRT-I. *Biosci. Biotechnol. Biochem*. 77, 1715–1721. doi: 10.1271/bbb.130280

Paris, N., Stanley, C. M., Jones, R. L., and Rogers, J. C. (1996). Plant cells contain two functionally distinct vacuolar compartments. *Cell* 85, 563–572. doi: 10.1016/S0092-8674(00)81256-8

Pihakaski, K. (1968). A study of the ultrastructure of the shoot apex and leaf cells in two liverworts, with special reference to the oil bodies. *Protoplasma* 66, 79–103. doi: 10.1007/BF01252526

Prag, G., Misra, S., Jones, E. A., Ghirlando, R., Davies, B. A., Horazdovsky, B. F., et al. (2003). Mechanism of ubiquitin recognition by the CUE domain of Vps9p. *Cell* 113, 609–620. doi: 10.1016/S0092-8674(03)00364-7

Pressel, S., Duckett, J. G., Ligrone, R., and Proctor, M. C. F. (2009). Effects of de- and rehydration in desiccation-tolerant liverworts: a cytological and physiological study. *Int. J. Plant Sci*. 170, 182–199. doi: 10.1086/595285

Pressel, S., Ligrone, R., and Duckett, J. G. (2008). Cellular differentiation in moss protonemata: a morphological and experimental study. *Ann. Bot*. 102, 227–245. doi: 10.1093/aob/mcn080

Radin, I., Richardson, R. A., Coomey, J. H., Weiner, E. R., Bascom, C. S., Li, T., et al. (2021). Plant PIEZO homologs modulate vacuole morphology during tip growth. *Science* 373, 586–590. doi: 10.1126/science.abe6310

Richards, A., Veses, V., and Gow, N. A. R. (2010). Vacuole dynamics in fungi. *Fungal Biol. Rev*. 24, 93–105. doi: 10.1016/j.fbr.2010.04.002

Rojo, E., Zouhar, J., Carter, C., Kovaleva, V., and Raikhel, N. V. (2003). A unique mechanism for protein processing and degradation in *Arabidopsis thaliana*. *Proc. Natl. Acad. Sci. U.S.A*. 100, 7389–7394. doi: 10.1073/pnas.1230987100

Rowntree, J. K., Duckett, J. G., Mortimer, C. L., Ramsay, M. M., and Pressel, S. (2007). Formation of specialized propagules resistant to desiccation and cryopreservation in the threatened moss *Ditrichum plumbicola* (Ditrichales, Bryopsida). *Ann. Bot*. 100, 483–496. doi: 10.1093/aob/mcm141

Sanmartin, M., Ordonez, A., Sohn, E. J., Robert, S., Sanchez-Serrano, J. J., Surpin, M. A., et al. (2007). Divergent functions of VTI12 and VTI11 in trafficking to storage and lytic vacuoles in Arabidopsis. *Proc. Natl. Acad. Sci. U.S.A*. 104, 3645–3650. doi: 10.1073/pnas.0611147104

Scheuring, D., Lofke, C., Kruger, F., Kittelmann, M., Eisa, A., Hughes, L., et al. (2016). Actin-dependent vacuolar occupancy of the cell determines auxin-induced growth repression. *Proc. Natl. Acad. Sci. U.S.A*. 113, 452–457. doi: 10.1073/pnas.1517445113

Schnepf, E., and Reinhard, C. (1997). Brachycytes in funaria protonemate: induction by abscisic acid and fine structure. *J. Plant Physiol*. 151, 166–175. doi: 10.1016/S0176-1617(97)80149-6

Shen, J., Zeng, Y., Zhuang, X., Sun, L., Yao, X., Pimpl, P., et al. (2013). Organelle pH in the Arabidopsis endomembrane system. *Mol. Plant*. 6, 1419–1437. doi: 10.1093/mp/sst079

Shimada, T., Takagi, J., Ichino, T., Shirakawa, M., and Hara-Nishimura, I. (2018). Plant vacuoles. *Annu. Rev. Plant Biol*. 69, 123–145. doi: 10.1146/annurev-arplant-042817-040508

Shimamura, M. (2016). Marchantia polymorpha: taxonomy, phylogeny and morphology of a model system. *Plant Cell Physiol*. 57, 230–256. doi: 10.1093/pcp/pcv192

Sohn, E. J., Kim, E. S., Zhao, M., Kim, S. J., Kim, H., Kim, Y. W., et al. (2003). Rha1, an Arabidopsis Rab5 homolog, plays a critical role in the vacuolar trafficking of soluble cargo proteins. *Plant Cell*. 15, 1057–1070. doi: 10.1105/tpc.009779

Soriano, G., Del-Castillo-Alonso, M.-Á., Monforte, L., Núñez-Olivera, E., and Martínez-Abaigar, J. (2019). Phenolic compounds from different bryophyte species and cell compartments respond specifically to ultraviolet radiation, but not particularly quickly. *Plant Physiol. Biochem*. 134, 137–144. doi: 10.1016/j.plaphy.2018.07.020

Takemoto, K., Ebine, K., Askani, J. C., Kruger, F., Gonzalez, Z. A., Ito, E., et al. (2018). Distinct sets of tethering complexes, SNARE complexes, and Rab GTPases mediate membrane fusion at the vacuole in Arabidopsis. *Proc. Natl. Acad. Sci. U.S.A*. 115, E2457–E2466. doi: 10.1073/pnas.1717839115

Tan, X., Li, K., Wang, Z., Zhu, K., Tan, X., and Cao, J. (2019). A review of plant vacuoles: formation, located proteins, and functions. *Plants* 8:327. doi: 10.3390/plants8090327

Thiébaut, G., Giamberini, L., and Ghanbaja, J. (2008). Cellular distribution of metals in a liverwort and a moss transplanted to two streams of differing acidity. *Water Air Soil Pollut*. 192, 263–272. doi: 10.1007/s11270-008-9653-8

Uemura, T., and Ueda, T. (2014). Plant vacuolar trafficking driven by RAB and SNARE proteins. *Curr. Opin. Plant Biol*. 22, 116–121. doi: 10.1016/j.pbi.2014.10.002

Uemura, T., Ueda, T., Ohniwa, R. L., Nakano, A., Takeyasu, K., and Sato, M. H. (2004). Systematic analysis of SNARE molecules in Arabidopsis: dissection of the post-Golgi network in plant cells. *Cell Struct. Funct*. 29, 49–65. doi: 10.1247/csf.29.49

Viotti, C., Kruger, F., Krebs, M., Neubert, C., Fink, F., Lupanga, U., et al. (2013). The endoplasmic reticulum is the main membrane source for biogenesis of the lytic vacuole in Arabidopsis. *Plant Cell* 25, 3434–3449. doi: 10.1105/tpc.113.114827

Wang, T., Li, L., and Hong, W. (2017). SNARE proteins in membrane trafficking. *Traffic* 18, 767–775. doi: 10.1111/tra.12524

Wang, X., Cai, Y., Wang, H., Zeng, Y., Zhuang, X., Li, B., et al. (2014). Trans-Golgi network-located AP1 gamma adaptins mediate dileucine motif-directed vacuolar targeting in Arabidopsis. *Plant Cell*. 26, 4102–4118. doi: 10.1105/tpc.114.129759

Wolf, L., Rizzini, L., Stracke, R., Ulm, R., and Rensing, S. A. (2010). The molecular and physiological responses of *Physcomitrella patens* to ultraviolet-B radiation. *Plant Physiol*. 153, 1123–1134. doi: 10.1104/pp.110.154658

Yip, K. L., and Rushing, A. E. (1999). An ultrastructural and developmental study of the sporophyte-gametophyte junction in *Ephemerum cohaerens*. *Bryologist* 102, 179–195. doi: 10.2307/3244358

Zhang, J., Fu, X. X., Li, R. Q., Zhao, X., Liu, Y., Li, M. H., et al. (2020). The hornwort genome and early land plant evolution. *Nat. Plants* 6, 107–118. doi: 10.1038/s41477-019-0588-4

Zhang, J., Martinoia, E., and Lee, Y. (2018). Vacuolar transporters for cadmium and arsenic in plants and their applications in phytoremediation and crop development. *Plant Cell Physiol*. 59, 1317–1325. doi: 10.1093/pcp/pcy006

Zhang, X., Li, H., Lu, H., and Hwang, I. (2021). The trafficking machinery of lytic and protein storage vacuoles: how much is shared and how much is distinct? *J. Exp. Bot*. 72, 3504–3512. doi: 10.1093/jxb/erab067

Zhao, Q., Shen, J., Gao, C., Cui, Y., Wang, Y., Cui, J., et al. (2019). RST1 is a FREE1 suppressor that negatively regulates vacuolar trafficking in Arabidopsis. *Plant Cell* 31, 2152–2168. doi: 10.1105/tpc.19.00003

Zhao, W., Li, Z., Hu, Y., Wang, M., Zheng, S., Li, Q., et al. (2019). Development of a method for protonema proliferation of peat moss (*Sphagnum squarrosum*) through regeneration analysis. *N. Phytol*. 221, 1160–1171. doi: 10.1111/nph.15394

Zwiewka, M., Feraru, E., Moller, B., Hwang, I., Feraru, M. I., Kleine-Vehn, J., et al. (2011). The AP-3 adaptor complex is required for vacuolar function in Arabidopsis. *Cell Res*. 21, 1711–1722. doi: 10.1038/cr.2011.99

Conflict of Interest: The authors declare that the research was conducted in the absence of any commercial or financial relationships that could be construed as a potential conflict of interest.

Publisher's Note: All claims expressed in this article are solely those of the authors and do not necessarily represent those of their affiliated organizations, or those of the publisher, the editors and the reviewers. Any product that may be evaluated in this article, or claim that may be made by its manufacturer, is not guaranteed or endorsed by the publisher.

frontiers | Frontiers in Plant Science

ORIGINAL RESEARCH
published: 16 June 2022
doi: 10.3389/fpls.2022.862398

Constitutive Active CPK30 Interferes With Root Growth and Endomembrane Trafficking in *Arabidopsis thaliana*

*Ren Wang[1,2], Ellie Himschoot[1,2], Jian Chen[1,2], Marie Boudsocq[3,4], Danny Geelen[5], Jiří Friml[6], Tom Beeckman[1,2] and Steffen Vanneste[1,2,5,7]**

[1] Department of Plant Biotechnology and Bioinformatics, Ghent University, Ghent, Belgium, [2] VIB Center for Plant Systems Biology, Ghent, Belgium, [3] Université Paris-Saclay, CNRS, INRAE, Univ. Evry, Institute of Plant Sciences Paris-Saclay (IPS2), Orsay, France, [4] Université de Paris, Institute of Plant Sciences Paris-Saclay (IPS2), Orsay, France, [5] Department of Plants and Crops, Ghent University, Ghent, Belgium, [6] Institute of Science and Technology Austria, Klosterneuburg, Austria, [7] Lab of Plant Growth Analysis, Ghent University Global Campus, Incheon, South Korea

Calcium-dependent protein kinases (CPK) are key components of a wide array of signaling pathways, translating stress and nutrient signaling into the modulation of cellular processes such as ion transport and transcription. However, not much is known about CPKs in endomembrane trafficking. Here, we screened for CPKs that impact on root growth and gravitropism, by overexpressing constitutively active forms of CPKs under the control of an inducible promoter in *Arabidopsis thaliana*. We found that inducible overexpression of an constitutive active CPK30 (CA-CPK30) resulted in a loss of root gravitropism and ectopic auxin accumulation in the root tip. Immunolocalization revealed that CA-CPK30 roots have reduced PIN protein levels, PIN1 polarity defects and impaired Brefeldin A (BFA)-sensitive trafficking. Moreover, FM4-64 uptake was reduced, indicative of a defect in endocytosis. The effects on BFA-sensitive trafficking were not specific to PINs, as BFA could not induce aggregation of ARF1- and CHC-labeled endosomes in CA-CPK30. Interestingly, the interference with BFA-body formation, could be reverted by increasing the extracellular pH, indicating a pH-dependence of this CA-CPK30 effect. Altogether, our data reveal an important role for CPK30 in root growth regulation and endomembrane trafficking in *Arabidopsis thaliana*.

Keywords: calcium-dependent kinase, CPK30, endosome, Brefeldin A, PIN, root, gravitropism, polarity

OPEN ACCESS

Edited by:
Ruixi Li,
Southern University of Science and Technology, China

Reviewed by:
Anindya Ganguly,
AgroSpheres Inc., United States
Lorena Pizarro,
Universidad de O'Higgins, Chile

****Correspondence:***
Steffen Vanneste
steffen.vanneste@ugent.be

Specialty section:
This article was submitted to Plant Physiology, a section of the journal Frontiers in Plant Science

Received: *25 January 2022*
Accepted: *02 May 2022*
Published: *16 June 2022*

Citation:
Wang R, Himschoot E, Chen J, Boudsocq M, Geelen D, Friml J, Beeckman T and Vanneste S (2022) Constitutive Active CPK30 Interferes With Root Growth and Endomembrane Trafficking in Arabidopsis thaliana. Front. Plant Sci. 13:862398. doi: 10.3389/fpls.2022.862398

INTRODUCTION

Calcium (Ca^{2+}) is one of the most conserved second messengers in living organisms, and is a central component of signal transduction networks mediating plant development and responses to numerous biotic and abiotic stresses (Shi et al., 2018), such as pathogens, drought, heat, salinity and cold, etc. A wide variety of endogenous and external stimuli can activate cytoplasmic Ca^{2+} signals that can be sensed and decoded by multiple classes of Ca^{2+} binding proteins that provide specificity in the signaling pathway: the calmodulins (CaM), the calcineurin B-like (CBL) proteins that mostly regulate the class of CBL-interacting protein kinases (CIPKs) in plants and the calcium-dependent protein kinases (CPKs) and their relatives CPK-related kinases (CRKs) (Yip Delormel and Boudsocq, 2019). CaM is highly conserved in all eukaryotes, whereas CBLs and CPKs are

only identified in plants and some protists (Day et al., 2002; Shi et al., 2018).

CPKs are serine/threonine protein kinases with an auto-inhibitory junction, and calmodulin-like domain in a single polypeptide. As a result, CPKs can be activated by direct binding of Ca^{2+} in its calmodulin-like domain (Cheng et al., 2002; Roberts and Harmon, 2003), and constitutive active variants can be generated by deleting the auto-inhibitory and calmodulin-like domains (Boudsocq et al., 2010; **Supplementary Figure 1A**). The Arabidopsis genome contains 34 CPK genes, operating in a diverse range of signaling pathways related to plant immunity, abiotic stress, hormonal signaling, regulation of the cytoskeleton, ion and water transport, nitrogen, and phospholipid metabolism (Rudd and Franklin-Tong, 2001; Boudsocq and Sheen, 2013; Simeunovic et al., 2016; Yip Delormel and Boudsocq, 2019). While some have a ubiquitous expression in most tissues, others are only expressed in specific tissues (Hong et al., 1996; Ye et al., 2009; Monaghan et al., 2014).

Several CPKs are also known to be involved in root development. A subclade of CPKs, including CPK10, 30, 32, have been implicated in a nitrate signaling cascade that controls root architecture (Liu et al., 2017). These CPKs modulate the function of important regulatory factors of the nitrate signaling pathway such as the transcription factor NIN-LIKE PROTEIN 7 (NLP7), presumably downstream of the transceptor NPF6.3/NRT1.1 (Liu et al., 2017). The CPK7 acts on root hydraulic conductivity by reducing the cellular abundance of water transporting aquaporins (Li et al., 2015). CPK3 was linked to lateral root formation by *in vitro* phosphorylation of the C-terminus of PLAIV (Rietz et al., 2010). Several calcium-dependent protein kinases (CPKs), including CPK4, can phosphorylate RopGEF1 to promote its degradation in root hair development (Li et al., 2018). Interestingly, CPK29 was found to impact on auxin-regulated development through modulation of auxin-transport by directly phosphorylating of PIN-type auxin transporters (Lee et al., 2021).

A plant cell, as well as any other eukaryotic cell, contains a network of intracellular membranes to facilitate protein transport, which consists of the plasma membrane, the ER, *trans*-Golgi network/early endosomes (TGN/EEs), the Golgi Apparatus, the multivesicular body/prevacuolar compartment/late endosomes (MVB/PVC/LEs), and the lytic and storage vacuole (Murphy et al., 2005; Jürgens and Geldner, 2007; Schellmann and Pimpl, 2009; Zárský and Potocký, 2010; Reyes et al., 2011; Robinson and Pimpl, 2014). Key regulators of endosome trafficking between distinct endomembrane compartments are ARF (ADP-ribosylation Factor) GTPases and their regulators ARF-GEFs (ARF-GUANINE NUCLEOTIDE EXCHANGE FACTORs) (Zárský and Potocký, 2010; Kania et al., 2014).

ARF GTPases control the budding of endosomal vesicles, and continuously cycle between a guanosine-5′-triphosphate (GTP)-bound (active) form, and a guanosine diphosphate (GDP)-bound (inactive) form. Switching between both forms relies on GTP hydrolysis, mediated by negative regulators named ARF GTPase-ACTIVATING PROTEINs (ARF-GAPs), and exchange of GDP for GTP, mediated by the positive regulators called ARF-GEFs (Yorimitsu et al., 2014). The Arabidopsis genome contains 8 large ARF-GEFs showing mutual significant functional redundancy (Anders and Jurgens, 2008). Due to the presence of several resistant ARF-GEFs in Arabidopsis, the fungal toxin Brefeldin A can be used to inhibit GNOM ARF-GEF-regulated processes in the root. At a concentration of 25 μM, BFA induces the formation of so-called BFA bodies that are aggregates of early endosomes/TGN surrounded by Golgi (Donaldson and Jackson, 2000; Geldner et al., 2001; Nebenfuhr et al., 2002), an effect that can be largely attributed to inhibition of GNOM (Peyroche et al., 1996; Geldner et al., 2003). In these BFA bodies, *de novo* synthesized and endocytosed cargoes destined for secretion and recycling, respectively, can be captured. Therefore, the accumulation of endosomal cargoes could be used as a proxy for endocytic rates (Geldner et al., 2001; Robert et al., 2010; Kitakura et al., 2011). However, caution should be taken when using this assay, as treatments that interfere with BFA-induced endosomal aggregation could complexify the interpretation of results (Narasimhan et al., 2021).

While CPKs have been found in various subcellular locations, most CPKs are targeted to the plasma membrane (PM), where they modulate the activity of PM-localized proteins such as ion channels like SLAH (Gutermuth et al., 2013) and transporters (Liu et al., 2017; Lee et al., 2021). However, not much is known about their effect on endomembrane trafficking (Himschoot et al., 2017). Here, we screened constitutive active CPKs for effects on root growth, and found that CPK30 and the related CPK13 strongly impair root growth and gravitropism. This phenotype was associated with defects in endosomal trafficking, and was pH dependent. These data provide a first link between CPK activity and the regulation of endomembrane dynamics.

MATERIALS AND METHODS

Plant Growth Conditions

Arabidopsis thaliana seeds were sterilized by using bleach gas (8 mL concentrated HCl to 150 mL bleach) overnight, afterward the seeds were sown on Petri dishes (12 cm × 12 cm) containing sterile half-strength Murashige and Skoog (1/2 × MS, Duchefa-biochemie, Haarlem) medium (1/2 × MS salts, 0.8% sucrose, 0.5 g/L 2-(N-morpholino) ethanesulfonic acid, pH 5.7, and 1% w/v agar), after 2 days stratification at 4°C in the dark then transfer to growth chamber. Plates are put vertically at 21°C under continuous light. The phenotype of Col-0, *CA-CPK* lines was determined by germinating seeds on 1/2 x MS, and transferring them after 5 days 1/2 × MS plates supplemented with 2.5 μM β-estradiol for another 7 days. CA-CPK30 was crossed to DR5rev:GFP (Friml et al., 2003) and analyzed in the F1 generation.

Cloning and Selection

The CA-CPK clones were previously created for transient expression assays (Boudsocq et al., 2010). These vectors were used as templates for subcloning in pDONR221 *via* BP reaction of a PCR fragments that were generated using attB1_CPKx_FW (GGGGACAAGTTTGTACAAAAAAGCAGGCTTGATCGTGC AACCCATCGGATCC) and AttB2_FLAG_REV (GGGGACC ACTTTGTACAAGAAAGCTGGGTTCACTTGTCATCGTCGT CC). The resulting entry vectors were confirmed by sequencing

and recombined with pEN-L4_RPS5A_XVE_R1 (Gao et al., 2018) into pH7m24GW,3 (Karimi et al., 2007) *via* LR recombination. Validated clones were transformed into wild-type Col-0 plants *via* floral dip transformation (Clough and Bent, 1998), and transformants were selected using Hygromycin selection.

Chemicals

The following chemicals were used: Brefeldin A (BFA, catalog Nr B6542-25MG-Sigma-Aldrich, Belgium), β-estradiol (catalog Nr E8875-5G-Sigma-Aldrich, Belgium). These drugs were dissolved in 100% dimethylsulfoxide (DMSO, catalog Nr D4540-500ML Sigma-Aldrich, Belgium) to make 50 mM stock solutions. The FM4-64 (T13320—Thermo Fisher Scientific, Belgium) stock in DMSO was set at 10 mM.

Immunodetection

The seedlings used for immunodetection are 3–4-day-old grown on 1/2 × MS, and then treated in liquid medium as indicated. For β-estradiol induction, 3-day-old seedlings were transferred to a plate 1/2 × MS medium containing β-estradiol (2.5 μM) for at least 24 h. The samples were fixed by paraformaldehyde (4%) (cat. no. P6148, Sigma-Aldrich, Belgium) in PBS for 1 h in vacuum. The following steps of the immunostaining were performed by the immuno-robot InsituPro Vsi II (Intavis, Tübingen, Germany), as described by Sauer (Sauer et al., 2006). In brief, immediately after fixation, the samples were transferred to the 30-well rack of the robot and subjected to 6 washes [3 in PBS pH 7.4 + 0.1%Triton X-100 (PBS-T); 3 in distilled water + 0.1%Triton X-100 (cat. no. 3051.2, Carl Roth, Germany); 5 min each], cell wall digestion [1.5% Driselase (cat. no. D9515, Sigma-Aldrich, Belgium) in PBS, 30 min at 37°C], 3 washes (PBS-T, 5 min), permeabilization (3% IGEPAL CA-630 (cat. no. I3021, Sigma-Aldrich, Belgium), 10% DMSO in PBS; 30 min room temperature), 3 washes (PBS-T, 5 min), blocking solution (3% BSA in PBS, 1 h 37°C), primary antibody solution (primary antibodies diluted in blocking solution, 4 h 37°C), 5 washes (PBS-T, 5 min), secondary antibody solution (secondary antibodies diluted in blocking solution, 3 h, 37°C), 5 washes (PBS-T, 5 min) and 5 washes (distilled water, 5 min). The dilutions of the primary antibodies used are: goat anti-PIN1 (1:600) (sc-27163, SantaCruz, CA, United States), rabbit anti-PIN1 (1:1,000) (Paciorek et al., 2005) and rabbit anti-PIN2 (1:1,000) (Abas et al., 2006). The dilutions of the secondary antibodies used are: AlexaFluor488 donkey anti-goat (1:600) (A-11055, Thermo Fisher Scientific, Belgium) and Alexafluor555 donkey anti-rabbit (1:600) (A-31572, Thermo Fisher Scientific, Belgium).

Microscopy and Image Analysis

A Leica SP2 or a Zeiss LSM 710 confocal laser scanning microscope equipped with a 63x water-corrected objective (Leica SP2) or 40x water-corrected objective (Zeiss LSM710) was used for detection. Settings for detection: Alexa488 (ex 488 nm/em 500–545 nm), Alexa555 (ex 561 nm/em 555–610 nm), the pinhole was always set to 1 airy unit. Images were analyzed using Fiji[1]: Eg. Root length (segmented line for tracing the root, Analyze-Measure (Analyze-set scale for calibration); Fiji was used to rotate (Image-Transform-Rotate) and crop images (Image-Crop). For the maximal projections: Stacks-z-Project + Image-Lookup Tables-Fire. Fluorescence measurements were done on 8-bit images. The proportion of cells with BFA bodies was scored manually and calculated by using Excel. BoxPlotR was used to generate the box plots (Spitzer et al., 2014).

Statistical Analysis

For statistical analysis of the immunolocalization experiments, a logistic regression was performed to compare the presence of BFA bodies in root cells of treated vs. untreated roots or wild type vs. mutant. A random effect was added to the model for the experiments with multiple repeats to consider the correlation between measurements done at the same time. The analysis was performed with the glimmix procedure from SAS (Version 9.4 of the SAS System for windows 7 64 bit. Copyright 2002–2012 SAS Institute Inc. Cary, NC, United States).[2] Maximum likelihood estimation was done with the default estimation method. A Wald-type test was performed to estimate the treatment/genotype effect on the presence of BFA bodies in the root cells.

RESULTS

A Gain-of-Function Screen Identifies Calcium-Dependent Protein Kinases Involved in Auxin-Regulated Root Growth

A gain-of-function screen was performed to identify CPKs involved in root growth and gravitropism. Therefore, we generated a collection of β-estradiol-inducible vectors for inducible overexpression of constitutive active (CA) variants, lacking the C-terminal Ca^{2+} regulatory and autoinhibitory domain, for 12 out of 34 CPKs in *Arabidopsis* (**Figure 1A** and **Supplementary Figure 1A**). The templates for cloning the CA-CPKs were previously used for transient expression in a protoplast system (Boudsocq et al., 2010; Liu et al., 2017), and the β-estradiol induction module was driven under the RPS5A promotor (Gao et al., 2018). We obtained at least 2 independent lines for Group I: CA-CPK2, CA-CPK4, CA-CPK11, CA-CPK12; Group II: CA-CPK22, CA-CPK27, CA-CPK29; Group III: CA-CPK8, CA-CPK13 and CA-CPK30; Group IV: CA-CPK28, and screened them at homozygosity for obvious β-estradiol-induced root phenotypes (**Figures 1B–M** and **Supplementary Figures 1B–M**). Seeds were germinated on control medium and transferred after 5 days to β-estradiol medium (2.5 μM) for another 7 days. The position of the root tip at time of transfer was marked to allow measuring the root growth during estradiol treatment. The β-estradiol treatment significantly reduced root growth in both independent lines for CA-CPK2, CA-CPK4, CA-CPK11, CA-CPK12, CA-CPK13, CA-CPK29, and CA-CPK30 (**Figure 1N**). The observation of root growth defects in 2 independent lines illustrates robustness of the

[1] https://imagej.net/Fiji

[2] www.sas.com

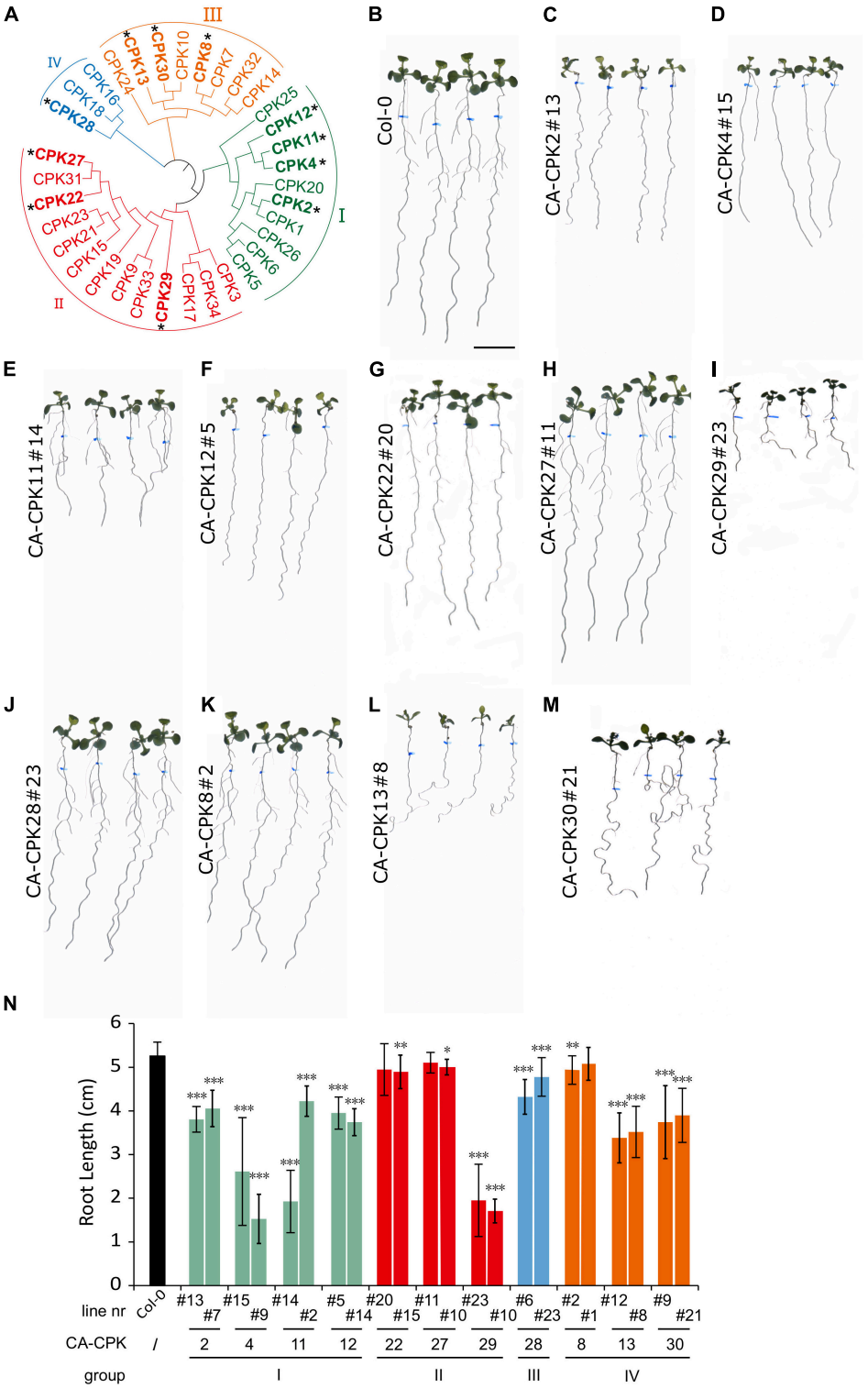

FIGURE 1 | Phenotypic screen of constitutive active CPKs. **(A)** Phylogenetic tree of the Arabidopsis CPK family, with indication of the four main subgroups (I-IV). CPKs indicated with an asterisk were analyzed *via* stable overexpression lines. **(B–M)** Overview of macroscopic phenotypes of CA-CPK lines relative to WT (Col-0). Seeds were grown for 5 days on 1/2 × MS medium then transferred to medium supplemented with 2.5 μM β-estradiol for another 7 days. Scale bar = 1 cm. **(N)** Quantification of root length for indicated CA-CPK lines. Data are represented as the mean ± SD of at two independent replications. $n \geq 12$ for all lines, except for CPK12#14 ($n = 6$) and CA-CPK22#20 ($n = 7$). Asterisk indicates significant difference (Unpaired Student's *t*-test; $^{*}P \leq 0.05$, $^{**}P \leq 0.01$, $^{***}P \leq 0.001$) between transgenic lines and WT (Col-0) plants.

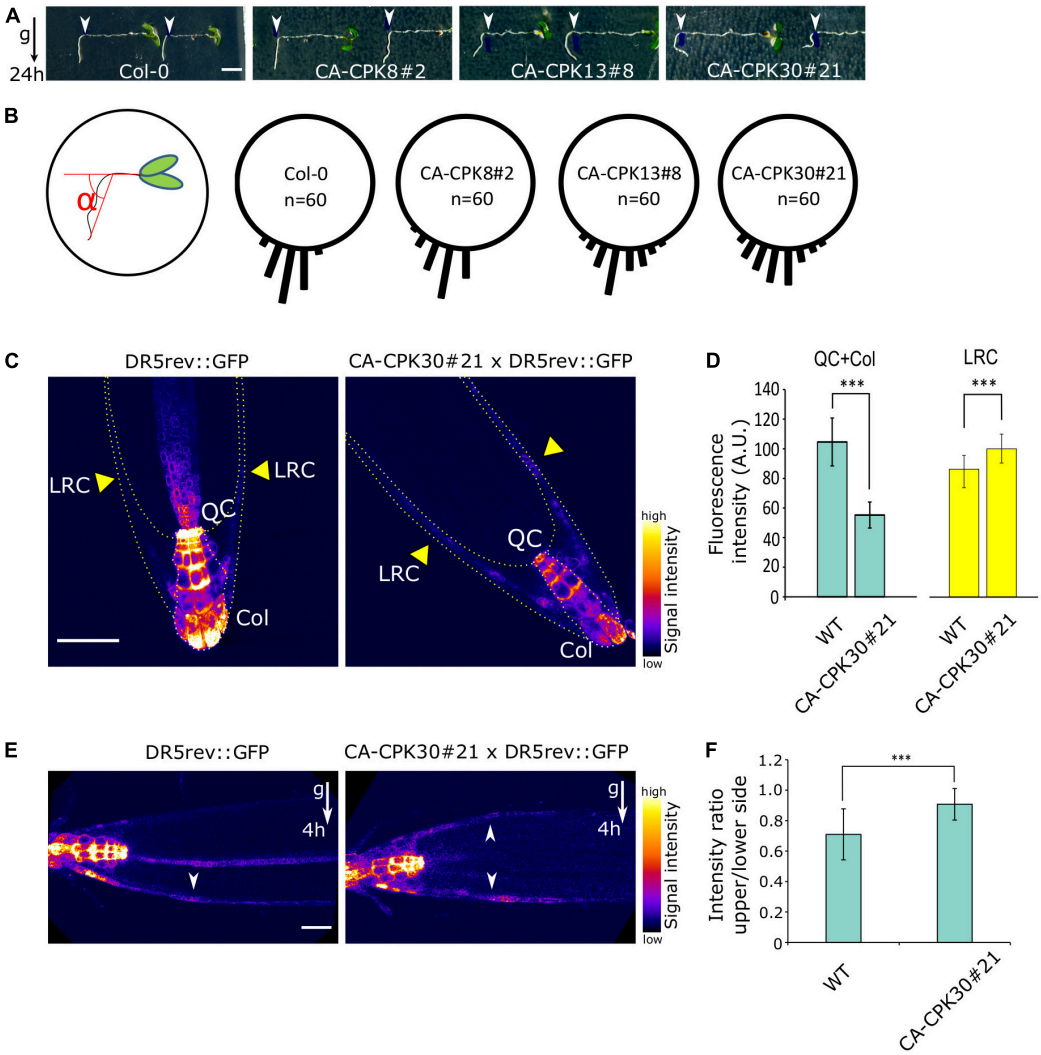

FIGURE 2 | Induction of CA-CPK30 causes agravitropic root growth. **(A)** Analysis of the root gravitropic response of Col-0, CA-CPK8#2, CA-CPK13#8 and CA-CPK30#21. 5-day-old seedlings were transferred to 2.5 μM β-estradiol medium and immediately gravistimulated for 24 h (90 degree rotation). White arrowheads mark the position of the root tip at the moment of transfer. Scale bar = 0.2 cm. **(B)** Quantification of the root angle distribution of **(A)**. $n = 60$ is the total number of roots analyzed from two replicates for each genotype. **(C)** Expression pattern of the auxin output response marker DR5rev::GFP in WT and CA-CPK30#21 backgrounds. 6-day-old seedlings were transferred to 2.5 μM β-estradiol medium for a 2 day induction. Yellow arrowheads indicate the lateral root cap (LRC). QC and Col, are quiescence center and columella, respectively. Scale bar = 50 μm. **(D)** Quantification of DR5rev::GFP fluorescence in WT and CA-CPK30#21 (shown in **C**), in the quiescence center and columella, lateral root cap. Measured areas are indicated in **(C)** by dashed lines. For DR5rev::GFP $n = 12$ in total, for CA-CPK30#21 × DR5rev::GFP $n = 10$ in total, from two replicates. Data are presented as the mean ± SD. (Unpaired Student's *t*-test; $^{***}P \leq 0.001$). **(E)** Expression pattern of the auxin output response marker DR5rev::GFP in WT and CA-CPK30 in response to gravity. 6-day-old seedlings were transplanted onto 2.5 μM β-estradiol-containing medium for 2 day induction, followed by a 4 h gravistimulation (90 degree rotation). Scale bar = 20μm. **(F)** Quantification of intensity ratio between the upper/lower side for DR5rev::GFP fluorescence in WT and CA-CPK30#21 (shown in **E**). Across 3 replicates, $n = 17$ for DR5rev::GFP and, $n = 24$ for CA-CPK3#21 × DR5rev::GFP. Data are presented as the mean ± SD. (Unpaired Student's *t*-test; $^{***}P \leq 0.001$).

observed phenotypes, and highlights the corresponding CPKs as regulators of processes that are important for root growth.

Constitutive Active CPK30 Interferes With Auxin Distribution and Gravitropism

In addition to a root length reduction, we noted that both lines of the closely related CA-CPK13 and CA-CPK30 displayed an exaggerated wavy root growth phenotype that was not seen for other CA-CPKs (**Figures 1L,M** and **Supplementary Figures 1L,M**). We further explored the root gravitropic growth in CA-CPK13#8 and CA-CPK30#21. Five-day-old seedlings were transferred to β-estradiol-containing medium and were rotated 90 degrees relative to the gravity vector followed by the assessment of gravitropic reorientation of the root tip after 24 h. As controls we used WT (Col-0) and CA-CPK8#2 that represents a more distant member of the group III CPKs, to which also CPK13 and CPK30 belong. In contrast to the

tight realignment to the gravity vector of these controls, the realignment of CA-CPK13#8 and CA-CPK30#21 roots appeared to occur randomly, indicating a defect in their gravitropic response (**Figures 2A,B**). These data suggest that CA-CPK13 and CA-CPK30 deregulate processes that are important for normal root growth and gravitropism.

Gravitropism is the result of stimulation and inhibition of cell elongation driven by differential accumulation of auxin on opposing sides of a gravistimulated root (Vanneste and Friml, 2009). Therefore, we suspected a defective auxin distribution in the roots of CA-CPK30. We crossed the auxin signaling output marker DR5rev::GFP to CA-CPK30#21, yielding a gravitropic root defect similar to the one seen in the original CA-CPK30#21 (**Supplementary Figures 2A,B**), suggesting that the DR5rev::GFP background did not modify CA-CPK30 effects on gravitropism.

Subsequently, we analyzed the effect of 2 days β-estradiol treatment on the DR5rev::GFP expression pattern in the root tip. In the WT, DR5rev::GFP was mainly expressed in the quiescence center (QC) and columella (Col), with little to no expression in the lateral root cap (LRC) (**Figure 2C**). In the CA-CPK30, the QC and Col signals were reduced, while its intensity in the LRC increased (**Figures 2C,D**).

Next, we assessed the response of the DR5rev::GFP signal to a gravistimulus. Seedlings were transferred to β-estradiol for 2 days, followed by a 4 h gravistimulation. The gravistimulus elicited a typical asymmetric DR5rev::GFP expression at the lower side of the gravistimulated root meristem, but not at its upper side (**Figures 2E,F**). This reflects a differential auxin accumulation that inhibits elongation on the lower side, to achieve root bending and realignment to the gravitropic field. In contrast, the establishment of an asymmetric DR5rev::GFP signal between the upper and lower sides of CA-CPK30#21 was impaired (**Figures 2E,F**). These data suggest that CA-CPK30 causes gravitropic defects in the root *via* ectopic auxin accumulation that is unresponsive to gravistimulation.

Constitutive Active CPK30 Impairs PIN Protein Levels and Polarity

The poor gravitropic response and auxin distribution defects in CA-CPK30 roots prompted us to analyze the expression and localization of the auxin transporters PIN1 and PIN2 *via* whole mount immunolocalization after 2 days induction with 2.5 μM β-estradiol. In CA-CPK30#21, both the anti-PIN1 signal and anti-PIN2 signals were significantly reduced compared to WT (**Figures 3A–D**). Interestingly, a prominent lateral PIN1 signal, that was not observed in WT, became apparent in the CA-CPK30#21 line (**Figures 3A,E**), suggesting a defect in PIN1 polarity. We expanded these analysis with other CA-CPK lines to provide a qualitative assessment of effects on PIN levels and polarization in them (**Supplementary Figures 3A,B**). Additionally, we generated maximal projections of 70 μm z-stacks across the root (Baster et al., 2013), to visualize the overall PIN protein levels in the roots (**Supplementary Figure 3C**). *Via* these analyses, we found that the reductions in PIN1 and PIN2 protein levels and PIN1 polarization seen in CA-CPK30#21, could also be detected in CA-CPK30#9, CA-CPK13#8 and CA-CPK13#12, with the effects on PIN1 polarization being less prominent in CA-CPK13#8 (**Supplementary Figures 3A–C**). In addition to the CA-CPK13 and CA-CPK30, both lines for CA-CPK2, CA-CPK4, CA-CPK11, CA-CPK12, and CA-CPK29 displayed clear reductions in PIN signals in their root meristems (**Supplementary Figure 3C**). The lines with reduced PIN levels largely corresponded with the CA-CPK lines in which root length was reduced (**Figure 1N**). Additionally, we observed a tendency toward more lateral PIN1 signals in CA-CPK22 (#20 and #15) and in CA-CPK29#10 (but not in #23) (**Supplementary Figure 3A**), suggesting that these CPKs are also potential regulators of PIN polarity. The reduced PIN1 polarity is consistent with a recent report demonstrating that CPK29 can interact with and phosphorylate PIN proteins (Lee et al., 2021).

Collectively, these data demonstrate that CA-CPK30 impairs not only PIN1 and PIN2 protein levels but also PIN1 polar distribution.

Constitutive Active CPK30 Impairs Brefeldin A-Sensitive Trafficking

CPK29 was recently shown not only to affect PIN polarity, but also to suppress its internalization rates (Lee et al., 2021). Therefore, we asked if internalization would be affected by CA-CPK30. We estimated PIN internalization rates using a short-term treatment with the fungal toxin Brefeldin A (BFA) that blocks recycling and causes aggregation of the endosomes and their cargoes in so-called BFA bodies (Geldner et al., 2001). Therefore, we simultaneously monitored the localization of PIN1 and the ARF1 GTPase, which labels the Golgi and TGN/EEs (Xu and Scheres, 2005). A 1 h treatment with 25 μM BFA induced the formation of BFA bodies in WT roots that were positive for both PIN1 and ARF1 (**Figures 3F,G**). In contrast, nearly no PIN1 signal was observed in internal structures, but was retained at the plasma membrane, nor were the ARF1-positive endosomes aggregated upon BFA treatment in CA-CPK30#20 (**Figures 3F,G**). To exclude that this was an artifact of CA-CPK30#21 on ARF1 localization to endosomes, we repeated this dual labeling experiment using anti-CLATHRIN HEAVY CHAIN (CHC) antibodies as a marker of the TGN/EEs (Shimizu et al., 2021). Similarly, CA-CPK30 interfered with the induction of PIN1- and CHC-labeled BFA bodies (**Supplementary Figures 4A,B**). This suggests that overexpression of CA-CPK30 impairs PIN endomembrane trafficking, and BFA-sensitive aggregation of endosomes.

To better understand this, we screened all our CA-CPK lines for BFA body formation (**Supplementary Figures 5A,B**). All of the CA-CPK13 and CA-CPK30 lines were almost devoid of PIN1 or PIN2 positive BFA bodies. Also, no BFA bodies could be discerned in CA-CPK4 and CA-CPK11 lines, while all other lines showed some signs of PINs accumulating in BFA bodies, even though their PIN protein levels were also reduced (**Supplementary Figure 3C**). This indicates that the inhibition of

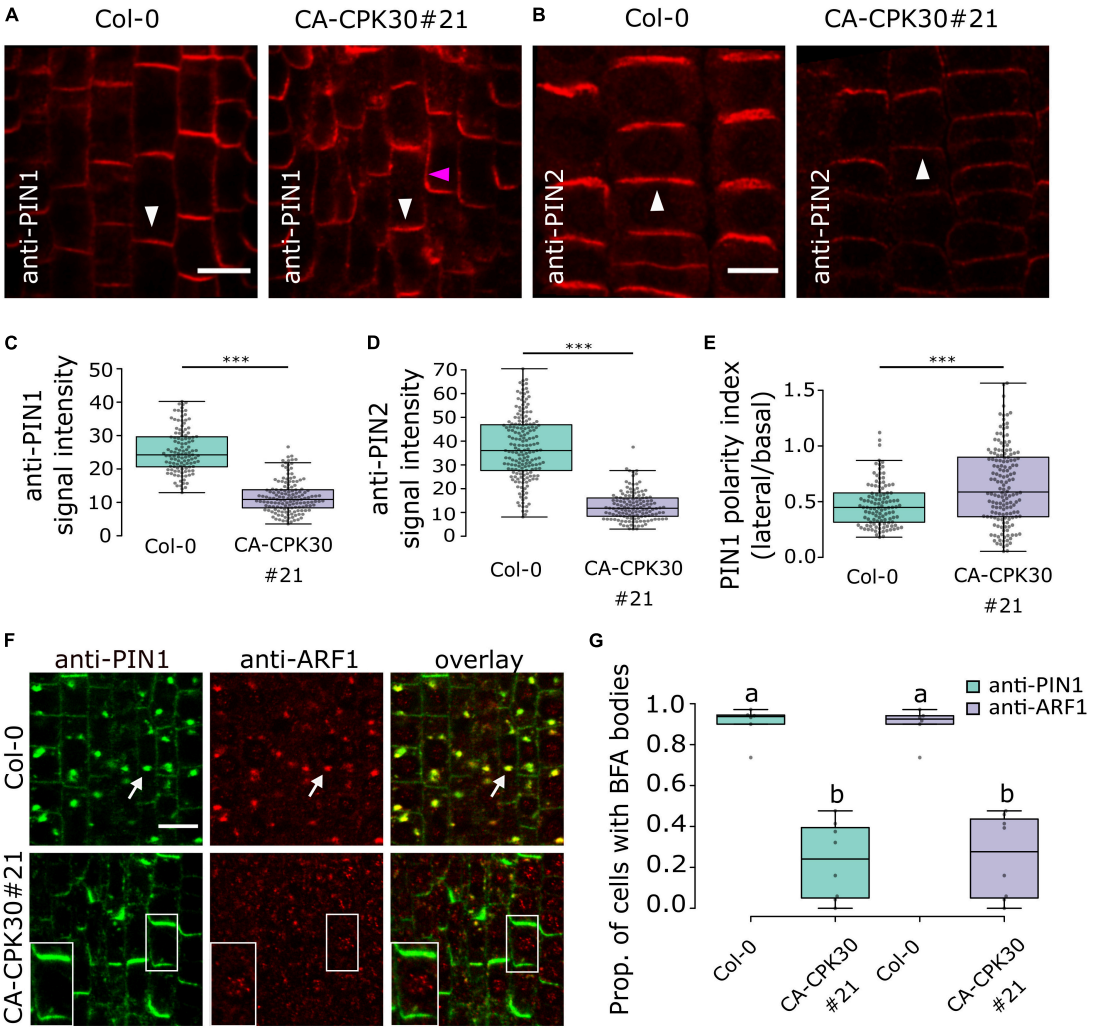

FIGURE 3 | Induction of CA-CPK30 causes endomembrane trafficking defects. **(A,B)** Immunolocalization of PIN1 **(A)** and PIN2 **(B)** in roots of β-estradiol-treated Col-0 and CA-CPK30#21. White arrowheads indicate the expected polar domain of the respective PINs. The pink arrowhead indicates ectopic, lateral PIN1 signal. Scale bar = 20 μm. **(C)** Quantification of anti-PIN1 signal intensity in the plasma membrane of stele cells for Col-0 and CA-CPK30#21. For Col-0 $n = 119$ cells from 11 roots, for CA-CPK30#21 $n = 147$ cells from 9 roots pooled from two replicates. **(D)** Quantification of anti-PIN2 intensity in the plasma membrane of epidermal cells for Col-0 and CA-CPK30#21. For Col-0 $n = 183$ cells from 12 roots, for CA-CPK30#21 $n = 140$ cells from 11 roots pooled from two replicates. **(E)** Quantification of PIN1 polarity, based on the ratio of the PIN1 signal in the lateral/basal side for individual cells in Col-0 and CA-CPK30#21. For Col-0: $n = 113$ cells from 11 roots, for CA-CPK30#21: $n = 158$ cells from 10 roots, two replicates. (Unpaired Student's *t*-test; *** $P \leq 0.001$ for **C–E**). **(F)** Whole-mount immunolocalization using anti-PIN1 and anti-ARF1 antibodies in 5 day-old seedling root meristems of BFA-treated Col-0 and CA-CPK30#21 seedlings. Seedlings were transferred for 1 day to 2.5 μM β-estradiol prior to 1 h BFA (25 μM) treatment. White arrows indicate PIN1, ARF1 co-localization in BFA bodies. Insets are magnifications of a single cell of the BFA-treated CA-CPK30#21. Scale bar = 10 μm. **(G)** Boxplot representation of the proportion of cells with BFA bodies for treatments to Col-0 and CA-CPK30#21 (for Col-0: $n = 6$ and for CA-CPK30#21: $n = 8$ in total from two replicates). Significant differences ($P \leq 0.05$, Wald-type test) are indicated by different lowercase letters. For all box plots, the central line indicates the median, the bottom and top edges of the box the interquartile range, and the box plot whiskers are plotted down to the minimum and up to the maximum value.

PIN1 accumulation in BFA bodies is not a universal feature of CA-CPKs that cause reduction of PIN protein levels.

Constitutive Active CPK30 Impacts on Endocytosis and Brefeldin A-Sensitive Trafficking

The agravitropism (**Figures 2A,B**), ectopic DR5rev::GFP in the LRC (**Figures 2C,D**), the reduced PIN1 polarization (**Figures 3A,E**) and the defect in PIN BFA body formation in CA-CPK30 (**Figures 3F,G**) are reminiscent of phenotypes induced by overexpression of a dominant negative fragment of CHC, which causes defects in clathrin-mediated endocytosis (Kitakura et al., 2011). Therefore, we monitored CA-CPK30's ability for uptake of the endocytic tracer dye FM4-64 (**Figures 4A,B**). After 10 min, the FM4-64 stained the plasma membrane and numerous endosomes in WT roots. In contrast, in CA-CPK30#21 nearly no FM4-64 signal could be detected in endosomes, suggesting

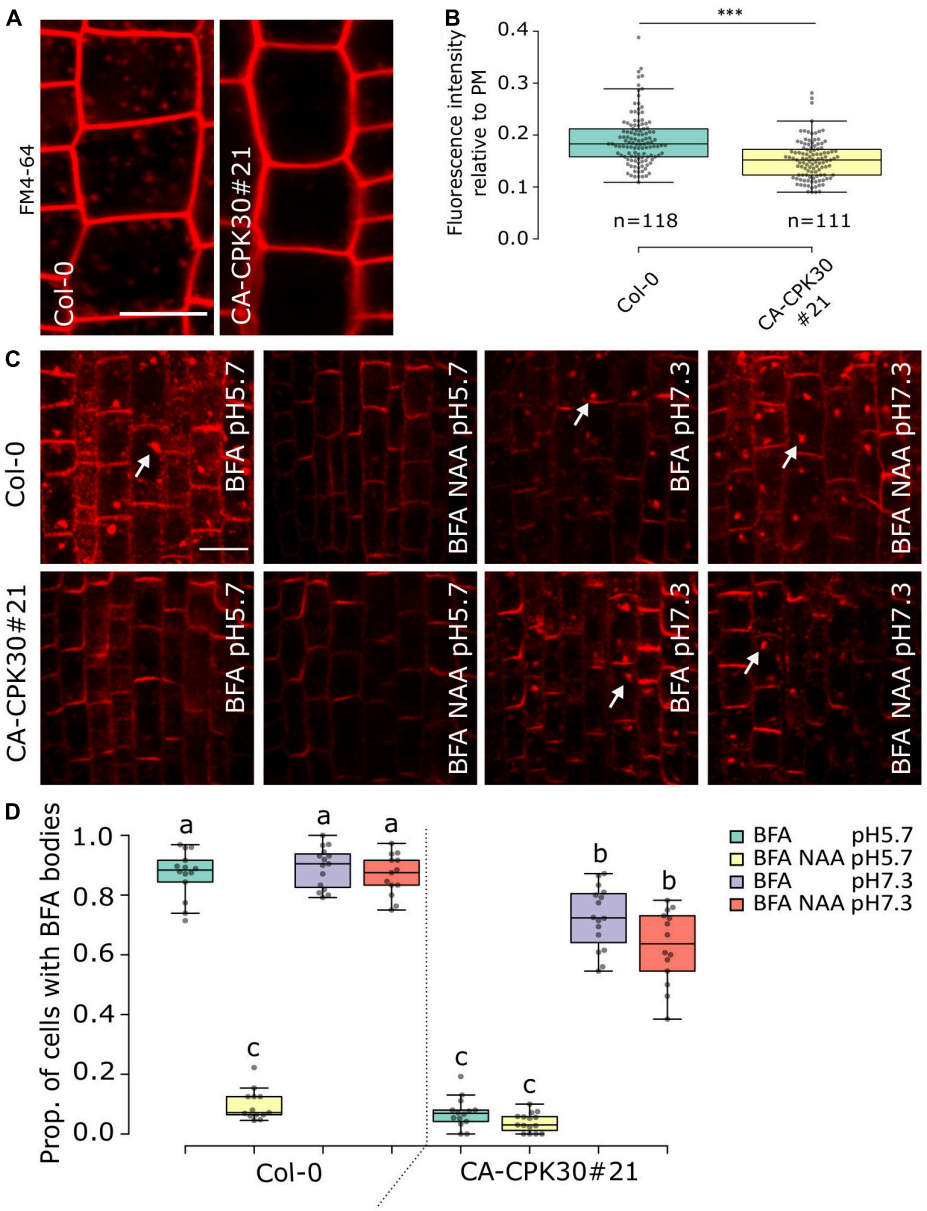

FIGURE 4 | BFA insensitivity in CA-CPK30 depends on the extracellular pH. **(A)** Representative confocal images of FM4-64 uptake in β-estradiol-treated (1 day, 2.5 μM) Col-0 and CA-CPK30#21 seedlings in root epidermal cells. The 5-days-old seedlings were pretreated with liquid medium for 20 min, followed by 10 min incubation in liquid medium containing 5 μM FM4-64. The contrast was equally enhanced in both pictures for illustrational purposes. Measurements were done on the original images without saturation of pixels. **(B)** Quantification of FM4-64 fluorescence intensity in the cytoplasm relative to the plasma membrane of Col-0 and CA-CPK30#21. Numbers (n) represent the cells analyzed from 11 individual seedlings for each line, over three replicates. Unpaired Student's *t*-test; $^{***}P < 0.001$. Scale bar = 20 μm. **(C)** Whole-mount immunolocalization using anti-PIN1 antibodies in 5 day-old seedling root meristems of β-estradiol treated wild-type (Col-0) and CA-CPK30#21 seedlings that were treated with BFA or BFA/NAA at pH5.7 and at pH 7.3. Seedlings were transferred for 1 day to 2.5 μM β-estradiol prior to different treatments. Seedlings were incubated in liquid β-estradiol-containing medium with pH 5.7 or pH 7.3 for 30 min then incubated with 25 μM BFA or combined with 10 μM NAA in pH 5.7 or pH 7.3 for 1 h. White arrows indicate PIN1 in BFA bodies. Scale bar = 20 μm. **(D)** Quantification of the proportion of cells with BFA bodies for treatments described in **(C)** (for Col-0: $n = 14$ in BFA, pH5.7; $n = 13$ in BFA/NAA, pH5.7; $n = 15$ in BFA, pH7.3; $n = 13$ in BFA/NAA, pH7.3) and (for CA-CPK30#21: $n = 14$ in BFA, pH5.7; $n = 15$ in BFA/NAA, pH5.7; $n = 16$ in BFA, pH7.3; $n = 14$ in BFA/NAA, pH7.3), three replicates. For the box plots, significant differences ($P \leq 0.05$, Wald-type test) are indicated by different lowercase letters. The central line indicates the median, the bottom and top edges of the box the interquartile range, and the box plot whiskers are plotted down to the minimum and up to the maximum value.

CA-CPK30 interferes with endocytosis. Importantly, however, our BFA experiments also revealed that CA-CPK30#21 was defective in BFA-induced endosomal aggregation, suggesting that endosomal motility is affected, thereby possibly precluding the efficient movement of FM4-64 positive endosomes into the cell's interior.

A similar effect on endosomal motility and FM4-64 uptake have previously also been reported for treatments with the protonophore Endosidin9 (Dejonghe et al., 2016) and the synthetic auxin, 1-NAA (Narasimhan et al., 2021). The effects of these molecules on endosomal dynamics could be, at least in part, reverted by increasing the apoplastic pH to reduce their effect on cytoplasmic acidification (Dejonghe et al., 2016; Narasimhan et al., 2021). Therefore, we asked if these effects of CA-CPK30 on BFA body formation could also be reverted at higher pH. We compared BFA body formation at the standard acidic pH 5.7, and the neutral pH7.3 (**Figures 4C,D**). As a positive control for the assay we used the pH-dependence of 1-NAA on BFA body formation (Narasimhan et al., 2021). The BFA treatment caused accumulation of PIN1 in BFA bodies and could be inhibited by 1-NAA co-treatment at pH 5.7 (**Figures 4C,D**). In contrast, 1-NAA lost its ability to inhibit PIN1 BFA body formation at pH 7.3 in WT (Col-0) (**Figures 4C,D**). Similarly, while CA-CPK30 strongly interfered with PIN1 BFA body formation at pH 5.7, it could no longer prevent BFA bodies at pH 7.3 (**Figures 4C,D**). Even a 1-NAA treatment of CA-CPK30 seedlings could not prevent BFA body formation at pH7.3 (**Figures 4C,D**). These data indicate that the CA-CPK30 effects on endosomal trafficking are pH-dependent, and thus that the effects on PIN endocytosis and polarity are possibly indirect.

DISCUSSION

The endomembrane system is undisputedly connected to Ca^{2+}. Its membranes separate the cytoplasm from Ca^{2+} that accumulates in lumen of organelles and the apoplast. Every fusion or fission event involves breaching the membrane integrity, during which Ca^{2+} can enter the cytoplasm. It is therefore not surprising that Ca^{2+} was recruited in the regulation of endomembrane trafficking. This is very well established during rapid tip-growth of pollen tubes and root hairs (Himschoot et al., 2017), and this likely also holds true in all cell types. However, very few Ca^{2+} sensors have been characterized as regulators of endomembrane trafficking. One recent example of this is that Ca^{2+} is required for the function of the endocytic TPLATE COMPLEX (Van Damme et al., 2011; Yperman et al., 2021). Here, we found that the Ca^{2+} binding kinase CPK30 can interfere with PIN trafficking, FM4-64 uptake and BFA-sensitive endosomal aggregation, providing a first link between a Ca^{2+} binding kinase and endomembrane trafficking. Notably, biochemical assays have suggested that CPK30 is activated by Ca^{2+} at concentrations that are lower than the cytoplasmic resting Ca^{2+} levels (Boudsocq et al., 2012; Liese and Romeis, 2013), implying its activity would be insensitive to cytoplasmic Ca^{2+} increases. However, CPK30 activity was found to be regulated by Ca^{2+} signals *in planta*, suggesting that CPK30 is kept in a low Ca^{2+} environment at the molecular level to allow activation by Ca^{2+} signals (Liu et al., 2017).

Recently, it was shown that nitrate coordinately stimulates cell elongation and cell proliferation and lateral root development *via* effects on PIN2-mediated auxin transport (Vega et al., 2021; Ötvös et al., 2021). This could be linked to nitrate regulated PIN2 phosphorylation changes that stimulated PIN2 secretion and recycling (Ötvös et al., 2021). We found that CPK30 impacts on root growth responses, and PIN2-mediated auxin transport at least *via* an effect on PIN2 abundance. Therefore, it would be of interest to evaluate if CPK30-like CPKs could directly phosphorylate PINs as part of the root's nitrate responses.

We noted that induction of CA-CPK30 interfered not only with PIN accumulation in BFA bodies, but rather with BFA-induced endosomal aggregation. A similar phenotype was previously also reported for treatments with the protonophore Endosidin9 (Dejonghe et al., 2016) and the synthetic auxin 1-NAA (Narasimhan et al., 2021). The effects of both treatments could be reverted by increasing the extracellular pH, and are thus linked to induction of cytoplasmic acidification. Such acidification possibly interferes with the protein recruitment to endomembranes *via* negative charges in acidic phospholipids (Himschoot et al., 2017), thereby explaining its disruptive effect on endomembrane processes. We found that the effect of induced CA-CPK30 activity on BFA body formation could also be reverted by increasing the extracellular pH. This suggests that CA-CPK30 inhibits BFA body formation by inducing cytoplasmic acidification, rather than by direct effects on endosomal machinery. Despite the pH-dependence of the BFA-resistance in CA-CPK30, it does not preclude direct effects on other endosomal components, as direct phosphorylation of the endocytic regulator DRP2B was reported for CPK5 (Yip Delormel et al., 2022).

Cytoplasmic acidification implies interference with proton efflux, activation of proton influx, or by a combination of both. Plasma membrane (PM) H^+ ATPases are prominent phosphorylation-regulated targets for many signaling pathways (Haruta et al., 2015), and could be even inhibited through phosphorylation by the Ca^{2+}-regulated PSK5/CIPK11 kinase (Fuglsang et al., 2007). Thus far, CPK30-like CPKs have been shown to inhibit K^+ influx by direct phosphorylation of the inward rectifying K^+ channel KAT2 and KAT1 in guard cells (Ronzier et al., 2014), but not in phosphorylation of PM H^+ ATPases. Yet, a grape berry group I CPK was found to phosphorylate and stimulate H^+ ATPases (Yu et al., 2006). Therefore, it will be of interest to determine how these group III CPKs could cause cytoplasmic acidification, and whether or not this involves a direct or indirect effect on PM H^+ ATPase activity.

Our analysis also provide a an entry point into exploring the role and impact of CPK-mediated signaling in the root. While we have focused here on CPK30, it is clear from our phenotypic screen that multiple CPKs control processes that are can modify root growth. While we did not analyze all features of these lines in detail *via* quantifications, we believe that the images can provide clues about other CPKs having a potential role in controlling PIN protein levels, trafficking and polarity. In example, our data indicate that CA-CPK29 has PIN polarity defects, which is consistent with a recent report about CPK29 controlling PIN polarity *via* direct interaction and phosphorylation (Lee et al., 2021). It will therefore be of interest to explore how these different CA-CPK

lines lead to defects in PIN protein levels, polarity and/or BFA-sensitive trafficking. This will provide the onset of research into how CPK-mediated signals converge on auxin-regulated root growth.

DATA AVAILABILITY STATEMENT

The original contributions presented in the study are included in the article and **Supplementary Material**, further inquiries can be directed to the corresponding author.

AUTHOR CONTRIBUTIONS

RW, EH, and JC performed the experiments. RW and SV analyzed the data and drew the figures. MB, DG, JF, TB, and SV planned and designed the study. All authors contributed to the article and approved the submitted version.

FUNDING

RW and JC predoctoral fellows that were supported by the Chinese Science Counsil. The IPS2 benefits from the support of the LabEx Saclay Plant Sciences-SPS (ANR-10-LABX-0040-SPS).

ACKNOWLEDGMENTS

We thank Jen Sheen for establishing and generously sharing the CKP family clone sets, and for providing useful feedback on the manuscript.

SUPPLEMENTARY MATERIAL

The Supplementary Material for this article can be found online at: https://www.frontiersin.org/articles/10.3389/fpls.2022.862398/full#supplementary-material

REFERENCES

Abas, L., Benjamins, R., Malenica, N., Paciorek, T., Wisniewska, J., Moulinier-Anzola, J. C., et al. (2006). Intracellular trafficking and proteolysis of the Arabidopsis auxin-efflux facilitator PIN2 are involved in root gravitropism. *Nat. Cell Biol.* 8, 249–256. doi: 10.1038/ncb1369

Anders, N., and Jurgens, G. (2008). Large ARF guanine nucleotide exchange factors in membrane trafficking. *Cell Mol. Life Sci.* 65, 3433–3445. doi: 10.1007/s00018-008-8227-7

Baster, P., Robert, S., Kleine-Vehn, J., Vanneste, S., Kania, U., Grunewald, W., et al. (2013). $SCF^{TIR1/AFB}$-auxin signalling regulates PIN vacuolar trafficking and auxin fluxes during root gravitropism. *EMBO J.* 32, 260–274. doi: 10.1038/emboj.2012.310

Boudsocq, M., Droillard, M. J., Regad, L., and Lauriere, C. (2012). Characterization of Arabidopsis calcium-dependent protein kinases: activated or not by calcium? *Biochem. J.* 447, 291–299. doi: 10.1042/BJ20112072

Boudsocq, M., and Sheen, J. (2013). CDPKs in immune and stress signaling. *Trends Plant Sci.* 18, 30–40. doi: 10.1016/j.tplants.2012.08.008

Boudsocq, M., Willmann, M. R., Mccormack, M., Lee, H., Shan, L., He, P., et al. (2010). Differential innate immune signalling *via* Ca(2+) sensor protein kinases. *Nature* 464, 418–422. doi: 10.1038/nature08794

Cheng, S. H., Willmann, M. R., Chen, H. C., and Sheen, J. (2002). Calcium signaling through protein kinases. The Arabidopsis calcium-dependent protein kinase gene family. *Plant Physiol.* 129, 469–485. doi: 10.1104/pp.005645

Clough, S. J., and Bent, A. F. (1998). Floral dip: a simplified method for Agrobacterium-mediated transformation of Arabidopsis thaliana. *Plant J.* 16, 735–743. doi: 10.1046/j.1365-313x.1998.00343.x

Day, I. S., Reddy, V. S., Shad Ali, G., and Reddy, A. S. (2002). Analysis of EF-hand-containing proteins in Arabidopsis. *Genome Biol.* 3:RESEARCH0056. doi: 10.1186/gb-2002-3-10-research0056

Dejonghe, W., Kuenen, S., Mylle, E., Vasileva, M., Keech, O., Viotti, C., et al. (2016). Mitochondrial uncouplers inhibit clathrin-mediated endocytosis largely through cytoplasmic acidification. *Nat. Commun.* 7:11710. doi: 10.1038/ncomms11710

Donaldson, J. G., and Jackson, C. L. (2000). Regulators and effectors of the ARF GTPases. *Curr. Opin. Cell Biol.* 12, 475–482. doi: 10.1016/s0955-0674(00)00119-8

Friml, J., Vieten, A., Sauer, M., Weijers, D., Schwarz, H., Hamann, T., et al. (2003). Efflux-dependent auxin gradients establish the apical-basal axis of Arabidopsis. *Nature* 426, 147–153. doi: 10.1038/nature02085

Fuglsang, A. T., Guo, Y., Cuin, T. A., Qiu, Q., Song, C., Kristiansen, K. A., et al. (2007). Arabidopsis protein kinase PKS5 inhibits the plasma membrane H+ -ATPase by preventing interaction with 14-3-3 protein. *Plant Cell* 19, 1617–1634. doi: 10.1105/tpc.105.035626

Gao, Z., Daneva, A., Salanenka, Y., Van Durme, M., Huysmans, M., Lin, Z., et al. (2018). KIRA1 and ORESARA1 terminate flower receptivity by promoting cell death in the stigma of Arabidopsis. *Nat. Plants* 4, 365–375. doi: 10.1038/s41477-018-0160-7

Geldner, N., Anders, N., Wolters, H., Keicher, J., Kornberger, W., Muller, P., et al. (2003). The Arabidopsis GNOM ARF-GEF mediates endosomal recycling, auxin transport, and auxin-dependent plant growth. *Cell* 112, 219–230. doi: 10.1016/s0092-8674(03)00003-5

Geldner, N., Friml, J., Stierhof, Y. D., Jurgens, G., and Palme, K. (2001). Auxin transport inhibitors block PIN1 cycling and vesicle trafficking. *Nature* 413, 425–428. doi: 10.1038/35096571

Gutermuth, T., Lassig, R., Portes, M. T., Maierhofer, T., Romeis, T., Borst, J. W., et al. (2013). Pollen tube growth regulation by free anions depends on the interaction between the anion channel SLAH3 and calcium-dependent protein kinases CPK2 and CPK20. *Plant Cell* 25, 4525–4543. doi: 10.1105/tpc.113.118463

Haruta, M., Gray, W. M., and Sussman, M. R. (2015). Regulation of the plasma membrane proton pump (H(+)-ATPase) by phosphorylation. *Curr. Opin. Plant Biol.* 28, 68–75. doi: 10.1016/j.pbi.2015.09.005

Himschoot, E., Pleskot, R., Van Damme, D., and Vanneste, S. (2017). The ins and outs of Ca(2+) in plant endomembrane trafficking. *Curr. Opin. Plant Biol.* 40, 131–137. doi: 10.1016/j.pbi.2017.09.003

Hong, Y., Takano, M., Liu, C. M., Gasch, A., Chye, M. L., and Chua, N. H. (1996). Expression of three members of the calcium-dependent protein kinase gene family in Arabidopsis thaliana. *Plant Mol. Biol.* 30, 1259–1275. doi: 10.1007/BF00019557

Jürgens, G., and Geldner, N. (2007). The high road and the low road: trafficking choices in plants. *Cell* 130, 977–979. doi: 10.1016/j.cell.2007.09.003

Kania, U., Fendrych, M., and Friml, J. (2014). Polar delivery in plants; commonalities and differences to animal epithelial cells. *Open Biol.* 4:140017. doi: 10.1098/rsob.140017

Karimi, M., Bleys, A., Vanderhaeghen, R., and Hilson, P. (2007). Building blocks for plant gene assembly. *Plant Physiol.* 145, 1183–1191. doi: 10.1104/pp.107.110411

Kitakura, S., Vanneste, S., Robert, S., Löfke, C., Teichmann, T., Tanaka, H., et al. (2011). Clathrin mediates endocytosis and polar distribution of PIN auxin transporters in Arabidopsis. *Plant Cell* 23, 1920–1931. doi: 10.1105/tpc.111.083030

Lee, H., Ganguly, A., Baik, S., and Cho, H.-T. (2021). Calcium-dependent protein kinase 29 modulates PIN-FORMED polarity and Arabidopsis development *via* its own phosphorylation code. *Plant Cell* 33, 3513–3531. doi: 10.1093/plcell/koab207

Li, G., Boudsocq, M., Hem, S., Vialaret, J., Rossignol, M., Maurel, C., et al. (2015). The calcium-dependent protein kinase CPK7 acts on root hydraulic conductivity. *Plant Cell Environ.* 38, 1312–1320. doi: 10.1111/pce.12478

Li, Z., Takahashi, Y., Scavo, A., Brandt, B., Nguyen, D., Rieu, P., et al. (2018). Abscisic acid-induced degradation of &It;em>Arabidopsis&It;/em> guanine nucleotide exchange factor requires calcium-dependent protein kinases. *Proc. Natl. Acad. Sci. U S A.* 115, E4522–E4531.

Liese, A., and Romeis, T. (2013). Biochemical regulation of in vivo function of plant calcium-dependent protein kinases (CDPK). *Biochim. Biophys. Acta* 1833, 1582–1589. doi: 10.1016/j.bbamcr.2012.10.024

Liu, K. H., Niu, Y., Konishi, M., Wu, Y., Du, H., Sun Chung, H., et al. (2017). Discovery of nitrate-CPK-NLP signalling in central nutrient-growth networks. *Nature* 545, 311–316. doi: 10.1038/nature22077

Monaghan, J., Matschi, S., Shorinola, O., Rovenich, H., Matei, A., Segonzac, C., et al. (2014). The calcium-dependent protein kinase CPK28 buffers plant immunity and regulates BIK1 turnover. *Cell Host Microbe* 16, 605–615. doi: 10.1016/j.chom.2014.10.007

Murphy, A. S., Bandyopadhyay, A., Holstein, S. E., and Peer, W. A. (2005). ENDOCYTOTIC CYCLING OF PM PROTEINS. *Annu. Rev. Plant Biol.* 56, 221–251. doi: 10.1146/annurev.arplant.56.032604.144150

Narasimhan, M., Gallei, M., Tan, S., Johnson, A., Verstraeten, I., Li, L., et al. (2021). Systematic analysis of specific and nonspecific auxin effects on endocytosis and trafficking. *Plant Physiol.* 186, 1122–1142. doi: 10.1093/plphys/kiab134

Nebenfuhr, A., Ritzenthaler, C., and Robinson, D. G. (2002). Brefeldin A: deciphering an enigmatic inhibitor of secretion. *Plant Physiol.* 130, 1102–1108. doi: 10.1104/pp.011569

Ötvös, K., Marconi, M., Vega, A., O'brien, J., Johnson, A., Abualia, R., et al. (2021). Modulation of plant root growth by nitrogen source-defined regulation of polar auxin transport. *EMBO J.* 40:e106862. doi: 10.15252/embj.2020106862

Paciorek, T., Zazímalová, E., Ruthardt, N., Petrásek, J., Stierhof, Y. D., Kleine-Vehn, J., et al. (2005). Auxin inhibits endocytosis and promotes its own efflux from cells. *Nature* 435, 1251–1256. doi: 10.1038/nature03633

Peyroche, A., Paris, S., and Jackson, C. L. (1996). Nucleotide exchange on ARF mediated by yeast Geal protein. *Nature* 384, 479–481. doi: 10.1038/384479a0

Reyes, F. C., Buono, R., and Otegui, M. S. (2011). Plant endosomal trafficking pathways. *Curr. Opin. Plant Biol.* 14, 666–673. doi: 10.1016/j.pbi.2011.07.009

Rietz, S., Dermendjiev, G., Oppermann, E., Tafesse, F. G., Effendi, Y., Holk, A., et al. (2010). Roles of Arabidopsis Patatin-Related Phospholipases A in Root Development Are Related to Auxin Responses and Phosphate Deficiency. *Mol. Plant* 3, 524–538. doi: 10.1093/mp/ssp109

Robert, S., Kleine-Vehn, J., Barbez, E., Sauer, M., Paciorek, T., Baster, P., et al. (2010). ABP1 mediates auxin inhibition of clathrin-dependent endocytosis in Arabidopsis. *Cell* 143, 111–121. doi: 10.1016/j.cell.2010.09.027

Roberts, D., and Harmon, A. C. (2003). Calcium-Modulated Proteins: Targets of Intracellular Calcium Signals in Higher Plants. *Annu. Rev. Plant Physiol.* 43, 375–414. doi: 10.1146/annurev.pp.43.060192.002111

Robinson, D. G., and Pimpl, P. (2014). Clathrin and post-Golgi trafficking: a very complicated issue. *Trends Plant Sci.* 19, 134–139. doi: 10.1016/j.tplants.2013.10.008

Ronzier, E., Corratge-Faillie, C., Sanchez, F., Prado, K., Briere, C., Leonhardt, N., et al. (2014). CPK13, a noncanonical Ca2+-dependent protein kinase, specifically inhibits KAT2 and KAT1 shaker K+ channels and reduces stomatal opening. *Plant Physiol.* 166, 314–326. doi: 10.1104/pp.114.240226

Rudd, J. J., and Franklin-Tong, V. E. (2001). Unravelling response-specificity in Ca2+ signalling pathways in plant cells. *New Phytol.* 151, 7–33. doi: 10.1046/j.1469-8137.2001.00173.x

Sauer, M., Balla, J., Luschnig, C., Wisniewska, J., Reinöhl, V., Friml, J., et al. (2006). Canalization of auxin flow by Aux/IAA-ARF-dependent feedback regulation of PIN polarity. *Genes Dev.* 20, 2902–2911. doi: 10.1101/gad.390806

Schellmann, S., and Pimpl, P. (2009). Coats of endosomal protein sorting: retromer and ESCRT. *Curr. Opin. Plant Biol.* 12, 670–676. doi: 10.1016/j.pbi.2009.09.005

Shi, S., Li, S., Asim, M., Mao, J., Xu, D., Ullah, Z., et al. (2018). The Arabidopsis Calcium-Dependent Protein Kinases (CDPKs) and Their Roles in Plant Growth Regulation and Abiotic Stress Responses. *Int. J. Mol. Sci.* 19:1900. doi: 10.3390/ijms19071900

Shimizu, Y., Takagi, J., Ito, E., Ito, Y., Ebine, K., Komatsu, Y., et al. (2021). Cargo sorting zones in the trans-Golgi network visualized by super-resolution confocal live imaging microscopy in plants. *Nat. Commun.* 12:1901. doi: 10.1038/s41467-021-22267-0

Simeunovic, A., Mair, A., Wurzinger, B., and Teige, M. (2016). Know where your clients are: subcellular localization and targets of calcium-dependent protein kinases. *J. Exp. Bot.* 67, 3855–3872. doi: 10.1093/jxb/erw157

Spitzer, M., Wildenhain, J., Rappsilber, J., and Tyers, M. (2014). BoxPlotR: a web tool for generation of box plots. *Nat. Methods* 11, 121–122. doi: 10.1038/nmeth.2811

Van Damme, D., Gadeyne, A., Vanstraelen, M., Inze, D., Van Montagu, M. C., De Jaeger, G., et al. (2011). Adaptin-like protein TPLATE and clathrin recruitment during plant somatic cytokinesis occurs *via* two distinct pathways. *Proc. Natl. Acad. Sci. U S A.* 108, 615–620. doi: 10.1073/pnas.1017890108

Vanneste, S., and Friml, J. (2009). Auxin: a trigger for change in plant development. *Cell* 136, 1005–1016. doi: 10.1016/j.cell.2009.03.001

Vega, A., Fredes, I., O'brien, J., Shen, Z., Ötvös, K., Abualia, R., et al. (2021). Nitrate triggered phosphoproteome changes and a PIN2 phosphosite modulating root system architecture. *EMBO Rep.* 22:e51813. doi: 10.15252/embr.202051813

Xu, J., and Scheres, B. (2005). Dissection of Arabidopsis ADP-RIBOSYLATION FACTOR 1 function in epidermal cell polarity. *Plant Cell* 17, 525–536. doi: 10.1105/tpc.104.028449

Ye, S., Wang, L., Xie, W., Wan, B., Li, X., and Lin, Y. (2009). Expression profile of calcium-dependent protein kinase (CDPKs) genes during the whole lifespan and under phytohormone treatment conditions in rice (Oryza sativa L. ssp. indica). *Plant Mol. Biol.* 70, 311–325. doi: 10.1007/s11103-009-9475-0

Yip Delormel, T., Avila-Ospina, L., Davanture, M., Zivy, M., Lang, J., Valentin, N., et al. (2022). In vivo identification of putative CPK5 substrates in Arabidopsis thaliana. *Plant Sci.* 314:111121. doi: 10.1016/j.plantsci.2021.111121

Yip Delormel, T., and Boudsocq, M. (2019). Properties and functions of calcium-dependent protein kinases and their relatives in Arabidopsis thaliana. *New Phytol.* 224, 585–604. doi: 10.1111/nph.16088

Yorimitsu, T., Sato, K., and Takeuchi, M. (2014). Molecular mechanisms of Sar/Arf GTPases in vesicular trafficking in yeast and plants. *Front. Plant Sci.* 5:411. doi: 10.3389/fpls.2014.00411

Yperman, K., Papageorgiou, A. C., Merceron, R., De Munck, S., Bloch, Y., Eeckhout, D., et al. (2021). Distinct EH domains of the endocytic TPLATE complex confer lipid and protein binding. *Nat. Commun.* 12:3050. doi: 10.1038/s41467-021-23314-6

Yu, X. C., Li, M. J., Gao, G. F., Feng, H. Z., Geng, X. Q., Peng, C. C., et al. (2006). Abscisic acid stimulates a calcium-dependent protein kinase in grape berry. *Plant Physiol.* 140, 558–579. doi: 10.1104/pp.105.074971

Zárský, V., and Potocký, M. (2010). Recycling domains in plant cell morphogenesis: small GTPase effectors, plasma membrane signalling and the exocyst. *Biochem. Soc. Trans.* 38, 723–728. doi: 10.1042/BST0380723

Conflict of Interest: The authors declare that the research was conducted in the absence of any commercial or financial relationships that could be construed as a potential conflict of interest.

Publisher's Note: All claims expressed in this article are solely those of the authors and do not necessarily represent those of their affiliated organizations, or those of the publisher, the editors and the reviewers. Any product that may be evaluated in this article, or claim that may be made by its manufacturer, is not guaranteed or endorsed by the publisher.

Advantages of publishing in Frontiers

OPEN ACCESS
Articles are free to read for greatest visibility and readership

FAST PUBLICATION
Around 90 days from submission to decision

HIGH QUALITY PEER-REVIEW
Rigorous, collaborative, and constructive peer-review

TRANSPARENT PEER-REVIEW
Editors and reviewers acknowledged by name on published articles

Frontiers
Avenue du Tribunal-Fédéral 34
1005 Lausanne | Switzerland

Visit us: www.frontiersin.org
Contact us: frontiersin.org/about/contact

REPRODUCIBILITY OF RESEARCH
Support open data and methods to enhance research reproducibility

DIGITAL PUBLISHING
Articles designed for optimal readership across devices

FOLLOW US
@frontiersin

IMPACT METRICS
Advanced article metrics track visibility across digital media

EXTENSIVE PROMOTION
Marketing and promotion of impactful research

LOOP RESEARCH NETWORK
Our network increases your article's readership